

PLACE IN RETURN BOX to remove this checkout from your record.
TO AVOID FINES return on or before date due.
MAY BE RECALLED with earlier due date if requested.

DATE DUE	DATE DUE	DATE DUE

**DECOMPOSITION
AND CONSECUTIVE DYNAMIC CONDENSATION METHODS
FOR STATIC AND DYNAMIC ANALYSIS OF SINGLE LAYER
LATTICE PLATES**

By

Vera Vladimirovna Galishnikova

A DISSERTATION

Submitted to
Michigan State University
in partial fulfillment of the requirements
for the degree of

DOCTOR OF PHILOSOPHY

Department of Civil and Environmental Engineering

2004

ABSTRACT

DECOMPOSITION AND CONSECUTIVE DYNAMIC CONDENSATION METHODS FOR STATIC AND DYNAMIC ANALYSIS OF SINGLE LAYER LATTICE PLATES

By

Vera Vladimirovna Galishnikova

Approximate yet accurate methods for analyzing large lattice structures are very efficient for the preliminary structural analysis and design, and parametric optimization of large lattice structures.

Two classes of new and effective approximate methods for static and dynamic analysis of large lattice single layer plates using decomposition and consecutive dynamic condensation techniques are developed in this work. These developments are extensions of the decomposition method proposed by Pshenichnov and the dynamic condensation method proposed by Ignatiev.

Simple and accurate approximate analytical formulas for the displacements, force responses, and first eigenvalue of the boundary value problems of thin plates with elastic supports are obtained using the decomposition method. Static and dynamic problems of latticed plates with elastic supports are efficiently solved using continuum modeling. The developed analytical dependencies are used to obtain optimal lattice geometries for a class of plate problems. Shear deformations and joint flexibility are not considered.

The decomposition method also is used with a finite difference formulation that is able to model the original discrete lattice plate. This alternate method has similar accuracy to that based on a continuum modeling for simple, regular lattices.

While the decomposition method is effective and accurate for static analysis and for estimating fundamental frequency of lattice plates, it is intractable for estimating higher frequencies and mode shapes.

An energy form of the consecutive dynamic condensation method is developed in this work. It is demonstrated that the combination of static condensation with the energy form of consecutive dynamic condensation yield accurate estimates of most frequencies and mode shapes of lattice plates. This technique is computationally efficient due to the resulting block diagonal equations and is suitable for implementation on parallel computers.

TO MY FAMILY

ACKNOWLEDGEMENTS

I would like to express my sincere gratitude to Professor Ronald S. Harichandran, my advisor, for his encouragement and significant help as well as for his friendly attitude over the years of my study.

I wish to acknowledge Professors Ronald C. Averill, Rigoberto Burgueño, and Amit H. Varma, the members of advisory committee, for their interest in my work and suggestions.

I would like to express my deepest appreciation to Dr. Thomas L. Maleck for providing financial support that made it possible for me to finish this work. I extend my gratitude to Dr. Salvatore Castronovo who was a kind and generous host for me during one of my semesters at MSU.

I would like to thank all my friends at MSU, and especially Professors Emeriti William E. Saul, William C. Taylor, and Frank Hatfield for their constant friendly support and encouragement.

I wish to appreciate my collaborators, colleagues and friends at the Volgograd State University of Architecture and Civil Engineering and Saratov State Technical University (Russia).

Last, but not least, I want to thank my family for sharing all the challenge with me: my father Vladimir Aleksandrovich Ignatiev for inspiration and guidance, my husband Evgeny Lebed for his understanding and faith, and professional help with the software development, and my sons Aleksander and Ilia for being the main source of cheer for me.

TABLE OF CONTENTS

LIST OF TABLES.....	ix
LIST OF FIGURES.....	xii
CHAPTER 1	
INTRODUCTION AND LITERATURE REVIEW.....	1
1.1 Introduction.....	1
1.2 Motivation.....	2
1.3 Background.....	3
1.3.1 Substructuring Methods.....	4
1.3.2 Order Reduction Methods.....	5
1.3.3 Continuum Modeling.....	8
CHAPTER 2	
DECOMPOSITION METHOD	
FOR SOLVING PROBLEMS OF STRUCTURAL MECHANICS.....	10
2.1 Main Concept of the Decomposition Method.....	10
2.2 Bending of Rectangular Plate with Non-Symmetric Elastic Supports.....	12
2.2.1 Problem Statement.....	12
2.2.2 Decomposition of the Problem.....	15
2.2.3 Numerical Results.....	21
2.3 Symmetric Bending Problem of Rectangular Plates with Elastic Supports.....	23
2.3.1 Problem Statement.....	23
2.3.2 Decomposition of the Problem.....	24
2.3.3 Solution techniques for the interconnection equation.....	27
2.3.4 Solution of the Problem for the Case of a Non-uniform Load.....	36
2.4 Bending of Rectangular Plate with One Free Edge and Three Elastically Supported Edges.....	39
2.4.1 Problem Statement.....	39
2.4.2 Decomposition of the problem.....	40
2.4.3 Numerical results.....	44

2.5	Transverse Free Vibration of a Plate with Elastic Supports.....	50
CHAPTER 3		
STATIC AND DYNAMIC ANALYSIS OF SINGLE LAYER LATTICE PLATES: CONTINUUM MODELING AND SOLUTION BY THE DECOMPOSITION METHOD.....		
		55
3.1	Calculation Model of Lattice Plate.....	55
3.2	Solution of Bending Problem for Lattice Plate with Elastic Supports.....	59
3.3	Comparative Analysis for Different Types of Lattices.....	65
3.4	Transverse Free Vibration of Lattice Plate with Elastic Supports.....	72
CHAPTER 4		
STATIC AND DYNAMIC ANALYSIS OF SINGLE LAYER LATTICE PLATES BY THE DECOMPOSITION METHOD BASED ON FINITE DIFFERENCE DISCRETIZATION.....		
		89
4.1	Notations and the Main Operators of the Finite Difference Formulation.....	90
4.2	Constitutive Equations for Regular Rectangular Grid Stated in Finite Difference Form.....	93
	4.2.1 Method of Virtual Work.....	94
	4.2.2 Displacement Method and Mixed Method.....	98
4.3	Governing Finite Difference Bending Equation for Lattice Plate.....	102
4.4	Boundary Conditions.....	105
4.5	Solution of the Bending of Lattice Plates with Orthogonal Grids.....	107
4.6	Free Vibration Problem of Lattice Plate with an Orthogonal Grid.....	119
CHAPTER 5		
DYNAMIC ANALYSIS OF LATTICE PLATES BY CONSECUTIVE DYNAMIC CONDENSATION.....		
		124

5.1	Problem Statement.....	124
5.2	Frequency - Dynamic Condensation Method.....	126
5.2.1	Condensation based on the Displacement Method.....	126
5.2.2	Condensation based on the Method of Forces.....	128
5.3	Consecutive Dynamic Condensation Method.....	130
5.4	Energy Form of the Consecutive Dynamic Condensation Method.....	132
5.4.1	Condensation Using the Smallest Natural Frequency of Partial Systems.....	133
5.4.2	Condensation Using the Reduced Spectrum of Eigenvalues and Eigenvectors of Partial Systems.....	135
5.4.3	Combined Static and Consecutive Dynamic Condensation.....	140
CHAPTER 6		
CONCLUSIONS AND RECOMMENDATIONS.....		160
APPENDICES.....		164
APPENDIX A		
ARBITRARY FUNCTIONS FOR THE PROBLEM		
PRESENTED IN SECTION 2.4.2.....		165
APPENDIX B		
PROGRAM "PLAS" FOR STATIC ANALYSIS		
OF LATTICE PLATES.....		169
APPENDIX C		
FORMULAE FOR THE MAIN DIFFERENCES AND SUMS.....		179
APPENDIX D		
ELEMENTS OF MATRICES OF COEFFICIENTS		
FOR THE PROBLEM PRESENTED IN SECTION 4.5.....		180
APPENDIX E		
EXAMPLES OF DYNAMIC ANALYSIS USING		
THE COMBINED STATIC AND CONSECUTIVE DYNAMIC		
CONDENSATION METHOD.....		181
REFERENCES.....		190

LIST OF TABLES

TABLE 2.1.	Accuracy of results obtained using Bubnov-Galerkin condition (2.30).....	22
TABLE 2.2.	Accuracy of results obtained using Bubnov-Galerkin conditions (2.46).....	28
TABLE 2.3.	Calculation results for $k_1 = k_2 = 0$ (fixed supports) obtained using (2.47).....	29
TABLE 2.4.	Calculation results for $k_1 = k_2 = 1$ (pinned supports) obtained using (2.47).....	31
TABLE 2.5.	Calculation results for $k_1 = k_2 = 0$ (fixed supports) obtained using (2.48).....	33
TABLE 2.6.	Calculation results for $k_1 = k_2 = 1$ (pinned supports) obtained using (2.48).....	34
TABLE 2.7.	Calculation results for rectangular plate under non-uniform load for $k_1 = k_2 = 1$ (pinned supports) obtained using (2.47).....	37
TABLE 2.8.	Maximum deflection of the free edge for $k_l = 1$ (pinned supports).....	45
TABLE 2.9.	Deflection at the middle of the plate for $k_l = 1$ (pinned supports).....	46
TABLE 2.10.	Maximum bending moment for $k_l = 1$ (pinned supports).....	47
TABLE 2.11.	Maximum deflection of the free edge for $k_l = 0$ (fixed supports).....	48
TABLE 2.12.	Deflection at the middle of the plate for $k_l = 0$ (fixed supports).....	49
TABLE 2.13.	Expressions for P for different types of supports.....	54
TABLE 3.1.	Results for $k_1 = k_2 = 1$ (pinned supports).....	64
TABLE 3.2.	Results for $k_1 = k_2 = 0$ (fixed supports).....	64
TABLE 3.3.	Main types of support conditions and corresponding expressions for the square of the first frequency of free vibration.....	76
TABLE 3.4.	Results for lattice plate with pinned supports and governing angle of $\varphi = 45^\circ$	77

TABLE 3.5.	Results for lattice plate with fixed supports and governing angle of $\varphi = 45^0$	78
TABLE 3.6.	Results for lattice plate with pinned supports and governing angle of $\varphi = 30^0$	79
TABLE 3.7.	Results for lattice plate with fixed supports and governing angle of $\varphi = 30^0$	80
TABLE 3.8.	Results for lattice plate with pinned supports and governing angle of $\varphi = 60^0$	81
TABLE 3.9.	Results for lattice plate with fixed supports and governing angle of $\varphi = 60^0$	82
TABLE 3.10.	Results for lattice plate with supports of Type 1 obtained by (3.41).....	83
TABLE 3.11.	Results for lattice plate with supports of Type 2 obtained by (3.42).....	84
TABLE 3.12.	Results for lattice plate with supports of Type 3 obtained by (3.43).....	85
TABLE 3.13.	Results for lattice plate with supports of Type 4 obtained by (3.44).....	86
TABLE 3.14.	Results for lattice plate with supports of Type 5 obtained by (3.45).....	87
TABLE 3.15.	Results for lattice plate with supports of Type 6 obtained by (3.46).....	88
TABLE 4.1	Lower-order central difference operators.....	92
TABLE 4.2	Deflections at the middle of the plate for the different types of grid for $k_1 = 1$ (pinned support).....	117
TABLE 4.3	Bending moments for the plate with the 16x16 grid for $\tilde{k}_1 = 1$ (pinned support) and $\tilde{k}_1 = 0$ (fixed support).....	117
TABLE 4.4	Deflections in the middle of the plate with the 16x16 grid for different values of support rigidity \tilde{k}_1	118
TABLE 4.5.	Dimensionless values of the first free vibration frequency.....	123

TABLE 5.1.	Results for Test Problem 1	135
TABLE 5.2	Arrangement of the primary degrees of freedom for the Test Problem 2.....	138
TABLE 5.3	Results for Test Problem 2.....	139
TABLE 5.4.	Variants of condensation for Test Problem 3.....	142
TABLE 5.5.	Results for the Test Problem 3 for the case with 22 primary d.o.f.	145
TABLE 5.6.	Results for Test Problem 4 (condensation to 11 primary d.o.f.).....	150
TABLE 5.7.	Results for Test Problem 4 (condensation to 8 primary d.o.f.).....	153
TABLE 5.8.	Results for Test Problem 4 (condensation to 3 primary d.o.f.).....	154
TABLE 5.9.	Results for Test Problem 5.....	157
TABLE E.1.	Results for Problem 1	183
TABLE E.2.	Results for Problem 2.....	187

LIST OF FIGURES

Figure 1.1.	Examples of latticed structures.....	1
Figure 2.1.	Rectangular plate with non-symmetric elastic supports.....	13
Figure 2.2.	Rectangular plate with symmetric elastic supports.....	23
Figure 2.3.	Maximum deflections at the middle of the plate obtained by (2.47) for $k_1 = k_2 = 0$ (fixed supports).....	30
Figure 2.4.	Maximum bending moments on the edge of the plate obtained by (2.47) for $k_1 = k_2 = 0$ (fixed supports).....	30
Figure 2.5.	Maximum deflections at the middle of the plate obtained by (2.47) for $k_1 = k_2 = 1$ (pinned supports).....	31
Figure 2.6.	Maximum bending moments at the middle of the plate obtained by (2.47) for $k_1 = k_2 = 1$ (pinned supports).....	32
Figure 2.7.	Maximum deflections at the middle of the plate obtained by (2.48) for $k_1 = k_2 = 0$ (fixed supports).....	33
Figure 2.8.	Maximum bending moments at the middle of the plate obtained by (2.48).for $k_1 = k_2 = 0$ (fixed supports).....	34
Figure 2.9.	Maximum bending moments on the edge of the plate obtained by (2.48) for $k_1 = k_2 = 0$ (fixed supports).....	34
Figure 2.10.	Maximum deflections at the middle of the plate obtained by (2.48) for $k_1 = k_2 = 1$ (pinned supports).....	35
Figure 2.11.	Maximum bending moments at the middle of the plate obtained by (2.48) for $k_1 = k_2 = 1$ (pinned supports).....	36
Figure 2.12.	Deflections at the middle of the plate under non-uniform load for $k_1 = k_2 = 1$ (pinned supports) obtained using (2.47).....	38
Figure 2.13.	Bending moments at the middle of the plate under non-uniform load for $k_1 = k_2 = 1$ (pinned supports) obtained using (2.47).....	38
Figure 2.14.	Rectangular plate with one free edge.....	39
Figure 2.14.	Maximum deflection of the free edge for $k_1 = 1$ (pinned supports).....	45

Figure 2.15. Deflection at the middle of the plate for $k_1 = 1$ (pinned supports).....	46
Figure 2.16. Maximum bending moment for $k_1 = 1$ (pinned supports).....	47
Figure 2.17. Maximum deflection of the free edge for $k_1 = 0$ (fixed supports).....	48
Figure 2.18. Deflection at the middle of the plate for $k_1 = 0$ (fixed supports).....	49
Figure 3.1 Lattice plate with elastic supports.....	56
Figure 3.2 Internal forces and moments in a rod.....	57
Figure 3.3 Distributed internal forces and moments in the continuum model.....	57
Figure 3.4 Types of grids for lattice plates.....	60
Figure 3.5. Plate with an orthogonal lattice.....	64
Figure 3.6. Maximum deflection at the middle of the plate for $k_1 = k_2 = 0$ (fixed supports).....	68
Figure 3.7. Maximum moment at the middle of the plate for $k_1 = k_2 = 0$	68
Figure 3.8. Maximum deflection at the middle of the plate for $k_1 = k_2 = 1$ (pinned supports).....	69
Figure 3.9. Maximum moment at the middle of the plate for $k_1 = k_2 = 1$ (pinned supports).....	69
Figure 3.10. Maximum deflection at the middle of the plate for $k_1 = k_2 = 0.5$	70
Figure 3.11. Maximum moment at the middle of the plate for $k_1 = k_2 = 0.5$	70
Figure 3.12. Maximum deflection at the middle of the plate for different combinations of support rigidities.....	71
Figure 3.13 Lattice plate with non-symmetric elastic supports.....	72
Figure 3.14. First frequency of free vibration of lattice plate with pinned supports and governing angle of $\varphi = 45^\circ$	77
Figure 3.15. First frequency of free vibration of lattice plate with fixed supports and governing angle of $\varphi = 45^\circ$	78
Figure 3.16. First frequency of free vibration of lattice plate with pinned supports and governing angle of $\varphi = 30^\circ$	79

Figure 3.17.	First frequency of free vibration of lattice plate with fixed supports and governing angle of $\varphi = 30^0$	80
Figure 3.18.	First frequency of free vibration of lattice plate with pinned supports and governing angle of $\varphi = 60^0$	81
Figure 3.19.	First frequency of free vibration of lattice plate with fixed supports and governing angle of $\varphi = 60^0$	82
Figure 3.20.	First frequency of free vibration of lattice plate with supports of Type 1 obtained by (3.41).....	83
Figure 3.21.	First frequency of free vibration of lattice plate with supports of Type 2 obtained by (3.42).....	84
Figure 3.22.	First frequency of free vibration of lattice plate with supports of Type 3 obtained by (3.43).....	85
Figure 3.23.	First frequency of free vibration of lattice plate with supports of Type 4 obtained by (3.44).....	86
Figure 3.24.	First frequency of free vibration for lattice plate with supports of Type 5 obtained by (3.45).....	87
Figure 3.25.	First frequency of free vibration of lattice plate with supports of Type 6 obtained by (3.46).....	88
Figure 4.1	Lattice plate with regular rectangular grid.....	89
Figure 4.2	The original beam and auxiliary load cases for Example 1.....	95
Figure 4.3	Auxiliary load states for the system of orthogonal beams for Example 2.....	97
Figure 4.4	The original beam and the main systems of the displacement method and the mixed method for Example 3.....	99
Figure 4.5	Boundary conditions for the beam in Example 4.....	105
Figure 4.7	Deflections in the middle of the plate with the grid 16x16 for different values of support rigidity \tilde{k}_1	118
Figure 4.8.	Lattice plate with an orthogonal grid and concentrated nodal masses....	119
Figure 5.1.	Simply supported beam with equidistant masses for test problems 1 and 2.....	134

Figure 5.2.	Location of the primary d.o.f. and secondary d.o.f. blocks for the case with 22 primary d.o.f. for Test Problem 3.....	144
Figure 5.3.	Graphs of errors for Test Problem 3 for the case with 22 primary d.o.f.	147
Figure 5.4.	Graphs of errors for the Test Problem 3 for the case with 14 primary d.o.f.	147
Figure 5.5.	Graphs of errors for Test Problem 3 for the case with 10 primary d.o.f.	148
Figure 5.6.	Graphs of errors for Test Problem3 for the case with 6 primary d.o.f.	148
Figure 5.7.	Location of the primary d.o.f. and secondary d.o.f. blocks for Test Problem 4.....	149
Figure 5.8.	Results for Test Problem 4 (condensation to 11 primary d.o.f.).....	150
Figure 5.9.	Mode shapes for Test Problem 4 (condensation to 11 primary d.o.f.)....	151
Figure 5.10.	Results for Test Problem 4 (condensation to 8 primary d.o.f.).....	153
Figure 5.11.	Graphs of errors for Test Problem 4.....	154
Figure 5.12.	Rectangular lattice plate with a 16x16 orthogonal grid.....	155
Figure 5.13.	Condensation schemes for Test Problem 5: (a) to 29 primary nodes; (b) to 49 primary nodes; and (c) to 81 primary nodes.....	156
Figure 5.14.	Graphs of errors for Test Problem 5.....	158
Figure E.1.	(a) The frame for Problem 1; (b) Arrangement of the primary d.o.f. and secondary d.o.f. blocks for Problem 1.....	182
Figure E.2.	Results for Problem 1.....	184
Figure E.3.	Graphs of errors for Problem 1.....	184
Figure E.4.	Location of condensation nodes for Problem 2: (a) condensation to 63 d.o.f.; (b) condensation to 75 d.o.f.; (c) condensation to 99 d.o.f.	186
Figure E.5.	Results for Problem 2.....	189
Figure E.6.	Graphs of errors for Problem 2.....	189

CHAPTER 1

INTRODUCTION AND LITERATURE REVIEW

1.1 Introduction

A latticed structure consists of a very large number of elements or cells interconnected to form a periodic (repetitive) array. Such structures are used extensively in different areas of engineering. In civil construction their potential for freedom of form over long spans makes them architecturally attractive. From the engineering point of view they have advantages such as lightness, high rigidity and rapid erection.

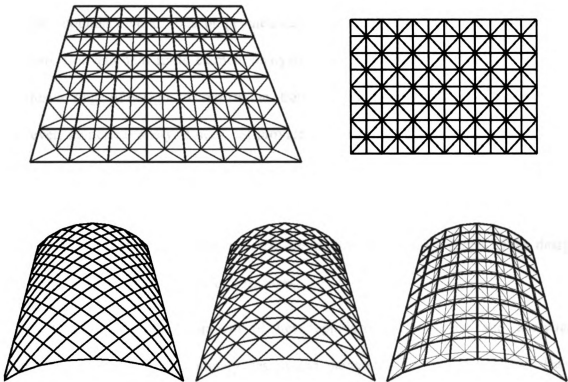


Figure 1.1. Examples of latticed structures

A review of early studies in this area is available in “Lattice Structure: State-of-the Art Report” (1976) and a comprehensive bibliography is given by Sherman (1972). The development of large space structures (LSS) has provided new impetus for research. Latticed structures having dimensions of the order of 10^2 - 10^3 m are the dominant form for LSS, due to their low weight and high stiffness as well as ease of transporting and assembling in space.

1.2 Motivation

The finite element method can be used to solve most problems involving lattice structures. Nevertheless, the large-scale algebraic systems that result in many cases pose significant challenges. Linear static finite element analysis of a large lattice structure may involve the solution of thousands of linear simultaneous algebraic equations. Adding complex boundary conditions or geometrical or physical nonlinearity complicates the problem. Conventional finite element analysis for such problems is usually used at the conclusive stage of design, to confirm the strength, stability and stiffness of the structure. However, numerical analysis does not provide the analytical dependence between force and deformation characteristics, which is desirable for the prediction of the overall structural behavior and optimal design. Further, because the calculation process is cumbersome, it is difficult to use it during the iterative preliminary stages of the design and for parametric studies of lattice structures.

Therefore, the development of new approximate numerical and analytical methods convenient for preliminary design and parametric studies is desirable. These methods provide practical solutions for global structural behavior. They are efficient

during preliminary design to develop the optimal lattice arrangement and estimate the initial cross section of members.

Another area of application for such methods is the dynamic and stability analysis of large lattice structures. Computation of the responses due to dynamic loadings requires the solution of thousands of coupled differential equations. The computational difficulties of solving such equations often limit the use of full-scale dynamic analysis in design. Stability analysis of large lattice structures also represents a complicated problem. Accurate approximate methods for conducting dynamic and stability analyses of such structures can be very useful in preliminary design.

1.3 Background

Approximate methods that have been proposed for simplified structural analysis can be divided into three main types: substructure synthesis, order reduction methods and continuum modeling. The first type involves methods of decomposing or breaking up a large complex problem into a set of subproblems of lower dimensionality, the union of which is equivalent to the original problem. This approach includes substructuring methods, methods of domain decomposition and equation decomposition. The second type includes techniques for reducing the degrees of freedom in complex structural systems, and has been referred to as reduction methods or condensation methods. The third type includes methods that substitute the actual lattice structure by a continuum model with equivalent properties. These three types of methods are briefly explained below.

1.3.1 Substructuring Methods

The main concept in substructure synthesis methods is to represent a complex structure as a set of substructures, each representing an aggregate of basic finite elements. In this approach, each substructure is defined in a convenient system of selected coordinates and analyzed independently with boundaries common to the other substructures. This analysis provides a more compact and tractable stiffness matrix of the substructure and its nodal loading matrix. The substructure for which such matrices have been defined is sometimes called a superelement.

The system of equations written for the boundary nodes of the superelements expresses the equilibrium conditions of the entire structure as an aggregate of superelements. This system of equations contains far fewer unknowns than if the entire system is modeled by standard finite elements. Computation of displacements of the substructure nodes referred to as the “forward step,” comprises the first major step.

In the so-called “backward step,” each substructure is analyzed for the given loading and the boundary displacements found in the forward step. These calculations offer no particular difficulty since the substructures are invariably described by relatively small systems of equations. From the viewpoint of the classic method of displacements, each substructure (superelement) in such an approach represents a complex element of the main system of the displacement method (Przemieniecki 1963, 1968).

The conventional form of substructure analysis has several drawbacks. These include computations in several stages, storage of the stiffness matrices of substructures at all levels, and limitations of the static condensation procedure which prohibits blockwise elimination of the boundary nodes in the Gauss method.

During the past decades the concept of substructuring was extended to the dynamic response of structures. Hurty (1960) proposed the component mode synthesis method. Craig and Bampton (1968) further developed this method. Substructure synthesis also includes such methods as branch-mode analysis (Gladwell, 1964), and component mode substitution (Bajan et al., 1969). A general review of substructuring methods developed in 1960s and 1970s is provided by Nelson (1979).

Further research in this area yielded solution procedures for extracting eigenvalues and eigenvectors from linear dynamic systems using the finite element method. Eigensolution techniques that provide only a partial eigensolution are efficient because they extract only a subset (normally the lowest) of the eigenvalues and eigenvectors required for the analysis of systems. These techniques include the subspace iteration method, the Lanczos method, the conjugate gradient method, the Ritz vector method, the substructure synthesis method, condensation techniques, etc.

1.3.2 Order Reduction Methods

Techniques for reducing the degrees of freedom (d.o.f.) in complex structural systems are referred to as reduction methods or condensation methods. The basic concept in reduction methods is to condense a large system (of algebraic and/or differential equations) to a similar much smaller system of substitute equations. In dynamic problems, the full set of equations of complex systems is reduced by selecting a set of master d.o.f. and eliminating all other (slave) d.o.f. from the primary governing equation. Guyan (1965) first proposed a consistent method of reducing both the stiffness and mass matrices. Methods of static and dynamic condensation based on reducing the order of the

characteristic matrix by exchanging all secondary (auxiliary) d.o.f. have gained considerable application in recent years.

The method of *static condensation* (Guyan 1965) is one of the most convenient and simple methods of reducing the unknowns in the substructuring method of solving dynamic problems. The slave coordinates are those in which, at low frequency, the inertia forces are considered negligible compared to the static forces. This technique can greatly reduce the computational effort necessary to calculate the system eigenpairs. However it has some shortcomings. The major drawback is the error arising from the assumption that the inertial forces in the secondary nodes are negligible. Another drawback is that the accuracy of the result depends on the selection of the condensed nodes (master d.o.f.).

Dynamic condensation by modal synthesis of substructures has been discussed in several works (Hurty 1965, Bathe and Wilson, 1972). Displacements of the secondary (slave) nodes of the substructure are represented as the sum of their static displacements caused by displacements of the primary nodes and displacements of firmly fixed primary nodes in the substructure represented in term of natural modes of vibrations. The dynamic condensation techniques can yield solutions of very high accuracy depending on the number of modes used. The frequencies of the first few modes barely differ from those calculated by the static condensation method. Therefore, the use of dynamic condensation methods for determining only the lower frequencies is not recommended.

Meirovitch and Hale (1981) demonstrated that the component mode synthesis is essentially a different form of the Rayleigh-Ritz method. Based on this, Meirovitch and Kwak (1991) proposed the construction of an approximate eigensolution from the space of admissible functions, and not necessarily from the component modes. They also

proposed choosing the trial vectors from the space of quazi-comparison functions, a new class of functions with high convergence characteristics. These functions represent linear combinations of admissible functions that act like comparison functions. A comparison function satisfies the boundary conditions but not necessarily the differential equation. Quazi-comparison functions obtained can satisfy natural boundary conditions to any degree of accuracy, and the eigensolutions obtained exhibit superior convergence characteristics compared to those based on admissible functions.

Jonsson et al. (1995) proposed a recursive substructuring of finite elements for repetitive structures. In each recursive step the problem is transformed into a new problem involving half the number of identical substructures. The computational work involved in factorization grows only logarithmically as opposed to linear growth in conventional methods.

Farhatt and Geradin (1994) developed a Hybrid Craig-Bampton method involving the original CB method for assembling substructures, hybrid variational formulation and finite element procedure for incompatible substructures. This method can be used as an interface reduction method.

Archer and Graham (2001) present the variation of the component mode technique for the dynamic substructuring of large-scale structural systems. The principal innovation of the proposed method is that the resulting matrix of the reduced substructures remains diagonal. The reduction is accomplished by transforming the degrees of freedom in the substructure using boundary shapes and internal shapes. Then diagonalization of the mass matrix takes place. To recover the accuracy, lost in the diagonalization, additional pseudo-rigid-body-mode shapes are included.

In recent years reduction methods have been extensively developed covering a wide range of problems. Newer techniques using reduction methods in conjunction with substructuring and operator splitting techniques also have been proposed.

1.3.3 Continuum Modeling

In the continuum approach, the actual lattice structure is substituted by a continuum model with equivalent properties derived from those of the discrete members. The behavior of a discrete structure can be determined by studying that of the continuous one. Large sets of algebraic equations used in numerical methods are replaced by a small number of partial differential equations that can be solved analytically or numerically. In many cases continuum modeling provides practical solution methods for global structural behavior, and can be used efficiently in preliminary design and parametric studies. It has been successfully applied to study the vibration and buckling of latticed structures.

Existing continuum modeling methods differ by how the appropriate relationships between the geometric and material properties of the original lattice structure and its continuum model are determined. Most of them fall into one of several main categories. One group of methods uses the relation between force or deformation characteristics of a repeating cell of a lattice structure and those of the continuum model (Wright 1965, Pshenichnov 1982, Necib and Sun 1989). Displacement equations for a lattice cell can be written in terms of finite difference operators and transformed to differential operators (Renton 1970, Kollar and Hegedus 1985). A second category includes methods using energy equivalencies between the lattice and continuum models (Noor, Andersen and Green 1978, Noor 1988, Dow and Huyer 1987, 1989, and Lee 1990, 1991, 1994, 1998).

Methods of the third category are based on the finite element model of a repeating cell. The model is subjected to static loading (Sun and Kim 1985, Sun, Kim and Bogdanoff 1988) or wave propagation (Abrate 1991) and the equivalent properties of the model are determined from the results of these studies. The method suggested by Nayfeh and Hefzy (1981) combines decomposition of the structural member array and an analytical geometry approach.

The detailed survey of the application of continuum modeling and an extensive bibliography in this area are available in the reviews by Noor and Mikulas (1988), and Abrate (1985, 1988, and 1991).

CHAPTER 2

DECOMPOSITION METHOD FOR SOLVING PROBLEMS OF STRUCTURAL MECHANICS

2.1 Main Concept of the Decomposition Method

The decomposition method for solving differential equations and boundary value problems was proposed by G.I. Pshenichnov (1985). Unlike the domain decomposition methods in which the structure is decomposed into substructures, this method decomposes the governing equation and boundary conditions into subproblems. The main concept in this method is to replace the task of solving the complex boundary value problem by the analysis of simpler auxiliary problems stated in terms of additional unknown functions. The form of these functions and their relationship to the field equation and the boundary conditions is the key to this method.

Assume that the solution $y = \{y_1(x), \dots, y_m(x)\}$ of the boundary value problem

$$L_i(y) = f_i(x), i = 1, \dots, m, x \in \Omega \quad (2.1)$$

$$l_j(y) = \varphi_j(x), j = 1, \dots, r, x \in \Gamma \quad (2.2)$$

is to be found, where L_i and l_j are the operators of the equations and the boundary conditions, respectively, $f_i(x)$ and $\varphi_j(x)$ are given functions, and $x = \{x_1, \dots, x_n\}$. The domain Γ consists of pieces of the whole boundary of the domain Ω , and may include some regions inside this domain. Domain Ω may be multiply connected, and the solution may be multivalued. Let the operators of the system be represented in the form

$$L_i = \sum_{k=1}^h L_{ik} \quad (2.3)$$

where some of the terms of the operators L_{ik} may not occur in L_i .

Introducing the notation

$$L_{ik}(y) = f_i^k(x) \quad (2.4)$$

it follows from equations (2.1), (2.3), and (2.4) that

$$f_i(x) = \sum_{k=1}^h f_i^k(x), \quad i = 1, \dots, m \quad (2.5)$$

The following h auxiliary problems for $y^k = \{y_1^k(x), \dots, y_m^k(x)\}$ are now added:

$$L_{ik}(y^k) = f_i^k(x), \quad x \in \Omega, i = 1, \dots, m, k = 1, \dots, h \quad (2.6)$$

$$l_j(y^k) = \varphi_j(x), \quad x \in \Gamma_{jk} \in \Gamma, \quad j = i_{1k}, \dots, i_{rk} \quad (2.7)$$

The conditions (2.7) are chosen so that conditions (2.2) are satisfied by at least one solution y^k at each fixed point on the contour Γ .

The solutions of the problem described by (2.1) and (2.2) coincide with the solutions common to all the problems characterized by (2.6) and (2.7). Boundary conditions will be satisfied as a consequence of the selections in (2.7). Furthermore, (2.1) will be satisfied as well, since (2.3), (2.5), and (2.6) hold. On the other hand, a solution y of the problem described by (2.1) and (2.2) is a solution of each of the h problems characterized by (2.6) and (2.7) as well. Consequently, the task of solving the boundary value problem may be replaced by that of finding solutions of the auxiliary problems

(2.6), containing $m \times h$ unknown functions $f^k(x)$ with the addition of $m \times h$ conditions (2.7) on the solutions.

The merit of this method is the flexibility in the decomposition of the original problem, which provides wide latitude for choosing the auxiliary problems that facilitate the construction of the desired solution. As a result, simple and highly accurate approximate analytical formulas for displacements, force responses, and eigenvalues of the boundary value problems can be obtained in many cases, where other methods must usually resort to numerical solutions.

In this work the decomposition method is developed for the bending and free vibration problems of thin isotropic and single-layer lattice plates with elastic supports.

2.2 Bending of Rectangular Plate with Non-Symmetric Elastic Supports

The application of the decomposition method is first illustrated with a non-symmetric problem of bending of the rectangular thin isotropic plate shown in Figure 2.1 subjected to a uniform transverse load.

2.2.1 Problem Statement

In the Cartesian coordinate system the differential equation governing the bending problem has the well-known form

$$\frac{\partial^4 w}{\partial x^4} + 2 \frac{\partial^4 w}{\partial x^2 \partial y^2} + \frac{\partial^4 w}{\partial y^4} = \frac{q(x)}{D} \quad (2.8)$$

where w is the transverse deflection, q is the uniformly distributed transverse load intensity, and D is the plate's flexural rigidity.

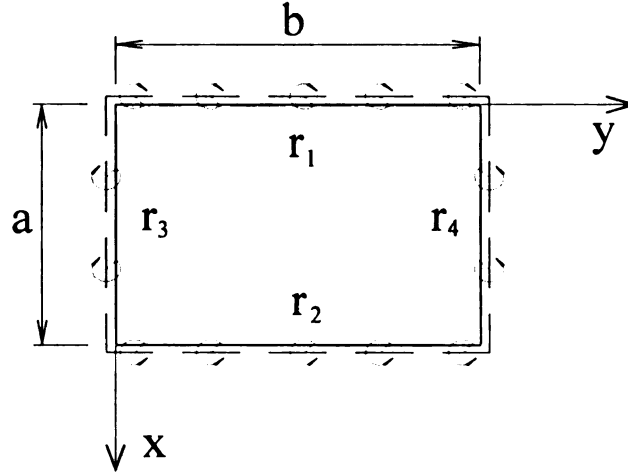


Figure 2.1. Rectangular plate with non-symmetric elastic supports

Assuming flexible elastic supports along the edges of the plate, (2.8) must be solved under the following boundary conditions:

$$w = 0, \quad M_1 = -r_1 \frac{\partial w}{\partial x} \quad (x = 0)$$

$$w = 0, \quad M_1 = r_2 \frac{\partial w}{\partial x} \quad (x = a)$$

$$w = 0, \quad M_2 = -r_3 \frac{\partial w}{\partial x} \quad (y = 0) \quad (2.9)$$

$$w = 0, \quad M_2 = r_4 \frac{\partial w}{\partial x} \quad (y = b)$$

where r_i is the stiffness per unit length of the distributed rotational springs along the corresponding support ($0 \leq r_i < \infty$). Using the moment-curvature relationships

$M_x = -D(\partial^2 w / \partial x^2)$ and $M_y = -D(\partial^2 w / \partial y^2)$, the boundary conditions may be written as:

$$\begin{aligned}
 w = 0, \quad D \frac{\partial^2 w}{\partial x^2} - r_1 \frac{\partial w}{\partial x} &= 0 \quad (x = 0) \\
 w = 0, \quad D \frac{\partial^2 w}{\partial x^2} + r_2 \frac{\partial w}{\partial x} &= 0 \quad (x = a) \\
 w = 0, \quad D \frac{\partial^2 w}{\partial y^2} - r_3 \frac{\partial w}{\partial y} &= 0 \quad (y = 0) \\
 w = 0, \quad D \frac{\partial^2 w}{\partial y^2} + r_4 \frac{\partial w}{\partial y} &= 0 \quad (y = b)
 \end{aligned} \tag{2.10}$$

For a rigid support, the stiffness coefficient is infinity, and the equations above are inconvenient for obtaining the analytical dependencies. It is expedient to introduce the following expressions for the dimensionless stiffness coefficients of the elastic supports:

$$\begin{aligned}
 k_1 &= \frac{1}{1+r_1 a/D}, \quad k_2 = \frac{1}{1+r_2 a/D} \\
 k_3 &= \frac{1}{1+r_3 b/D}, \quad k_4 = \frac{1}{1+r_4 b/D}
 \end{aligned} \tag{2.11}$$

Since $0 \leq r_i < \infty$, it follows that $0 \leq k_i \leq 1$, and the extreme cases $k_i = 0$ and $k_i = 1$ correspond to rigid and hinged supports at the edges of the plate. Furthermore, the following notations are introduced to reduce the whole problem to non-dimensional form:

$$\begin{aligned}
 \alpha = x/a, \quad \beta = y/b, \quad \lambda = b/a \geq 1 \\
 v = w \frac{D}{qa^4}
 \end{aligned} \tag{2.12}$$

where v = dimensionless deflection function.

The dimensionless differential equation corresponding to (2.8) is

$$\frac{\partial^4 v}{\partial \alpha^4} + \frac{2}{\lambda^2} \frac{\partial^4 v}{\partial \alpha^2 \partial \beta^2} + \frac{1}{\lambda^4} \frac{\partial^4 v}{\partial \beta^4} = 1 \quad (2.13)$$

and the dimensionless boundary conditions corresponding to (2.10) are

$$\begin{aligned} v = 0, \quad k_1 \frac{\partial^2 v}{\partial \alpha^2} - (1 - k_1) \frac{\partial v}{\partial \alpha} &= 0 \quad (\alpha = 0) \\ v = 0, \quad k_2 \frac{\partial^2 v}{\partial \alpha^2} + (1 - k_2) \frac{\partial v}{\partial \alpha} &= 0 \quad (\alpha = 1) \\ v = 0, \quad k_3 \frac{\partial^2 v}{\partial \alpha^2} - (1 - k_3) \frac{\partial v}{\partial \alpha} &= 0 \quad (\beta = 0) \\ v = 0, \quad k_4 \frac{\partial^2 v}{\partial \alpha^2} + (1 - k_4) \frac{\partial v}{\partial \alpha} &= 0 \quad (\beta = 1) \end{aligned} \quad (2.14)$$

2.2.2 Decomposition of the Problem

The boundary value problem characterized by (2.13) and (2.14) is solved by the decomposition method. The dimensionless deflection $v(\alpha, \beta)$ is represented in the three forms v_1, v_2 , and v_3 . Three auxiliary problems, two of which are boundary value problems, are introduced to determine these forms.

The first auxiliary problem (boundary value problem) is to find the solution to the differential equation

$$\frac{\partial^4 v_1}{\partial \alpha^4} = f_1(\alpha, \beta) \quad (2.15)$$

subject to the conditions

$$\begin{aligned}
 v_1 = 0, \quad k_1 \frac{\partial^2 v_1}{\partial \alpha^2} - (1 - k_1) \frac{\partial v_1}{\partial \alpha} = 0 \quad (\alpha = 0) \\
 v_1 = 0, \quad k_2 \frac{\partial^2 v_1}{\partial \alpha^2} + (1 - k_2) \frac{\partial v_1}{\partial \alpha} = 0 \quad (\alpha = 1)
 \end{aligned}
 \tag{2.16}$$

The second auxiliary problem (boundary value problem) is to find the solution to the differential equation

$$\frac{\partial^4 v_2}{\partial \beta^4} = f_2(\alpha, \beta)
 \tag{2.17}$$

subject to the conditions

$$\begin{aligned}
 v_2 = 0, \quad k_3 \frac{\partial^2 v_2}{\partial \alpha^2} - (1 - k_3) \frac{\partial v_2}{\partial \alpha} = 0 \quad (\beta = 0) \\
 v_2 = 0, \quad k_4 \frac{\partial^2 v_2}{\partial \alpha^2} + (1 - k_4) \frac{\partial v_2}{\partial \alpha} = 0 \quad (\beta = 1)
 \end{aligned}
 \tag{2.18}$$

The third auxiliary problem is to find the solution to the interconnection differential equation

$$\frac{2}{\lambda^2} \frac{\partial^4 v_3}{\partial \alpha^2 \partial \beta^2} = -f_1(\alpha, \beta) - \frac{1}{\lambda^4} f_2(\alpha, \beta) + 1
 \tag{2.19}$$

These problems include two unknown functions $f_1(\alpha, \beta)$ and $f_2(\alpha, \beta)$.

Assuming that

$$v = v_1 = v_2 = v_3
 \tag{2.20}$$

and separately summing the left- and right-hand terms of the equations in the three auxiliary problems, yields the left- and right-hand terms of the original problem in (2.13). Similarly, summation of the boundary conditions of the auxiliary problems results in the boundary conditions of the original problem (2.14). Thus, the solution of the boundary value problem (2.13) and (2.14) can be replaced by the solution of auxiliary problems (2.15), (2.17), and (2.19) satisfying conditions (2.20).

If the condition (2.20) is satisfied exactly, the three forms of the solution v_1 , v_2 , and v_3 coincide, and the exact solution of the original boundary value problem is obtained. In this work an approximate solution is sought by representing of the unknown functions $f_1(\alpha, \beta)$ and $f_2(\alpha, \beta)$ as power series. These functions do not depend upon boundary conditions, and therefore can be represented by the same system of basic functions. Since the fourth derivative of v_3 is approximated by these functions, retaining only a few terms of the power series expansion can still yield accurate results for v . Assume that

$$\begin{aligned} f_1(\alpha, \beta) &= \psi_1(\beta) \\ f_2(\alpha, \beta) &= \psi_2(\alpha) \end{aligned} \tag{2.21}$$

where $\psi_1(\beta)$ and $\psi_2(\alpha)$ are arbitrary functions.

Consider the first auxiliary problem (2.15) and (2.16). The integration of (2.15) yields

$$v_1 = \psi_1(\beta) \left(\frac{\alpha^4}{24} + C_3 \frac{\alpha^3}{6} + C_2 \frac{\alpha^2}{2} + C_1 \alpha + C_0 \right) \tag{2.22}$$

which C_i , $i = 0...3$, are the integration constants depending on the values of λ (the aspect ratio of the plate) and k_i (the dimensionless stiffness coefficients of the elastic supports).

These constants are found by satisfying boundary conditions (2.16):

$$\begin{aligned}
C_0 &= 0 \\
C_1 &= \frac{1}{12} \cdot \frac{k_1(1+5k_2)}{3(1+k_1)(1+k_2)-2(1-k_1k_2)} = \frac{1}{12} \cdot \frac{k_1(1+5k_2)}{R_{12}} \\
C_2 &= \frac{1}{12} \cdot \frac{(1-k_1)(1+5k_2)}{3(1+k_1)(1+k_2)-2(1-k_1k_2)} = \frac{1}{12} \cdot \frac{(1-k_1)(1+5k_2)}{R_{12}} \\
C_3 &= -\frac{2(1+2k_2)R_{12} + (1+5k_2)(1-k_1k_2)}{6R_{12}(1+k_2)}
\end{aligned} \tag{2.23}$$

where $R_{12} = 3(1+k_1)(1+k_2) - 2(1-k_1k_2) = 1 + 3(k_1+k_2) + 5k_1k_2$.

The expression for the first form of the deflection function can now be written as

$$\begin{aligned}
v_1 &= \frac{\psi_1(\beta)}{72} \left\{ 3\alpha^4 - \frac{2}{R_{12}(1+k_2)} \left[2R_{12}(1+2k_2) + (1+5k_2)(1-k_1k_2) \right] \alpha^3 \right. \\
&\quad \left. + \frac{3(1+5k_2)}{R_{12}} \left[(1-k_1)\alpha^2 + 2k_1\alpha \right] \right\}
\end{aligned} \tag{2.24}$$

A similar procedure for the second auxiliary problem (2.17) and (2.18) yields

$$\begin{aligned}
v_2 &= \frac{\psi_2(\alpha)}{72} \left\{ 3\beta^4 - \frac{2}{R_{34}(1+k_4)} \left[2R_{34}(1+2k_4) + (1+5k_4)(1-k_3k_4) \right] \beta^3 \right. \\
&\quad \left. + \frac{3(1+5k_4)}{R_{34}} \left[(1-k_3)\beta^2 + 2k_3\beta \right] \right\}
\end{aligned} \tag{2.25}$$

where $R_{34} = 3(1 + k_3)(1 + k_4) - 2(1 - k_3 k_4) = 1 + 3(k_3 + k_4) + 5k_3 k_4$

Satisfying condition $v_1 = v_2$ from (2.20) yields the arbitrary functions $\psi_1(\beta)$ and $\psi_2(\alpha)$:

$$\psi_1(\beta) = p \left\{ 3\beta^4 - \frac{2}{R_{34}(1+k_4)} \left[2R_{34}(1+2k_4) + (1+5k_4)(1-k_3k_4) \right] \beta^3 + \frac{3(1+5k_4)}{R_{34}} \left[(1-k_3)\beta^2 + 2k_3\beta \right] \right\} \quad (2.26)$$

or $\psi_1(\beta) = p\phi_1(\beta)$

$$\psi_2(\alpha) = p \left\{ 3\alpha^4 - \frac{2}{R_{12}(1+k_2)} \left[2R_{12}(1+2k_2) + (1+5k_2)(1-k_1k_2) \right] \alpha^3 + \frac{3(1+5k_2)}{R_{12}} \left[(1-k_1)\alpha^2 + 2k_1\alpha \right] \right\} \quad (2.27)$$

or $\psi_2(\alpha) = p\phi_2(\alpha)$

where p is an unknown constant. Substituting $\psi_1(\beta)$ and $\psi_2(\alpha)$ into (2.24) and (2.25) yields the following expression for the dimensionless deflection function:

$$v = v_1 = v_2 = \frac{p}{72} \left\{ 3\alpha^4 - \frac{2}{R_{12}(1+k_2)} \left[2R_{12}(1+2k_2) + (1+5k_2)(1-k_1k_2) \right] \alpha^3 + \frac{3(1+5k_2)}{R_{12}} \left[(1-k_1)\alpha^2 + 2k_1\alpha \right] \right\} \times \left\{ 3\beta^4 - \frac{2}{R_{34}(1+k_4)} \left[2R_{34}(1+2k_4) + (1+5k_4)(1-k_3k_4) \right] \beta^3 + \frac{3(1+5k_4)}{R_{34}} \left[(1-k_3)\beta^2 + 2k_3\beta \right] \right\} \quad (2.28)$$

Equation (2.28) is an approximate solution to the original problem with the unknown constant to be determined by solving the third auxiliary problem.

The approximate solution of the third auxiliary problem (2.19) is found by assuming $v_3 = v_1 = v_2 = v$. The following the discrepancy function based on (2.13), (2.15), and (2.17) is proposed:

$$\Phi(\alpha, \beta) = f_1(\alpha, \beta) + \frac{2}{\lambda^2} \frac{\partial^4 v_3}{\partial \alpha^2 \partial \beta^2} + \frac{1}{\lambda^4} f_2(\alpha, \beta) - 1 \quad (2.29)$$

If the solution is exact, the function $\Phi(\alpha, \beta)$ is identically zero. In the approximate solution that is sought, the arbitrary constant p is determined by minimizing the discrepancy function $\Phi(\alpha, \beta)$ using the Bubnov-Galerkin method. The vanishing condition for the discrepancy function can be written as:

$$\int_0^1 \int_0^1 \Phi(\alpha, \beta) \varphi_2(\alpha) \varphi_1(\beta) d\alpha d\beta = 0 \quad (2.30)$$

Using the notations in (2.26), (2.27), and (2.28) yields the expression

$$\int_0^1 \int_0^1 \left[\frac{p}{72} \varphi_1(\beta) + \frac{2}{\lambda^2} \frac{p}{72} \varphi_2''(\alpha) \varphi_1''(\beta) + \frac{p}{72} \frac{1}{\lambda^4} \varphi_1(\beta) \right] \varphi_2(\alpha) \varphi_1(\beta) d\alpha d\beta = 0$$

where the primes denote derivatives with respect to the arguments of the functions. Performing the integrations and necessary transformations yields the following expression for the arbitrary constant

$$p = \frac{49 R_{12} R_{34} G_{12} G_{34}}{7 R_{12} G_{12} F_{34} + \frac{4}{\lambda^2} H_{12} H_{34} + \frac{7}{\lambda^4} R_{34} G_{34} F_{12}} \quad (2.31)$$

where

$$R_{12} = 1 + 3(k_1 + k_2) + 5k_1 k_2, \quad R_{34} = 1 + 3(k_3 + k_4) + 5k_3 k_4$$

$$G_{12} = 1 + 8(k_1 + k_2) + 55k_1k_2, \quad G_{34} = 1 + 8(k_3 + k_4) + 55k_3k_4$$

$$H_{12} = 1 + 13(k_1 + k_2) + 58(k_1^2 + k_2^2) + 154k_1k_2 + 625(k_1^2k_2 + k_1k_2^2) + 2125k_1^2k_2^2$$

$$H_{34} = 1 + 13(k_3 + k_4) + 58(k_3^2 + k_4^2) + 154k_3k_4 + 625(k_3^2k_4 + k_3k_4^2) + 2125k_3^2k_4^2$$

$$F_{12} = 1 + 15(k_1 + k_2) + 60(k_1^2 + k_2^2) + 208k_1k_2 + 765(k_1^2k_2 + k_1k_2^2) + 2575k_1^2k_2^2$$

$$F_{34} = 1 + 15(k_3 + k_4) + 60(k_3^2 + k_4^2) + 208k_3k_4 + 765(k_3^2k_4 + k_3k_4^2) + 2575k_3^2k_4^2$$

After the value of p is obtained from (2.31), the dimensionless deflection can be computed using (2.28). The actual deflection and bending moments at any point of the plate are calculated using the formulas

$$w = \frac{qa^4}{D} v$$

$$M_1 = -qa^2 \left(\frac{\partial^2 v}{\partial \alpha^2} + \nu \frac{\partial^2 v}{\partial \beta^2} \right) \quad (2.32)$$

$$M_2 = -qa^2 \left(\nu \frac{\partial^2 v}{\partial \alpha^2} + \frac{\partial^2 v}{\partial \beta^2} \right)$$

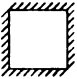
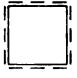
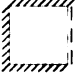
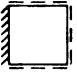
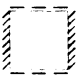
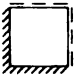
2.2.3 Numerical Results

Test results were obtained from the decomposition method for an isotropic square plate with different combinations of boundary conditions under the uniformly distributed load and compared with accurate solutions (Timoshenko and Voinowsky-Krieger 1959). The calculation results and the associated errors are presented in Table 2.1.

The error in the deflections computed by the decomposition method do not exceed 5%, but the error in the computed bending moments is significant and reaches 20%. This

is because the bending moment is related to the second derivative of the displacement which is prone to greater error. The number of terms in the series expansion should be increased to improve the results for the bending moment.

TABLE 2.1. Accuracy of results obtained using Bubnov-Galerkin condition (2.30)

Support Type	$v(0, 0) \times 10^3$			$M_0(0, 0) \times 10^2$		
	Exact value	DM	ε (%)	Exact value	$M_0(1, 0)$	ε (%)
	1.32	1.26	-4.8	2.77	2.31	-19.0
	4.14	4.04	-2.0	5.17	4.79	-9.0
	1.61	1.57	-2.5	3.26	2.83	-15.9
	2.82	2.80	-0.7	4.31	3.90	-10.4
	1.98	1.92	-3.12	2.77	2.44	-13.5
	2.40	2.30	-4.3	3.02	2.81	-7.5

Notations:  fixed support,  pinned support

2.3 Symmetric Bending Problem of Rectangular Plates with Elastic Supports

In this section the decomposition method is used to obtain the bending response of the thin isotropic rectangular plate with elastic supports shown in Figure 2.2 under an arbitrarily distributed load. Collocation methods are introduced for minimizing the discrepancy function.

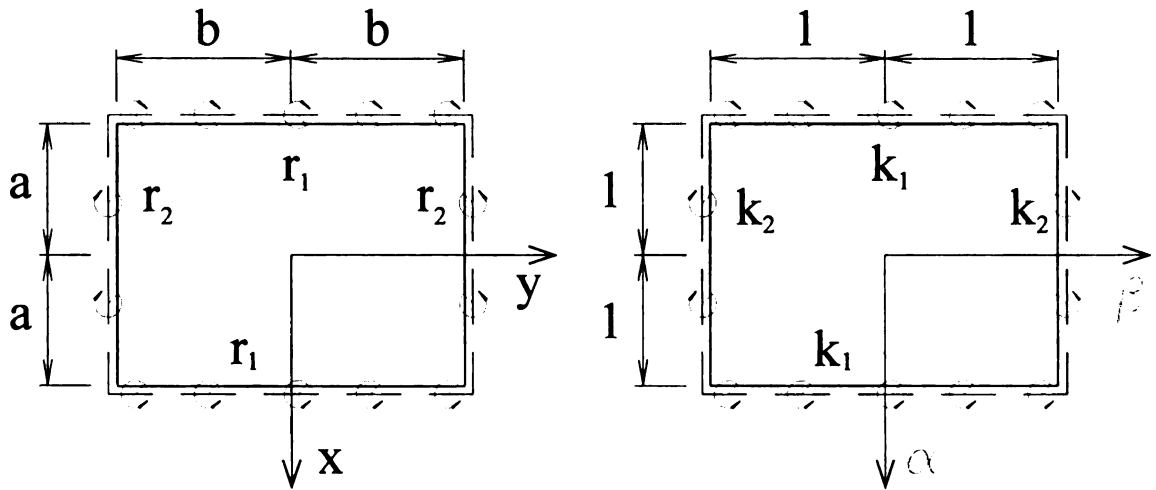


Figure 2.2. Rectangular plate with symmetric elastic supports

2.3.1 Problem Statement

The differential equation for the bending problem is

$$\frac{\partial^4 w}{\partial x^4} + 2 \frac{\partial^4 w}{\partial x^2 \partial y^2} + \frac{\partial^4 w}{\partial y^4} = \frac{Z}{D} \quad (2.33)$$

where Z is the arbitrary distributed transverse load.

Assuming symmetrical elastic supports along the opposite edges of the plate, (2.33) must be solved under the following boundary conditions:

$$w = 0, \quad D \frac{\partial^2 w}{\partial x^2} \pm r_1 \frac{\partial w}{\partial x} = 0 \quad (x = \pm a)$$

$$w = 0, \quad D \frac{\partial^2 w}{\partial y^2} \pm r_2 \frac{\partial w}{\partial y} = 0 \quad (y = \pm b)$$
(2.34)

Using the notations (2.11) and (2.12), the problem is reduced to the non-dimensional form:

$$\frac{\partial^4 v}{\partial \alpha^4} + \frac{2}{\lambda^2} \frac{\partial^4 v}{\partial \alpha^2 \partial \beta^2} + \frac{1}{\lambda^4} \frac{\partial^4 v}{\partial \beta^4} = q(\alpha, \beta)$$
(2.35)

where $q(\alpha, \beta) = \frac{Z}{|Z_{\max}|}$ = the dimensionless load function. The dimensionless boundary conditions corresponding to (2.34) are

$$v = 0, \quad k_1 \frac{\partial^2 v}{\partial \alpha^2} \pm (1 - k_1) \frac{\partial v}{\partial \alpha} = 0 \quad (\alpha = \pm 1)$$
(2.36a)

$$v = 0, \quad k_2 \frac{\partial^2 v}{\partial \beta^2} \pm (1 - k_2) \frac{\partial v}{\partial \beta} = 0 \quad (\beta = \pm 1)$$
(2.36b)

2.3.2 Decomposition of the Problem

The boundary value problem characterized by (2.35) and (2.36) is solved by the decomposition method using three auxiliary problems. The first auxiliary problem (boundary value problem) is to find the solution to the differential equation

$$\frac{\partial^4 v_1}{\partial \alpha^4} = f_1(\alpha, \beta)$$
(2.37)

subject to the conditions (2.36a), where $v = v_1$.

The second auxiliary problem (boundary value problem) is to find the solution to the differential equation

$$\frac{\partial^4 v_2}{\partial \beta^4} = f_2(\alpha, \beta) \quad (2.38)$$

subject to the conditions (2.36b), where $v = v_2$.

The third auxiliary problem (solution of the differential equation) is

$$\Phi(\alpha, \beta) \equiv \frac{2}{\lambda^2} \frac{\partial^4 v_3}{\partial \alpha^2 \partial \beta^2} + f_1(\alpha, \beta) + \frac{1}{\lambda^4} f_2(\alpha, \beta) - q(\alpha, \beta) = 0 \quad (2.39)$$

These problems include two unknown functions $f_1(\alpha, \beta)$ and $f_2(\alpha, \beta)$. An approximate solution is sought by retaining the first two terms of the power series expansion of $f_1(\alpha, \beta)$ and $f_2(\alpha, \beta)$. Due to symmetry in the coordinates α and β , it is assumed that

$$f_1(\alpha, \beta) = f_1(\beta) + \alpha^2 f_3(\beta), \quad f_2(\alpha, \beta) = f_2(\alpha) + \beta^2 f_4(\alpha) \quad (2.40)$$

where $f_1(\beta), f_2(\alpha), f_3(\beta), f_4(\alpha)$ are arbitrary functions.

Solutions of the boundary value problems (2.37) and (2.38) are then obtained as

$$\begin{aligned} v_1 = & \frac{1}{24} \left[\alpha^4 - 2(1 + 2k_1)\alpha^2 + 1 + 4k_1 \right] f_1(\beta) \\ & + \frac{1}{360} \left[\alpha^6 - 3(1 + 4k_1)\alpha^2 + 2(1 + 6k_1) \right] f_3(\beta) \end{aligned} \quad (2.41)$$

$$\begin{aligned}
v_2 &= \frac{1}{24} \left[\beta^4 - 2(1 + 2k_2) \beta^2 + 1 + 4k_2 \right] f_2(\alpha) \\
&+ \frac{1}{360} \left[\beta^6 - 3(1 + 4k_2) \beta^2 + 2(1 + 6k_2) \right] f_4(\alpha)
\end{aligned} \tag{2.42}$$

Satisfying conditions (2.20) yields

$$\begin{aligned}
v_1 = v_2 &= \frac{1}{24} \psi_1^{(1)}(\alpha) \left[p_1 \psi_1^{(2)}(\beta) + p_3 \psi_2^{(2)}(\beta) \right] \\
&+ \frac{1}{360} \psi_2^{(1)}(\alpha) \left[p_2 \psi_1^{(2)}(\beta) + p_4 \psi_2^{(2)}(\beta) \right]
\end{aligned} \tag{2.43}$$

where

$$\begin{aligned}
\psi_1^{(1)}(\alpha) &= \alpha^4 - 2(1 + 2k_1) \alpha^2 + 1 + 4k_1 \\
\psi_2^{(1)}(\alpha) &= \alpha^6 - 3(1 + 4k_1) \alpha^2 + 2(1 + 6k_1) \\
\psi_1^{(2)}(\beta) &= \beta^4 - 2(1 + 2k_2) \beta^2 + 1 + 4k_2 \\
\psi_2^{(2)}(\beta) &= \beta^6 - 3(1 + 4k_2) \beta^2 + 2(1 + 6k_2)
\end{aligned} \tag{2.44}$$

and $p_i =$ arbitrary constants.

Equation (2.43) is an approximate solution to the original problem with four constants to be determined by solving the third auxiliary problem. Satisfying conditions (2.20) and using (2.39) and (2.43) yields

$$\begin{aligned}
\Phi(\alpha, \beta) &= p_1 \left[\psi_1^{(2)}(\beta) + \frac{1}{12\lambda^2} \psi_1^{(1)''}(\alpha) \psi_1^{(2)''}(\beta) + \frac{1}{\lambda^4} \psi_1^{(1)}(\alpha) \right] \\
&+ p_2 \left[\alpha^2 \psi_1^{(2)}(\beta) + \frac{1}{180\lambda^2} \psi_2^{(1)''}(\alpha) \psi_1^{(2)''}(\beta) + \frac{1}{15\lambda^4} \psi_2^{(1)}(\alpha) \right]
\end{aligned}$$

$$\begin{aligned}
& + p_3 \left[\psi_2^{(2)}(\beta) + \frac{1}{12\lambda^2} \psi_1^{(1)''}(\alpha) \psi_2^{(2)''}(\beta) + \frac{15}{\lambda^4} \beta^2 \psi_1^{(1)}(\alpha) \right] \\
& + p_4 \left[\alpha^2 \psi_2^{(2)}(\beta) + \frac{1}{180\lambda^2} \psi_2^{(1)''}(\alpha) \psi_2^{(2)''}(\beta) + \frac{1}{\lambda^4} \beta^2 \psi_2^{(1)}(\alpha) \right] - q(\alpha, \beta) = 0 \quad (2.45)
\end{aligned}$$

The primes denote derivatives with respect to the arguments of the functions.

2.3.3 Solution techniques for the interconnection equation

The third auxiliary problem (interconnection equation) can be solved by different methods. For the problem at hand, three different approaches were used to evaluate the arbitrary constants p_i : the Bubnov-Galerkin method and two forms of the collocation method. The load was assumed to be uniformly distributed: $q(\alpha, \beta) = 1$.

Bubnov-Galerkin Method. In the first approach using the Bubnov-Galerkin method, the vanishing conditions for the discrepancy function can be written as:

$$\begin{aligned}
\int_0^1 \int_0^1 \Phi(\alpha, \beta) \psi_1^{(1)}(\alpha) \psi_1^{(2)}(\beta) d\alpha d\beta &= 0 \\
\int_0^1 \int_0^1 \Phi(\alpha, \beta) \psi_2^{(1)}(\alpha) \psi_2^{(2)}(\beta) d\alpha d\beta &= 0 \\
\int_0^1 \int_0^1 \Phi(\alpha, \beta) \psi_1^{(1)}(\alpha) \psi_2^{(2)}(\beta) d\alpha d\beta &= 0 \\
\int_0^1 \int_0^1 \Phi(\alpha, \beta) \psi_2^{(1)}(\alpha) \psi_1^{(2)}(\beta) d\alpha d\beta &= 0
\end{aligned} \tag{2.46}$$

Substituting the discrepancy function (2.45) into (2.46) and performing the integrations yields a system of four linear algebraic equations which can be solved to obtain the four unknowns p_1 , p_2 , p_3 , and p_4 . The dimensionless deflection at any point of

the plate is then obtained from (2.43) and bending moments are computed using the moment curvature relationships. Results obtained from the decomposition method for a square plate with three different types of boundary conditions, and the associated errors compared with accurate solutions (Timoshenko and Voinowsky-Krieger 1959) are given in Table 2.2. The example demonstrates the accuracy of the technique for the case of square plates.

TABLE 2.2. Accuracy of results obtained using Bubnov-Galerkin conditions (2.46)

Support Type	$v(0, 0)$	ε (%)	$M_0(0, 0)$	ε (%)	$M_0(1, 0)$	ε (%)
Pinned supports ($k_1 = k_2 = 1$)	0.00406	0	0.0474	1.04	0	0
Fixed supports ($k_1 = k_2 = 0$)	0.00126	0	0.0228	1.2	0.0512	0.3
Mixed supports ($k_1 = 0, k_2 = 1$)	0.00192	0.1	0.0246	-0.6	0.0668	1.3

However, the solution using this approach loses the accuracy for aspect ratios other than 1. Also, the Bubnov-Galerkin method for solving the third auxiliary problem is cumbersome and does not lend itself to automation. An alternate method is to obtain the equations for determining the unknown constants by equating the discrepancy function or its derivatives to zero at several collocation points.

Collocation Method with Single Point. In the second approach the arbitrary constants are determined by minimizing $\Phi(\alpha, \beta)$ in the middle section of the plate. Accordingly, the function and some of its lower derivatives with respect to α and β are set to zero at the center of the plate.

$$\Phi(0,0) = 0, \quad \frac{\partial^2 \Phi}{\partial \alpha^2}(0,0) = 0, \quad \frac{\partial^2 \Phi}{\partial \beta^2}(0,0) = 0, \quad \frac{\partial^4 \Phi}{\partial \alpha^4}(0,0) = 0 \quad (2.47)$$

Since all odd derivatives are zero at the center of the plate owing to symmetry, these are not used in (2.47).

Using (2.39) and (2.47) results in a system of four linear algebraic equations, the solution of which yield the constants p_i . The values of these constants are then substituted into (2.43) to compute the dimensionless deflection function. The real deflections and moments can be calculated using (2.32). Results obtained from this technique are compared with accurate solutions (Timoshenko and Voinowsky-Krieger 1959) in Tables 2.3 and 2.4, and Figures (2.3) through (2.6). It can be seen that this approach provides reasonably good results for square plates and for long plates with high aspect ratios, but yields large discrepancies for intermediate aspect ratios.

TABLE 2.3. Calculation results for $k_1 = k_2 = 0$ (fixed supports) obtained using (2.47)

$\lambda = \frac{b}{a}$	$\nu(0, 0) \times 10^3$			$-M_0(1, 0) \times 10^2$		
	Exact Value	Decomp. Method	ε (%)	Exact Value	Decomp. Method	ε (%)
1.0	20.16	20.29	0.64	20.52	20.42	-0.49
1.1	24.00	23.74	-1.08	23.24	22.80	-1.89
1.2	27.52	26.75	-2.80	25.56	24.79	-3.01
1.3	30.56	29.30	-4.12	27.48	26.43	-3.82
1.4	33.12	31.42	-5.13	29.04	27.75	-4.44
1.5	35.20	33.16	-5.80	30.28	28.81	-4.85
1.6	36.80	34.59	-6.00	31.20	29.65	-4.97
1.7	38.08	35.75	-6.12	31.96	30.32	-5.13
1.8	39.20	36.70	-6.38	32.48	30.86	-4.99
1.9	39.84	37.48	-5.92	32.88	31.28	-4.87
2.0	40.64	38.12	-6.20	33.16	31.63	-4.61
∞	41.60	41.67	0.17	33.32	33.33	0.03

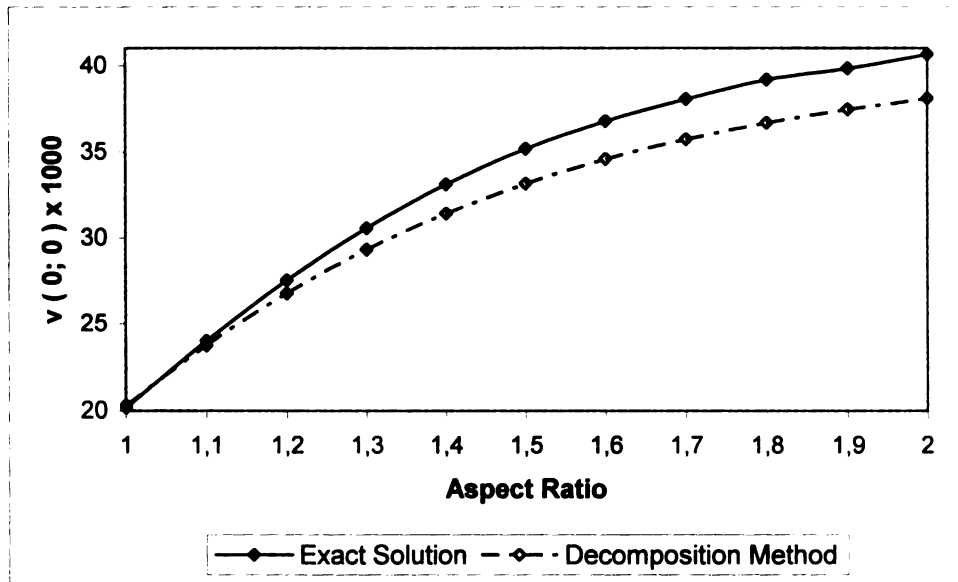


Figure 2.3. Maximum deflections at the middle of the plate obtained by (2.47) for $k_1 = k_2 = 0$ (fixed supports)

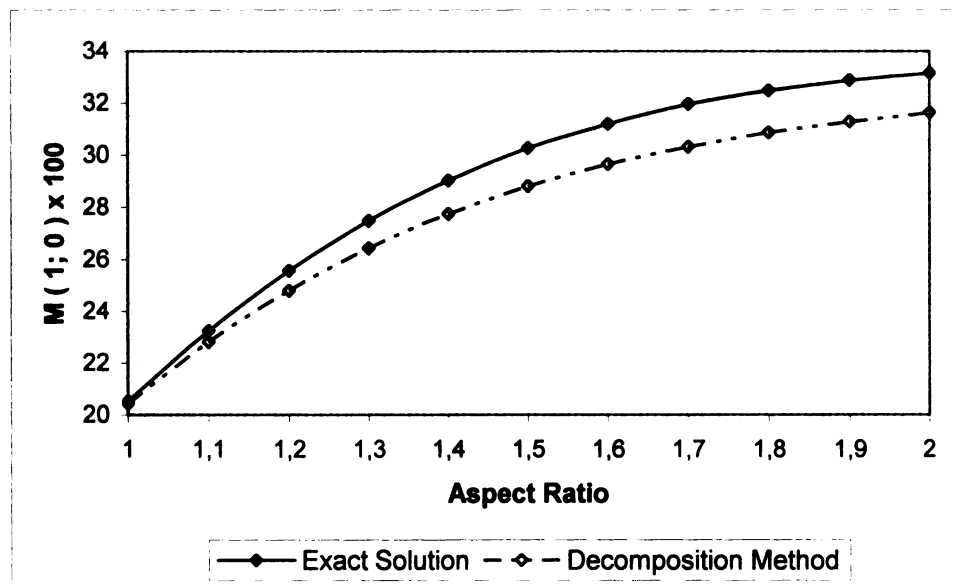


Figure 2.4. Maximum bending moments on the edge of the plate obtained by (2.47) for $k_1 = k_2 = 0$ (fixed supports)

TABLE 2.4 Calculation results for $k_1=k_2=1$ (pinned supports) obtained using (2.47)

$\lambda = \frac{b}{a}$	$v(0, 0) \times 10^2$			$M_0(0, 0) \times 10^2$		
	Exact Value	Decomp. Method	ε (%)	Exact Value	Decomp. Method	ε (%)
1.0	6.50	6.41	-1.38	19.16	18.97	-0.99
1.2	9.02	8.78	-2.66	25.08	26.24	4.62
1.4	11.28	10.88	-3.55	30.20	32.60	7.95
1.6	13.28	12.66	-4.67	34.48	37.88	9.86
1.8	14.90	14.12	-5.23	37.92	42.10	11.0
2.0	16.16	15.31	-5.26	40.80	45.40	11.3
3.0	19.52	18.62	-4.61	47.56	53.28	11.9
4.0	20.48	19.83	-3.17	49.40	54.77	10.9
5.0	20.80	20.33	-2.26	49.84	54.53	9.41
∞	20.80	20.80	0	50.00	50.57	0.01

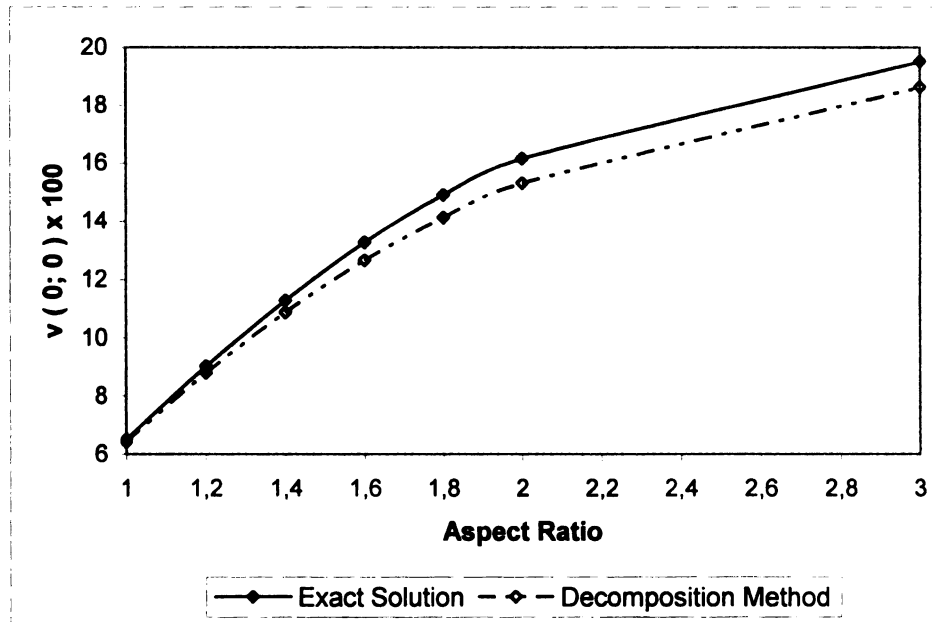


Figure 2.5. Maximum deflections at the middle of the plate obtained by (2.47)

for $k_1 = k_2 = 1$ (pinned supports)

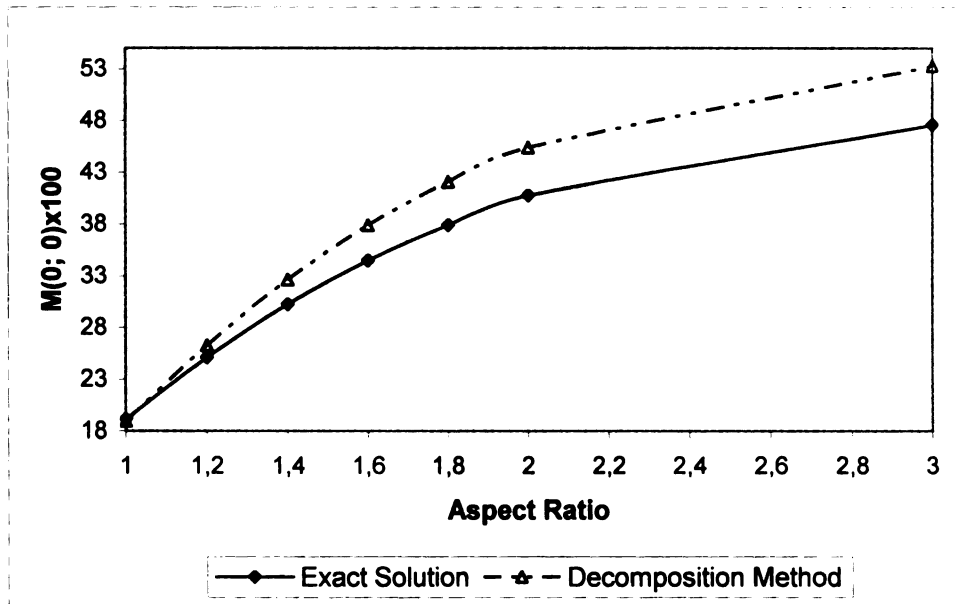


Figure 2.6. Maximum bending moments at the middle of the plate obtained by (2.47) for $k_1 = k_2 = 1$ (pinned supports)

Collocation Method with Multiple Points. The third approach is to obtain the equations for determining the unknown constants by equating the discrepancy function to zero at several collocation points. For the given symmetrical problem, only a quarter of the plate needs to be analyzed. For four equidistant collocation points, the linear algebraic equations can be solved to obtain p_1 , p_2 , p_3 , and p_4 :

$$\Phi(0,0)=0, \quad \Phi(0,0.5)=0, \quad \Phi(0.5,0)=0, \quad \Phi(0.5,0.5)=0 \quad (2.48)$$

Tables 2.5 and 2.6 show the results calculated for plates with fixed and pinned supports, respectively, for different aspect ratios. These results are also illustrated in Figures 2.7 through 2.11. The collocation method was used to obtain the results shown in these tables. The comparison of deflections and bending moments with exact solutions show the high accuracy of this method.

TABLE 2.5. Calculation results for $k_1 = k_2 = 0$ (fixed supports) obtained using (2.48)

$\lambda = \frac{b}{a}$	$\nu(0, 0) \times 10^3$			$M_0(0, 0)$			$M_0(1, 0)$		
	Exact Value	Decomp. Method	ε (%)	Exact Value	Decomp. Method	ε (%)	Exact Value	Decomp. Method	ε (%)
1.0	20.16	20.11	-0.25	9.24	9.14	-1.06	20.52	20.13	-1.88
1.1	24.00	23.96	-0.14	10.56	10.64	0.71	23.24	22.98	-1.11
1.2	27.52	27.41	-0.41	11.96	11.93	-0.23	25.56	25.41	-0.57
1.3	30.56	30.37	-0.62	13.08	13.02	-0.45	27.48	27.43	-0.20
1.4	33.12	32.86	-0.79	13.96	13.91	-0.34	29.04	29.05	0.03
1.5	35.20	34.91	-0.82	14.72	14.53	-1.28	30.28	30.34	0.19
1.6	36.80	36.58	-0.61	15.24	15.20	-0.24	31.20	31.34	0.46
1.7	38.08	37.92	-0.42	15.68	15.65	-0.17	31.96	32.12	0.49
1.8	39.20	38.99	-0.54	16.04	16.00	-0.22	32.48	32.71	0.70
1.9	39.84	39.84	0.00	16.28	16.28	-0.03	32.88	33.15	0.83
2.0	40.64	40.51	-0.32	16.48	16.48	0.02	33.16	33.49	0.98
∞	41.60	41.67	0.16	-	-	-	33.32	33.33	0.04

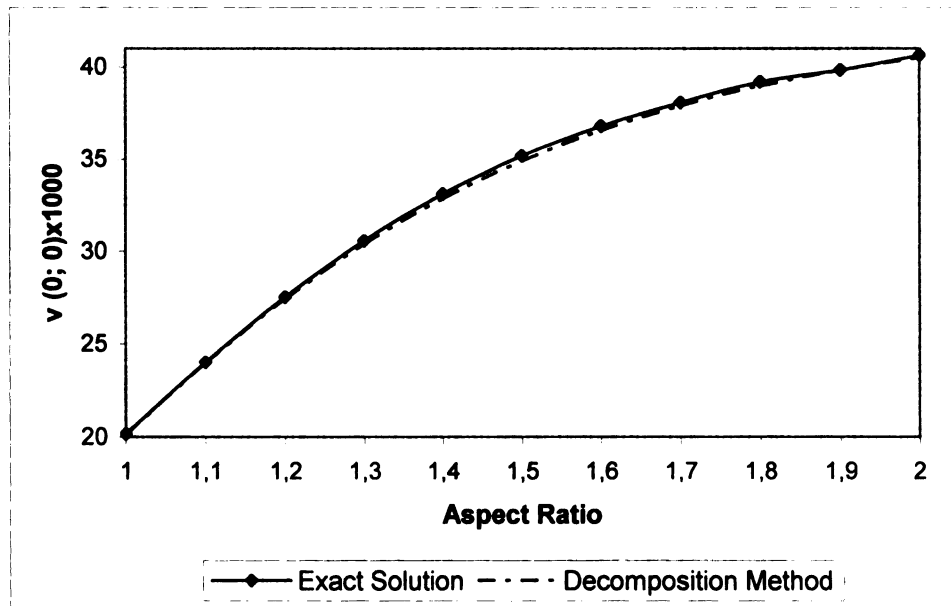
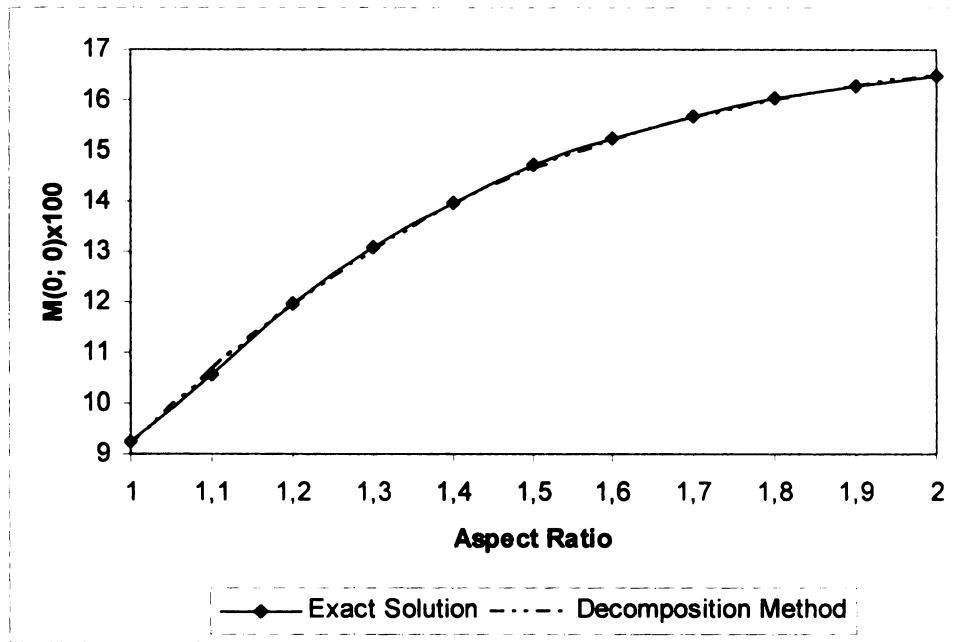
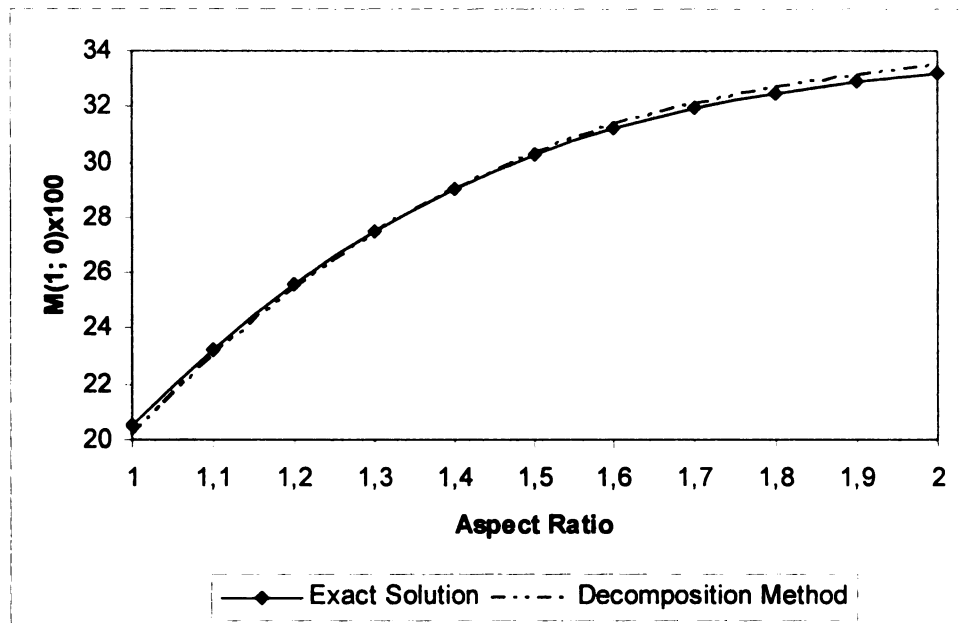


Figure 2.7. Maximum deflections at the middle of the plate obtained by (2.48)

for $k_1 = k_2 = 0$ (fixed supports)



**Figure 2.8. Maximum bending moments at the middle of the plate obtained by (2.48)
for $k_1 = k_2 = 0$ (fixed supports)**



**Figure 2.9. Maximum bending moments on the edge of the plate obtained by (2.48)
for $k_1 = k_2 = 0$ (fixed supports)**

TABLE 2.6. Calculation results for $k_1 = k_2 = 1$ (pinned supports) obtained using (2.48)

$\lambda = \frac{b}{a}$	$\nu(0, 0) \times 10^2$			$M_0(0, 0) \times 10^2$		
	Exact Value	Decomp. Method	ε (%)	Exact Value	Decomp. Method	ε (%)
1.0	6.50	6.41	-1.45	19.16	18.96	-1.07
1.2	9.02	8.91	-1.27	25.08	24.76	-1.28
1.4	11.28	11.15	-1.13	30.20	29.79	-1.34
1.6	13.28	13.06	-1.63	34.48	33.97	-1.49
1.8	14.90	14.64	-1.76	37.92	37.34	-1.53
2.0	16.16	15.91	-1.54	40.68	40.03	-1.60
3.0	19.52	19.33	-0.98	47.56	47.08	-1.02
4.0	20.48	20.45	-0.17	49.40	49.31	-0.19
5.0	20.80	20.82	0.11	49.84	50.04	0.41
∞	20.80	20.83	0.16	50.00	50.00	0.00

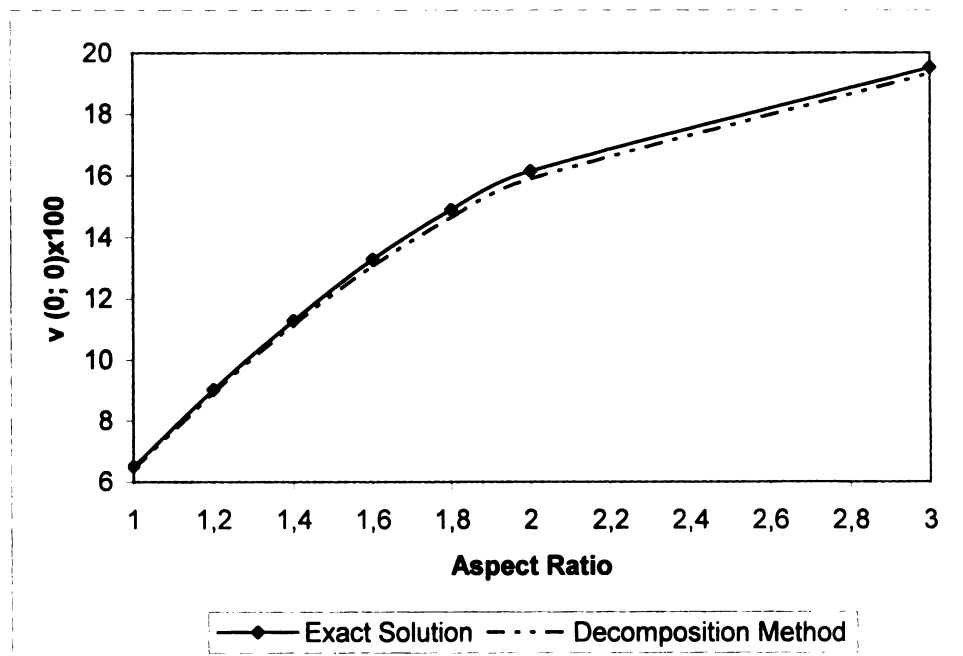


Figure 2.10. Maximum deflections at the middle of the plate obtained by (2.48)

for $k_1 = k_2 = 1$ (pinned supports)

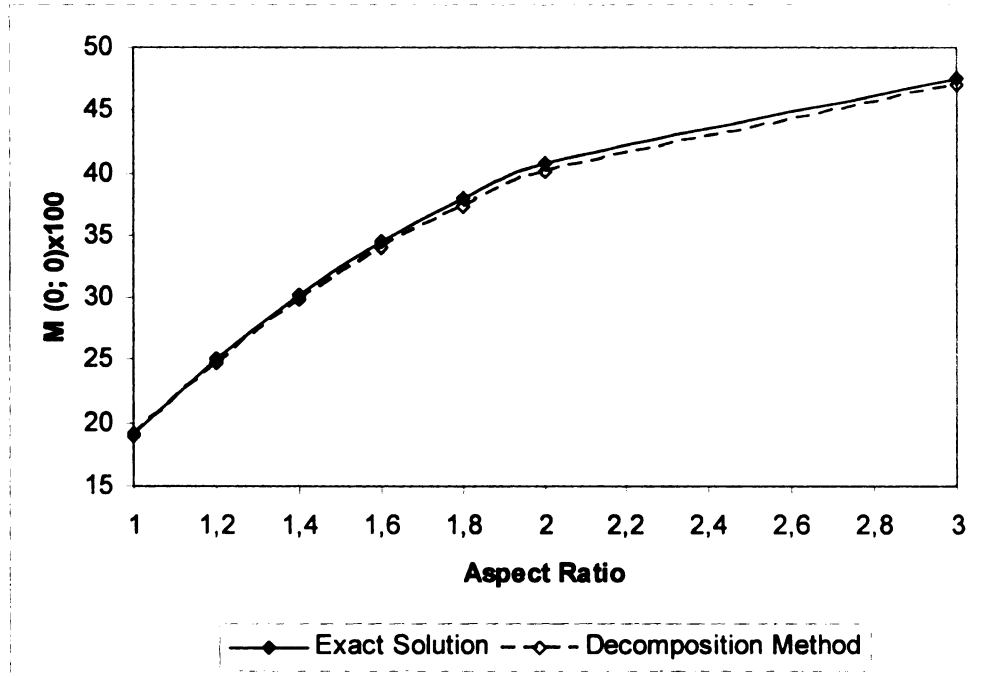


Figure 2.11. Maximum bending moments at the middle of the plate obtained by (2.48) for $k_1 = k_2 = 1$ (pinned supports)

2.3.4 Solution of the Problem for the Case of a Non-uniform Load

For the rectangular plate with pinned supports the boundary value problem has the form (2.35) and (2.36). Assume the load distribution function as

$$q(\alpha, \beta) = \cos \frac{n\pi\alpha}{2} \cos \frac{m\pi\beta}{2} \quad (2.49)$$

$$n, m = 1, 3, 5, \dots$$

The approximate solution of the problem has the form (2.43) with respect to (2.44). The arbitrary constants p_i are to be determined from the conditions (2.47). Using the

notations $\lambda_n = \frac{n\pi}{2}$, $\lambda_m = \frac{m\pi}{2}$, the values of the load function and its low even

derivatives at the central point of the plate are determined as

$$q(0,0) = 1, \quad \frac{\partial^2 q}{\partial \alpha^2}(0,0) = -\lambda_n^2, \quad \frac{\partial^2 q}{\partial \beta^2}(0,0) = -\lambda_m^2, \quad \frac{\partial^4 q}{\partial \alpha^4}(0,0) = -\lambda_n^4, \quad (2.50)$$

Using the expression (2.35) for discrepancy function and applying conditions (2.47) yields the system of four linear algebraic equations with four unknown constants. The resulting values of constants are then substituted into (2.43) to obtain the equation of the dimensionless deflection function.

The non-dimensional values of deflections and bending moments for the plates with different aspect ratios obtained from this technique are presented in the Table 2.7 and Figures 2.12 and 2.13. To estimate the accuracy, the solution by Timoshenko method was obtained. The comparison shows a reasonable accuracy of the proposed technique.

TABLE 2.7. Calculation results for rectangular plate under non-uniform load for $k_1=k_2=1$ (pinned supports) obtained using (2.47)

$\lambda = \frac{b}{a}$	$v(0,0) \times 10^2$			$M_0(0,0) \times 10^2$		
	Exact Value	Decomp. Method	ε (%)	Exact Value	Decomp. Method	ε (%)
1.0	4.11	4.16	1.2	10.1	10.2	1.0
1.2	5.72	5.68	-0.7	18.3	18.3	0.0
1.4	7.20	7.09	-1.5	23.1	22.8	-1.2
1.6	8.49	8.28	-2.5	27.2	26.8	-1.8
1.8	9.59	9.32	-2.8	30.8	30.1	-2.0
2.0	10.5	10.2	-2.8	33.7	32.9	-2.1
3.0	13.3	12.8	-3.3	42.7	41.9	-1.9
4.0	14.5	14.1	-3.2	46.6	46.1	-1.2
5.0	15.2	14.7	-3.1	48.7	48.4	-0.7
10.0	16.1	15.7	-2.6	51.6	52.0	0.6

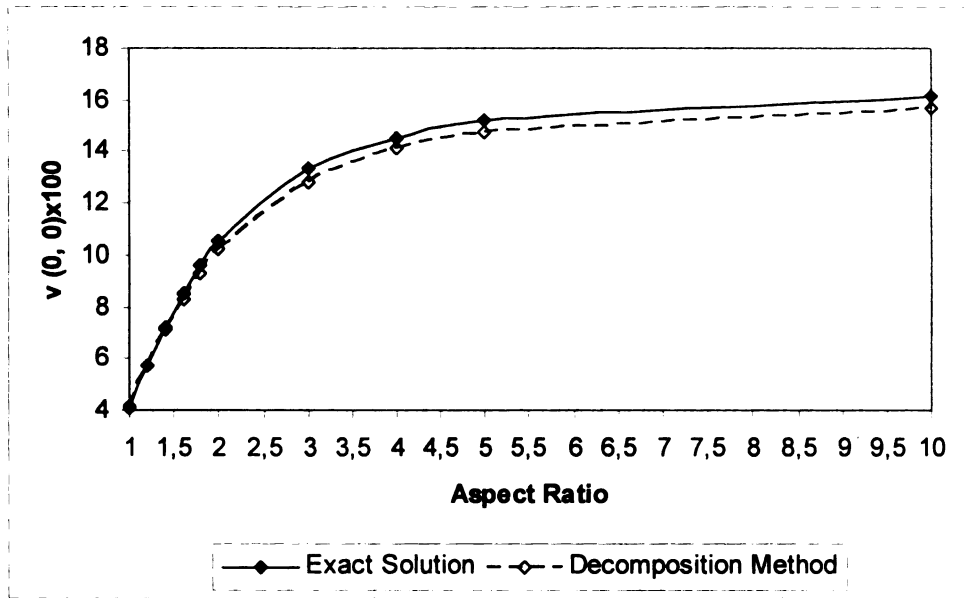


Figure 2.12. Deflections at the middle of the plate under non-uniform load for $k_1 = k_2 = 1$ (pinned supports) obtained using (2.47)

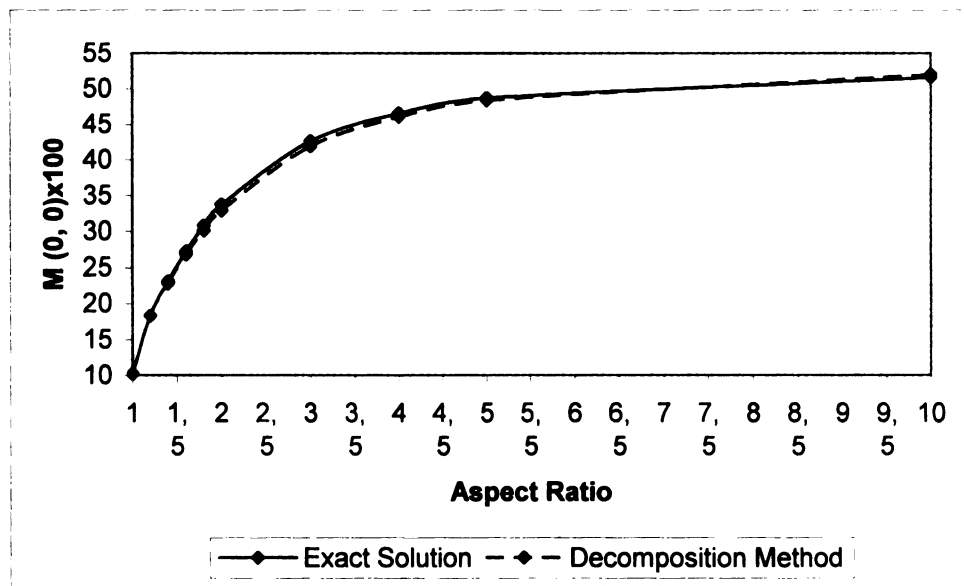


Figure 2.13. Bending moments at the middle of the plate under non-uniform load for $k_1 = k_2 = 1$ (pinned supports) obtained using (2.47)

2.4 Bending of Rectangular Plate with One Free Edge and Three Elastically Supported Edges

The transverse bending of a thin isotropic rectangular plate with one free edge and elastic supports along the three other edges is investigated (Figure 2.14). The load is assumed to be uniformly distributed.

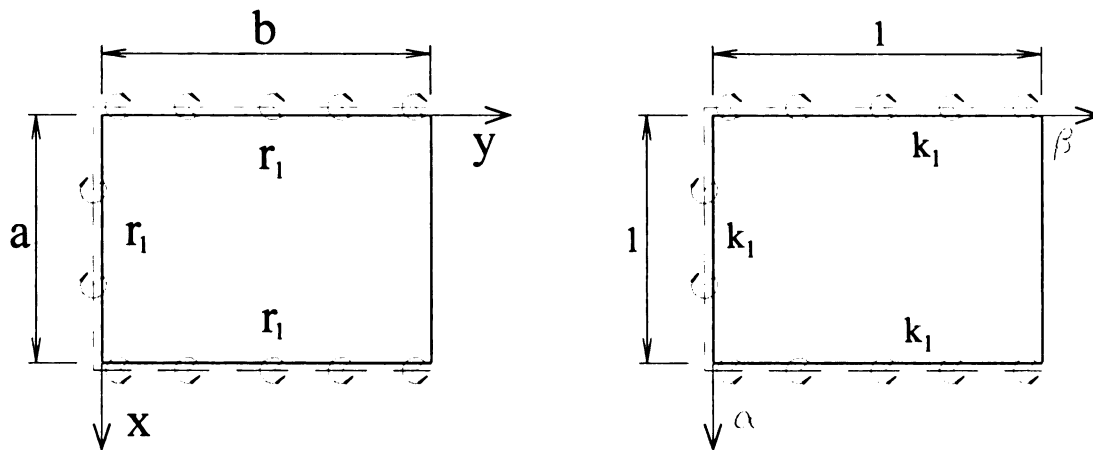


Figure 2.14. Rectangular plate with one free edge

2.4.1 Problem Statement

The problem is stated in the non-dimensional form with respect to notations (2.10). Assume that the edges $\alpha = 0$, $\alpha = 1$, and $\beta = 0$ are supported elastically, and the edge $\beta = 1$ is free. In this case the boundary value problem can be written as

$$\frac{\partial^4 v}{\partial \alpha^4} + \frac{2}{\lambda^2} \frac{\partial^4 v}{\partial \alpha^2 \partial \beta^2} + \frac{1}{\lambda^4} \frac{\partial^4 v}{\partial \beta^4} = 1 \quad (2.51)$$

$$v = 0, \quad k_1 \frac{\partial^2 v}{\partial \alpha^2} \pm (1 - k_1) \frac{\partial v}{\partial \alpha} = 0 \quad (\alpha = 0, \quad \alpha = 1) \quad (2.52a)$$

$$v = k_1 \frac{\partial^2 v}{\partial \beta^2} - (1 - k_1) \frac{\partial v}{\partial \beta} = 0 \quad (\beta = 0) \quad (2.52b)$$

$$V_\beta = - \left[\frac{(2 - \mu)}{\lambda} \frac{\partial^3 v}{\partial \alpha^2 \partial \beta} + \frac{1}{\lambda^3} \frac{\partial^3 v}{\partial \beta^3} \right] = 0 \quad (2.52c)$$

$$M_\beta = - \left[\frac{1}{\lambda^2} \frac{\partial^2 v}{\partial \beta^2} + \mu \frac{\partial^2 v}{\partial \alpha^2} \right] = 0 \quad (\beta = 1)$$

2.4.2 Decomposition of the problem

The boundary value problem characterized by (2.51) and (2.52) is solved by the decomposition method using three auxiliary problems. The first auxiliary problem (boundary value problem) is to find the solution to the differential equation

$$\frac{\partial^4 v_1}{\partial \alpha^4} = f_1(\alpha, \beta) \quad (2.53)$$

subject to the conditions (2.52a), where $v = v_1$:

$$v_1 = k_1 \frac{\partial^2 v_1}{\partial \alpha^2} \pm (1 - k_1) \frac{\partial v_1}{\partial \alpha} = 0 \quad (\alpha = 0, \quad \alpha = 1) \quad (2.54)$$

The second auxiliary problem (boundary value problem) is to find the solution to the differential equation

$$\frac{\partial^4 v_2}{\partial \beta^4} = f_2(\alpha, \beta) \quad (2.55)$$

subject to the conditions (2.52b) and (2.52c):

$$v_2 = k_1 \frac{\partial^2 v_2}{\partial \beta^2} - (1 - k_1) \frac{\partial v_2}{\partial \beta} = 0 \quad (\beta = 0) \quad (2.56a)$$

$$V_\beta = - \left[\frac{(2 - \mu)}{\lambda} \frac{\partial^2 v_1}{\partial \alpha^2} \frac{\partial v_2}{\partial \beta} + \frac{1}{\lambda^3} \frac{\partial^3 v_2}{\partial \beta^3} \right] = 0 \quad (2.56b)$$

$$M_\beta = - \left[\frac{1}{\lambda^2} \frac{\partial^2 v_2}{\partial \beta^2} + \mu \frac{\partial^2 v_1}{\partial \alpha^2} \right] = 0 \quad (\beta = 1)$$

Note that boundary conditions (2.56b) now include the derivatives of the deflection function in both directions. For this case it is more convenient to use the “weaker” form of the boundary conditions. To obtain it, the summation of work done by tractions along the edge $\beta = 1$ is set equal to zero:

$$U_V = \frac{(2 - \mu)}{\lambda} \frac{\partial v_2}{\partial \beta} \int_0^1 \frac{\partial^2 v_1}{\partial \alpha^2} v_1 d\alpha + \frac{1}{\lambda^3} \frac{\partial^3 v_2}{\partial \beta^3} \int_0^1 v_1 d\alpha = 0 \quad (2.56c)$$

$$U_M = \frac{1}{\lambda^2} \frac{\partial^2 v_2}{\partial \beta^2} \int_0^1 \frac{\partial v_1}{\partial \alpha} d\alpha + \mu \int_0^1 \frac{\partial^2 v_1}{\partial \alpha^2} \frac{\partial v_1}{\partial \alpha} d\alpha = 0 \quad (\beta = 1)$$

The third auxiliary problem (solution of the interconnection differential equation) is

$$\Phi(\alpha, \beta) \equiv \frac{2}{\lambda^2} \frac{\partial^4 v_3}{\partial \alpha^2 \partial \beta^2} + f_1(\alpha, \beta) + \frac{1}{\lambda^4} f_2(\alpha, \beta) - 1 = 0 \quad (2.57)$$

Note that solutions of the auxiliary problems must satisfy the condition

$$v = v_1 = v_2 = v_3 \quad (2.58)$$

The approximating functions are taken in the following forms:

$$f_1(\alpha, \beta) = f_1(\beta), \quad f_2(\alpha, \beta) = \beta f_2(\alpha) + \beta^2 f_3(\alpha) + \beta^3 f_4(\alpha) \quad (2.59)$$

where $f_i(t)$, $i = 1, \dots, 4$, are arbitrary functions of the arguments α and β .

The solution of the first boundary value problem has the form

$$v_1 = \frac{1}{24} \left[\alpha^4 - 2\alpha^3 - 2(-1 + k_1)/(1 + k_1)\alpha^2 + 2k_1\alpha/(1 + k_1) \right] f_1(\beta) \quad (2.60)$$

Consider the second auxiliary problem. Integration of the differential equation (2.55) yields

$$\begin{aligned} v_2 = & f_2(\alpha) \left(\frac{1}{120} \beta^5 + \frac{\beta^3}{6} C_3 + \frac{\beta^2}{2} C_2 + \beta C_1 + C_0 \right) \\ & + f_3(\alpha) \left(\frac{1}{360} \beta^6 + \frac{\beta^3}{6} C_7 + \frac{\beta^2}{2} C_6 + \beta C_5 + C_4 \right) \\ & + f_4(\alpha) \left(\frac{1}{840} \beta^7 + \frac{\beta^3}{6} C_{11} + \frac{\beta^2}{2} C_{10} + \beta C_9 + C_8 \right) \end{aligned} \quad (2.61)$$

where C_i , $i = 1, \dots, 11$, are the integration constants depending on the values of λ (the aspect ratio of the plate) and k_1 (the dimensionless stiffness coefficient of the elastic supports).

These constants are found by satisfying the boundary conditions (2.56a) and (2.56c). The expressions for C_i are obtained using the Maple computer algebra system, and are given in Appendix A.

Satisfying condition $v_1 = v_2$ from (2.58) yields:

$$\begin{aligned} f_1(\beta) &= p_1 \psi_1^{(2)}(\beta) + p_2 \psi_2^{(2)}(\beta) + p_3 \psi_3^{(2)}(\beta) \\ f_2(\alpha) &= f_3(\alpha) = f_4(\alpha) = \frac{1}{24} \psi_1^{(1)}(\alpha) \end{aligned} \quad (2.62)$$

where

$$\psi_1^{(1)}(\alpha) = \alpha^4 - 2\alpha^3 - 2(-1 + k_1)/(1 + k_1)\alpha^2 + 2k_1\alpha/(1 + k_1)$$

$$\psi_1^{(2)}(\beta) = \frac{1}{120}\beta^5 + \frac{\beta^3}{6}C_3 + \frac{\beta^2}{2}C_2 + \beta C_1 + C_0$$

$$\psi_2^{(2)}(\beta) = \frac{1}{360}\beta^6 + \frac{\beta^3}{6}C_7 + \frac{\beta^2}{2}C_6 + \beta C_5 + C_4 \quad (2.63)$$

$$\psi_3^{(2)}(\beta) = \frac{1}{840}\beta^7 + \frac{\beta^3}{6}C_{11} + \frac{\beta^2}{2}C_{10} + \beta C_9 + C_8$$

The expression for the deflection function can now be written as

$$v_1 = v_2 = \frac{1}{24}\psi_1^{(1)}(\alpha) \left(p_1 \psi_1^{(2)}(\beta) + p_2 \psi_2^{(2)}(\beta) + p_3 \psi_3^{(2)}(\beta) \right) \quad (2.64)$$

where p_1 , p_2 , and p_3 are arbitrary constants that are to be determined from the third auxiliary problem with respect to the conditions in (2.58).

Substituting the expression (2.64) into (2.57) and using (2.63) yields

$$\begin{aligned} \Phi(\alpha, \beta) = & p_1 \left[\psi_1^{(2)}(\beta) + \frac{1}{12\lambda^2} \psi_1^{(1)''}(\alpha) \psi_1^{(2)''}(\beta) \right] \\ & + p_2 \left[\psi_2^{(2)}(\beta) + \frac{1}{12\lambda^2} \psi_1^{(1)''}(\alpha) \psi_1^{(2)''}(\beta) \right] \\ & + p_3 \left[\psi_3^{(2)}(\beta) + \frac{1}{12\lambda^2} \psi_1^{(1)''}(\alpha) \psi_2^{(2)''}(\beta) \right] \\ & + \frac{1}{24\lambda^4} \psi_1^{(1)''}(\alpha) (\beta + \beta^2 + \beta^3) - 1 = 0 \end{aligned} \quad (2.65)$$

An overdefined point collocation method is used for the solution of this problem, with 90 collocation points spaced equidistantly over the surface of the plate. For each point the following condition is applied:

$$\int_0^1 \int_0^1 \Phi(\alpha, \beta) W_i d\alpha d\beta = 0 \quad (2.66)$$

$$W_i = \delta(\alpha - \alpha_i, \beta - \beta_i), \quad i = 1, 2, \dots, K, K, K, N$$

where δ is Dirac delta-function, and (α_i, β_i) are coordinates of the collocation points.

The constants p_1, p_2 and p_3 are obtained as the least-square solution of the resulting overdefined system of linear algebraic equations. The dimensionless deflection function is determined using (2.64), and the real deflections and bending moments are calculated using the expressions in (2.32).

2.4.3 Numerical results

Test results were obtained from the decomposition method for an isotropic rectangular plate with different aspect ratios under the uniformly distributed load and compared with available accurate solutions (Timoshenko and Voinowsky-Krieger 1959) and finite element solutions. The finite element analysis was performed using the LIRA software (Kiev, 2000). A refined mesh of quadrilateral finite elements was used to achieve convergent solutions. All dimensional values of deflections obtained by the finite element method were converted into non-dimensional form. Calculation results are presented in Tables 2.8 through 2.12 and in Figures 2.14 through 2.18.

TABLE 2.8. Maximum deflection of the free edge for $k_I=1$ (pinned supports)

$\lambda = \frac{b}{a}$	$\nu(0.5; 1) \times 10^3$					
	Timoshenko solution	FEM	ε (%)	Decomp. method DM	ε (%)	ε (%) DM/ FEM
0.5	7.1	7.09	-0.14	717	1.02	1.11
0.67	9.68	9.68	0.00	9.79	1.13	1.14
0.71	10.23	10.28	0.49	10.40	1.65	1.11
0.77	10.92	10.91	-0.09	11.03	0.98	1.03
0.83	11.58	11.56	-0.17	11.67	0.75	0.93
0.91	12.32	12.21	-0.89	12.30	-0.13	0.80
1.0	12.86	12.85	-0.08	12.93	0.51	0.59
1.1	13.41	13.39	-0.15	13.46	0.38	0.51
1.2	13.84	13.82	-0.14	13.88	0.25	0.40
1.3	14.17	14.15	-0.15	14.20	0.19	0.34
1.4	14.42	14.40	-0.13	14.45	0.19	0.33
1.5	14.62	14.59	-0.18	14.65	0.18	0.37
2.0	15.07	15.05	-0.14	15.24	1.12	1.25

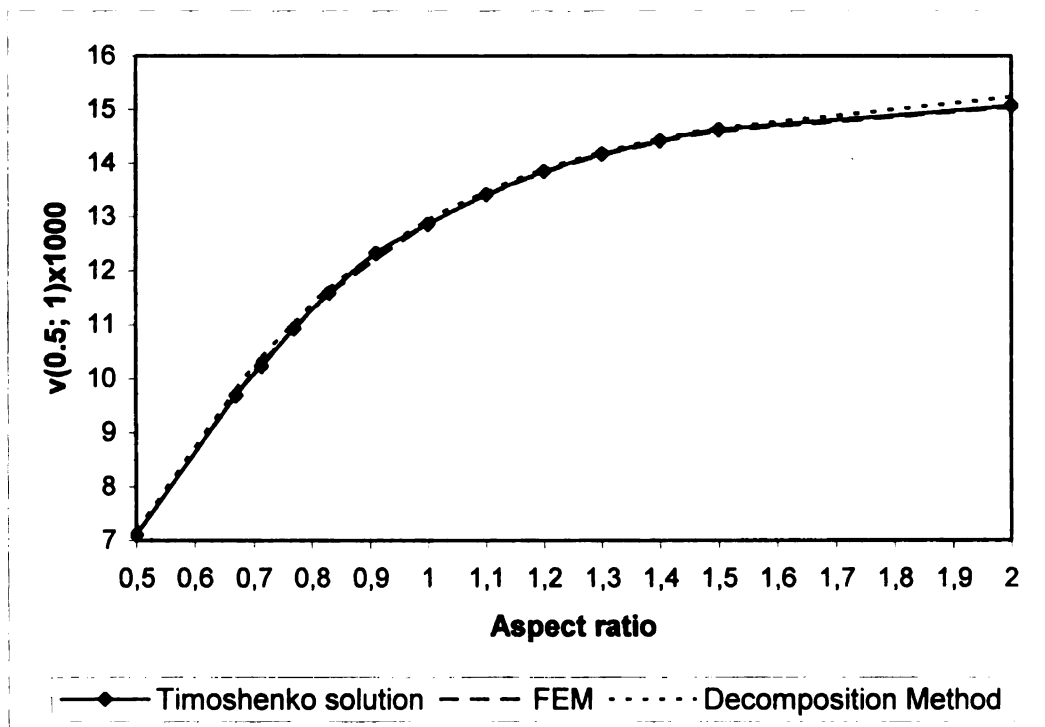


Figure 2.14. Maximum deflection of the free edge for $k_I=1$ (pinned supports)

TABLE 2.9. Deflection at the middle of the plate for $k_I=1$ (pinned supports)

$\lambda = \frac{b}{a}$	$\nu(0.5; 0.5) \times 10^3$		
	FEM	Decomp. method DM	ε (%) DM vs. FEM
0.5	3.81	3.87	1.57
0.67	5.43	5.53	1.77
0.71	5.82	5.96	2.43
0.77	6.31	6.42	1.74
0.83	6.81	6.92	1.70
0.91	7.35	7.47	1.64
1.0	7.94	8.06	1.57
1.1	8.51	8.64	1.52
1.2	9.02	9.15	1.50
1.3	9.47	9.61	1.49
1.4	9.87	10.02	1.50
1.5	10.22	10.38	1.53
2.0	11.50	11.69	1.65

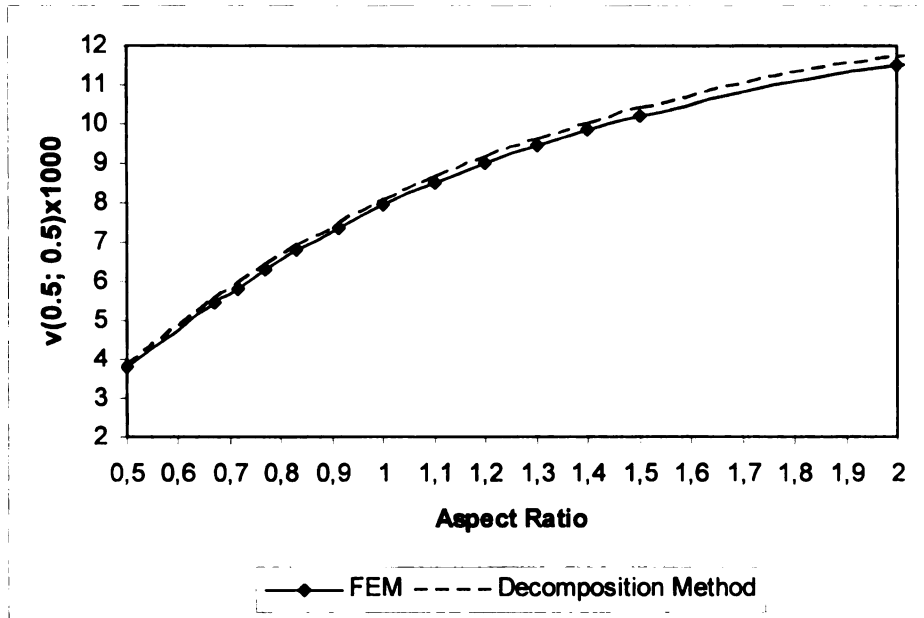


Figure 2.15. Deflection at the middle of the plate for $k_I=1$ (pinned supports)

TABLE 2.10. Maximum bending moment for $k_I=1$ (pinned supports)

$\lambda = \frac{b}{a}$	M (0.5; 1) × 10²		
	Timoshenko solution	Decomp. method DM	ε (%)
0.5	6.0	6.25	4.16
0.67	8.3	8.53	2.75
0.71	8.8	9.06	2.94
0.77	9.4	9.61	2.20
0.83	10.0	10.16	1.63
0.91	10.7	10.72	0.18
1.0	11.2	11.26	0.54
1.1	11.7	11.73	0.23
1.2	12.1	12.09	-0.10
1.3	12.4	12.37	-0.26
1.4	12.6	12.59	-0.11
1.5	12.8	12.76	-0.31
2.0	13.2	13.27	0.53

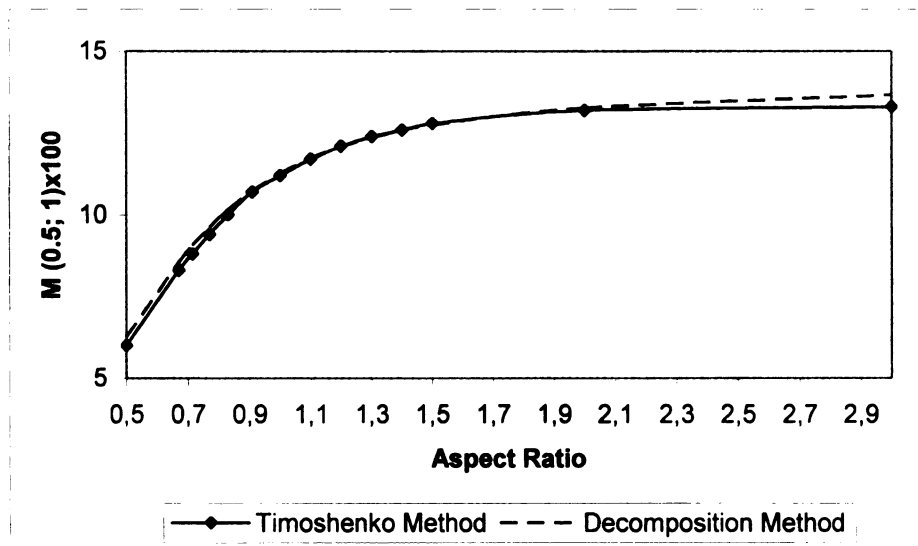


Figure 2.16. Maximum bending moment for $k_I=1$ (pinned supports)

TABLE 2.11. Maximum deflection of the free edge for $k_l=0$ (fixed supports)

$\lambda = \frac{b}{a}$	$v(0.5; 1) \times 10^4$		
	FEM	Decomp. method	ε (%) DM vs FEM
0.6	22.24	22.10	0.63
0.7	24.88	24.65	0.92
0.8	26.44	26.16	1.06
0.9	27.27	26.97	1.10
1.0	27.66	27.33	1.19
1.25	27.78	27.34	1.58
1.5	27.55	27.06	1.78

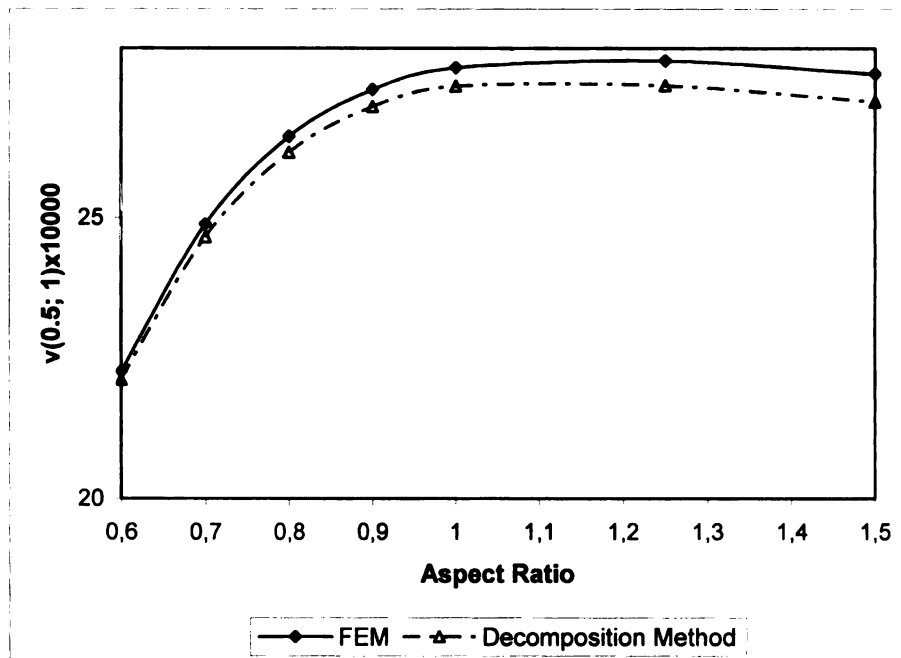


Figure 2.17. Maximum deflection of the free edge for $k_l=0$ (fixed supports)

TABLE 2.12. Deflection at the middle of the plate for $k_I=0$ (fixed supports)

$\lambda = \frac{b}{a}$	$v(0.5; 0.5) \times 10^4$			
	FEM	Decomp. method DM	ε (%)	ε (%) DM vs FEM
0.6	10.89	10.90	15.5	0.16
0.7	13.34	13.27	16.5	-0.48
0.8	15.48	15.35	17.0	-0.85
0.9	17.35	17.19	17.8	-0.95
1.0	18.96	18.82	18.2	-0.76
1.25	22.01	22.14	17.7	0.59
1.5	25.32	24.53	15.4	-3.12

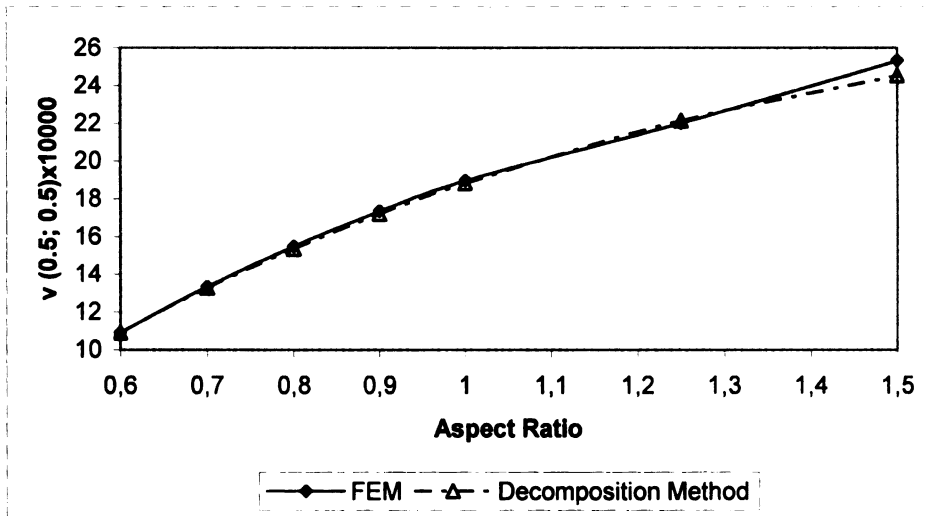


Figure 2.18. Deflection at the middle of the plate for $k_I=0$ (fixed supports)

Percentage errors are reported in the tables for comparisons between the decomposition method and the Timoshenko solution, the FEM and the Timoshenko solution, and the decomposition method and the FEM. The results clearly demonstrate

that the collocation form of the decomposition method yields accurate analytical dependencies for displacements and force responses. The proposed technique is easy for computer implementation. Depending on the point where the solution is sought one can use a different distribution and density of collocation points.

2.5 Transverse Free Vibration of a Plate with Elastic Supports

Consider an isotropic elastic rectangular plate of constant thickness shown in Figure 2.1. The differential equation governing the transverse free vibration of the plate is

$$\frac{\partial^4 w}{\partial x^4} + 2 \frac{\partial^4 w}{\partial x^2 \partial y^2} + \frac{\partial^4 w}{\partial y^4} = \frac{\rho h \omega^2}{D} \quad (2.67)$$

where ω = circular natural frequency of free vibration, w = transverse displacement, ρ = mass density, h = plate thickness, and D = flexural rigidity of the plate.

Using the dimensionless stiffness coefficients of elastic supports (2.11); the boundary conditions can be written in the form:

$$\begin{aligned} w = 0, \quad k_1 a \frac{\partial^2 w}{\partial x^2} - (1 - k_1) \frac{\partial w}{\partial x} &= 0 \quad (x = 0) \\ w = 0, \quad k_2 a \frac{\partial^2 w}{\partial x^2} + (1 - k_2) \frac{\partial w}{\partial x} &= 0 \quad (x = a) \\ w = 0, \quad k_3 b \frac{\partial^2 w}{\partial y^2} - (1 - k_3) \frac{\partial w}{\partial y} &= 0 \quad (y = 0) \\ w = 0, \quad k_4 b \frac{\partial^2 w}{\partial y^2} + (1 - k_4) \frac{\partial w}{\partial y} &= 0 \quad (y = b) \end{aligned} \quad (2.68)$$

The homogeneous equation (2.67) and the homogeneous boundary conditions (2.68) represent an eigenvalue problem, and the lowest value of ω which provides a non-trivial solution is the fundamental natural frequency of the plate.

Using the decomposition method, the solution w is sought in terms of three components w_1 , w_2 , and w_3 that constitute the unknowns in three auxiliary problems.

The first problem is

$$\frac{\partial^4 w_1}{\partial x^4} = f_1(x, y) \quad (2.69)$$

subject to the boundary conditions

$$\begin{aligned} w_1 = 0, \quad k_1 a \frac{\partial^2 w_1}{\partial x^2} - (1 - k_1) \frac{\partial w_1}{\partial x} = 0 \quad (x = 0) \\ w_1 = 0, \quad k_2 a \frac{\partial^2 w_1}{\partial x^2} + (1 - k_2) \frac{\partial w_1}{\partial x} = 0 \quad (x = a) \end{aligned} \quad (2.70)$$

The second auxiliary problem is

$$\frac{\partial^4 w_2}{\partial y^4} = f_2(x, y) \quad (2.71)$$

subject to the boundary conditions

$$\begin{aligned} w_2 = 0, \quad k_3 b \frac{\partial^2 w_2}{\partial y^2} - (1 - k_3) \frac{\partial w_2}{\partial y} = 0 \quad (y = 0) \\ w_2 = 0, \quad k_4 b \frac{\partial^2 w_2}{\partial y^2} + (1 - k_4) \frac{\partial w_2}{\partial y} = 0 \quad (y = b) \end{aligned} \quad (2.72)$$

The third auxiliary problem is

$$\Phi(\alpha, \beta) \equiv 2 \frac{\partial^4 w_3}{\partial x^2 \partial y^2} - \frac{\rho h \omega^2}{D} w_3 + f_1(x, y) + f_2(x, y) = 0 \quad (2.73)$$

where $\Phi(\alpha, \beta)$ is the discrepancy function.

To find the approximate solution to the original problem, it is assumed that

$$w_1 = w_2 = w_3 \quad (2.74)$$

and the functions $f_1(x, y)$ and $f_2(x, y)$ are

$$\begin{aligned} f_1(x, y) &= f_1(y) \\ f_2(x, y) &= f_2(x) \end{aligned} \quad (2.75)$$

Integrating (2.69) four times and satisfying the boundary conditions (2.70) yields

$$\begin{aligned} w_1 = \frac{f_1(y)}{72} \left\{ 3x^4 - \frac{2}{R_{12}(1+k_2)} \cdot [2R_{12}(1+2k_2) + (1-k_1k_2)(1+5k_2)] ax^3 \right. \\ \left. + \frac{3(1+5k_2)}{R_{12}} [(1-k_1)a^2 x^2 + 2k_1 a^3 x] \right\} \end{aligned} \quad (2.76)$$

where $R_{12} = 1 + 3(k_1 + k_2) + 5k_1k_2$. Similarly, the solution to the second auxiliary problem (2.71) and (2.72) is

$$\begin{aligned} w_2 = \frac{f_2(x)}{72} \left\{ 3y^4 - \frac{2}{R_{34}(1+k_4)} \cdot [2R_{34}(1+2k_4) + (1-k_3k_4)(1+5k_4)] by^3 \right. \\ \left. + \frac{3(1+5k_4)}{R_{34}} [(1-k_3)b^2 y^2 + 2k_3 b^3 y] \right\} \end{aligned} \quad (2.77)$$

where $R_{34} = 1 + 3(k_3 + k_4) + 5k_3k_4$.

To satisfy (2.74), $f_1(y)$ and $f_2(x)$ must be proportional to the quantities in braces in (2.76) and (2.77), respectively, and hence

$$w_1 = w_2 = \frac{c}{72} \varphi(x) \varphi(y) \quad (2.78)$$

where

$$\begin{aligned} \varphi(x) = & 3x^4 - \frac{2}{R_{12}(1+k_2)} \cdot [2R_{12}(1+2k_2) + (1-k_1k_2)(1+5k_2)] ax^3 \\ & + \frac{3(1+5k_2)}{R_{12}} [(1-k_1)a^2 x^2 + 2k_1 a^3 x] \end{aligned} \quad (2.79)$$

$$\begin{aligned} \varphi(y) = & 3y^4 - \frac{2}{R_{34}(1+k_4)} \cdot [2R_{34}(1+2k_4) + (1-k_3k_4)(1+5k_4)] by^3 \\ & + \frac{3(1+5k_4)}{R_{34}} [(1-k_3)b^2 y^2 + 2k_3 b^3 y] \end{aligned} \quad (2.80)$$

Setting $w_3 = w_1$ and using the Bubnov-Galerkin method with (2.73) yields:

$$\iint_{00}^{ba} \left[2 \frac{\partial^4 w_1}{\partial x^2 \partial y^2} - \frac{\rho h \omega^2}{D} w_1 + f_1(y) + f_2(x) \right] w_1 dx dy = 0 \quad (2.81)$$

Integrating (2.81) yields the expression for square of the first natural frequency of the plate

$$\frac{\rho h \omega^2}{D} = \frac{504 R_{12} G_{12}}{a^4 F_{12}} + \frac{288 H_{12} H_{34}}{a^2 b^2 F_{12} F_{34}} + \frac{504 R_{34} G_{34}}{b^4 F_{34}}, \quad (2.82)$$

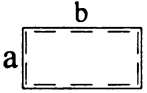
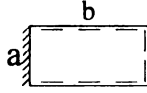
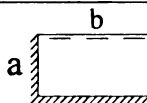
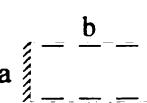
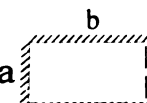
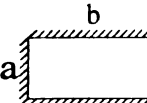
where $R_{12}, R_{34}, G_{12}, G_{34}, H_{12}, H_{34}, F_{12},$ and F_{34} have the same values as in (2.31).

Formula (2.82) is symmetric with respect to coefficients k_i and the side lengths a and b , and yields the following dimensionless parameter proportional to the lowest natural frequency:

$$P = \omega b^2 \sqrt{\frac{\rho h}{D}} \quad (2.83)$$

Expressions for P obtained for the six possible combinations of fixed ($k = 0$) and pinned ($k = 1$) supports for the plate are given in Table 2.13. Comparison of the results with exact solutions (Umansky 1973) shows that the error in (2.83) does not exceed 0.5%, and confirms the high accuracy of the decomposition method.

TABLE 2.13. Expressions for P for different types of supports

Boundary Conditions	$P = \omega b^2 \sqrt{\rho h/D}$		Maximum Error	
	Decomposition Method	Exact Solution	ε (%)	Location λ
	$9.88(1 + \lambda^2)$	$9.87(1 + \lambda^2)$	0.1	All values
	$9.88\sqrt{1 + 2.30\lambda^2 + 2.45\lambda^4}$	$9.87\sqrt{1 + 2.33\lambda^2 + 2.44\lambda^4}$	0.1	0
	$15.45\sqrt{1 + 1.08\lambda^2 + \lambda^4}$	$15.42\sqrt{1 + 1.12\lambda^2 + \lambda^4}$	0.5	1
	$9.88\sqrt{1 + 2.43\lambda^2 + 5.17\lambda^4}$	$9.87\sqrt{1 + 2.49\lambda^2 + 5.14\lambda^4}$	0.2	0.57
	$22.45\sqrt{1 + 0.54\lambda^2 + 0.47\lambda^4}$	$22.37\sqrt{1 + 0.57\lambda^2 + 0.47\lambda^4}$	0.4	1.21
	$22.45\sqrt{1 + 0.57\lambda^2 + \lambda^4}$	$22.37\sqrt{1 + 0.61\lambda^2 + \lambda^4}$	0.4	1

Notations: $\lambda = b/a$,  fixed support,  pinned support

CHAPTER 3

STATIC AND DYNAMIC ANALYSIS OF SINGLE LAYER LATTICE PLATES: CONTINUUM MODELING AND SOLUTION BY THE DECOMPOSITION METHOD

3.1 Calculation Model of Single Layer Lattice Plate

In order to compute the responses of single layer lattice plates, a continuum model based on the theory of lattice plates and shells by Pshenichnov (1993) is used. Constitutive equations of the model that are based on the lattice structure and material are obtained by relating force and deformation characteristics of the rods that constitute the lattice plate to those of the continuum model. In this work all members of the lattice plate are assumed to lie in a single plane. While a continuum model can be developed for lattice plates constructed of 3-D trusses, such a model would need to include shear deformations. Flexibility of joints in the lattice plate is neglected. Joint flexibility can be approximately accounted for in a continuum model by a shear deformable plate. This is beyond the scope of this work.

Figure 3.1 illustrates a single layer lattice plate with n families of rods. The position of the axes of the i^{th} family of rods ($1 \leq i \leq n$) is characterized by the angle φ_i measured from the x -axis to the y -axis.

A rod's deformation is assumed to be equal to that of the mid-surface in the continuum model. Using the transformation relations for the components of deformation

in the theory of elasticity, the following expressions are obtained for the components of deformation of the axis of the i^{th} family of rods:

$$\kappa_i^* = \kappa_1 c_i^2 + \kappa_2 s_i^2 + \kappa_{12} \sin 2\varphi_i, \quad \theta_i^* = s_i c_i (\kappa_2 - \kappa_1) + \kappa_{12} \cos 2\varphi_i \quad (3.1)$$

where $s_i = \sin \varphi_i$, $c_i = \cos \varphi_i$, $\kappa_1 = -\partial^2 w / \partial x^2$, $\kappa_2 = -\partial^2 w / \partial y^2$,

and $\kappa_{12} = -\partial^2 w / (\partial x \partial y)$ are bending and twisting curvatures of the plate's mid-surface,

and κ_i^* and θ_i^* are the curvature and twist angle of the i^{th} family of rods.

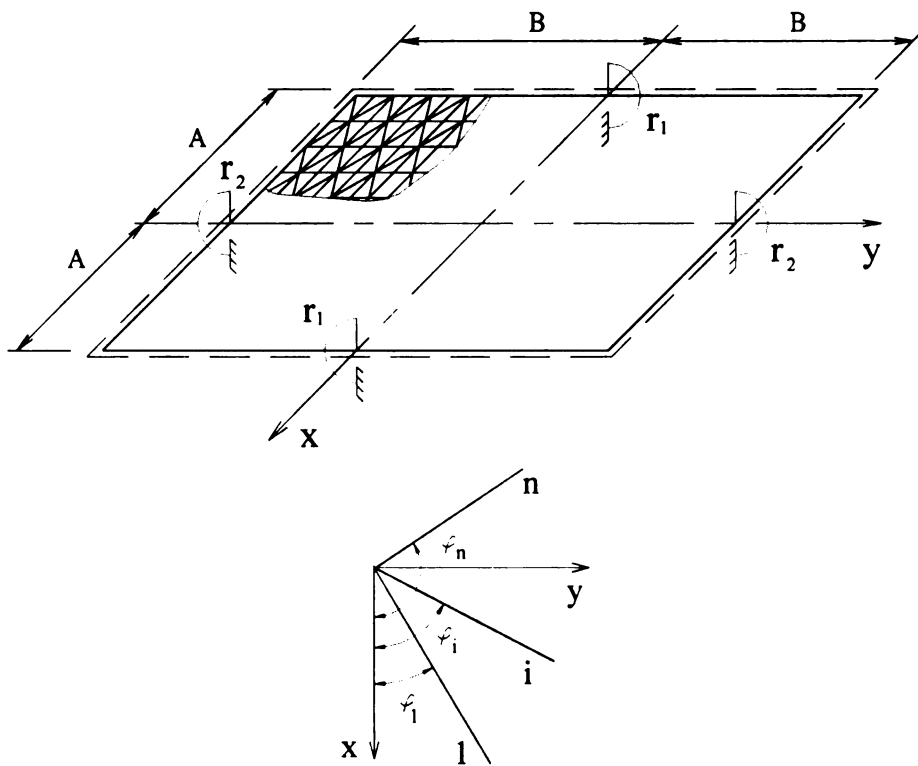


Figure 3.1 Lattice plate with elastic supports

The positive directions of internal forces and bending and twisting moments in a rod are shown in Fig. 3.2. Their dependence on the deformation components is assumed to be

$$M_i = -E_i I_i \kappa_i^*, \quad T_i = -G_i J_i \theta_i^*, \quad Q_i = -\nabla_i M_i \quad (3.2)$$

where $\nabla_i = c_i \frac{\partial}{\partial x} + s_i \frac{\partial}{\partial y}$ is a linear differential operator, $E_i =$ Young's modulus,

$G_i =$ shear modulus, $I_i =$ moment of inertia, and $J_i =$ torsion moment of inertia.

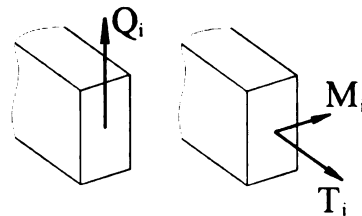


Figure 3.2 Internal forces and moments in a rod

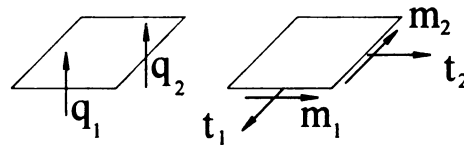


Figure 3.3 Distributed internal forces and moments in the continuum model

Assuming that the rod's forces and moments are distributed continuously across the continuum model's cross section, the following expressions are obtained for the forces and moments in the continuum model shown in Figure 3.3:

$$\begin{aligned}
q_1 &= \sum_{i=1}^n (Q_i c_i) / a_i, & q_2 &= \sum_{i=1}^n (Q_i s_i) / a_i \\
m_1 &= \sum_{i=1}^n (M_i c_i^2 + T_i s_i c_i) / a_i, & m_2 &= \sum_{i=1}^n (M_i s_i^2 - T_i s_i c_i) / a_i \\
t_1 &= -\sum_{i=1}^n (M_i s_i c_i - T_i c_i^2) / a_i, & t_2 &= -\sum_{i=1}^n (M_i s_i c_i + T_i s_i^2) / a_i
\end{aligned} \tag{3.3}$$

where a_i = distance between the axes of the i^{th} family of rods. By substituting (3.2) into (3.3) and taking (3.1) into account, the following constitutive equations are obtained for the continuum model:

$$\begin{aligned}
m_1 &= \sum_{i=1}^n \frac{1}{a_i} c_i \nabla_i (E_i I_i c_i \nabla_i - G_i J_i s_i \Delta_i) w, \\
m_2 &= \sum_{i=1}^n \frac{1}{a_i} s_i \nabla_i (E_i I_i s_i \nabla_i - G_i J_i c_i \Delta_i) w \\
t_1 &= -\sum_{i=1}^n \frac{1}{a_i} c_i \nabla_i (E_i I_i s_i \nabla_i - G_i J_i c_i \Delta_i) w, \\
t_2 &= -\sum_{i=1}^n \frac{1}{a_i} s_i \nabla_i (E_i I_i c_i \nabla_i + G_i J_i s_i \Delta_i) w
\end{aligned} \tag{3.4}$$

where $\Delta_i = s_i \frac{\partial}{\partial x} - c_i \frac{\partial}{\partial y}$ is a linear differential operator orthogonal to the axes of the i^{th} family of rods.

Equilibrium equations for an element of the plate has the form

$$\frac{\partial q_1}{\partial x} + \frac{\partial q_2}{\partial y} + Z = 0, \quad \frac{\partial t_1}{\partial x} - \frac{\partial m_2}{\partial y} - q_2 = 0, \quad \frac{\partial t_2}{\partial y} - \frac{\partial m_1}{\partial x} - q_1 = 0 \tag{3.5}$$

Using (3.4) in the last two equations of (3.5) yields

$$\begin{aligned}
q_1 &= -\sum_{i=1}^n \frac{1}{a_i} \nabla_i^2 (E_i I_i c_i \nabla_i + G_i J_i s_i \Delta_i) w, \\
q_2 &= -\sum_{i=1}^n \frac{1}{a_i} \nabla_i^2 (E_i I_i s_i \nabla_i - G_i J_i c_i \Delta_i) w
\end{aligned} \tag{3.6}$$

while the first equation in (3.5) yields

$$L(w) - Z = 0 \tag{3.7}$$

where the linear differential operator L has the form

$$L(w) = \sum_{i=1}^n \frac{1}{a_i} \nabla_i^2 (E_i I_i \nabla_i^2 + G_i J_i \Delta_i^2) w \tag{3.8}$$

3.2 Solution of Bending Problem for Lattice Plate with Elastic Supports

Consider a plate with the lattice type shown in Figure 3.4(a). It consists of four families of rods ($n = 4$) and the rods of the first and second families are identical. For this specific case

$$\begin{aligned}
\varphi_1 &= \varphi, \quad \varphi_2 = -\varphi, \quad \varphi_3 = \pi/2, \quad \varphi_4 = 0 \\
a_1 &= a_2 = a, \quad a = 2a_3 s = 2a_4 c \\
E_1 I_1 &= E_2 I_2 = EI, \quad G_1 J_1 = G_2 J_2 = GJ
\end{aligned} \tag{3.9}$$

With respect to (3.9), the constitutive equations can be written as

$$\begin{aligned}
m_1 &= \beta_{11} \kappa_1 + \beta_{12} \kappa_2, & m_2 &= \beta_{12} \kappa_1 + \beta_{22} \kappa_2, \\
t_1 &= \beta_{31} \kappa_{12}, & t_2 &= \beta_{41} \kappa_{12}
\end{aligned} \tag{3.10}$$

where the coefficients β depend upon geometrical and physical characteristics of the lattice:

$$\begin{aligned}
 \beta_{11} &= -2(EIc^4 + E_4I_4c + GJs^2c^2)/a \\
 \beta_{12} &= -2s^2c^2(EI - GJ)/a \\
 \beta_{22} &= -2(EIs^4 + E_3I_3s + GJs^2c^2)/a \\
 \beta_{31} &= (EI \sin^2 2\varphi + 2GJc^2 \cos 2\varphi + 2G_4J_4c)/a \\
 \beta_{41} &= (EI \sin^2 2\varphi - 2GJs^2 \cos 2\varphi + 2G_3J_3s)/a
 \end{aligned}
 \tag{3.11}$$

Note that the parameters without subscripts refer to the first two families of rods.

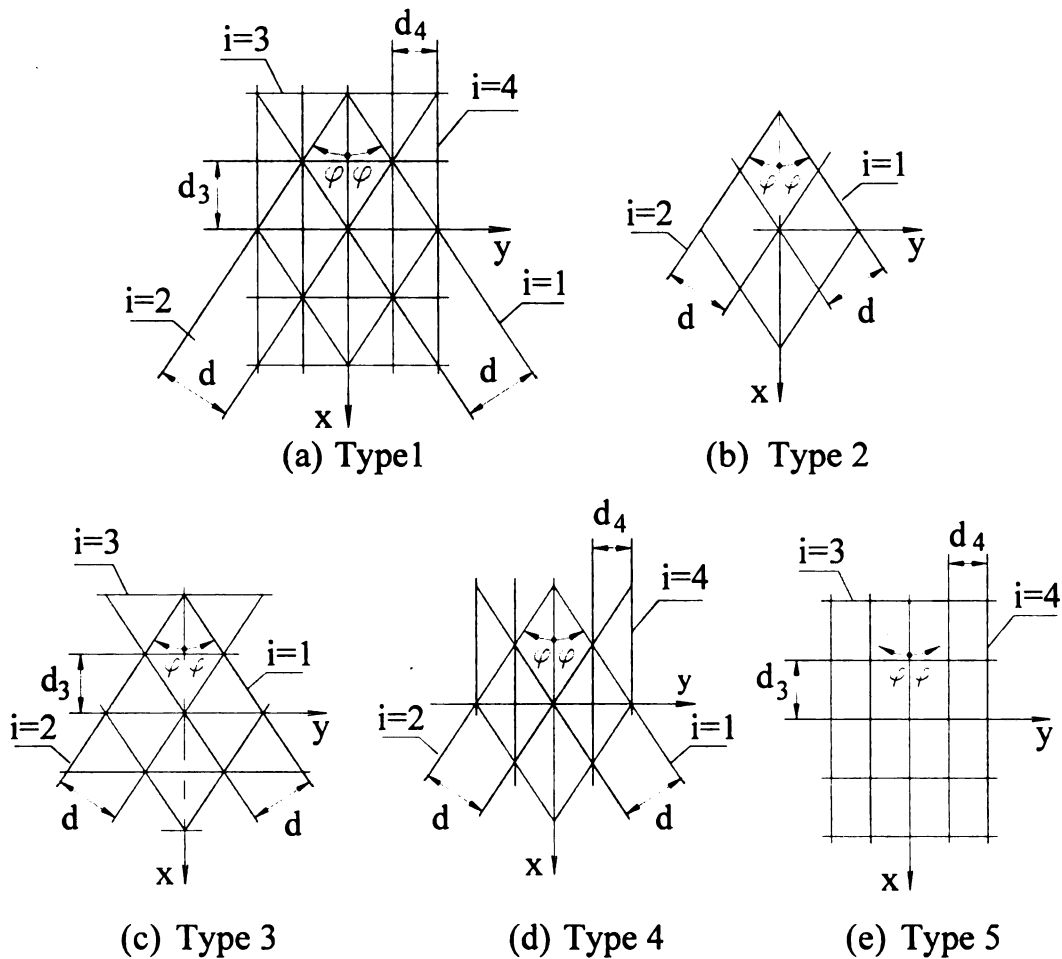


Figure 3.4 Types of grids for lattice plates

Using (3.7) and (3.8) yields the bending equation for the continuum model as

$$D_1 \frac{\partial^4 w}{\partial x^4} + D_2 \frac{\partial^4 w}{\partial x^2 \partial y^2} + D_3 \frac{\partial^4 w}{\partial y^4} = \frac{a}{2EI} Z \quad (3.12)$$

where

$$\begin{aligned} D_1 &= c^4 + \gamma s^2 c^2 + g_4 c \\ D_2 &= 6c^2 s^2 + \gamma(s^4 - 4c^2 s^2 + c^4) + \gamma_3 s + \gamma_4 c \\ D_3 &= s^4 + \gamma c^2 s^2 + g_3 s \\ g_i &= E_i I_i / EI \\ \gamma_i &= G_i J_i / EI \end{aligned} \quad (3.13)$$

Bending equations for plates with other types of lattice geometries shown in Figures 3.4(b) to 3.4(e) may be obtained from (3.12) and (3.13) by considering the terms of coefficients corresponding to the family of rods that are not present to be zero.

Since the plates are assumed to have elastic supports, (3.12) must be solved under the following boundary conditions:

$$w = 0, \quad M_1 = \pm r_1 \frac{\partial w}{\partial x} \quad (x = \pm A)$$

$$w = 0, \quad M_2 = \pm r_2 \frac{\partial w}{\partial y} \quad (y = \pm B)$$

Here r_1 and r_2 are the stiffness per unit length of the distributed rotational springs along the supports. Using (3.10) and (3.11), these boundary conditions may be expressed as

$$w = 0, \quad \beta_{11} \frac{\partial^2 w}{\partial x^2} \pm r_1 \frac{\partial w}{\partial x} = 0 \quad (x = \pm A) \quad (3.14a)$$

$$w = 0, \quad \beta_{22} \frac{\partial^2 w}{\partial y^2} \pm r_2 \frac{\partial w}{\partial y} = 0 \quad (y = \pm B) \quad (3.14b)$$

The following notations are introduced to reduce the problem to non-dimensional form:

$$\alpha = x/A, \quad \beta = y/B, \quad \lambda = B/A, \quad \eta_1 = D_2/D_1, \quad \eta_2 = D_3/D_1$$

$$p_Z = \max|Z|, \quad f_Z(\alpha, \beta) = Z/p_Z, \quad v = w \frac{2EI D_1}{aA^4 p_Z}$$

where $f_Z(\alpha, \beta)$ = dimensionless load function, and v = dimensionless deflection function.

Non-dimensional forms of the stiffness coefficients of the elastic supports are taken as $k_1 = \beta_{11}/(\beta_{11} + r_1 A)$ and $k_2 = \beta_{22}/(\beta_{22} + r_2 B)$, where $0 \leq k_{1,2} \leq 1$.

The dimensionless form of (3.12) is

$$\frac{\partial^4 v}{\partial \alpha^4} + \frac{\eta_1}{\lambda^2} \frac{\partial^4 v}{\partial \alpha^2 \partial \beta^2} + \frac{\eta_2}{\lambda^4} \frac{\partial^4 v}{\partial \beta^4} = f_Z(\alpha, \beta) \quad (3.15)$$

to be solved under the boundary conditions

$$v = 0, \quad k_1 \frac{\partial^2 v}{\partial \alpha^2} \pm (1 - k_1) \frac{\partial v}{\partial \alpha} = 0 \quad (\alpha = \pm 1) \quad (3.16a)$$

$$v = 0, \quad k_2 \frac{\partial^2 v}{\partial \beta^2} \pm (1 - k_2) \frac{\partial v}{\partial \beta} = 0 \quad (\beta = \pm 1) \quad (3.16b)$$

The boundary value problem characterized by (3.15) and (3.16) is solved by the decomposition method as described in Section 2.3. The interconnection equation of the problem is solved by the multiple-point collocation method. The dimensionless

displacement is computed using (2.43), from which the actual displacement is recovered. The internal forces in the rods are finally computed using (3.1) and (3.2). The displacement and internal forces in the rods are given by

$$w = \frac{A^4 a p_Z}{2D_1 EI} v \quad (3.17)$$

$$M_i = -g_i \frac{A^2 a p_Z}{2D_1} \kappa_i^* \quad (3.18)$$

$$T_i = \gamma_i \frac{A^2 a p_Z}{2D_1} \theta_i^* \quad (3.19)$$

$$Q_i = - \left(\frac{c_i}{A} \frac{\partial}{\partial \alpha} + \frac{s_i}{B} \frac{\partial}{\partial \beta} \right) M_i \quad (3.20)$$

Numerical example

Consider the rectangular lattice plate shown in Fig. 3.5 which is uniformly loaded at the joints with the loads $P_y = 1$ N. The lattice consists of two orthogonal families of rods with the following characteristics: $l_1 = 0.1$ m, $l_2 = 0.15$ m, $EI_1 = EI_2 = 10^5$ N.m². For simplicity and without any loss of generalization, torsional rigidities were assumed to be zero, i.e. $GJ_{k,1} = GJ_{k,2} = 0$. Deflections and bending moments are calculated at the four locations indicated in Fig. 6 for pinned and fixed supports. Table 3.1 shows the results obtained using the finite element method (FEM) and the decomposition method (DM). In the FEM, each rod was taken as a separate finite element.

The example demonstrates that the continuum model, together with the decomposition method, yields an accuracy of within 2% for displacements and bending moments, which is adequate for preliminary design and optimization purposes.

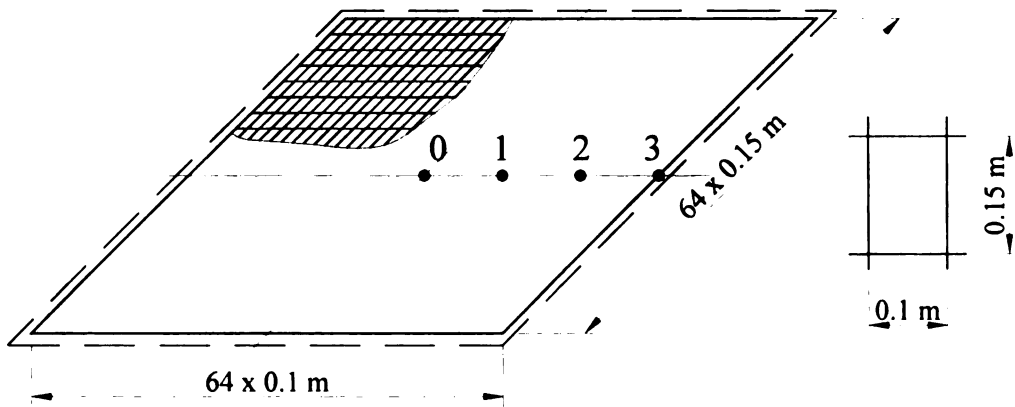


Figure 3.5. Plate with an orthogonal lattice

TABLE 3.1. Results for $k_1 = k_2 = 1$ (pinned supports)

Location Number	w ($\times 10^3$ m)			M ($\times 10^{-1}$ N.m)		
	FEM	DM	ε (%)	FEM	DM	ε (%)
0	2.29	2.30	0.1	4.96	5.01	1.2
1	1.93	1.96	0.2	4.41	4.46	1.1
2	1.15	1.16	0.8	2.77	2.83	1.0
3	0	0	-	0	0	-

TABLE 3.2. Results for $k_1 = k_2 = 0$ (fixed supports)

Location Number	w ($\times 10^3$ m)			M ($\times 10^{-1}$ N.m)		
	FEM	DM	ε (%)	FEM	DM	ε (%)
0	0.555	0.560	0.9	1.40	1.42	1.4
1	0.407	0.415	1.9	1.98	1.99	0.5
2	0.148	0.149	0.7	-0.265	-0.266	1.0
3	0	0	-	-3.12	-3.125	0.4

3.3 Comparative Analysis for Different Types of Lattices

In this section the bending problem of a lattice plate is analyzed for the different types of lattices shown in Figure 3.4, and different values of support rigidities. The rod's material volume per unit area of the middle surface of the plate is fixed, i.e.,

$$\frac{F_1}{a_1} + \frac{F_2}{a_2} + \frac{F_3}{a_3} + \frac{F_4}{a_4} = \bar{v} = \text{const} \quad (3.21)$$

where F_i = the cross-section area of a rod in the i^{th} family. The rods of all four families are assumed to be made of the same material and to have the same cross-section

$$F_1 = F_2 = F_3 = F_4 = F \quad (3.22)$$

With respect to (3.22) and notations (3.9), the condition (3.21) can be written as

$$\bar{v} = \frac{2F}{a} (\delta_1 + \delta_3 s + \delta_4 c) \quad (3.23)$$

Coefficients δ_1 , δ_3 , and δ_4 take the values of 1 if the corresponding family of rods is present or 0 if the corresponding family of rods is absent. The coefficient of torsional rigidity of the i^{th} family of rods is defined as $\gamma_i = \delta_i \gamma$, where γ is determined by (3.13). The formulae for the coefficients η_1 and η_2 of the bending equation become

$$\eta_1 = \frac{6\delta_1 \sin^2 \varphi \cos \varphi + \delta_1 \gamma (\cos^{-1} \varphi - 6\sin^2 \varphi \cos \varphi + \delta_3 \text{tg} \varphi + \delta_4)}{\delta_1 \cos^3 \varphi + \delta_4 + \delta_1 \gamma \sin^2 \varphi \cos \varphi} \quad (3.24)$$

$$\eta_2 = \frac{\sin^3 \varphi \text{tg} \varphi + \delta_3 \text{tg} \varphi + \delta_1 \gamma \sin^2 \varphi \cos \varphi}{\delta_1 \cos^3 \varphi + \delta_4 + \delta_1 \gamma \sin^2 \varphi \cos \varphi} \quad (3.25)$$

Taking the angle φ as the controlling parameter, using (3.23) the other variable a can be expressed in terms of φ since the material volume is kept constant:

$$a = 2(\delta_1 + \delta_3 s + \delta_4 c) F / \bar{v}$$

or

(3.26)

$$a = a_0(\delta_1 + \delta_3 s + \delta_4 c), \quad \text{where} \quad a_0 = \frac{2F}{\bar{v}}$$

Substituting this value into (3.17) and (3.18) and assuming a uniform transverse load, the equations for deflection and bending moments can be written as

$$w = w^0 \frac{A^4 q a_0}{EI} \tag{3.25}$$

$$M_i = -M_i^0 A^2 q a_0 \tag{3.26}$$

where

$$w^0 = v \frac{(\delta_1 + \delta_3 s + \delta_4 c)}{2D_1} \tag{3.27}$$

$$M_i^0 = \kappa_i^* g_i \frac{(\delta_1 + \delta_3 s + \delta_4 c)}{2D_1} \tag{3.28}$$

The dimensionless displacement function is determined by (2.43) and (2.44), and the curvature κ_i^* is found from (3.1). The dimensionless coefficient D_1 is given in (3.13). The $a_0 = F/\bar{v}$ ratio is constant for the particular problem and is known from the problem definition.

The technique described above was implemented into the PLAST computer program for analyzing rectangular lattice plates with different types of lattices and

different values of support rigidities. PLAST is written in the C programming language and can be used on personal computers. The listing of the program is given in Appendix B. Some of the results obtained using the program are shown in graphical form below.

Figures 3.6 through 3.11 represent the dependencies of maximum values w_{\max}^0 and $M_{i \max}^0$ on the angle φ for the values $k_i=0, 1, \text{ and } 0.5$. The three curves on the graphs correspond to three different types of lattices shown in Figure 3.4. The graphs identify the optimal lattice type and governing angle value for each type of support condition. Figures 3.8 and 3.9 show that for pinned supports the optimal lattice type that minimizes moments and deflections is rhombic (Type 2) and the optimal value of the angle is $\varphi = 45^\circ$. For fixed supports (Figures 3.6 and 3.7) the rhombic lattice with a 45° angle yields smaller moments but at the same time gives larger deflections than lattices with the governing angle close to 0° or 90° . For partially restrained supports (Figures 3.10 and 3.11) the rhombic lattice is also optimal.

Figure 3.12 shows examples of similar dependencies of w_{\max}^0 on angle φ for different combinations of support rigidities.

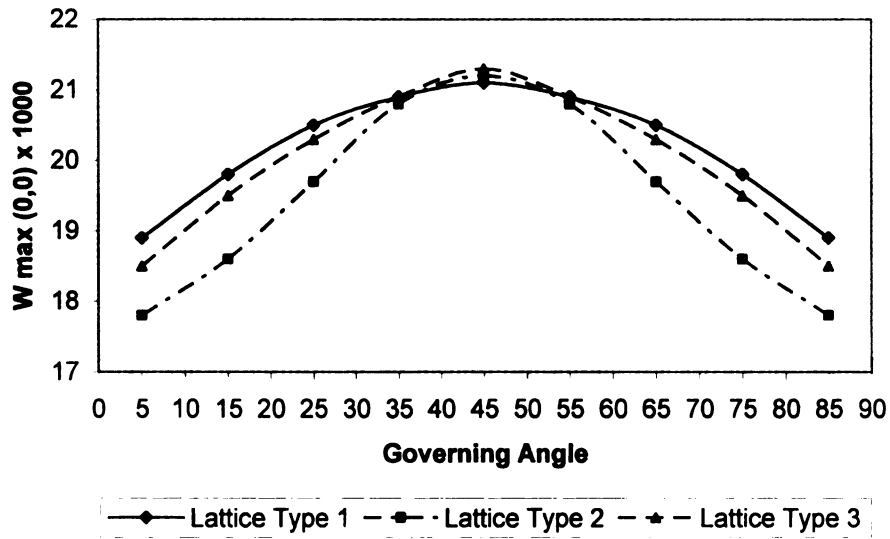


Figure 3.6. Maximum deflection at the middle of the plate for $k_1 = k_2 = 0$ (fixed supports)

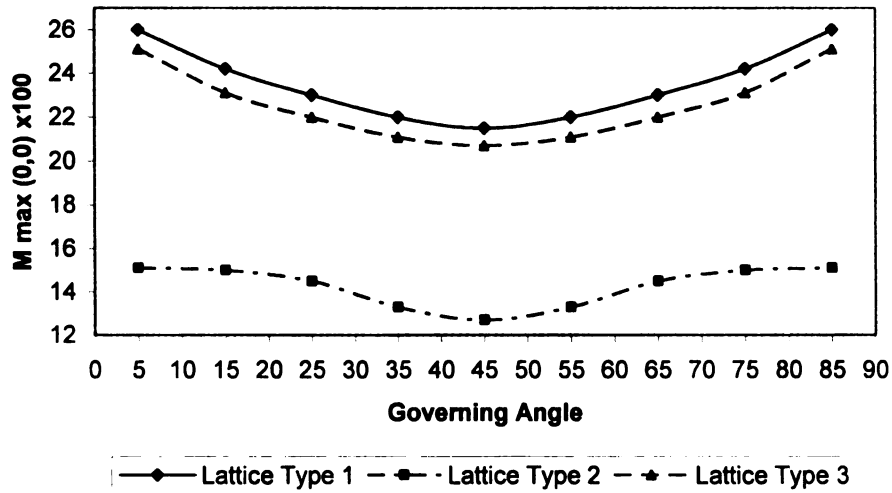


Figure 3.7. Maximum moment at the middle of the plate for $k_1 = k_2 = 0$ (fixed supports)

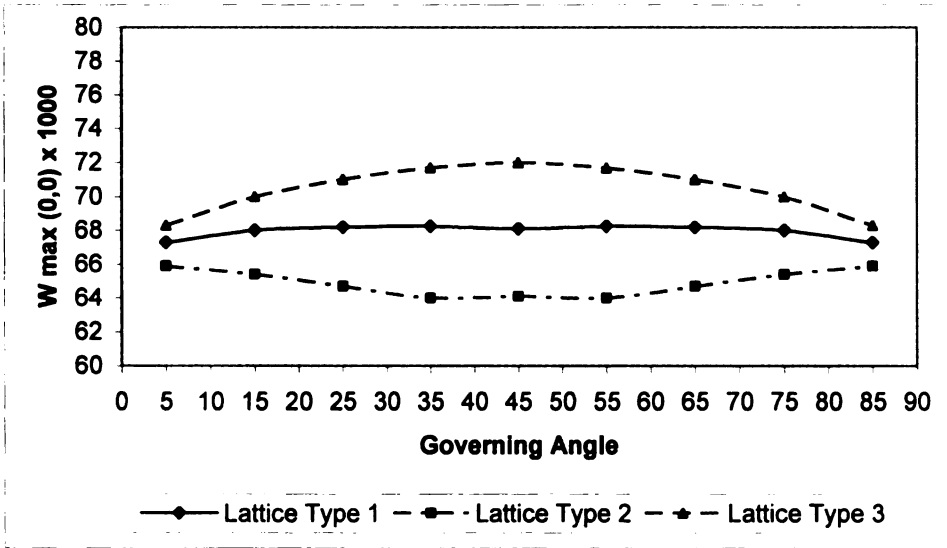


Figure 3.8. Maximum deflection at the middle of the plate for $k_1 = k_2 = 1$ (pinned supports)

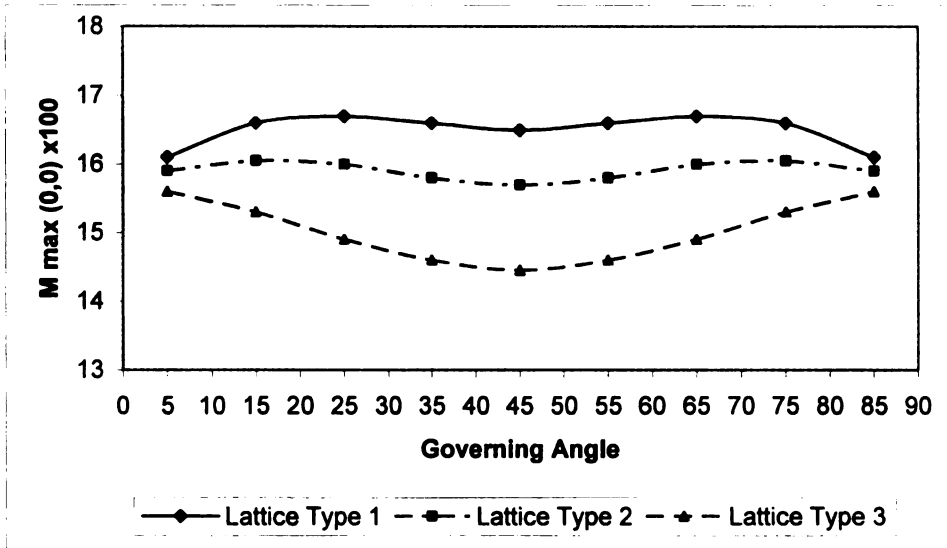


Figure 3.9. Maximum moment at the middle of the plate for $k_1 = k_2 = 1$ (pinned supports)

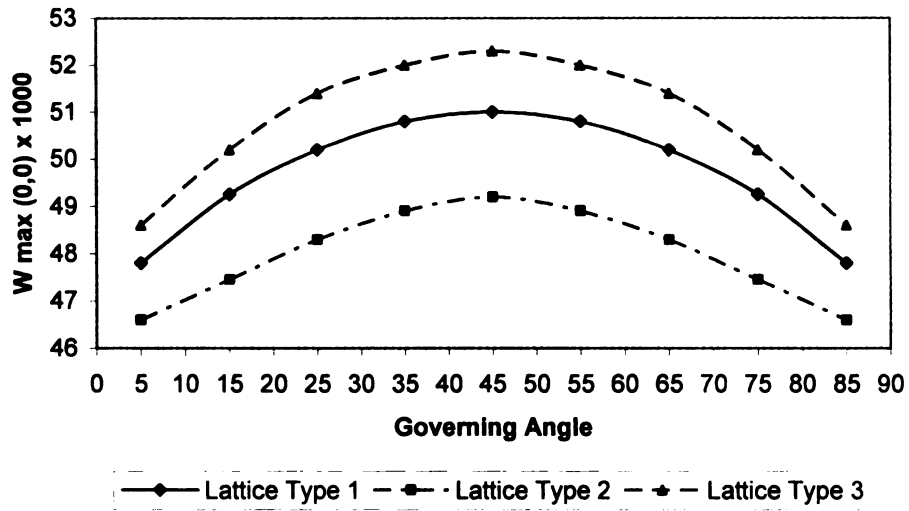


Figure 3.10. Maximum deflection at the middle of the plate for $k_1 = k_2 = 0.5$

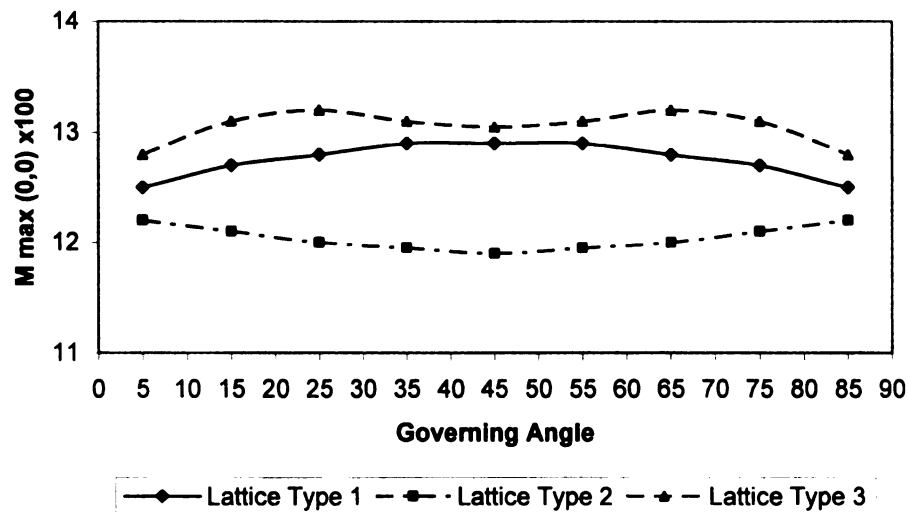


Figure 3.11. Maximum moment at the middle of the plate for $k_1 = k_2 = 0.5$

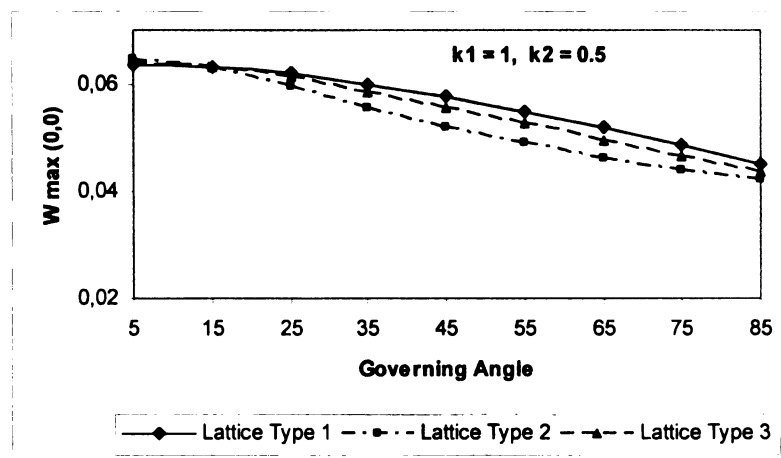
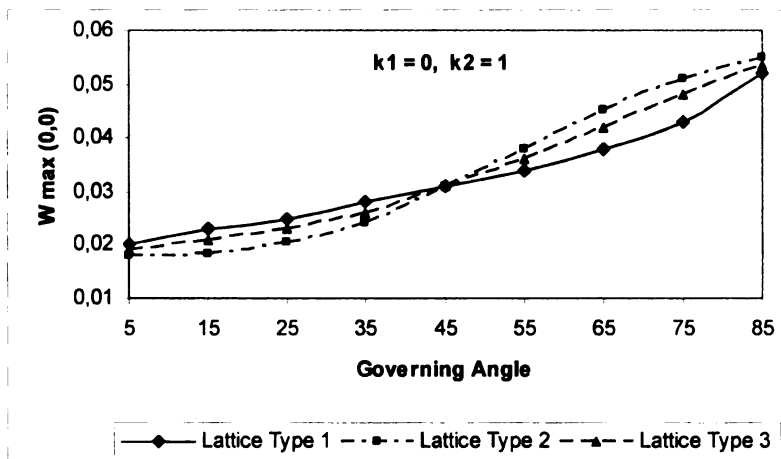
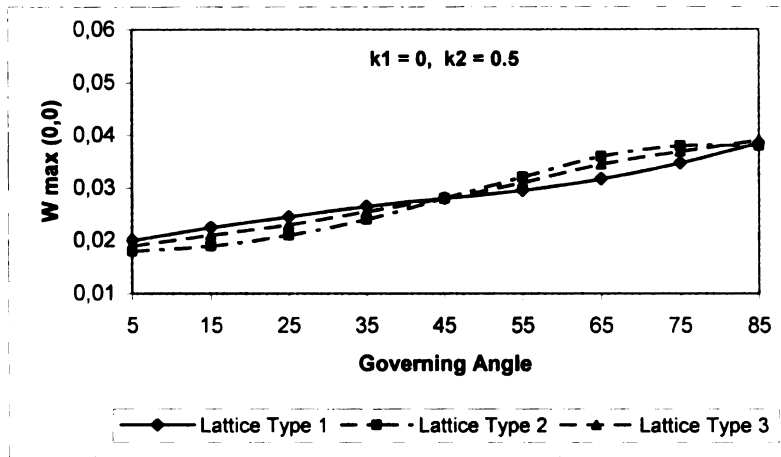


Figure 3.12. Maximum deflection at the middle of the plate for different combinations of support rigidities

3.4 Transverse Free Vibration of Lattice Plate with Elastic Supports

Consider the plate shown in Figure 3.13 with non-symmetric elastic supports. The lattice consists of four families of rods ($n = 4$), as shown in Figure 3.4(a), and the cross-section of the rods in all the families are identical. The continuum model described in Section 3.1 is used for this problem.

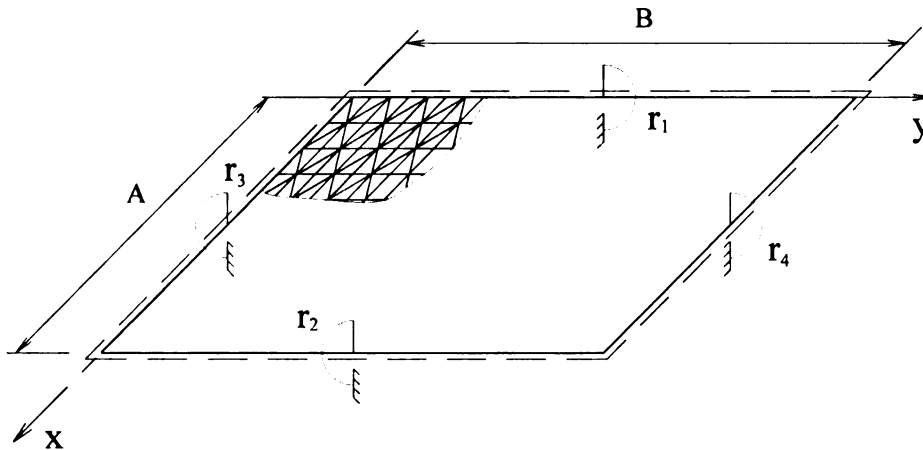


Figure 3.13 Lattice plate with non-symmetric elastic supports

The differential equation governing the transverse free vibration of the plate can be obtained from the bending equation (3.12) by substituting the external load Z by the inertia forces due to its movement:

$$Z = -\frac{\partial^2 w}{\partial t^2} \sum_{i=1}^n \frac{\rho_i F_i}{a_i} \quad (3.29)$$

where ρ_i is the density of material of the i^{th} family of rods. For the case of steady harmonic free vibration at the frequency ω

$$Z = \omega^2 w \sum_{i=1}^n \frac{\rho_i F_i}{a_i} = \frac{2\omega^2 \rho F}{a} (1 + \sin \varphi + \cos \varphi) \quad (3.30)$$

Substituting this value into the right-hand side of (3.12), the governing equation becomes

$$D_1 \frac{\partial^4 w}{\partial x^4} + D_2 \frac{\partial^4 w}{\partial x^2 \partial y^2} + D_3 \frac{\partial^4 w}{\partial y^4} = \frac{\omega^2 \rho}{Er^2 \cos \varphi} (1 + \sin \varphi + \cos \varphi) \quad (3.31)$$

where r is the radius of gyration of the rods, and the coefficients D_1 , D_2 , and D_3 are defined by (3.13). The boundary conditions for the problem using the non-dimensional coefficients of support rigidity are

$$w = k_1 A \frac{\partial^2 w}{\partial x^2} - (1 - k_1) \frac{\partial w}{\partial x} = 0, \quad (x = 0) \quad (3.32a)$$

$$w = k_2 A \frac{\partial^2 w}{\partial x^2} - (1 - k_2) \frac{\partial w}{\partial x} = 0, \quad (x = A) \quad (3.32b)$$

$$w = k_3 B \frac{\partial^2 w}{\partial y^2} - (1 - k_3) \frac{\partial w}{\partial y} = 0, \quad (y = 0) \quad (3.32c)$$

$$w = k_4 B \frac{\partial^2 w}{\partial y^2} - (1 - k_4) \frac{\partial w}{\partial y} = 0, \quad (y = B) \quad (3.32d)$$

The three auxiliary problems introduced in the decomposition method have the form:

1.
$$D_1 \frac{\partial^4 w_1}{\partial x^4} = f_1(x, y) \quad (3.33)$$

subject to the boundary conditions (3.32a,b);

$$2. \quad D_2 \frac{\partial^4 w_2}{\partial y^4} = f_2(x, y) \quad (3.34)$$

subject to the boundary conditions (3.32c,d); and

$$3. \quad D_3 \frac{\partial^4 w_3}{\partial x^2 \partial y^2} - \frac{\omega^2 \rho}{E r^2 \cos \varphi} (1 + \sin \varphi + \cos \varphi) = -f_1(x, y) - f_2(x, y) \quad (3.35)$$

The approximating functions are taken in the form

$$f_1(x, y) = \psi_1(y), \quad f_2(x, y) = \psi_2(x)$$

From the solution of the first two boundary value problems and satisfying condition $w_1 = w_2$

$$w_1 = w_2 = \psi_1(y) \psi_2(x) \quad (3.36)$$

where

$$\psi_1(y) = \frac{1}{24 D_2} \times \frac{y(y-B)}{(1+3k_3+3k_4+5k_3k_4)} \times \left[y^2 (1+3k_3+3k_4+5k_3k_4) - yB(1+k_3+5k_4+5k_3k_4) - 2B^2(k_3+5k_3k_4) \right] \quad (3.37)$$

$$\psi_2(x) = \frac{1}{24 D_1} \times \frac{x(x-A)}{(1+3k_1+3k_2+5k_1k_2)} \times \left[x^2 (1+3k_1+3k_2+5k_1k_2) - xA(1+k_1+5k_2+5k_1k_2) - 2A^2(k_1+5k_1k_2) \right]$$

The Bubnov-Galerkin method is used for solving the third auxiliary problem, assuming that $w_3 \equiv w_1$:

$$\int_0^B \int_0^A \left[D_3 \frac{\partial^4 w_1}{\partial x^2 \partial y^2} + \psi_1(y) + \psi_2(x) - w_1 \frac{\omega^2 \rho}{E r^2 \cos \varphi} (1 + \sin \varphi + \cos \varphi) \right] w_1 dx dy = 0 \quad (3.38)$$

The expression for ω^2 is determined from (3.38). For $k_i = 1$ (pinned support):

$$\omega^2 = \frac{108}{961} \times \frac{(868D_1A^4 + 867D_3A^2B^2 + 868D_2B^4)Er^2 \cos \varphi}{\rho A^4 B^4 (1 + \sin \varphi + \cos \varphi)} \quad (3.39)$$

For $k_i = 0$ (fixed support):

$$\omega^2 = \frac{72(7D_1A^4 + 2D_3A^2B^2 + 7D_2B^4)Er^2 \cos \varphi}{\rho A^4 B^4 (1 + \sin \varphi + \cos \varphi)} \quad (3.40)$$

Expressions for ω^2 determined for six different types of support combinations are summarized in Table (3.3).

Numerical examples

Consider the rectangular lattice plate shown in Figure 3.13. The lattice consists of four families of rods (Type 1 in Figure 3.4). The rods are standard steel tubes. The values of the first frequency of free vibration ω are calculated using the decomposition method and compared with the solutions obtained by the FEM using the LIRA software (Kiev 2000).



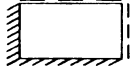
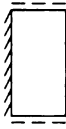


Tables 3.4 – 3.9 and Figures 3.14 – 3.19 demonstrate the results obtained for lattice plates with pinned and fixed supports and the values of the governing angle of the lattice $\varphi = 45^0, 30^0, \text{ and } 60^0$. The longer side of the plate was taken as $b=5$ m, and the step of the lattice along side b was taken 1 m.

Tables 3.10 – 3.15 and Figures 3.20 – 3.25 show the results obtained using expressions (3.41) – (3.46) for lattice plates with different combinations of supports and

different aspect ratios. The results presented correspond to the case when $b=10$ m, and $\varphi = 45^\circ$.

The results demonstrate that the decomposition method yields sufficient accuracy for preliminary design applications. The analytical dependencies obtained can be used for optimization purposes.

TABLE 3.3. Main types of support conditions and corresponding expressions for the square of the first frequency of free vibration

Type of supports		Expression for ω^2	
1		$\omega^2 = \frac{72}{19} \frac{(63 D_1 A^4 + 36 D_3 A^2 B^2 + 133 D_2 B^4) E r^2 \cos \varphi}{\rho A^4 B^4 (1 + \sin \varphi + \cos \varphi)}$	(3.41)
2		$\omega^2 = \frac{72}{19} \frac{(133 D_1 A^4 + 36 D_3 A^2 B^2 + 63 D_2 B^4) E r^2 \cos \varphi}{\rho A^4 B^4 (1 + \sin \varphi + \cos \varphi)}$	(3.42)
3		$\omega^2 = \frac{648}{361} \frac{(133 D_1 A^4 + 72 D_3 A^2 B^2 + 133 D_2 B^4) E r^2 \cos \varphi}{\rho A^4 B^4 (1 + \sin \varphi + \cos \varphi)}$	(3.43)
4		$\omega^2 = \frac{216}{589} \frac{(266 D_1 A^4 + 306 D_3 A^2 B^2 + 651 D_2 B^4) E r^2 \cos \varphi}{\rho A^4 B^4 (1 + \sin \varphi + \cos \varphi)}$	(3.44)
5		$\omega^2 = \frac{72}{31} \frac{(42 D_1 A^4 + 51 D_3 A^2 B^2 + 217 D_2 B^4) E r^2 \cos \varphi}{\rho A^4 B^4 (1 + \sin \varphi + \cos \varphi)}$	(3.45)
6		$\omega^2 = \frac{216}{589} \frac{(651 D_1 A^4 + 306 D_3 A^2 B^2 + 266 D_2 B^4) E r^2 \cos \varphi}{\rho A^4 B^4 (1 + \sin \varphi + \cos \varphi)}$	(3.46)

Notations:  fixed support,  pinned support

**TABLE 3.4. Results for lattice plate with pinned supports
and governing angle of $\varphi = 45^\circ$**

$\lambda = \frac{b}{a}$	Mass (metric ton)	First frequency of free vibration $\omega, \left(\frac{1}{\text{sec}}\right)$		
		FEM	DM	ε (%)
1	1.147	85.64	87.17	1.8
1.2	1.370	72.42	72.77	0.5
1.4	1.593	64.44	64.36	-0.1
1.6	1.816	59.26	59.04	-0.4
1.8	2.039	55.70	55.46	-0.4
2	2.262	53.16	52.94	-0.4
3	3.378	47.14	47.02	-0.3
4	4.493	45.04	44.94	-0.2
5	5.608	44.08	43.95	-0.3

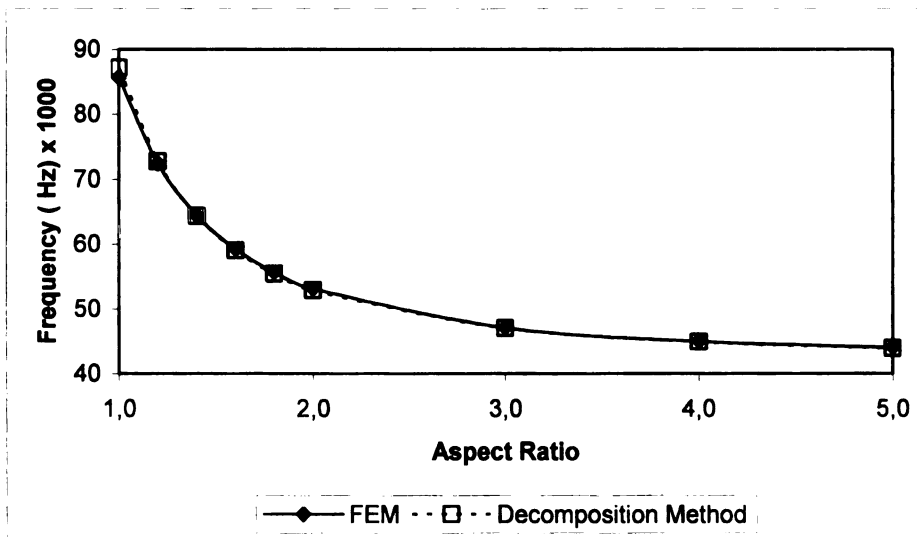


**Figure 3.14. First frequency of free vibration of lattice plate with pinned supports
and governing angle of $\varphi = 45^\circ$**

TABLE 3.5. Results for lattice plate with fixed supports

and governing angle of $\phi = 45^\circ$

$\lambda = \frac{b}{a}$	Mass (metric ton)	First frequency of free vibration $\omega, \left(\frac{1}{\text{sec}}\right)$		
		FEM	DM	$\varepsilon(\%)$
1	1.147	163.5	164.2	0.4
1.2	1.370	139.2	138.2	-0.7
1.4	1.593	126.1	124.4	-1.3
1.6	1.816	118.4	116.4	-1.6
1.8	2.039	113.4	111.4	-1.7
2	2.262	109.7	108.1	-1.4
3	3.378	103.7	101.1	-2.5
4	4.493	101.7	98.86	-2.8
5	5.608	100.8	97.77	-3.0

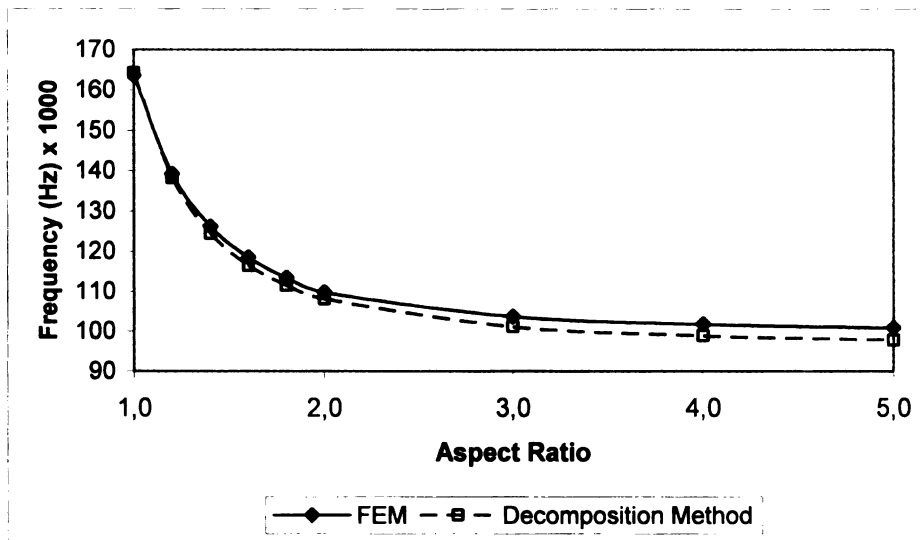
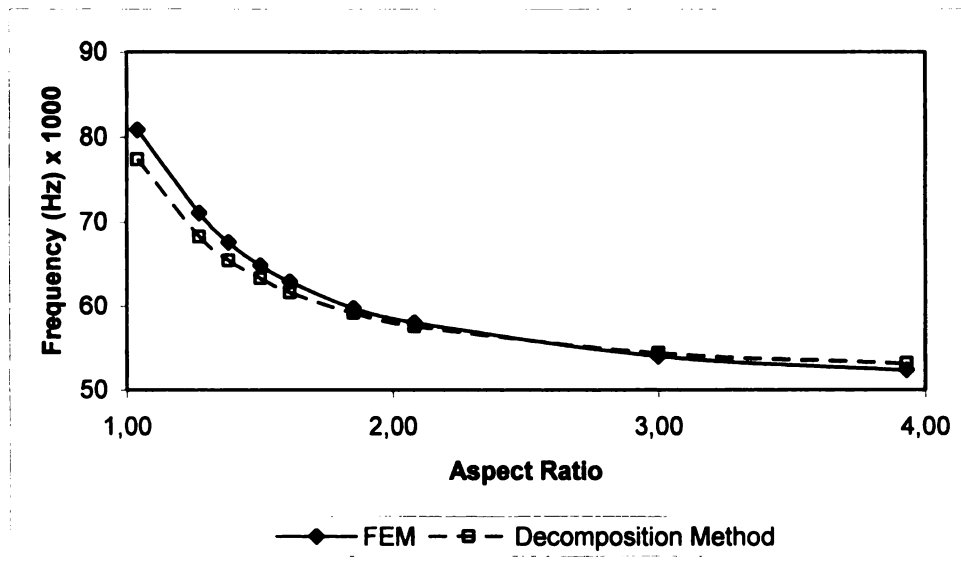


Figure 3.15. First frequency of free vibration of lattice plate with fixed supports

and governing angle of $\phi = 45^\circ$

**TABLE 3.6. Results for lattice plate with pinned supports
and governing angle of $\varphi = 30^0$**

$\lambda = \frac{b}{a}$	Mass (metric ton)	First frequency of free vibration $\omega, \left(\frac{1}{\text{sec}}\right)$		
		FEM	DM	ε (%)
1.04	0.845	80.83	77.38	-4.3
1.27	1.026	71.07	68.26	-4.0
1.38	1.116	67.57	65.44	-3.2
1.50	1.207	64.84	63.30	-2.4
1.61	1.297	62.91	61.61	-2.1
1.85	1.478	59.74	59.17	-1.0
2.08	1.658	57.99	57.55	-0.8
3.00	2.381	53.98	54.37	0.7
3.93	3.104	52.34	53.16	1.6
4.96	3.916	51.48	52.48	1.9



**Figure 3.16. First frequency of free vibration of lattice plate
with pinned supports and governing angle of $\varphi = 30^0$**

**TABLE 3.7. Results for lattice plate with fixed supports
and governing angle of $\varphi = 30^0$**

$\lambda = \frac{b}{a}$	Mass (metric ton)	First frequency of free vibration $\omega, \left(\frac{1}{\text{sec}}\right)$		
		FEM	DM	ε (%)
1.04	0.845	147.2	147.5	0.2
1.27	1.026	132.9	133.9	0.8
1.38	1.116	128.8	130.1	1.0
1.50	1.207	125.8	127.3	1.2
1.61	1.297	123.5	125.3	1.5
1.85	1.478	120.4	122.4	1.7
2.08	1.658	118.4	120.7	1.9
3.00	2.381	115.0	117.5	2.2
3.93	3.104	113.9	116.4	2.2
4.96	3.916	113.4	115.8	2.1

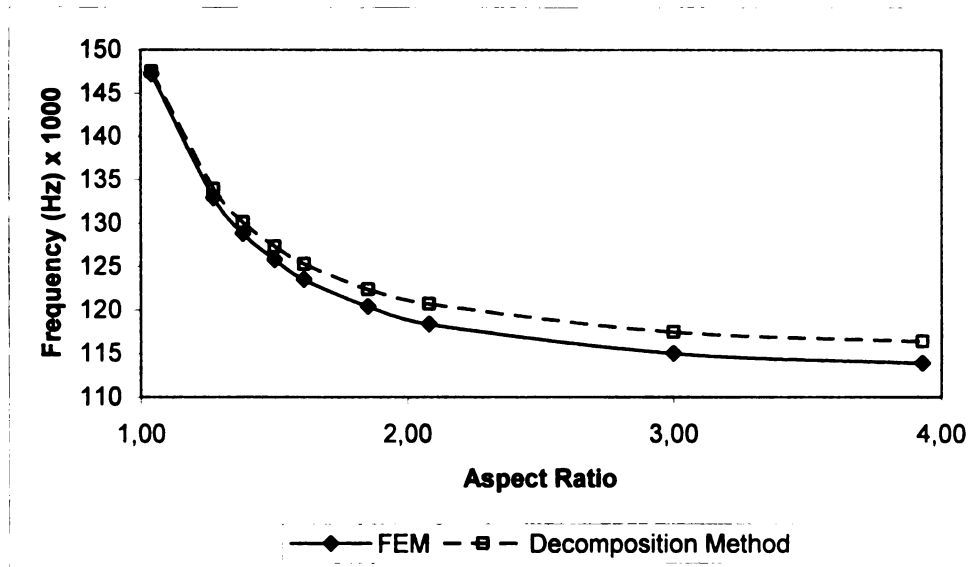


**Figure 3.17. First frequency of free vibration of lattice plate with fixed supports
and governing angle of $\varphi = 30^0$**

**TABLE 3.8. Results for lattice plate with pinned supports
and governing angle of $\varphi = 60^\circ$**

$\lambda = \frac{b}{a}$	Mass (metric ton)	First frequency of free vibration $\omega, \left(\frac{1}{\text{sec}}\right)$		
		FEM	DM	ε (%)
1.04	0.435	81.61	82.94	1.6
1.38	0.569	61.07	59.88	-1.9
1.73	0.703	51.3	49.69	-3.1
2.08	0.838	45.9	44.35	-3.4
2.42	0.972	42.6	41.22	-3.2
2.77	1.106	40.46	39.27	-2.9
3.11	1.241	38.98	37.89	-2.8
3.46	1.375	37.91	37.01	-2.4
3.81	1.510	37.13	36.28	-2.3
4.16	1.644	36.53	35.76	-2.1
4.50	1.778	36.06	35.35	-2.0
4.85	1.913	35.69	34.91	-2.2
5.20	2.047	35.39	34.65	-2.1

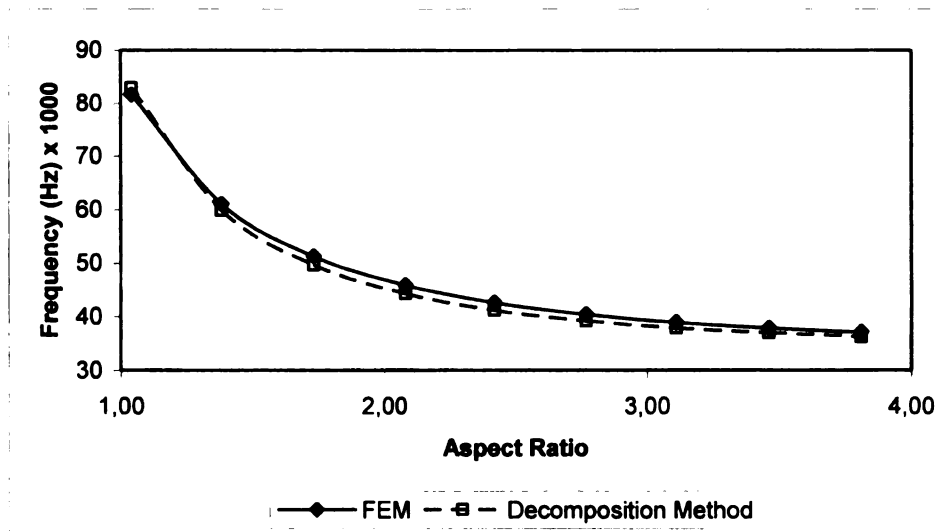


**Figure 3.18. First frequency of free vibration of lattice plate with pinned supports
and governing angle of $\varphi = 60^\circ$**

**TABLE 3.9. Results for lattice plate with fixed supports
and governing angle of $\phi = 60^\circ$**

$\lambda = \frac{b}{a}$	Mass (metric ton)	First frequency of free vibration $\omega, \left(\frac{1}{\text{sec}}\right)$		
		FEM	DM	ε (%)
1.04	0.435	135.96	142.35	4.7
1.38	0.569	103.72	108.56	4.7
1.73	0.703	90.41	94.42	4.4
2.08	0.838	84.15	87.59	4.1
2.42	0.972	80.82	83.74	3.6
2.77	1.106	78.89	81.58	3.4
3.11	1.241	77.67	79.99	3.0
3.46	1.375	76.86	78.85	2.6
3.81	1.510	76.29	77.99	2.2
4.16	1.644	75.88	77.35	1.9
4.50	1.778	75.57	76.86	1.7
4.85	1.913	75.34	76.45	1.5
5.20	2.047	75.15	76.14	1.3

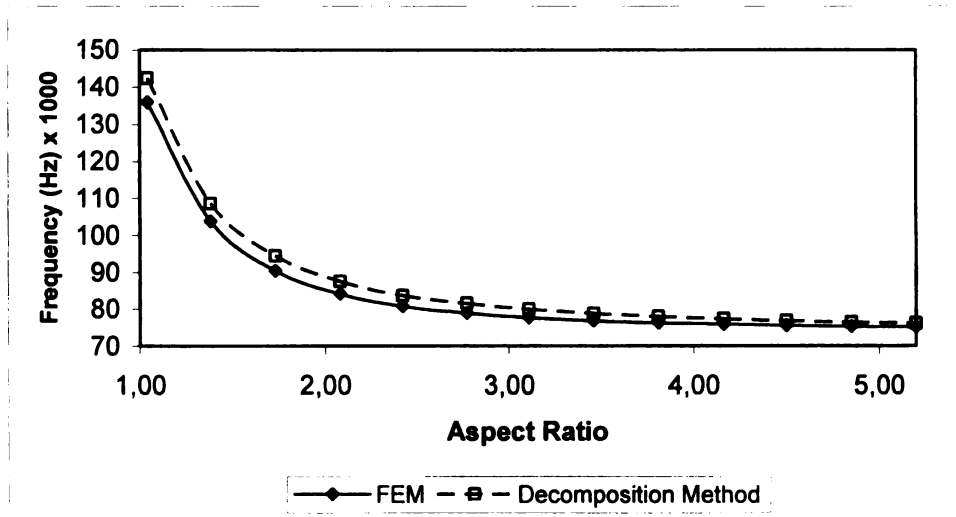


**Figure 3.19. First frequency of free vibration of lattice plate with fixed supports
and governing angle of $\phi = 60^\circ$**

**TABLE 3.10. Results for lattice plate with supports of Type 1
obtained by (3.41)**

$\lambda = \frac{b}{a}$	First frequency of free vibration $\omega, \left(\frac{1}{\text{sec}}\right)$		
	FEM	DM	ε (%)
1.0	33.92	34.24	0.9
1.1	31.79	31.94	0.5
1.2	30.25	30.31	0.2
1.3	29.11	29.09	-0.1
1.4	28.25	28.18	-0.2
1.5	27.57	27.47	-0.4
1.6	27.05	26.91	-0.5
1.7	26.62	26.46	-0.6
1.8	26.28	26.10	-0.7
1.9	26.0	25.08	-0.8
2.0	25.76	25.54	-0.9
2.5	25.02	24.72	-1.2
3.0	24.66	24.29	-1.5

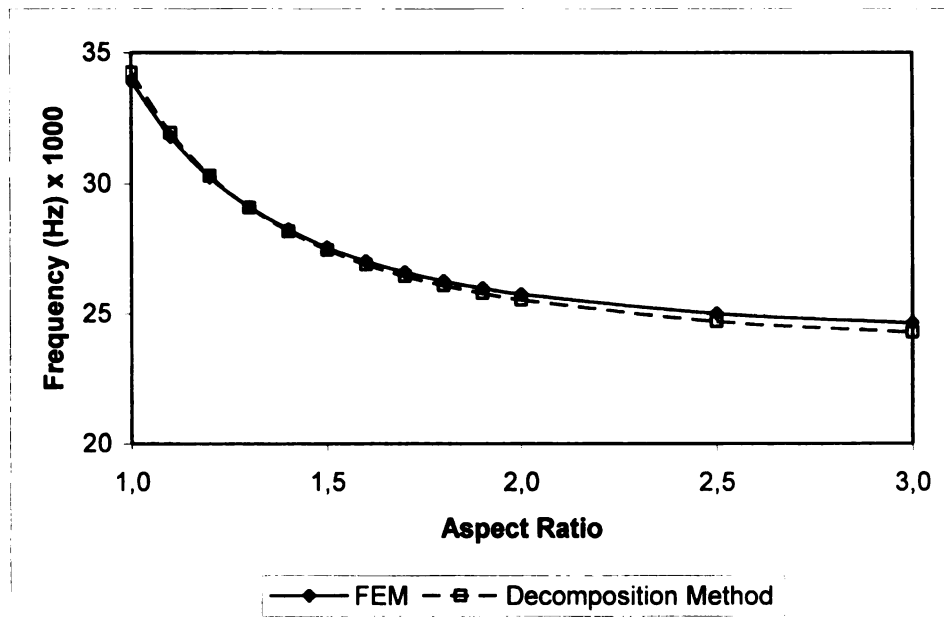


**Figure 3.20. First frequency of free vibration of lattice plate
with supports of Type 1 obtained by (3.41)**

**TABLE 3.11. Results for lattice plate with supports of Type 2
obtained by (3.42)**

$\lambda = \frac{b}{a}$	First frequency of free vibration $\omega, \left(\frac{1}{\text{sec}}\right)$		
	FEM	DM	ϵ (%)
1.0	33.92	34.24	0.9
1.1	30.29	30.31	0.1
1.2	27.62	27.46	-0.6
1.3	25.61	25.34	-1.1
1.4	24.07	23.73	-1.4
1.5	22.87	22.50	-1.6
1.6	21.92	21.53	-1.8
1.7	21.16	20.75	-1.9
1.8	20.55	20.13	-2.0
1.9	20.04	19.63	-2.0
2.0	19.63	19.21	-2.1
2.5	18.33	17.92	-2.2
3.0	17.70	17.29	-2.3

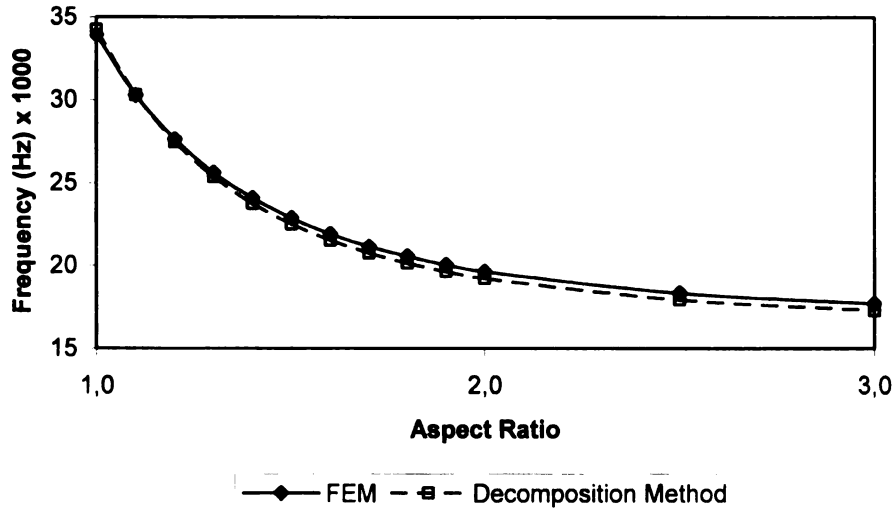


**Figure 3.21. First frequency of free vibration of lattice plate
with supports of Type 2 obtained by (3.42)**

**TABLE 3.12. Results for lattice plate with supports of Type 3
obtained by (3.43)**

$\lambda = \frac{b}{a}$	First frequency of free vibration $\omega, \left(\frac{1}{\text{sec}}\right)$		
	FEM	DM	ε (%)
1.0	29.02	28.87	-0.5
1.1	26.53	26.24	-1.1
1.2	24.69	24.32	-1.5
1.3	23.30	22.89	-1.8
1.4	22.23	21.80	-1.9
1.5	21.38	20.95	-2.0
1.6	20.71	20.28	-2.1
1.7	20.16	19.74	-2.1
1.8	19.72	19.30	-2.1
1.9	19.35	18.93	-2.2
2.0	19.04	18.62	-2.2
2.5	18.05	17.65	-2.2
3.0	17.54	17.14	-2.3

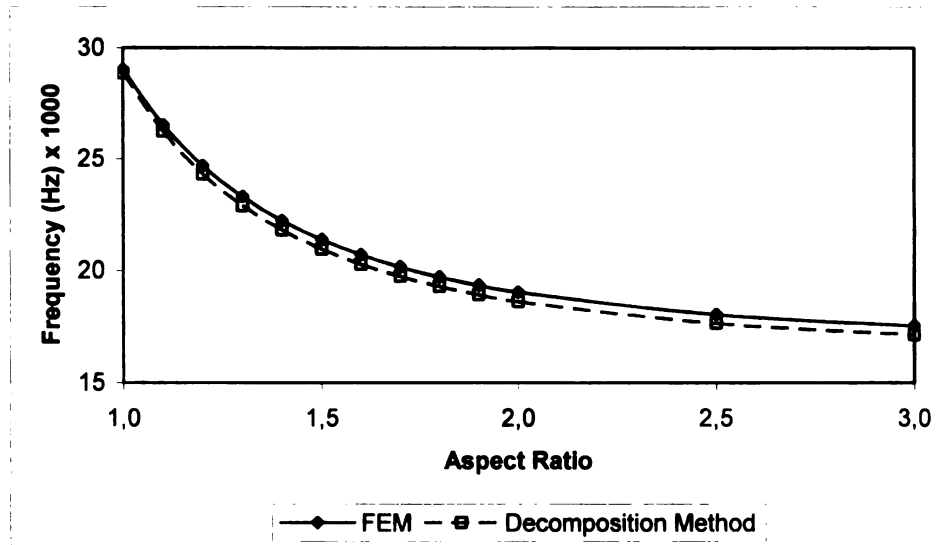


**Figure 3.22. First frequency of free vibration of lattice plate
with supports of Type 3 obtained by (3.43)**

TABLE 3.13. Results for lattice plate with supports of Type 4 obtained by (3.44)

$\lambda = \frac{b}{a}$	First frequency of free vibration $\omega, \left(\frac{1}{\text{sec}}\right)$		
	FEM	DM	ϵ (%)
1.0	25.47	26.44	3.8
1.1	23.82	24.58	3.2
1.2	22.58	23.21	2.8
1.3	21.63	22.17	2.5
1.4	20.89	21.36	2.2
1.5	20.29	20.72	2.1
1.6	19.81	20.20	2.0
1.7	19.42	19.78	1.9
1.8	19.09	19.43	1.8
1.9	18.82	19.14	1.7
2.0	18.58	18.88	1.6
2.5	17.82	18.06	1.3
3.0	17.41	17.60	1.1

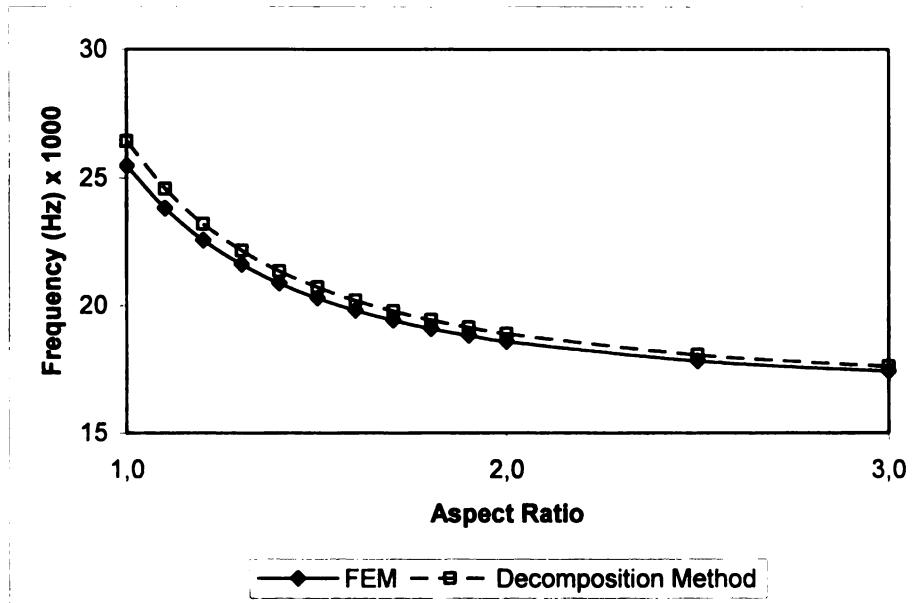
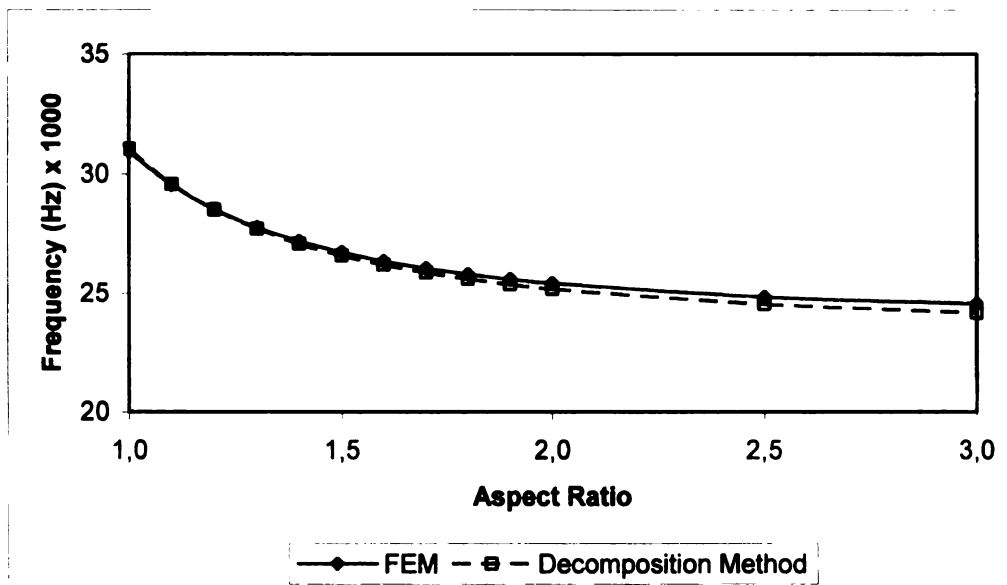


Figure 3.23. First frequency of free vibration of lattice plate with supports of Type 4 obtained by (3.44)

**TABLE 3.14. Results for lattice plate with supports of Type 5
obtained by (3.45)**

$\lambda = \frac{b}{a}$	First frequency of free vibration $\omega, \left(\frac{1}{\text{sec}}\right)$		
	FEM	DM	ε (%)
1.0	30.94	31.06	0.4
1.1	29.56	29.59	0.1
1.2	28.55	28.52	-0.1
1.3	27.79	27.72	-0.3
1.4	27.20	27.09	-0.4
1.5	26.73	26.60	-0.5
1.6	26.36	26.20	-0.6
1.7	26.06	25.88	-0.7
1.8	25.81	25.61	-0.8
1.9	25.60	25.38	-0.9
2.0	25.43	25.18	-1.0
2.5	24.86	24.54	-1.3
3.0	24.56	24.18	-1.5



**Figure 3.24. First frequency of free vibration for lattice plate
with supports of Type 5 obtained by (3.45)**

**TABLE 3.15. Results for lattice plate with supports of Type 6
obtained by (3.46)**

$\lambda = \frac{b}{a}$	First frequency of free vibration $\omega, \left(\frac{1}{\text{sec}}\right)$		
	FEM	DM	ε (%)
1.0	30.94	31.87	3.0
1.1	27.00	27.68	2.5
1.2	24.03	24.56	2.2
1.3	21.78	22.17	1.8
1.4	20.02	20.32	1.5
1.5	18.62	18.86	1.3
1.6	17.49	17.68	1.1
1.7	16.58	16.71	0.8
1.8	15.83	15.92	0.6
1.9	15.20	15.26	0.4
2.0	14.68	14.72	0.3
2.5	13.02	13.02	0.0
3.0	12.19	12.19	0.0

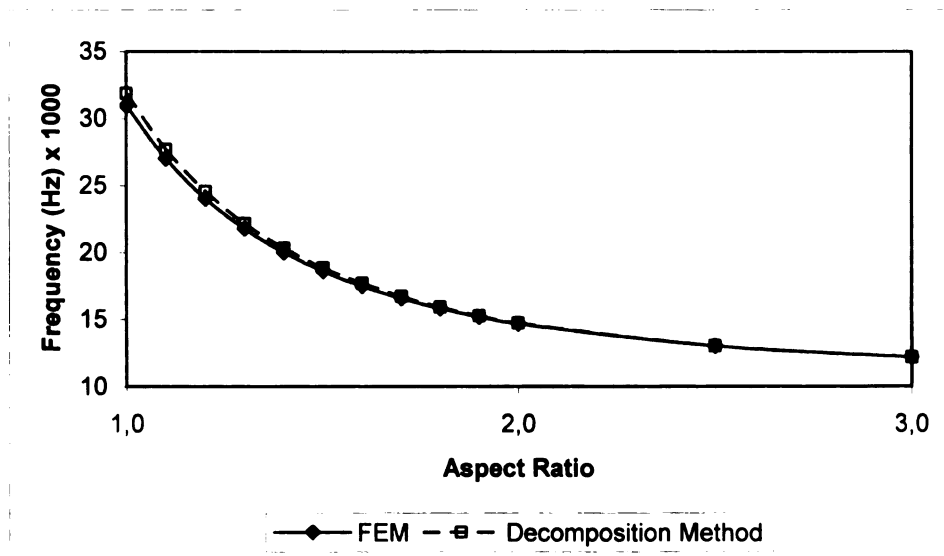


**Figure 3.25. First frequency of free vibration of lattice plate
with supports of Type 6 obtained by (3.46)**

CHAPTER 4

STATIC AND DYNAMIC ANALYSIS OF SINGLE LAYER LATTICE PLATES BY THE DECOMPOSITION METHOD BASED ON FINITE DIFFERENCE DISCRETIZATION

Lattice plates with a regular rectangular grid as shown in Figure 4.1 are investigated in this chapter. The governing equations for bending and free vibrations stated in the finite difference formulation are obtained. The decomposition method is then used to obtain solutions.

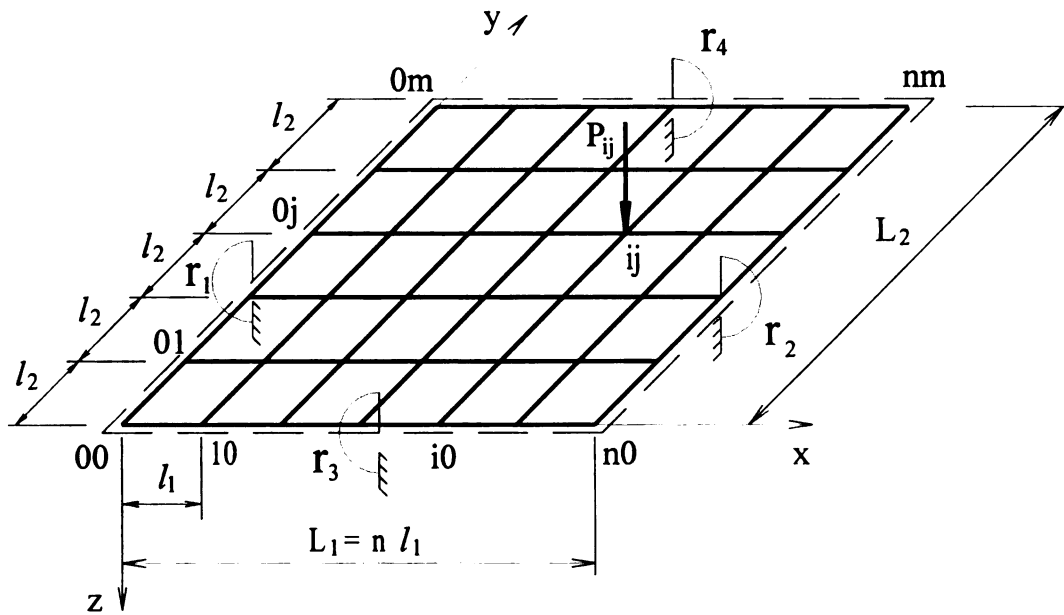


Figure 4.1 Lattice plate with regular rectangular grid

4.1 Notations and the Main Operators of the Finite Difference Formulation

This chapter follows the notations introduced by A. Markov (1911) and used in the works of Bleich and Melan (1936), and Ignatiev (1979).

Assume that $\Phi_x = f(x_i)$ is a function for the discrete argument x defined in the interval $[a, b]$. The discrete argument x takes the values

$$x_i = x_0 + hi, \quad i = 0, \pm 1, \pm 2, \dots \pm n \quad (4.1)$$

where x_0 is a fixed number, and $h > 0$ is the step size. Without any loss of generality it is assumed that $x_0 = 0$ and $h = 1$. All functions Φ_x introduced in this work are assumed to be single-valued, real, and bounded.

The main operator of the finite difference calculus is the difference operator of the first order Δ (the forward difference operator) defined as

$$\Delta_i = \Delta f(x_i) = f(x_i + h) - f(x_i) \quad (4.2)$$

or, in short notation

$$\Delta_i = \Delta f_i = f_{i+1} - f_i, \quad h = 1 \quad (4.3)$$

The backward difference operator is defined as

$$\nabla_i = \nabla f_i = f_i - f_{i-1}, \quad h = 1 \quad (4.4)$$

The forward and backward shift operators, E and E^{-1} , are defined as

$$E f(x_i) = f(x_{i+1}), \quad E^{-1} f(x_i) = f(x_{i-1}) \quad (4.5)$$

or in short notation:

$$E = 1_{i+1}, \quad E^{-1} = 1_{i-1} \quad (4.6)$$

Higher-order shift operators can be written as

$$E^k f = 1_{i+k}, \quad E^{-k} f = 1_{i-k} \quad (4.7)$$

The following identities exist for the difference and shift operators:

$$E = 1 + \Delta, \quad E^{-1} = 1 - \nabla, \quad \Delta f_i = \nabla f_{i+1}, \quad \nabla f_i = \Delta f_{i-1} \quad (4.8)$$

The higher-order differences may be expressed in terms of the following recurrent dependencies:

$$\begin{aligned} \Delta_i^n &= \Delta^{n-1}(\Delta f_i) = \Delta^{n-1} f_{i+1} - \Delta^{n-1} f_i \\ \nabla_i^n &= \nabla^{n-1}(\nabla f_i) = \nabla^{n-1} f_i - \nabla^{n-1} f_{i-1} \end{aligned} \quad (4.9)$$

These differences can be expressed in terms of the values of the function as

$$\begin{aligned} \Delta_i^n &= \sum_{r=0}^n (-1)^r C(n, r) f[i + (n - r)] \\ \nabla_i^n &= \Delta_{i-n}^n \end{aligned} \quad (4.10)$$

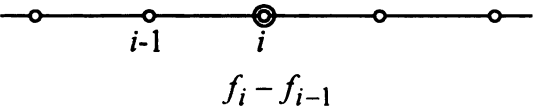
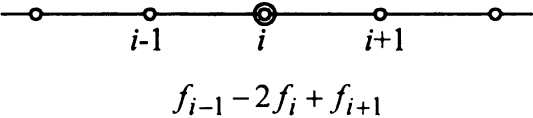
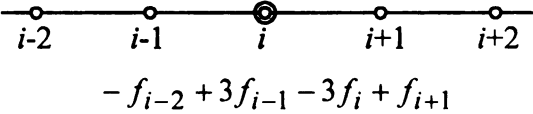
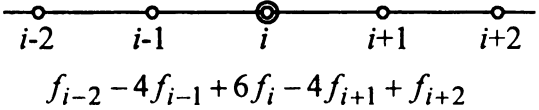
where $C(n, r) = \frac{n^{(r)}}{r!}$ are the binomial coefficients, n is a whole number, and $n^{(r)}$ is a factorial polynomial.

The central difference operators defined in the domain of equidistantly located points $i = 0, \pm 1, \pm 2, \dots, \pm n$ are used to obtain the constitutive equations for a regular lattice plate. The central difference operator can be expressed in terms of the forward difference operator as

$${}^* \Delta_i^n = \left[\Delta_{i+(-1)^n}^{n-1} - \Delta_i^{n-1} \right] (-1)^n = \Delta_{i-1}^{n-2} - 2\Delta_i^{n-2} + \Delta_{i+1}^{n-2} \quad (4.11)$$

The formulae and graphical templates for some lower-order central difference operators are given in Table 4.1.

TABLE 4.1 Lower-order central difference operators

Notation	Graphical template and analytical formulation
${}^* \Delta_i$	
${}^* \Delta_i^2$	
${}^* \Delta_i^3$	
${}^* \Delta_i^4$	

Using the central difference operators yields easier formulations that maintain the symmetric structure of the main equations. Only this type of operator is used in this work, and henceforth the asterisk is omitted for simplicity.

In finite difference calculus, the function G_i is called the sum of f_i if its first difference in the given domain is equal to f_i :

If $\Delta G_i = f_i$, then $S\Delta G_i = G_i = Sf_i$

and

$$S_a^{a+nh} \Delta G_i = |G_i|_a^{a+nh} = S_a^{a+nh} f_i \quad (4.12)$$

The operator of summation, S , is the inverse of the difference operator. Therefore the summation formulae can be obtained by inverting the difference formulae. For the general case of a factorial polynomial

$$\Delta_{i(t)} = t(i-1)^{(t-1)} \quad (4.13)$$

$$S_{i(t)} = \frac{(i+1)^{(t+1)}}{t+1} + C \quad (4.14)$$

The main differences and sums used in this work are given in Appendix C.

Note that the operator of finite difference summation is related to the operator of algebraic summation as follows:

$$S = \sum_a^b \sum_a^{b-1} \quad (4.15)$$

4.2 Constitutive Equations for Regular Rectangular Grid Stated in Finite Difference Form

The finite difference equations obtained from a system of algebraic equations yield a banded coefficient matrix. The first and the last equations of these systems usually serve as the boundary conditions.

Different methods are used to obtain the band structure of the coefficient matrix. Three different approaches using the principle of virtual work, the displacement method and the mixed method are illustrated in this chapter.

4.2.1 Method of Virtual Work

In the first approach, auxiliary states of the system are introduced when localized self-equilibrating groups of forces are applied to any possible statically determinate system obtained from the original system. The virtual-work equation is then constructed for the displacements of the original system.

Example 1. Consider the prismatic beam shown in Figure 4.2(a), loaded at equidistant points. The virtual state shown in Figure 4.2(c) that results in a localized bending moment diagram is used to obtain the main bending equation for the beam in finite differences. Equating the virtual work of external and internal forces gives

$$-y_{i-1} + 2y_i - y_{i+1} = \frac{l^2}{6EI} (M_{i-1} + 4M_i + M_{i+1})$$

Using the finite difference notation this may be expressed as

$$\Delta_i^2 (y_i) = -\frac{l^2}{6EI} (\Delta^2 + 6)_i (M_i) \quad (4.16)$$

From the equilibrium condition for node i , it follows that

$$\frac{M_i - M_{i-1}}{l} - \frac{M_{i+1} - M_i}{l} = P_i$$

or

$$\frac{1}{l} \Delta_i^2 (M_i) = P_i \quad (4.17)$$

The set of equations for all node numbers i yields the full system of algebraic equations for the original problem.

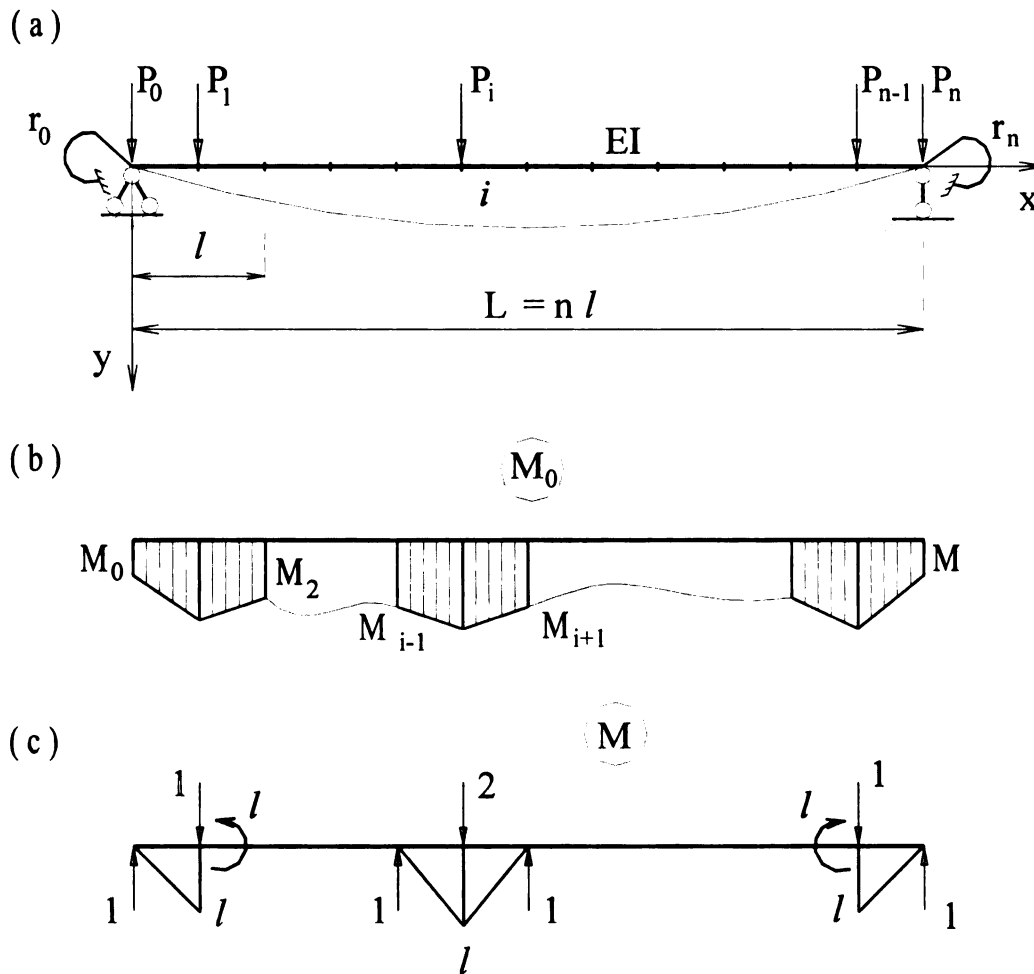


Figure 4.2 The original beam and auxiliary load cases for Example 1

Equations (4.16) and (4.17) can be transformed to yield the finite difference equation with respect to the unknown displacements y_i :

$$\Delta_i^4(y_i) = \frac{l^3}{6EI} (\Delta^2 + 6)_i(P_i) \quad (4.18)$$

Further, (4.16) and (4.17) can also be manipulated to yield expressions for the bending moment in the i^{th} nodal section and the shear force between nodes $i-1$ and i :

$$M_i = \frac{EI}{l^2}(-y_{i-1} + 2y_i - y_{i+1}) + \frac{P_i l}{6} = \frac{EI}{l^2} \Delta^2 y_i + \frac{P_i l}{6} \quad (4.19)$$

$$Q_i = \frac{M_i - M_{i-2}}{l} = \frac{EI}{l^3} \Delta^3 y_i + \frac{1}{6} \Delta P_i \quad (4.20)$$

The limits of the expressions (4.16), (4.17), (4.19), and (4.20)

$$\lim_{l \rightarrow dx} \frac{\Delta^2 y_i}{l^2} = \frac{d^2 y_x}{dx^2}, \quad \lim_{l \rightarrow dx} \left[-\frac{1}{6EI} (\Delta^2 + 6)_i M_i \right] = -M_x$$

$$\lim_{l \rightarrow dx} \frac{P_i}{l} = q_x, \quad \lim_{l \rightarrow dx} \frac{\Delta^2 M_i}{l^2} = \frac{d^2 M_x}{dx^2}$$

$$\lim_{l \rightarrow dx} \frac{\Delta^4 y_i}{l^4} = \frac{d^4 y_x}{dx^4}, \quad \lim_{l \rightarrow dx} \left[\frac{1}{6EI} (\Delta^2 + 6)_i \left(\frac{P_i}{l} \right) \right] = q_x$$

$$\lim_{l \rightarrow dx} \frac{M_i - M_{i-1}}{l} = 0, \quad \lim_{l \rightarrow dx} \left[\frac{EI}{l^3} \Delta^3 y_i + \frac{1}{6} \Delta P_i \right] = EI y'''$$

demonstrate that these relations are the difference analogues of the corresponding differential identities. Note that the inverse transformation from the differential identities to those written in finite difference form does not necessarily yield the original form of the latter.

Example 2. Consider the plate with the regular rectangular grid shown in Figure 4.1 loaded with arbitrary nodal forces. This plate can be treated as a system of orthogonal beams in the two directions i and j . Assume that the elements of the grid have zero

torsional rigidity ($GJ_k = 0$). The auxiliary load state ij in the form of the two groups of self-equilibrating forces shown in Fig. 4.3 is used to obtain constitutive equations.

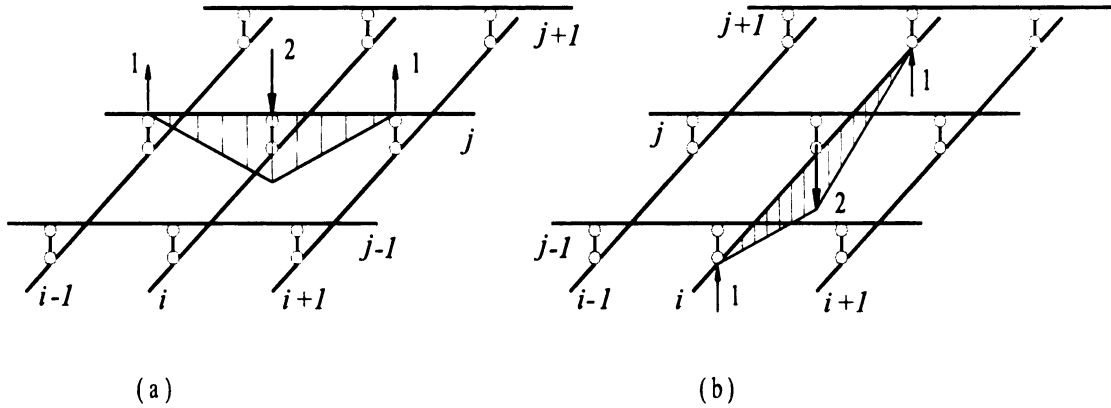


Figure 4.3 Auxiliary load states for the system of orthogonal beams for Example 2

The first group of forces is applied to the j^{th} beam in the statically determinate system obtained from the original system as shown in Fig.4.3 (a):

$$L_{ij}^{(1)}(P) = L_i(P)$$

The second group of forces is applied to the i^{th} beam in the statically determinate system obtained from the original system as shown in Fig.4.3 (b):

$$L_{ij}^{(2)}(P) = L_j(P)$$

The operators in these expressions have the following form

$$L_i(P) = -1_{i-1} + 2_i - 1_{i+1}$$

$$L_j(P) = -1_{j-1} + 2_j - 1_{j+1}$$

Two equations similar to (4.16) are obtained using the virtual work method:

$$\Delta_i^2(Z_{ij}) + \frac{l_1^2}{6EI_1} (\Delta^2 + 6)_i (M_{ij}^I) = 0 \quad (4.21)$$

$$\Delta_j^2(Z_{ij}) + \frac{l_2^2}{6EI_2} (\Delta^2 + 6)_j (M_{ij}^{II}) = 0 \quad (4.22)$$

where M_{ij}^I and M_{ij}^{II} are nodal bending moments in the i^{th} and j^{th} beams, respectively.

The third equation is obtained from the equilibrium condition of the node ij of the system:

$$\frac{\Delta_i^2}{l_1} (M_{ij}^I) + \frac{\Delta_j^2}{l_2} (M_{ij}^{II}) = P_{ij} \quad (4.23)$$

The three equations (4.21), (4.22), and (4.23) form the full system of constitutive finite difference equations resulting from the method of virtual work for the original system.

4.2.2 Displacement Method and Mixed Method

Example 3. Consider the prismatic beam shown in Figure 4.4(a) under the distributed load. The main system of the displacement method shown in Fig. 4.4(b) is formed by introducing nodal constraints in the form of clamps and rollers. The main system of the mixed method shown in Figure 4.4 (c) is formed by introducing nodal vertical supports (rollers), hinges and nodal moments as redundant.

For the triplet of nodes $i-1$, i , and $i+1$ of the main system shown in Figure 4.4 (b), reactions in the i^{th} node due to unit displacements of all restraints obtained from the slope-deflection diagrams are

$$R_i = \frac{12EI}{l^3}(y_{i-1} - 2y_i + y_{i+1}) + \frac{6EI}{l^2}(\varphi_{i-1} - \varphi_{i+1}) - P_i = 0$$

$$M_i = \frac{6EI}{l^2}(y_{i-1} - y_{i+1}) + \frac{2EI}{l}(\varphi_{i-1} + 4\varphi_i - \varphi_{i+1}) + 0 = 0$$

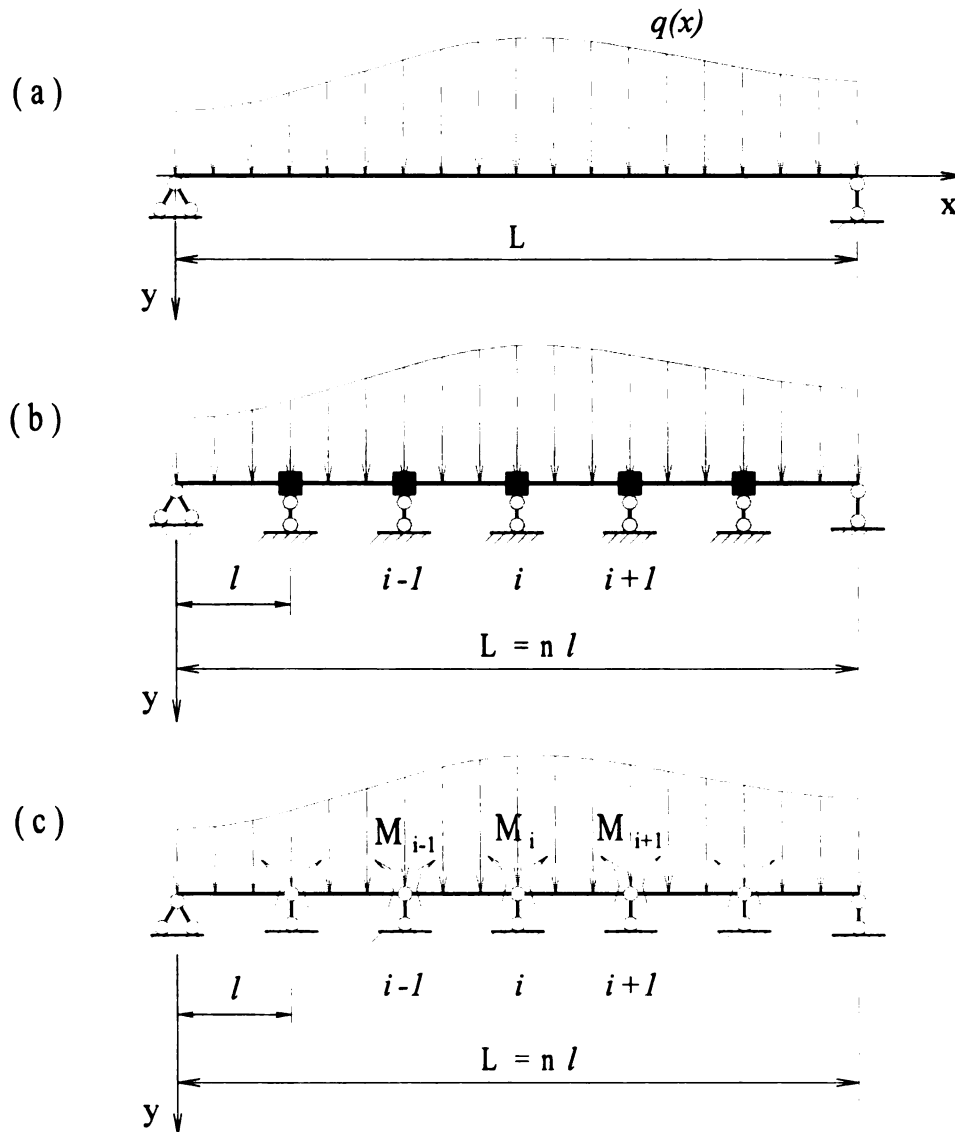


Figure 4.4 The original beam and the main systems of the displacement method and the mixed method for Example 3

The system of finite difference equations of the displacement method can be written in the operator form as

$$\begin{aligned} L_{11}(y_i) + L_{12}(\varphi_i) &= L_1(q) \\ L_{21}(y_i) + L_{22}(\varphi_i) &= L_2(q) \end{aligned} \quad (4.24)$$

where

$$\begin{aligned} L_{11} &= 12EI(1_{i-1} - 2_i + 1_{i+1})/l^3 \\ L_{21} = L_{12} &= 6EI(1_{i-1} - 1_{i+1})/l^2 \\ L_{22} &= 2EI(1_{i-1} + 4_i + 1_{i+1})/l \end{aligned}$$

If $q(x) = q = \text{constant}$, then $L_1(q) = ql/2$, $L_2(q) = 0$.

For the main system of the mixed method (Figure 4.4 c) reactions in the i^{th} node due to the unit displacements and unit moments in the triplet of nodes $i-1$, i , and $i+1$ are

$$\begin{aligned} R_i &= 0 + \frac{1}{l}(M_{i-1} - 2M_i + M_{i+1}) - P_i = 0 \\ \varphi_i &= \frac{1}{l}(y_{i-1} - 2y_i + y_{i+1}) + \frac{l}{6EI}(M_{i-1} + 4M_i + M_{i+1}) = 0 \end{aligned}$$

This system can be written in the operator form as

$$\begin{aligned} L_{11}(y_i) + L_{12}(M_i) &= L_1(q) \\ L_{21}(y_i) + L_{22}(M_i) &= L_2(q) \end{aligned} \quad (4.25)$$

where

$$\begin{aligned} L_{11} &= 0 \\ L_{12} &= (1_{i-1} - 2_i + 1_{i+1})/l^2 \end{aligned}$$

$$L_{21} = (1_{i-1} - 2_i + 1_{i+1})/l$$

$$L_{22} = \frac{l}{6EI} (1_{i-1} + 4_i + 1_{i+1})$$

Generalization of this approach on the regular system of orthogonal beams in Example 2 yields systems of finite difference equations similar to (4.24) and (4.25). The system of the displacement method has the form

$$\begin{aligned} L_{11}(Z_{ij}) + L_{12}(\varphi_{ij}^{(y)}) + L_{13}(\varphi_{ij}^{(x)}) &= L_1(P_{ij}) \\ L_{21}(Z_{ij}) + L_{22}(\varphi_{ij}^{(y)}) + 0 &= 0 \\ L_{31}(Z_{ij}) + 0 + L_{33}(\varphi_{ij}^{(x)}) &= 0 \end{aligned} \quad (4.26)$$

where

$$\begin{aligned} L_{11} &= 2(A\Delta_i^2 + B\Delta_j^2), \quad A = 6EI/l_1^3, \quad B = 6EI_2/l_2^3, \quad L_1 = -1 \\ L_{12} = L_{21} &= \frac{6EI_1}{l_1^2} (1_{i-1} - 1_{i+1}), \quad L_{13} = L_{31} = \frac{6EI_2}{l_2^2} (1_{j-1} - 1_{j+1}) \\ L_{22} &= \frac{2EI_1}{l_1} (\Delta^2 + 6)_j, \quad L_{33} = \frac{2EI_2}{l_2} (\Delta^2 + 6)_j \end{aligned} \quad (4.27)$$

For the main system of the mixed method the finite difference equations have the form

$$\begin{aligned} L_{11}(M_{ij}^I) + 0 + L_{13}(z_{ij}) &= 0 \\ 0 + L_{22}(M_{ij}^{II}) + L_{23}(z_{ij}) &= 0 \\ L_{31}(M_{ij}^I) + L_{32}(M_{ij}^{II}) + L_{33}(z_{ij}) &= L(P_{ij}) \end{aligned} \quad (4.28)$$

where

$$\begin{aligned}
L_{11} &= (\Delta^2 + 6)_i / Al_1^2, \quad L = -1 \\
L_{12} &= L_{21} = 0 \\
L_{22} &= (\Delta^2 + 6)_i / Bl_1^2, \quad L_{23} = L_{32} = \Delta_i^2 / l_2, \\
L_{13} &= L_{31} = \Delta_i^2 / l_1, \quad L_{33} = 0
\end{aligned} \tag{4.28a}$$

Equations (4.28) written in the full form are identical to equations (4.21), (4.22), and (4.23) obtained earlier using the virtual work method.

4.3 Governing Finite Difference Bending Equation for Lattice Plate

The systems of equations in (4.26) and (4.28) include three unknowns. Using operator transformations, both systems can be reduced to one equation in one unknown. System (4.28) can be transformed to one equation with respect to any of the three unknowns M_{ij}^I , M_{ij}^{II} , or Z_{ij} :

$$(L_{11}L_{23}L_{32} + L_{22}L_{13}L_{31})(M_{ij}^I) = L_{22}L_{13}L(P_{ij}) \tag{4.29a}$$

$$(L_{11}L_{23}L_{32} + L_{22}L_{13}L_{31})(M_{ij}^{II}) = L_{11}L_{23}L(P_{ij}) \tag{4.29b}$$

$$(L_{11}L_{23}L_{32} + L_{22}L_{13}L_{31})(z_{ij}) = L_{11}L_{22}L(P_{ij}) \tag{4.29c}$$

Similarly the system of equations (4.26) is reduced to the equation

$$L(Z_{ij}) = (L_{11}L_{23}L_{33} + L_{13}^2L_{22} + L_{12}^2L_{33})(Z_{ij}) = L_{22}L_{33}(P_{ij}) \tag{4.30}$$

Substituting the corresponding expressions for operators L into equations (4.29c) and (4.30) and performing transformations yields the same equation

$$\left\{ A \left[\Delta_i^4 (\Delta^2 + 6)_j \right] + B \left[\Delta_j^4 (\Delta^2 + 6)_i \right] \right\} (z_{ij}) = \left[(\Delta^2 + 6)_i (\Delta^2 + 6)_j \right] (P_{ij}) \quad (4.31)$$

where $A = 6EI_1/l_1^3$ and $B = 6EI_2/l_2^3$. Equation (4.31) is a finite difference analogue of a differential bending equation of the thin isotropic plate.

The system of equations resulting from the mixed method is more general since it allows the governing equation to be obtained both in terms of internal forces and displacements.

Accounting for torsion and shear, the operators (4.27) of the finite difference equation (4.26) become

$$\begin{aligned} L_{11} &= (A_1 \Delta_i^2 + A_2 \Delta_j^2), \quad L = -1 \\ L_{12} &= L_{21} = B_1 L_i, \quad L_{13} = L_{31} = B_2 L_j \\ L_{22} &= (D_1 \Delta_i^2 - F_2 \Delta_j^2 + G_1), \quad L_{33} = (D_2 \Delta_j^2 - F_1 \Delta_i^2 + G_2) \end{aligned} \quad (4.32)$$

where

$$\begin{aligned} \eta_1 &= \frac{EI_1 \bar{\gamma}_1}{l_1^2}, \quad \eta_2 = \frac{EI_2 \bar{\gamma}_2}{l_2^2} \\ A_1 &= \frac{12EI_1}{l_1^3} \frac{1}{1+12\eta_1}, \quad A_2 = \frac{12EI_2}{l_2^3} \frac{1}{1+12\eta_2} \\ B_1 &= \frac{1}{2} A_1 l_1, \quad B_2 = \frac{1}{2} A_2 l_2 \\ D_1 &= \frac{2EI_1}{l_1} \frac{(1-6\eta_1)}{1+12\eta_1}, \quad D_2 = \frac{2EI_2}{l_2} \frac{(1-6\eta_2)}{1+12\eta_2} \\ G_1 &= A_1 l_1^2, \quad G_2 = A_2 l_2^2, \quad F_1 = \frac{GI_{k1}}{l_1}, \quad F_2 = \frac{GI_{k2}}{l_2} \\ L_i &= 1_{i-1} - 1_{i+1}, \quad L_j = 1_{j-1} - 1_{j+1} \end{aligned} \quad (4.33)$$

where $\bar{\gamma}_1$ and $\bar{\gamma}_2$ are the engineering shear strains. If shear deformations are neglected

i.e., $\bar{\gamma}_1 = \bar{\gamma}_2 = 0$, then the coefficients in (4.33) become

$$\begin{aligned}
 \eta_1 &= \eta_2 = 0 \\
 A_1 &= \frac{12EI_1}{l_1^3}, \quad A_2 = \frac{12EI_2}{l_2^3}, \quad B_1 = \frac{1}{2}A_1l_1, \quad B_2 = \frac{1}{2}A_2l_2 \\
 D_1 &= \frac{2EI_1}{l_1} = A_1 \frac{l_1^2}{6}, \quad D_2 = \frac{2EI_2}{l_2} = A_2 \frac{l_2^2}{6} \\
 G_1 &= A_1 l_1^2, \quad G_2 = A_2 l_2^2, \quad F_1 = \frac{GI_{k1}}{l_1}, \quad F_2 = \frac{GI_{k2}}{l_2} \\
 L_i &= 1_{i-1} - 1_{i+1}, \quad L_j = 1_{j-1} - 1_{j+1}
 \end{aligned} \tag{4.34}$$

Substituting (4.34) into (4.30) and simplifying yields

$$\begin{aligned}
 &\left\{ -6 \left[\left(\frac{F_2 A_2}{l_1^2 A_1} \right) \Delta_j^6 + \left(\frac{F_1 A_1}{l_2^2 A_2} \right) \Delta_i^6 \right] + \frac{72}{l_1^2 l_2^2} \left[F_1 \left(\frac{l_1^2}{6} - \frac{F_2}{A_2} \right) \Delta_i^4 \Delta_j^2 \right. \right. \\
 &+ \left. \left. F_2 \left(\frac{l_2^2}{6} - \frac{F_1}{A_1} \right) \Delta_i^2 \Delta_j^4 + (F_1 l_2^2 + F_2 l_1^2) \Delta_i^2 \Delta_j^2 \right] + A_1 \Delta_i^4 (\Delta^2 + 6)_j \right. \\
 &+ \left. A_2 \Delta_j^4 (\Delta^2 + 6)_i \right\} (z_{ij}) = \left\{ \frac{12}{l_1^2 l_2^2} \left[- \left(\frac{l_2^2 F_2}{A_1} \right) \Delta_j^4 - \left(\frac{l_1^2 F_1}{A_2} \right) \Delta_i^4 \right. \right. \\
 &+ \left. \left. \frac{6F_1 F_2}{A_1 A_2} \Delta_i^2 \Delta_j^2 - \frac{6F_1 l_2^2}{A_1} \Delta_j^2 - \frac{6F_1 l_1^2}{A_2} \Delta_i^2 \right] + 2 \left[(\Delta^2 + 6)_i (\Delta^2 + 6)_j \right] \right\} (P_{ij}) \tag{4.35}
 \end{aligned}$$

which is the finite difference analogue of the corresponding differential equation.

4.4 Boundary Conditions

Example 4. In this example the boundary conditions for the cantilever beam with the left end fixed and the right end free (Figure 4.5) are obtained.

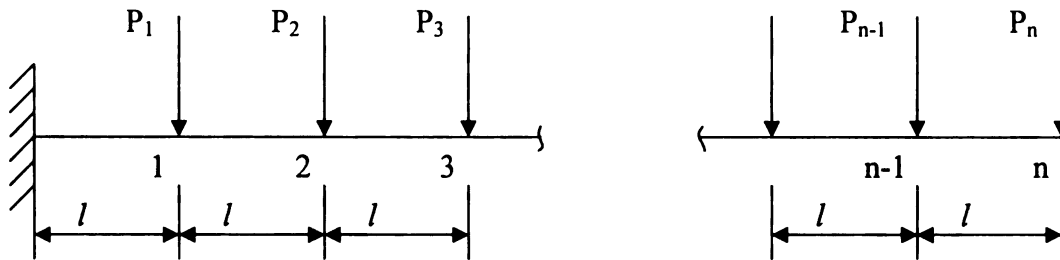


Figure 4.5 Boundary conditions for the beam in Example 4

The system of equations resulting from the displacement method for this case has the following form

$$\left. \begin{aligned} R_1 &= \frac{12EI}{l^3}(2y_1 - y_2) - \frac{6EI}{l^2}\varphi_2 - P_1 = 0 \\ M_1 &= -\frac{6EI}{l^2}(y_2) + \frac{2EI}{l}(4\varphi_1 + \varphi_2) = 0 \end{aligned} \right\} \text{node 1}$$

.....

$$\left. \begin{aligned} R_i &= \frac{12EI}{l^3}(-y_{i-1} + 2y_i - y_{i+1}) + \frac{6EI}{l^2}(-\varphi_{i-1} + \varphi_{i+1}) - P_i = 0 \\ M_i &= -\frac{6EI}{l^2}(-y_{i-1} + y_{i+1}) + \frac{2EI}{l}(\varphi_{i-1} + 4\varphi_i + \varphi_{i+1}) = 0 \end{aligned} \right\} \text{interior node } i$$

... ..

$$\left. \begin{aligned} R_n &= \frac{12EI}{l^3}(y_n - y_{n-1}) + \frac{6EI}{l^2}(-\varphi_n + \varphi_{n-1}) - P_n = 0 \\ M_n &= -\frac{6EI}{l^2}(y_n - y_{n-1}) + \frac{2EI}{l}(2\varphi_n + \varphi_{n-1}) = 0 \end{aligned} \right\} \text{node } n$$

The general case equations for an interior node i apply to all nodes except for nodes 1 and n . Therefore, the two equations corresponding to nodes 1 and n are the boundary conditions for the system. When changing from the system of two equations to one equation with one unknown function, only one boundary equation containing one unknown function for each end of the beam needs to be obtained.

For the left support, the first equation of the system for node 1 yields

$$\varphi_2 = \frac{l^2}{6EI} \left[P_1 - \frac{12EI}{l^3}(4y_1 + y_2) \right]$$

Substituting it into the second equation for node 1 yields

$$\varphi_1 = \frac{l^2}{24EI} \left[-P_1 - \frac{6EI}{l^3}(4y_1 + y_2) \right]$$

Substituting these expressions for φ_1 and φ_2 into the first and the second equations for node 2 produces two expressions for φ_3 , and equating these yields one boundary equation with one unknown function:

$$9y_1 - 4.5y_2 + y_3 = \frac{l^3}{12EI}(7P_1 + P_2)$$

For the right end of the beam the equations for R_n and R_{n-1} yield

$$\varphi_{n-1} = \frac{l^2}{6EI} \left[P_n - \frac{6EI}{l^3} \varphi_n - \frac{12EI}{l^3} (y_n - y_{n-1}) \right]$$

$$\varphi_{n-2} = \frac{l^2}{6EI} \left[P_n - \frac{6EI}{l^3} \varphi_n - \frac{12EI}{l^3} (y_n - 2y_{n-1} + y_{n-2}) \right]$$

Substituting these expressions into the equations for M_n and M_{n-1} and equating the resulting expressions for φ_n yields the boundary equation

$$\frac{6EI}{l^3} (y_n - 2y_{n-1} + y_{n-2}) = 6P_n + P_{n-1}$$

Boundary conditions for lattice plates can be constructed similarly since at every edge of the boundary either a displacement or a force has a fixed value. Using the operator transformation allows the original system of finite difference equations to be reduced to one equation similar to the corresponding differential equation for a continuous structure. This transformation allows the same methods and algorithms that are used for the solution of differential equations, such as the decomposition method, to be used.

4.5 Solution of the Bending of Lattice Plates with Orthogonal Grids

Consider the rectangular lattice plate shown in Figure 4.1 formed by two orthogonal families of rods that are parallel to the edges of the plate. The plate has elastic supports along the edges. The external load is applied at the nodes of the grid. Assuming that the torsional rigidities of the elements of the grid are negligible, the bending equation has the form (4.31). This equation can be written in the non-dimensional form

$$\left[A_1 \Delta_i^4 (\Delta_j^2 + 6_j) + A_2 \Delta_j^4 (\Delta_i^2 + 6_i) \right] (\tilde{w}_{ij}) = (\Delta_i^2 + 6_i) (\Delta_j^2 + 6_j) (\tilde{P}_{ij}) \quad (4.36)$$

where

$$A_1 = \frac{6EI_1 l_0^3}{EI_0 l_1^3}, \quad A_2 = \frac{6EI_2 l_0^3}{EI_0 l_2^3}, \quad \tilde{w}_{ij} = \frac{1}{w_0} w_{ij}, \quad \tilde{P}_{ij} = \frac{P_{ij} l_0^3}{EI_0 w_0} \quad (4.37)$$

A_1 and A_2 are dimensionless coefficients, \tilde{w}_{ij} is the dimensionless displacement of the node ij , and \tilde{P}_{ij} is the dimensionless load. The subscript 0 denotes a reference value of the corresponding function.

According to the decomposition method the original problem (4.36) can be replaced by the following three auxiliary problems:

$$1. \quad 6A_1 \Delta_i^4 (\tilde{w}_{ij}^I) = f_1(i, j) \quad (4.38)$$

$$2. \quad 6A_2 \Delta_j^4 (\tilde{w}_{ij}^{II}) = f_2(i, j) \quad (4.39)$$

$$3. \quad \left[A_1 (\Delta_i^4 \Delta_j^2) + A_2 (\Delta_i^2 \Delta_j^4) \right] (\tilde{w}_{ij}^{III}) = (\Delta_i^2 + 6_i) (\Delta_j^2 + 6_j) (\tilde{P}_{ij}) - f_1(i, j) - f_2(i, j) \quad (4.40)$$

where $f_1(i, j)$ and $f_2(i, j)$ are unknown functions of discrete arguments. Solutions to these auxiliary problems must be subject to condition

$$\tilde{w}_{ij}^I = \tilde{w}_{ij}^{II} = \tilde{w}_{ij}^{III} \quad (4.41)$$

Equations (4.38) and (4.39) can be regarded as the bending equations of the non-interconnected beams in the directions i and j . The beams have elastic supports in the form of rotational springs. Boundary conditions for the first auxiliary problem for the beam parallel to the x -axis (i -direction) can be written as

$$\tilde{w}_{0j}^I = 0$$

$$\tilde{w}_{1,j}^I (5 + 4\tilde{k}_1) - \tilde{w}_{2,j}^I (4 + 0.5\tilde{k}_1) + \tilde{w}_{3,j}^I = \frac{1}{A_1} [\tilde{P}_{1,j} (4 - 0.5\tilde{k}_1) + \tilde{P}_{2,j}] \quad (4.42a)$$

$$\text{at } i = 0$$

$$\tilde{w}_{nj}^I = 0$$

$$\tilde{w}_{n-1,j}^I (5 + 4\tilde{k}_1) - \tilde{w}_{n-2,j}^I (4 + 0.5\tilde{k}_1) + \tilde{w}_{n-3,j}^I = \frac{1}{A_1} [\tilde{P}_{n-1,j} (4 - 0.5\tilde{k}_1) + \tilde{P}_{n-2,j}] \quad (4.42b)$$

$$\text{at } i = n$$

where $\tilde{k}_1 = (1 + r_1 l_1 / 3EI_1)^{-1}$ is the dimensionless stiffness coefficients of the elastic supports. Boundary conditions for the second auxiliary problem have a similar form with corresponding subscripts and superscripts.

An approximate solution to the problem is found by approximating the functions of discrete argument $f_1(i, j)$ and $f_2(i, j)$. For the case of symmetric load it is assumed that

$$\begin{aligned} f_1(i, j) &= \psi_1(j) - \psi_2(j) \left[\left(i^{(2)} + i^{(1)} - ni^{(1)} \right) \frac{4}{m^2} - 1 \right] \\ f_2(i, j) &= \psi_1(i) - \psi_2(i) \left[\left(j^{(2)} + j^{(1)} - mj^{(1)} \right) \frac{4}{m^2} - 1 \right] \end{aligned} \quad (4.43)$$

where $\psi_1(j), \psi_2(j), \psi_1(i)$, and $\psi_2(i)$ are arbitrary functions, and $i^{(t)}$, and $j^{(t)}$ are factorial polynomials: $i^{(t)} = i(i-1)(i-2)\dots(i-t+1)$, $j^{(t)} = j(j-1)(j-2)\dots(j-t+1)$.

The first auxiliary problem can be considered as one-dimensional and can be written in the following form

$$6A_1 \Delta_i^4 (\tilde{w}_{ij}^I) = D_1 + D_2 i^{(1)} + D_3 i^{(2)} \quad (4.44)$$

where $D_1 = \psi_1(j) + \psi_2(j)$, $D_2 = (n-1)\frac{4}{n^2}\psi_2(j)$, $D_3 = -\frac{4}{n^2}\psi_2(j)$.

Using formula (4.14), the solution to the first auxiliary problem is

$$\tilde{w}_{ij}^I = \frac{1}{6A_1} \left[D_1 \frac{i^{(4)}}{24} + D_2 \frac{(i+2)^{(5)}}{120} + D_3 \frac{(i+2)^{(6)}}{360} \right] + C_1 \frac{i^{(3)}}{6} + C_2 \frac{i^{(2)}}{2} + C_3 i^{(1)} + C_4 \quad (4.45)$$

with the arbitrary constants C_i to be obtained from the boundary conditions (4.42).

Comparing equation (4.44) of the first auxiliary problem with the known bending equation of the beam loaded at equidistantly located points

$$A_1 \Delta_i^4 (\tilde{w}_{ij}^I) = (\Delta_i^2 + 6_i) (\tilde{P}_{ij}^I)$$

implies that

$$\frac{1}{6} [D_1 + D_2 i^{(1)} + D_3 i^{(2)}] = (\Delta_i^2 + 6_i) (\tilde{P}_{ij}^I)$$

Solving for \tilde{P}_{ij}^I yields

$$\tilde{P}_{ij}^I = \frac{1}{36} \left[\left(D_1 - \frac{1}{3} D_3 \right) + D_2 i^{(1)} + D_3 i^{(2)} \right]$$

From the first condition of (4.42) it follows that $C_4 = 0$. The other three conditions yield the following system of equations:

$$C_1 + C_2 (-0.5\tilde{k}_1 - 1) + C_3 (3\tilde{k}_1) C_1 = \frac{1}{36A_1} \left[D_1 (5 - 0.5\tilde{k}_1) + D_2 (6 - \tilde{k}_1) + D_3 \left(\frac{1}{3} + \frac{1}{6} \tilde{k}_1 \right) \right]$$

$$C_1 \frac{n^{(3)}}{6} + C_2 \frac{n^{(2)}}{2} + C_3 n = \frac{1}{36} \left[D_1 \frac{n^{(4)}}{4} + D_2 \frac{n^{(5)}}{20} + D_3 \frac{n^{(6)}}{60} \right]$$

$$\begin{aligned}
& C_1 \left[\frac{(n-1)^{(3)}}{6} (5 + 4\tilde{k}_1) - (4 + 0.5\tilde{k}_1) \frac{(n-2)^{(3)}}{6} + \frac{(n-3)^{(3)}}{6} \right] \\
& + C_2 \left[\frac{(n-1)^{(2)}}{2} (5 + 4\tilde{k}_1) - (4 + 0.5\tilde{k}_1) \frac{(n-2)^{(2)}}{2} + \frac{(n-3)^{(3)}}{2} \right] \\
& + C_3 \left[(n-1)(5 + 4\tilde{k}_1) - (4 + 0.5\tilde{k}_1)(n-2) + (n-3) \right] \\
& = \frac{1}{36A_1} \left\{ D_1 \left[5 - 0.5\tilde{k}_1 - (5 + 4\tilde{k}_1) \frac{(n-1)^{(4)}}{4} + (4 + 0.5\tilde{k}_1) \frac{(n-2)^{(4)}}{4} - \frac{(n-3)^{(4)}}{4} \right] \right. \\
& + D_2 \left[(4 - 0.5\tilde{k}_1)(n-1) + (n+2) - (5 + 4\tilde{k}_1) \frac{(n-1)^{(5)}}{20} + (4 + 0.5\tilde{k}_1) \frac{(n-2)^{(5)}}{20} - \frac{(n-3)^{(5)}}{20} \right] \\
& + D_3 \left[(4 - 0.5\tilde{k}_1) \left((n-1)^{(2)} - \frac{1}{3} \right) + (n+2)^{(2)} - \frac{1}{3} - (5 + 4\tilde{k}_1) \frac{(n-1)^{(6)}}{60} \right. \\
& \left. \left. + (4 + 0.5\tilde{k}_1) \frac{(n-2)^{(6)}}{60} - \frac{(n-3)^{(6)}}{60} \right] \right\}
\end{aligned}$$

For convenience this system can be written in the matrix form

$$[B_n] \{C^I\} = \frac{1}{36A_1} [G_n] \{D^I\} \quad (4.46)$$

In this equation $\{C^I\} = [C_1 \ C_2 \ C_3]^T$, $\{D^I\} = [D_1 \ D_2 \ D_3]^T$, and $[B_n]$ and

$[G_n]$ are the matrices of coefficients of C_i and D_i correspondingly. The elements of

these matrices are given in Appendix D. From (4.46)

$$\{C^I\} = [B_n]^{-1} [G_n] \{D^I\} \frac{1}{36A_1}$$

and substituting it into (4.45) yields the following expression for the dimensionless deflection function

$$\tilde{w}_{ij}^I = \{D^I\}^T \{f_i\} \quad (4.47)$$

where

$$\begin{aligned} \{f_i\} &= \frac{1}{36A_1} \left(\{a_i\} + [G_n]^T [B_n^{-1}]^T \{b_i\} \right) \\ \{a_i\} &= \left[\frac{i^{(4)}}{4} \quad \frac{(i+2)^{(5)}}{20} \quad \frac{(i+2)^{(6)}}{60} \right]^T \\ \{b_i\} &= \left[\frac{i^{(3)}}{6} \quad \frac{i^{(2)}}{2} \quad i^{(1)} \right]^T \end{aligned} \quad (4.48)$$

Similarly, the solution for the second auxiliary problem is

$$\tilde{w}_{ij}^{II} = \{D^{II}\}^T \{f_j\} \quad (4.49)$$

where

$$\begin{aligned} \{D^{II}\} &= [\tilde{D}_1 \quad \tilde{D}_2 \quad \tilde{D}_3]^T \\ \tilde{D}_1 &= \psi_1(i) + \psi_2(i), \quad \tilde{D}_2 = (m-1) \frac{4}{m^2} \psi_2(i), \quad \tilde{D}_3 = -\frac{4}{m^2} \psi_2(i) \end{aligned} \quad (4.50)$$

$$\{f_j\} = \frac{1}{36A_2} \left(\{a_j\} + [G_m]^T [B_m^{-1}]^T \{b_j\} \right)$$

Expressions (4.47) and (4.49) with respect to (4.44) and (4.50) can be written in the form

$$\begin{aligned}\tilde{w}_{ij}^I &= \varphi_1(i) \psi_1(j) + \varphi_2(i) \psi_2(j) \\ \tilde{w}_{ij}^{II} &= \varphi_1(j) \psi_1(i) + \varphi_2(j) \psi_2(i)\end{aligned}\tag{4.51}$$

where

$$\begin{aligned}\varphi_1(i) &= [d_1] \{f_i\}, \quad \varphi_2(i) = [d_{1,n}] \{f_j\} \\ \varphi_1(j) &= [d_1] \{f_j\}, \quad \varphi_2(j) = [d_{1,m}] \{f_j\}\end{aligned}\tag{4.52}$$

$$[d_1] = [1 \quad 0 \quad 0], \quad [d_{1,n}] = \left[1 \quad \frac{4}{n^2}(n-1) \quad -\frac{4}{n^2} \right]$$

$$[d_{1,m}] = \left[1 \quad \frac{4}{m^2}(m-1) \quad -\frac{4}{m^2} \right]$$

Accounting for the symmetry of the system, the arbitrary functions $\psi_1(i)$ and $\psi_2(i)$ can be assumed as follows:

$$\begin{aligned}\psi_1(i) &= \alpha_1 \varphi_1(i) + \alpha_2 \varphi_2(i), \quad \psi_2(i) = \alpha_3 \varphi_1(i) + \alpha_4 \varphi_2(i) \\ \psi_1(j) &= \tilde{\alpha}_1 \varphi_1(j) + \tilde{\alpha}_2 \varphi_2(j), \quad \psi_2(j) = \tilde{\alpha}_3 \varphi_1(j) + \tilde{\alpha}_4 \varphi_2(j)\end{aligned}\tag{4.53}$$

Satisfying $\tilde{w}_{ij}^I = \tilde{w}_{ij}^{II}$ from (4.41) implies that

$$\tilde{\alpha}_1 = \alpha_1, \quad \tilde{\alpha}_2 = \alpha_2, \quad \tilde{\alpha}_3 = \alpha_3, \quad \tilde{\alpha}_4 = \alpha_4\tag{4.54}$$

Coefficients α are determined from the third auxiliary problem. Introducing the discrepancy function $\Phi(i, j)$, the third auxiliary problem can be written as

$$\begin{aligned} \Phi(i, j) = & \left[A_1 (\Delta_i^4 \Delta_j^2) + A_2 (\Delta_i^2 \Delta_j^4) \right] (\tilde{w}_{ij}^{III}) - \left[(\Delta_i^2 + 6_i)(\Delta_j^2 + 6_j) \right] (\tilde{P}_{ij}) \\ & + f_1(i, j) + f_2(i, j) = 0 \end{aligned} \quad (4.55)$$

Assuming $\tilde{P}_{ij} = P = \text{constant}$ and performing algebraic manipulations yields

$$\begin{aligned} \Phi(i, j) = & \alpha_1 \left[A_1 \Delta_j^4 \varphi_1(i) \Delta_i^2 \varphi_1(j) + A_2 \Delta_i^2 \varphi_1(i) \Delta_j^4 \varphi_1(j) \right] \\ & + \alpha_2 \left[A_1 \Delta_j^4 \varphi_2(i) \Delta_i^2 \varphi_1(j) + A_2 \Delta_i^2 \varphi_2(i) \Delta_j^4 \varphi_1(j) \right] \\ & + \alpha_3 \left[A_1 \Delta_j^4 \varphi_2(i) \Delta_i^2 \varphi_2(j) + A_2 \Delta_i^2 \varphi_1(i) \Delta_j^4 \varphi_2(j) \right] \\ & + \alpha_4 \left[A_1 \Delta_j^4 \varphi_2(i) \Delta_i^2 \varphi_2(j) + A_2 \Delta_i^2 \varphi_2(i) \Delta_j^4 \varphi_2(j) \right] \\ & + \alpha_1 [\varphi_1(i) + \varphi_1(j)] + \alpha_2 [\varphi_1(i) + \varphi_1(j)] f(i, n) \\ & + \alpha_3 [\varphi_2(j) + \varphi_1(i)] f(j, m) \\ & + \alpha_4 [-\varphi_2(i)] f(j, m) - \varphi_2(j) f(i, n) - 36P = 0 \end{aligned} \quad (4.56)$$

where $f(i, n) = \left(i^{(2)} + i^{(1)} - ni^{(1)} \right) \frac{4}{n^2} - 1$ and $f(j, m) = \left(j^{(2)} + j^{(1)} - mj^{(1)} \right) \frac{4}{m^2} - 1$

The third auxiliary problem is solved by setting $\Phi(i, j)$ and some of its even lower differences to zero at the center of the plate:

$$\begin{aligned} \Phi(i, j) = 0, \quad \Delta_i^2 [\Phi(i, j)] = 0, \quad \Delta_j^2 [\Phi(i, j)] = 0, \quad \Delta_i^2 \Delta_j^2 [\Phi(i, j)] = 0 \\ i = n/2, \quad j = m/2 \end{aligned} \quad (4.57)$$

The arbitrary constants α_i are obtained by solving the resulting system of linear algebraic equations. The values of α_i are then substituted into the expression (4.53).

Using (4.53), (4.54) and (4.41), the equation for the deflection function can be written as

$$\tilde{w}_{ij} = [\alpha] \begin{bmatrix} \varphi_i(i) & \varphi_i(j) \end{bmatrix} \quad (4.58)$$

where

$$[\alpha] = [\alpha_1 \quad \alpha_2 \quad \alpha_3 \quad \alpha_4]$$

$$\begin{bmatrix} \varphi(i) & \varphi(j) \end{bmatrix} = \begin{bmatrix} \varphi_1(i) & \varphi_1(j) \\ \varphi_2(i) & \varphi_1(j) \\ \varphi_1(i) & \varphi_2(j) \\ \varphi_1(i) & \varphi_2(j) \end{bmatrix} \quad (4.59)$$

The value of bending moment in any rod of the lattice can be found using the expressions

$$M_{ij}^I = \frac{EI}{l} (-w_{i-1} + 2w_i - w_{i+1}) + \frac{P_{ij}}{6}$$

$$M_{ij}^{II} = \frac{EI}{l} (-w_{j-1} + 2w_j - w_{j+1}) + \frac{P_{ij}}{6} \quad (4.60)$$

Using notation (4.37), the equation for the dimensionless bending moment in any j^{th} beam in the i^{th} direction can be written as

$$\tilde{M}_{ij}^I = -(\tilde{w}_{i-1,j} - 2\tilde{w}_{i,j} + \tilde{w}_{i+1,j}) + \frac{1}{A_1} \tilde{P}_{ij}^I \quad (4.61)$$

where

$$\tilde{M}_{ij}^I = M_{ij} \left(\frac{l_1^2}{w_0 EI_1} \right), \quad A_1 = \frac{6l_0^3}{EI_0 w_0} \quad (4.62)$$

In equation (4.61), \tilde{P}_{ij}^I is the nodal load applied to the beams in the first direction (i).

Using (4.44) and (4.53)

$$\tilde{P}_{ij}^I = \frac{1}{36} [\alpha] \{D(i, j)\} \quad (4.63)$$

where

$$\begin{aligned} \{D(i, j)\} &= [D_1(i, j) \quad D_2(i, j) \quad D_3(i, j) \quad D_4(i, j)]^T \\ D_1(i, j) &= \varphi_1(j), \quad D_2(i, j) = \varphi_1(j)D(i, n), \quad D_3(i, j) = \varphi_2(j) \\ D(i, n) &= 1 + \frac{3}{n^2} + (n-1) \frac{4i^{(1)}}{n^2} - \frac{4i^{(2)}}{n^2} \end{aligned} \quad (4.64)$$

Numerical examples

The square lattice plate shown in Figure 4.1 ($L_1 = L_2$) uniformly loaded at the joints with unit loads was analyzed for six types of grids differing by the number of rods in the two directions ($m=n= 8, 16, 24, 32, 64,$ and 128). The following characteristics of the lattice were assumed: $l_1 = l_2 = l$, $EI_1 = EI_2 = EI$, $GJ_1 = GJ_2 = 0$.

Table 4.2 shows the maximum dimensionless values of deflections obtained for the plate with pinned support for six different types of grid using the decomposition method (DM) in finite difference formulation and differential formulation based on the continuum model. The results are compared with those obtained using the finite element method (FEM). The LIRA software (Kiev 2000) was used for the finite element analysis.

Maximum bending moments for the plate with a 16x16 grid are shown in Table 4.3 for the cases of pinned and fixed support. Table 4.4 demonstrates the maximum deflections of the same plate with varying coefficients of support rigidities. The results presented in Table 4.4 are illustrated in Figure 4.7.

Table 4.2 Deflections at the middle of the plate for the different types of grid
 $\tilde{k}_1=1$ (pinned support)

	$\tilde{w} \left(\frac{n}{2}, \frac{m}{2} \right) \times \left(\frac{EI}{PL^3} \right)$ for the type of grid					
	8x8	16x16	24x24	32x32	64x64	128x128
FEM	0.06403	0.13085	0.19636	0.26213	0.52487	1.05003
DM (finite difference model)	0.06289	0.13076	0.19737	0.26352	0.52997	1.07959
ε (%)	-1.78	-0.07	0.51	0.53	0.97	2.82
DM (continuous model)	0.06768	0.13530	0.20170	0.26381	0.52539	1.05108
ε (%)	5.7	3.4	2.72	0.64	0.1	0.1

Table 4.3 Bending moments for the plate with the 16x16 grid
for $\tilde{k}_1=1$ (pinned support) and $\tilde{k}_1=0$ (fixed support)

Support Type	$\tilde{M}_{ij}^I \left(\frac{n}{2}, \frac{m}{2} \right) \times \left(\frac{1}{PL} \right)$			$-\tilde{M}_{ij}^I \left(0, \frac{m}{2} \right) \times \left(\frac{1}{PL} \right)$		
	FEM	DM	ε (%)	FEM	DM	ε (%)
Pinned supports $\tilde{k}_1=1$	1.2305	1.2329	0.20	-	-	-
Fixed supports $\tilde{k}_1=0$	0.4083	0.4059	-0.58	0.9109	0.9152	0.47

Table 4.4 Deflections in the middle of the plate with the 16x16 grid for different values of support rigidity \tilde{k}_1

\tilde{k}_1	$\tilde{w}(n/2, m/2) \times \left(\frac{EI}{PL^3} \right)$		
	FEM	Decomposition Method	ε (%)
1.0	0.13085	0.13076	-0.06
0.99	0.11028	0.11055	0.25
0.95	0.07268	0.07287	0.25
0.8	0.04162	0.04162	0.0
0.6	0.03283	0.03273	-0.3
0.17	0.02772	0.02753	-0.6
0	0.02663	0.02642	-0.8

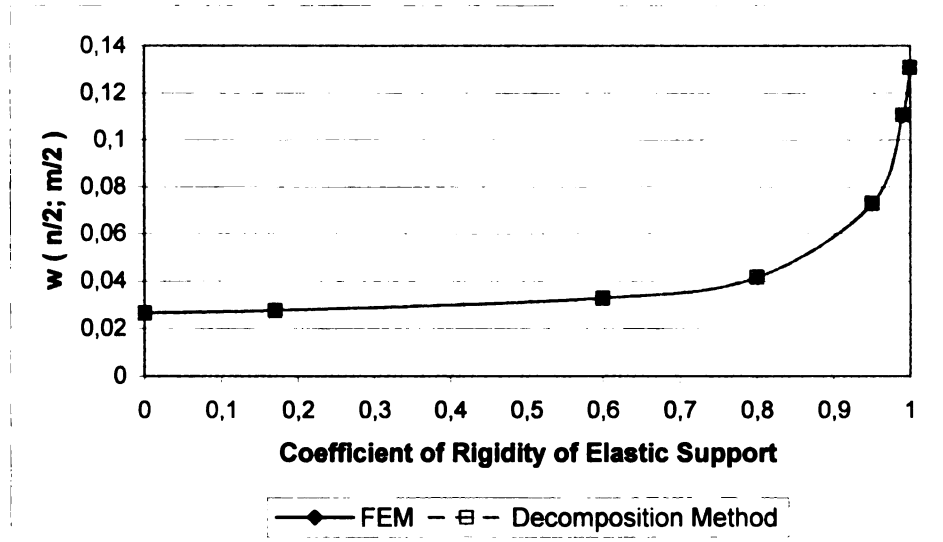


Figure 4.7 Deflections in the middle of the plate with the grid 16x16 for different values of support rigidity \tilde{k}_1

Results obtained demonstrate sufficient accuracy of the decomposition method stated in finite differences for bending problems of lattice plates with different types of grids and support rigidities. The finite difference formulation of the method provides better results than the differential formulation for sparse grids. However, for dense grids the results have similar accuracy.

4.6 Free Vibration Problem of Lattice Plate with an Orthogonal Grid

Consider a free vibration problem of a rectangular lattice plate with an orthogonal grid shown in Figure 4.8 with concentrated masses at the nodes.

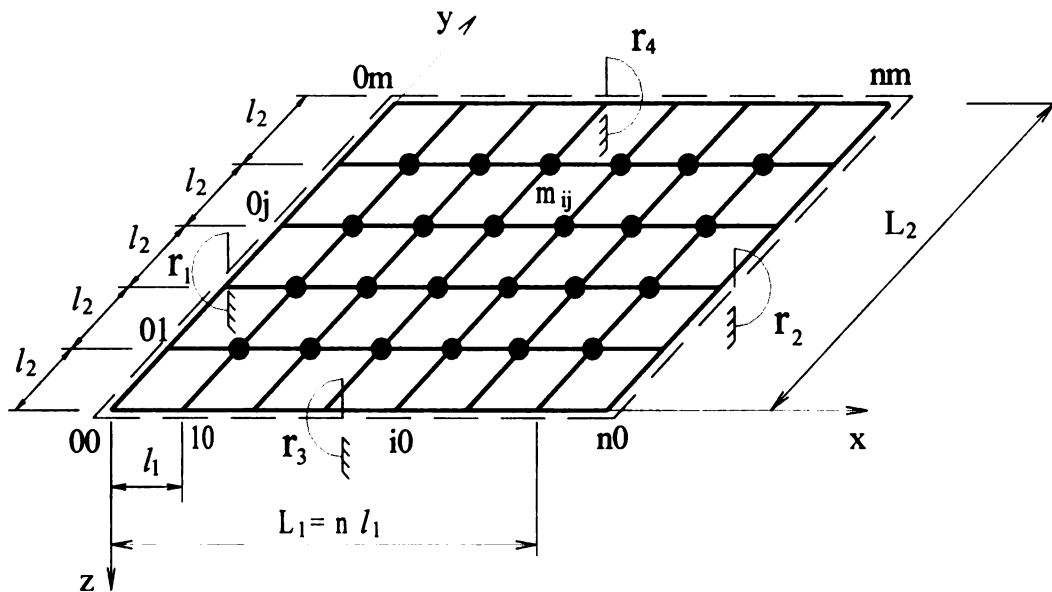


Figure 4.8. Lattice plate with an orthogonal grid and concentrated nodal masses

The governing equation of the problem has the form (Ignatiev, 1981)

$$\left[A_1 \Delta_i^4 (\Delta_j^2 + 6_i) + A_2 \Delta_j^4 (\Delta_i^2 + 6_j) \right] (\tilde{w}_{ij}) = \left[(\Delta_i^2 + 6_i) + (\Delta_j^2 + 6_j) \right] (\tilde{m}_{ij} \omega^2 \tilde{w}_{ij}) \quad (4.65)$$

where $\tilde{m}_{ij} = m_{ij} l_0^3 / EI_0$, m_{ij} is a point mass at the node i, j , and ω is the frequency of free vibration. The problem is subject to the boundary conditions (4.42).

The decomposition method is used to solve the problem, introducing the three auxiliary problems. The first two boundary value problems have the form (4.38) and (4.39). The third auxiliary problem stated in the form of discrepancy function is written as

$$\begin{aligned} \Phi(i, j) = & \left[A_1 (\Delta_i^4 \Delta_j^2) + A_2 (\Delta_i^2 \Delta_j^4) \right] (\tilde{w}_{ij}) - \left[(\Delta_i^2 + 6_i) (\Delta_j^2 + 6_j) \right] (\tilde{m}_{ij} \omega^2 \tilde{w}_{ij}) \\ & + f_1(i, j) + f_2(i, j) = 0 \end{aligned} \quad (4.66)$$

The solutions for the first two auxiliary problems are known from Section 4.5, and are given by (4.51), (4.52), and (4.53). Substituting expressions for $f_1(i, j)$ and $f_2(i, j)$ from (4.43), and \tilde{w}_{ij} from (4.51) into (4.65) and performing algebraic manipulations yields

$$\begin{aligned} \Phi(i, j) = & \alpha_1 \left[A_1 \Delta_j^4 \varphi_1(i) \Delta_i^2 \varphi_1(j) + A_2 \Delta_i^2 \varphi_1(i) \Delta_j^4 \varphi_1(j) \right] \\ & + \alpha_2 \left[A_1 \Delta_j^4 \varphi_2(i) \Delta_i^2 \varphi_1(j) + A_2 \Delta_i^2 \varphi_2(i) \Delta_j^4 \varphi_1(j) \right] \\ & + \alpha_3 \left[A_1 \Delta_j^4 \varphi_2(i) \Delta_i^2 \varphi_2(j) + A_2 \Delta_i^2 \varphi_1(i) \Delta_j^4 \varphi_2(j) \right] \end{aligned}$$

$$\begin{aligned}
& + \alpha_4 \left[A_1 \Delta_j^4 \varphi_2(i) \Delta_i^2 \varphi_2(j) + A_2 \Delta_i^2 \varphi_2(i) \Delta_j^4 \varphi_2(j) \right] \\
& + \alpha_1 \left[\varphi_1(j) + \varphi_1(j) - \tilde{m}_{ij} \omega^2 \varphi_1(i) \varphi_1(j) \right] \\
& + \alpha_2 \left[\varphi_2(i) - \varphi_1(j) f(i, n) - \tilde{m}_{ij} \omega^2 \varphi_2(i) \varphi_1(j) \right] \\
& + \alpha_3 \left[\varphi_2(j) - \varphi_1(i) f(j, m) - \tilde{m}_{ij} \omega^2 \varphi_1(i) \varphi_2(j) \right] \\
& + \alpha_4 \left[-\varphi_2(i) f(j, m) - \varphi_2(j) f(i, n) - \tilde{m}_{ij} \omega^2 \varphi_2(i) \varphi_2(j) \right] = 0
\end{aligned} \tag{4.67}$$

The third auxiliary problem is solved using the collocation method by setting $\Phi(i, j)$ to zero at the following four collocation points:

$$\left(\frac{n}{2}; \frac{m}{2} \right), \quad \left(\frac{n}{2}; \frac{m}{4} \right), \quad \left(\frac{n}{4}; \frac{m}{2} \right), \quad \left(\frac{n}{4}; \frac{m}{4} \right)$$

The resulting system of four linear algebraic equations can be written in matrix form as follows

$$\left[A - \omega^2 B \right] [\alpha] = 0 \tag{4.68}$$

where

$$[\alpha] = [\alpha_1 \quad \alpha_2 \quad \alpha_3 \quad \alpha_4] \tag{4.69}$$

and A, and B are the matrices of coefficients. The members of the matrix A are determined as

$$a_{1k} = A_1 \Delta_i^4 \varphi_1(i) \Delta_j^2 \varphi_1(j) + A_2 \Delta_i^2 \varphi_1(i) \Delta_j^4 \varphi_1(j) + \varphi_1(j) + \varphi_1(j)$$

$$\begin{aligned}
a_{2k} &= A_1 \Delta_i^4 \varphi_2(i) \Delta_j^2 \varphi_1(j) + A_2 \Delta_i^2 \varphi_2(i) \Delta_j^4 \varphi_1(j) + \varphi_2(i) - \varphi_1(j) f(i, n) \\
a_{3k} &= A_1 \Delta_i^4 \varphi_2(i) \Delta_j^2 \varphi_2(j) + A_2 \Delta_i^2 \varphi_1(i) \Delta_j^4 \varphi_2(j) + \varphi_2(j) - \varphi_1(i) f(j, m) \\
a_{4k} &= A_1 \Delta_i^4 \varphi_2(i) \Delta_j^2 \varphi_2(j) + A_2 \Delta_i^2 \varphi_1(i) \Delta_j^4 \varphi_2(j) + \varphi_2(j) - \varphi_1(i) f(j, m)
\end{aligned} \tag{4.70}$$

and the members of matrix B are

$$\begin{aligned}
b_{1k} &= \tilde{m}_{ij} \varphi_1(i) \varphi_1(j) \\
b_{2k} &= \tilde{m}_{ij} \varphi_2(i) \varphi_1(j) \\
b_{3k} &= \tilde{m}_{ij} \varphi_1(i) \varphi_2(j) \\
b_{4k} &= \tilde{m}_{ij} \varphi_2(i) \varphi_2(j)
\end{aligned} \tag{4.71}$$

where the subscript $k = 1 \dots 4$ denote the four collocation points.

For the general case $[\alpha] \neq 0$, therefore

$$|A - \omega^2 B| = 0 \tag{4.72}$$

Multiplying this equation from the right by B^{-1} , (4.72) can be written as the eigenvalue problem

$$|C - \lambda I| = 0 \tag{4.73}$$

where $\lambda = \omega^2$, $C = A B^{-1}$, and I is the identity matrix.

Solving (4.73) yields the four eigenvalues from which the smallest is chosen.

Results for the systems of orthogonal beams shown in Figure 4.8 with pinned support and six different grid sizes are presented in Table 4.5. The problem was solved in the dimensionless form using the following assumptions: $l_1 = l_2 = l$, $EI_1 = EI_2 = EI$, and $m_{ij} = m$. The results obtained by the decomposition method are compared with the exact solutions obtained by Ignatiev (1979).

TABLE 4.5. Dimensionless values of the first free vibration frequency

Grid size	$\tilde{\omega}_1 \times 10^3$					
	8x8	16x16	24x24	32x32	64x64	128x128
Decomposition method	211.045	54.5811	24.3659	13.6513	3.43240	0.854986
Exact solution	218.086	54.5223	24.2322	13.6306	3.40764	0.851912
ε (%)	-3.22	0.11	0.55	0.15	0.72	0.36

The results demonstrate that the decomposition method yields good accuracy for the first frequency. To obtain higher frequencies, the other forms of approximation functions must be used. However, the higher forms of vibration are hard to predict, and formal approximation may not be exact. For this reason, the number of sequence members retained in the approximating function must be at least four times greater than the number of frequencies to be determined. The resulting procedure is hard to implement by means of the decomposition method. Therefore, other approximate methods have to be developed for determining larger spectrum of natural frequencies for dynamic problems. The consecutive dynamic condensation method for solving the eigenproblems of lattice plates is presented in the next chapter.

CHAPTER 5

DYNAMIC ANALYSIS OF LATTICE PLATES BY CONSECUTIVE DYNAMIC CONDENSATION

Free vibration problems of complex structures involve the solution of large systems of algebraic equations ($N \cong 10^3 - 10^5$). Since only a limited number of eigenvalues and corresponding eigenvectors are required in practice the approximate methods of static and dynamic condensation can be used. The work presented in this chapter is based on the frequency dynamic condensation method (Grinenko, Mokeev 1988), and the consecutive dynamic condensation method proposed by Ignatiev (1992). A brief overview of these methods is given in Sections 5.2 and 5.3 of this chapter.

The energy form of the consecutive dynamic condensation method is developed in this chapter and three different techniques of using it to solve dynamic problems are described: condensation using the smallest natural frequency of subsystems; condensation using the eigenvectors of subsystems; and condensation using preliminary static condensation in the form of the displacement method.

5.1 Problem Statement

The problem of free vibration or stability of a system described by a discrete analytical model is characterized by the eigenvalue problem

$$[C - \lambda I]\{z\} = 0 \quad (5.1)$$

In scalar form, the above equation represents a system of homogeneous linear equations. A non-trivial solution of this system is possible when the determinant of the matrix of coefficients is equal to zero:

$$\det[C - \lambda I] = 0 \quad (5.2)$$

The matrix of coefficients $[C - \lambda I]$ in (5.1) is called the characteristic matrix of the given matrix C, and (5.2) is the characteristic equation of C with respect to λ . The roots of this equation are the eigenvalues $\lambda_i (i = 1, 2, \dots, N)$ that form the full matrix spectrum.

When the free vibration problem is solved by the displacement method (neglecting damping), the matrix C and the eigenvalue λ in (5.1) are determined as

$$C = M^{-1}K, \quad \lambda = \omega^2 \quad (5.3)$$

and (5.1) has the form

$$[K - \lambda M]\{z\} = 0 \quad (5.4)$$

where M and K are the mass and stiffness matrices, respectively; ω is the frequency of free vibration of the system, and $\{z\}$ is the vector of nodal displacements.

In the force method, the matrix C has the form

$$C = M\delta \quad (5.5)$$

and equation (5.1) becomes

$$[\delta M - \lambda I]\{z\} = 0 \quad (5.6)$$

where M is the mass matrix, δ is the flexibility matrix, $\lambda = 1/\omega^2$ is the eigenvalue, and I is the identity matrix.

5.2 Frequency - Dynamic Condensation Method

Similar to other reduction methods, this method divides the full set of degrees-of-freedom (d.o.f.) into primary (master) d.o.f. and secondary (auxiliary, or slave) d.o.f. The secondary d.o.f. are eliminated on the basis of the initial matrix equation, and the condensation of mass and stiffness (or flexibility) matrices is achieved by equating some frequencies of the condensed system with those of the original system.

5.2.1 Condensation based on the Displacement Method

Classifying all the d.o.f. of the system under consideration as primary and secondary, equation (5.4) can be written as

$$\left(\begin{bmatrix} k_{rr} & k_{rs} \\ k_{sr} & k_{ss} \end{bmatrix} - \lambda \begin{bmatrix} M_{rr} & M_{rs} \\ M_{sr} & M_{ss} \end{bmatrix} \right) \begin{Bmatrix} z_r \\ z_s \end{Bmatrix} = 0 \quad (5.7)$$

Subscripts r and s are used to denote the elements of matrices related to the primary and secondary d.o.f. correspondingly.

Eliminating the secondary unknowns z_s , (5.7) is condensed to one equation with the primary unknowns:

$$\left[(K_{rr} - \lambda M_{rr}) + D_{rr}^{(s)}(\lambda) \right] (z_r) = 0 \quad (5.8)$$

where

$$D_{rr}^{(s)}(\lambda) = -(K_{ss} - \lambda M_{rs})(K_{ss} - \lambda M_{ss})^{-1}(K_{sr} - \lambda M_{sr}) \quad (5.9)$$

Equation (5.8) can be approximated as

$$\left[(K_{rr} - \lambda M_{rr}) + (K_{rr}^{(s)} - \lambda M_{rr}^{(s)}) \right] (z_r) = 0 \quad (5.10)$$

where $K_{rr}^{(s)}$ and $M_{rr}^{(s)}$ are found from the assumption that the eigenvalues of the original equation (5.4) are equal to those of the condensed equation written in the forms (5.8) and (5.10). Using the two eigenvalues from (5.4) and equating (5.8) and (5.10), the following system of equations is obtained:

$$\begin{aligned} K_{rr}^{(s)} - \lambda_{1,rs} M_{rr}^{(s)} &= D_{rr}^{(s)}(\lambda_{1,rs}) \\ K_{rr}^{(s)} - \lambda_{2,rs} M_{rr}^{(s)} &= D_{rr}^{(s)}(\lambda_{2,rs}) \end{aligned} \quad (5.11)$$

where $\lambda_{1,rs}$ and $\lambda_{2,rs}$ are the limiting eigenvalues (λ_{\max} and λ_{\min}) of (5.4).

From system (5.11)

$$\begin{aligned} M_{rr}^{(s)} &= \frac{1}{(\lambda_{2,rs} - \lambda_{1,rs})} \left[D_{rr}^{(s)}(\lambda_{1,rs}) - D_{rr}^{(s)}(\lambda_{2,rs}) \right] \\ K_{rr}^{(s)} &= \frac{1}{(\lambda_{2,rs} - \lambda_{1,rs})} \left[\lambda_{2,rs} D_{rr}^{(s)}(\lambda_{1,rs}) - \lambda_{1,rs} D_{rr}^{(s)}(\lambda_{2,rs}) \right] \end{aligned} \quad (5.12)$$

The limiting eigenvalues $\lambda_{1,rs}$ and $\lambda_{2,rs}$, and the natural frequencies corresponding to them (basic frequencies, or condensation range) are obtained from available approximate solutions. The choice of the basic frequencies significantly affects the accuracy of approximation of dynamic conversion matrices (5.10). This is a serious drawback of this method.

5.2.2 Condensation based on the Method of Forces

After separating the full set of d.o.f. into r primary and s secondary ones, (5.6) can be written in the form

$$\left(\begin{bmatrix} \delta_{rr} & \delta_{rs} \\ \delta_{sr} & \delta_{ss} \end{bmatrix} \begin{bmatrix} M_r & 0 \\ 0 & M_s \end{bmatrix} - \lambda \begin{bmatrix} I_r & 0 \\ 0 & I_s \end{bmatrix} \right) \begin{Bmatrix} z_r \\ z_s \end{Bmatrix} = 0 \quad (5.13)$$

where I_r and I_s are identity matrices of orders r and s . Lumped mass system is used here yielding the diagonal mass matrix.

The relation between the primary z_r and secondary z_s unknowns is obtained from the second equation of (5.13):

$$z_s = -(\delta_{ss} M_s - \lambda I_s)^{-1} \delta_{sr} M_r z_r \quad (5.14)$$

Substituting (5.14) into the first equation of (5.13) yields

$$\left[(\delta_{rr} M_r - \lambda I_r) + D_{rr}^{(s)}(\lambda) \right] \{z_r\} = 0 \quad (5.15)$$

in which

$$D_{rr}^{(s)}(\lambda) = -\delta_{rs} M_s (\delta_{ss} M_s - \lambda I_s)^{-1} \delta_{sr} M_r \quad (5.16)$$

is the dynamic transformation matrix of auxiliary displacements. Matrix $D_{rr}^{(s)}$ can be approximated in the condensation range by

$$\tilde{D}_{rr}^{(s)}(\lambda) = \delta_{rr} M_r^{(s)} \quad (5.17)$$

where $M_r^{(s)}$ is the matrix of mass transport from auxiliary nodes s into primary nodes r .

Coefficients of this matrix are obtained from the condition that matrices $D_{rr}^{(s)}(\lambda)$ and $\tilde{D}_{rr}^{(s)}(\lambda)$ coincide in the minimal condensation range:

$$D_{rr}^{(s)}(\lambda_{\max,rs}) = \tilde{D}_{rr}^{(s)}(\lambda_{\max,rs}) \quad (5.18)$$

where $\lambda_{\max,rs} = 1/\omega_{\min}^2$ is the upper value of the condensation range calculated approximately by any known method.

From (5.17) and (5.18)

$$M_r^{(s)} = \delta_{rr}^{-1} \tilde{D}_{rr}^{(s)}(\lambda_{\max,rs}) \quad (5.19)$$

Accounting for (5.18), equation (5.15) can be written as

$$\left[\delta_{rr} M_r + D_{rr}^{(s)}(\lambda_{\max,rs}) - \lambda I_r \right] \{z_r\} = 0 \quad (5.20)$$

or

$$\left[\delta_{rr} (M_r + M_r^{(s)}) - \lambda I_r \right] \{z_r\} = 0 \quad (5.21)$$

The eigenvalues and the corresponding eigenvectors for the chosen condensation range are found from the characteristic equation

$$\left[\delta_{rr} (M_r + M_r^{(s)}) - \lambda I_r \right] = 0 \quad (5.22)$$

The drawback of this approach is the need to obtain the initial value of λ_{\max} by some method. It also involves conversion of high order matrices when the total number of d.o.f. is high, and the number of selected primary d.o.f. is low.

An advantage of the frequency-dynamic condensation method is the possibility of stepwise elimination of secondary d.o.f. and evaluation of correctness of their assignment

as secondary ones based on comparing the approximation errors of the dynamic conversion matrix in the condensation range.

5.3 Consecutive Dynamic Condensation Method

The main idea of the consecutive dynamic condensation method is to represent the entire characteristic matrix of the system (5.1) in block form. Thus, the secondary d.o.f. of the system are subdivided into several groups and each group is treated separately. For each group the corresponding partial eigenvalues are found by solving equation (5.13). Selecting λ_{\max} from these eigenvalues, dynamic transformation of the given group of masses to the primary group is performed using (5.19). This iterative procedure is repeated with each submatrix. After dynamic transformation of all groups of masses, the final equation for the reduced system is obtained as

$$\left| \delta_{rr} \left(M_r + \sum_{s=1}^t M_r^{(s)} \right) - \lambda I_r \right| = 0 \quad (5.23)$$

Thus the solution of the large-scale problem is substituted by the iterative procedure of finding the eigenvectors and eigenvalues of small matrices that requires minimum computer capacity. The method is particularly well-suited for implementation on parallel computers.

For the case when the original system is reduced to a system with a single d.o.f., (5.13) can be considered as a matrix system of two linear algebraic equations. Solution of this system yields

$$\lambda_{\max} = \frac{1}{2}(M_r \delta_{rr} + M_s \delta_{ss}) + \sqrt{\frac{1}{4}(M_r \delta_{rr} + M_s \delta_{ss}) - M_r M_s (\delta_{rr} \delta_{ss} - \delta_{rs} \delta_{sr})} \quad (5.24)$$

Substituting (5.24) into (5.19) and (5.16) and performing algebraic manipulations, the equation of mass transport from node s to node r is obtained in the following form:

$$M_r^{(s)} = \frac{\delta_{rs} \delta_{sr} M_s M_r}{\delta_{rr} (\delta_{ss} M_s - \lambda_{\max,rs})} \quad (5.25)$$

The coefficient of mass condensation to the main node is introduced as

$$k_{r,s} = \frac{M_r^{(s)}}{M_s} = \frac{\delta_{rs} \delta_{sr} M_r}{\delta_{rr} (\delta_{ss} M_s - \lambda_{\max,rs})} \quad (5.26)$$

The final equation for the reduced system becomes

$$\left| \delta_{rr} M_r \left(1 + \sum_{s=1}^N k_{r,s} \right) - \lambda \right| = 0 \quad (5.27)$$

where N is the total number of d.o.f. of the system.

From (5.27) the approximate equation for the maximum eigenvalue of the system is obtained that can be used for the following refined analysis:

$$\lambda_{\max} = \delta_{rr} M_r \left(1 + \sum_{\substack{s=1 \\ s \neq r}}^N k_{r,s} \right) \quad (5.28)$$

Test analyses of natural frequencies of beams and rectangular plates demonstrated the high accuracy of the results obtained by (5.28). However, the technique described provides accurate results only for the upper part of the eigenvalue spectrum (Ignatiev, 1992).

5.4 Energy Form of the Consecutive Dynamic Condensation Method

The energy form of the consecutive frequency-dynamic condensation method is based on the following assumptions:

- Equality of eigenvectors and eigenvalues of the reduced system and the corresponding part of the eigenvector and eigenvalue spectrum of the original system
- Equality of kinetic energies of the reduced system and the original system

The equation for the kinetic energy of the original system has the form:

$$U^{orig} = \frac{1}{2} \sum m_r \omega^2 z_r^2 + \frac{1}{2} \sum m_s \omega^2 z_s^2 \quad (5.29)$$

After mass transfer to the condensation nodes, kinetic energy of the reduced system becomes

$$U^{reduced} = \frac{1}{2} \sum m_r \omega^2 z_r^2 + \frac{1}{2} \sum m_r^{(s)} \omega^2 z_s^2 \quad (5.30)$$

where $m_r^{(s)}$ are the condensation additives resulting from transformation of all masses m_s to masses m_r .

Equating (5.29) and (5.30) yields

$$\sum_s m_s z_s^2 = \sum_r m_r^{(s)} z_r^2 \quad (5.31)$$

or, in matrix form

$$\{z_s\}^T [m_s] \{z_s\} = \{z_r\}^T [m_r^{(s)}] \{z_r\} \quad (5.32)$$

where $\{z_r\}$ and $\{z_s\}$ are the subvectors of the total vector of nodal displacements corresponding to the primary and secondary d.o.f.; and $[m_s]$ and $[m_r^{(s)}]$ are diagonal matrices of orders s and r , respectively.

5.4.1 Condensation Using the Smallest Natural Frequency of Partial Systems

For the first form of vibration corresponding to the fundamental (smallest) natural frequency ω_{\min} , equation (5.14) for the secondary nodal displacements can be written as

$$\{z_s\} = [D_{rr}^{(s)}(\lambda_{\max})] \{z_r\} \quad (5.33)$$

where

$$[D_{rr}^{(s)}(\lambda_{\max})] = -[\delta_{ss} M_s - \lambda I]^{-1} [\delta_{sr}] [M_r] \quad (5.34)$$

Substituting (5.33) into (5.32) yields the dependence

$$\{z_r\}^T [D_{rr}^{(s)}(\lambda_{\max})]^T [m_s] [D_{rr}^{(s)}(\lambda_{\max})] \{z_r\} = \{z_r\}^T [m_r^{(s)}] \{z_r\} \quad (5.35)$$

from which the matrix of condensation additives is found:

$$[m_r^{(s)}] = [D_{rr}^{(s)}(\lambda_{\max})]^T [m_s] [D_{rr}^{(s)}(\lambda_{\max})] \quad (5.36)$$

The right side of (5.36) results in a square matrix of order $r \times r$. In order to reduce it to the diagonal form corresponding to the structure of $[m_r^{(s)}]$, all the rows are added and the result are written in the diagonal form. For every partial system λ_{\max} is found solving (5.27).

Performing similar operations with all t groups of masses, the final equation for the reduced system becomes

$$\left| \delta_{rr} \left(M_r + \sum_{s=1}^t M_r^{(s)} \right) - \lambda I_r \right| = 0 \quad (5.37)$$

Test Problem 1

Consider the prismatic simply supported beam shown in Figure 5.1. The beam carries 12 equidistantly located point masses $m_i = 1$.

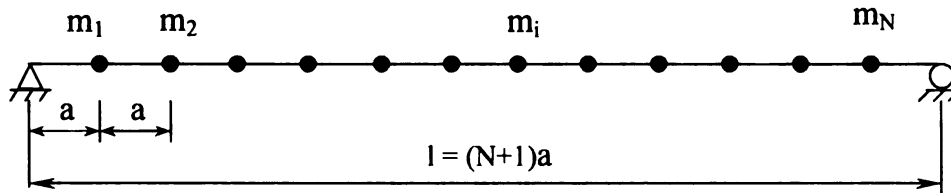
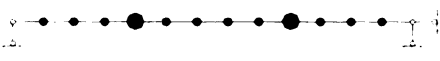
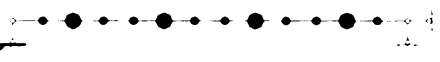
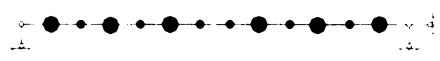


Figure 5.1. Simply supported beam with equidistant masses for test problems 1 and 2

The free vibration problem of the beam was analyzed by the energy form of the consecutive dynamic condensation method using the fundamental frequency of partial systems. Condensation was performed to two, four, and six primary d.o.f., by blocks of two secondary d.o.f. The results are presented in Table 5.1. The values of the natural frequencies obtained by the proposed technique are compared with accurate solutions calculated using the formula by Ignatiev (1979).

TABLE 5.1. Results for Test Problem 1

Arrangement of the primary d.o.f.	Order of frequency k	Frequency ω_k		
		Exact solution	Proposed technique	ε (%)
 $n = 2, s = 10$	1	0.13328	0.13409	0.61
	2	0.00833	0.01121	25.7
 $n = 4, s = 8$	1	0.13328	0.13341	0.09
	2	0.00833	0.00897	7.2
	3	0.00165	0.00206	20.1
	4	0.00052	0.00092	13.8
 $n = 6, s = 6$	1	0.13328	0.13375	0.35
	2	0.00833	0.00891	6.5
	3	0.00165	0.00182	9.3
	4	0.00052	0.00063	17.4
	5	0.00021	0.00031	32.2
	6	0.00010	0.00017	41.1

The results indicate that only the largest eigenvalue of the original system is determined with sufficient accuracy. The reason for this is that the condensation coefficient at each step accounts only for the largest eigenvalue of the characteristic matrix of the partial system.

5.4.2 Condensation Using the Reduced Spectrum of Eigenvalues and Eigenvectors of Partial Systems

In order to improve the accuracy of the computed natural frequencies, a different technique for determining the matrix of condensation coefficients is proposed in this section. As before, the set of d.o.f. of the original system is subdivided into primary and secondary d.o.f. The displacement vector is divided into two subvectors

$$\{z\} = [z_r \quad z_s]^T \quad (5.38)$$

The procedure is based on the method of forces. The main equation of the original system has the matrix form of (5.13) and the dependence between the primary and secondary unknown displacements z_r and z_s has the form (5.14).

Let us write (5.14) in the form

$$\{z_s\} = [A_{sr}] \{z_r\} \quad (5.39)$$

where $[A_{sr}]$ is the transformation matrix from secondary to primary unknowns.

Equation (5.39) is applicable for any k^{th} mode of vibration:

$$[z_{s,k}] = [A_{sr}] [z_{r,k}] \quad (5.40)$$

To construct the matrix $[A_{sr}]$ for the partial system the first r of n eigenvectors of the partial system are used ($k = r$). Since the matrix $[z_{r,k}]$ is square and nonsingular, $[A_{sr}]$ can be determined as

$$[A_{sr}] = [z_{s,k}] [z_{r,k}]^{-1} \quad (5.41)$$

Using the notation $k_{r,s}$ for the coefficient of mass condensation introduced earlier in (5.26), expression (5.32) can be written as

$$\{z_s\}^T [m_s] \{z_s\} = \{z_r\}^T [k_{r,s} m_r] \{z_r\} \quad (5.42)$$

Substituting (5.41) into (5.42) yields the matrix of the coefficients of condensation

$$[k_{r,s}] = [A_{sr}]^T [m_s] [A_{sr}] [1/m_r] \quad (5.43)$$

After determining the matrices of condensation coefficients for all partial systems, the matrix of condensed masses can be found as

$$[\tilde{M}_r] = [m_r] [I_r + \sum k_{r,s}] \quad (5.44)$$

The equation of the general type for the reduced system can be written as

$$[\delta_{rr} \tilde{M}_r - \lambda I_r] \{z_r\} = 0 \quad (5.45)$$

and the characteristic equation for the reduced system is

$$|\delta_{rr} \tilde{M}_r - \lambda I_r| = 0 \quad (5.46)$$

After solving (5.46) and (5.45), the reduced spectrum of eigenvalues and eigenvectors of the system is obtained. The eigenvectors corresponding to the secondary d.o.f. of the system can be determined by the backward transformation. Matrix $[A_{sr}]$ is constructed for each partial system and can be considered as the matrix of vibration modes of the i^{th} partial system. The matrix of vibration modes for the whole system can be written as

$$[B] = [I_r \ A_{sr}^1 \ \dots \ A_{sr}^{(t)}]^T \quad (5.47)$$

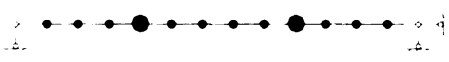
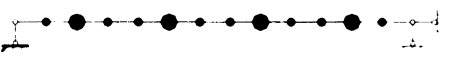

where t is the number of partial systems. The matrix of eigenvectors can be determined as

$$\{z\} = \begin{Bmatrix} z_r \\ z_s \end{Bmatrix} = [B] \{z_r\} \quad (5.48)$$

Test Problem 2

Consider the prismatic simply supported beam shown in Figure 5.1. The free vibration problem of the beam is analyzed by the energy form of the consecutive dynamic condensation method using the reduced spectrum of eigenvalues and eigenvectors of partial systems. The total number of d.o.f. of the system is twelve. Condensation was carried out using two, four, and six primary d.o.f. The schemes of the arrangements of condensation nodes are shown in Table 5.2. The total number s of the secondary d.o.f. was divided into b blocks. The number of blocks (b) and the number of secondary unknowns in each block (s_b) varied.

TABLE 5.2 Arrangement of the primary degrees of freedom for the Test Problem 2

Scheme No	Arrangement of the primary d.o.f.	n/s ratio	Block size $b \times s_b$
I	 $n = 2, s = 10$	1/5	10x1
			5x2
			2x5
II	 $n = 4, s = 8$	1/2	8x1
			4x2
			2x4
III	 $n = 6, s = 6$	1	6x1
			3x2
			2x3

Results are presented in Table 5.3. The eigenvalues obtained for the reduced system are compared with accurate values calculated using the equation obtained by Ignatiev (1979) for the case $N=12$:

$$\omega_k^2 = \frac{48EI}{ma^3} \left(\sin^4 \frac{k\pi}{2(N+1)} \right) \left/ \left(2 + \cos \frac{k\pi}{N+1} \right) \right.$$

TABLE 5.3 Results for Test Problem 2

Scheme No	n/s ratio	Order of frequency k	bxs_b	Frequency ω_k		
				Exact solution	Proposed technique	ϵ (%)
I	1/5	1	10x1	0.13328	0.13362	0.26
			5x2		0.13471	1.07
			2x5		0.13193	-1.01
		2	10x1	0.00833	0.00903	8.4
			5x2		0.00904	8.5
			2x5		0.01134	36.1
II	1/2	1	8x1	0.13328	0.13356	0.21
			4x2		0.13342	0.10
			2x4		0.13343	0.11
		2	8x1	0.00833	0.00849	1.92
			4x2		0.00862	3.48
			2x4		0.0085	2.04
		3	8x1	0.00165	0.00169	2.37
			4x2		0.00179	7.82
			2x4		0.00173	4.62
		4	8x1	0.00052	0.00062	16.13
			4x2		0.00059	11.86
			2x4		0.00058	10.34
III	1	1	6x1	0.13328	0.13345	0.13
			3x2		0.13347	0.14
			2x3		0.13343	0.11
		2	6x1	0.00833	0.0084	0.84
			3x2		0.00839	0.72
			2x3		0.00838	0.60
		3	6x1	0.00165	0.00167	1.20
			3x2		0.00175	5.71
			2x3		0.00168	1.79
		4	6x1	0.00052	0.00056	7.14
			3x2		0.00056	7.14
			2x3		0.00057	8.77
		5	6x1	0.00021	0.00023	8.70
			3x2		0.00023	8.70
			2x3		0.00028	25.00
		6	6x1	0.00010	0.00012	16.67
			3x2		0.00009	-11.11
			2x3		0.00019	47.37

The following observations are made:

- The proposed technique provides good accuracy for approximately 25% of the spectrum of eigenvalues
- The number of blocks does not affect the results significantly
- Increasing the number of condensation nodes improves accuracy. The recommended ratio of primary to secondary nodes is $\frac{1}{2} < n/s < 1$

5.4.3 Combined Static and Consecutive Dynamic Condensation

The eigenproblem stated in the form of the displacement method has the form (5.4). The technique proposed in this section combines the two methods presented earlier – static condensation and the energy form of consecutive dynamic condensation. After classifying all the d.o.f. of the system under consideration as primary and secondary, the main equation (5.4) transforms to (5.7). The system is then subdivided into a set of partial systems, and the secondary d.o.f. are represented in a block form.

In the first step Guyan's transformation is performed for the partial systems. The vector of displacements of the partial system is written as

$$\{z\} = \begin{Bmatrix} z_r \\ z_s \end{Bmatrix} = [A_r] \{z_r\} \quad (5.49)$$

where

$$[A_r] = \begin{bmatrix} I_r \\ -K_{ss}^{-1} K_{sr} \end{bmatrix} \quad (5.50)$$

is the matrix of static condensation.

The statically condensed stiffness and mass matrices of the partial system are obtained through

$$\begin{aligned} \left[K_{rr}^* \right] &= \left[A_r \right]^T \left[K \right] \left[A_r \right] = K_{rr} - K_{rs} K_{ss}^{-1} K_{sr} \\ \left[M_{rr}^* \right] &= \left[A_r \right]^T \left[M \right] \left[A_r \right] = M_{rr} - M_{rs} M_{ss}^{-1} M_{sr} \end{aligned} \quad (5.51)$$

The eigenvalues and eigenvectors of the partial system are then obtained from the solution of the characteristic equation

$$\left[\left[K_{rr}^* \right] - \lambda \left[M_{rr}^* \right] \right] \{z\} = 0 \quad (5.52)$$

In the second step, refined condensation is performed based on the energy form of the consecutive dynamic condensation method using the reduced spectrum of eigenvalues and eigenvectors of partial systems described in Section 5.4.2.

Condensed stiffness and mass matrices of the partial system are obtained through the transformation

$$\begin{aligned} \left[\tilde{K}_{rr}^{(i)} \right] &= \left[B \right]^T \left[K_{rr}^* \right] \left[B \right] \\ \left[\tilde{M}_{rr}^{(i)} \right] &= \left[B \right]^T \left[M_{rr}^* \right] \left[B \right] \end{aligned} \quad (5.53)$$

Performing condensation of all t blocks of secondary d.o.f., the final stiffness and mass matrices of the system are obtained by the summations

$$\left[\tilde{K}_{rr} \right] = \sum_{i=1}^t \left[\tilde{K}_{rr}^{(i)} \right] - (t-1) \left[K_{rr} \right] \quad (5.54)$$

$$[\tilde{M}_{rr}] = \sum_{i=1}^t [\tilde{M}_{rr}^i] - (t-1)[M_{rr}] \quad (5.55)$$

The eigenvalues and eigenvectors of the reduced system are obtained from the characteristic equation

$$\left[[\tilde{K}_{rr}] - \lambda [\tilde{M}_{rr}] \right] \{z\} = 0 \quad (5.56)$$

Test Problem 3

Consider a prismatic single-span beam with fixed ends loaded with a uniformly distributed mass of intensity $m = 1$. All geometrical and physical characteristics of the cross section are taken equal to unity. The beam is divided along the length into 72 linear finite elements. The length of each element is assumed to be $a = 1$.

TABLE 5.4. Variants of condensation for Test Problem 3

Total number of d.o.f N	Number of primary d.o.f n	$n/s, \%$	Number of blocks b	Number of secondary d.o.f. in one block s_b
142	6	4.4	2	68
			4	34
	10	7.6	2	66
			3	44
			6	22
	14	11	2	64
			4	32
			8	16
	22	18.3	2	60
			4	30
			6	20
			12	10

The problem was solved by the combined static and consecutive dynamic condensation method. Different variants of condensation were performed by varying the number of primary d.o.f. and the secondary d.o.f. blocks as shown in Table 5.4.

Figure 5.2 illustrates the location of the primary d.o.f. and secondary d.o.f. blocks for the case with 22 primary d.o.f. Results for this case are presented in Table 5.5. The eigenvalues obtained by both methods are compared with the results obtained by solving the full system of equations. Figure 5.3 illustrates the distribution of errors for the eigenvalues obtained by different techniques. Similar graphs for the other cases listed in Table 5.4 are shown in Figures 5.4 – 5.6.

Test Problem 4

Consider a beam described in Test Problem 3 with three equidistant intermediate roller supports added (Figure 5.7). Each span consists of 18 finite elements. The total number of d.o.f. of the structure is 139.

Condensation was performed using eleven, eight, and three primary d.o.f. Arrangement schemes of the primary d.o.f. and blocks of the secondary d.o.f. are shown in Figure 5.7(a), (b), and (c).

Results are presented in Tables 5.6, 5.7, and 5.8 and illustrated in Figures 5.8, 5.9, 5.10, and 5.11.

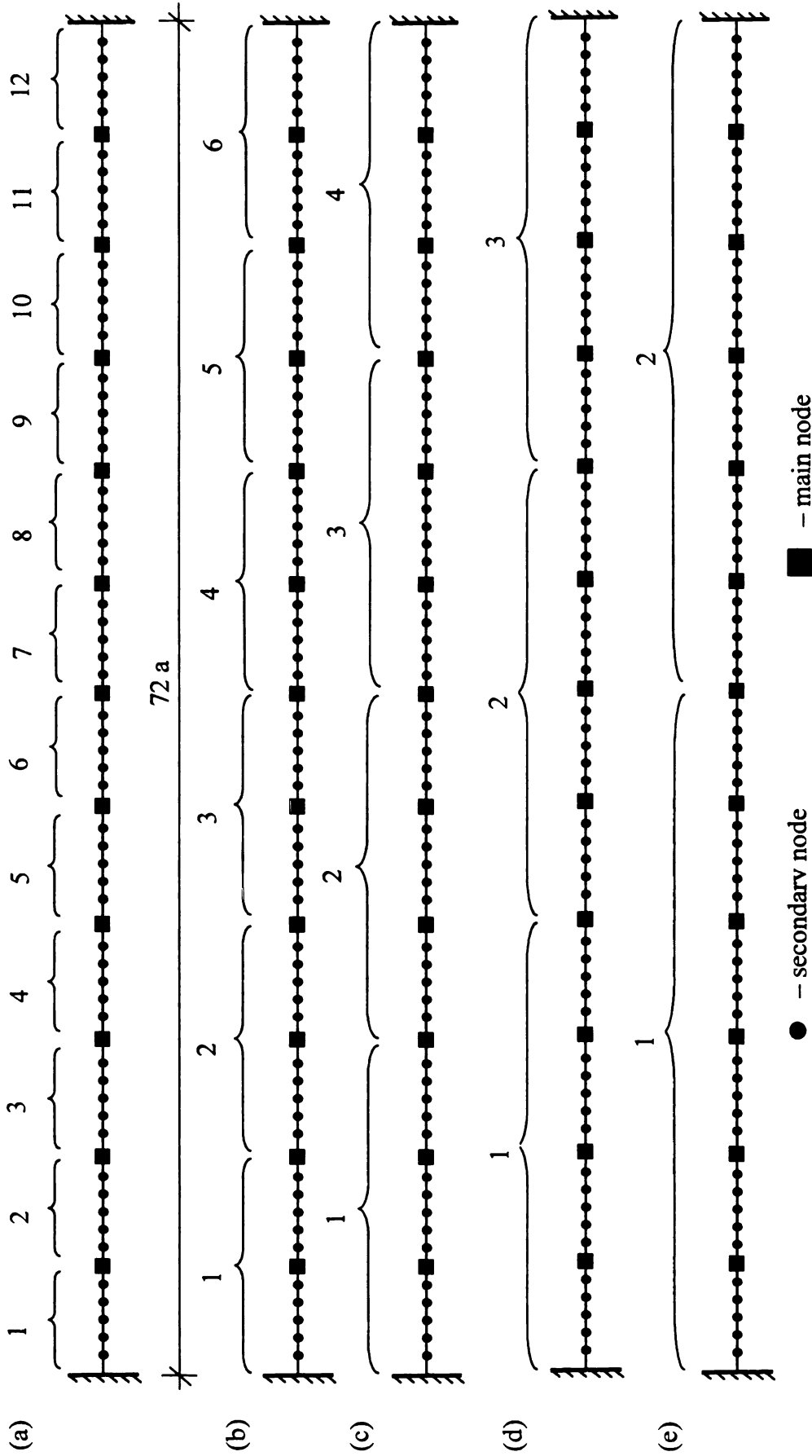


Figure 5.2. Location of the primary d.o.f. and secondary d.o.f. blocks for the case with 22 primary d.o.f. for Test Problem 3

TABLE 5.5. Results for the Test Problem 3 for the case with 22 primary d.o.f.

Eigenvalue Number		Eigenvalues obtained by													
		Solution of the full system $N = 142$		Static condensation to 22 primary d.o.f.		12x10		6x20		4x30		2x60			
				λ_k	ε (%)	λ_k	ε (%)	λ_k	ε (%)	λ_k	ε (%)	λ_k	ε (%)		
1	1.863×10^{-5}	1.863×10^{-5}	0.01	1.863×10^{-5}	0.00	1.863×10^{-5}	0.00	1.863×10^{-5}	0.00	1.863×10^{-5}	0.00	1.863×10^{-5}	0.00	1.863×10^{-5}	0.00
2	0.0001415	0.0001415	0.00	0.0001415	0.00	0.0001415	0.00	0.0001415	0.00	0.0001415	0.00	0.0001415	0.00	0.0001415	0.00
3	0.0005439	0.0005445	0.11	0.0005439	0.00	0.0005439	0.00	0.0005439	0.00	0.0005439	0.00	0.0005439	0.00	0.0005439	0.00
4	0.001486	0.001490	0.26	0.001486	0.00	0.001486	0.00	0.001486	0.00	0.001486	0.00	0.001486	0.00	0.001486	0.00
5	0.003317	0.003335	0.56	0.003317	0.00	0.003317	0.00	0.003317	0.00	0.003317	0.00	0.003317	0.00	0.003317	0.00
6	0.006470	0.006538	1.05	0.006470	0.00	0.006470	0.00	0.006470	0.00	0.006470	0.00	0.006470	0.00	0.006470	0.00
7	0.01147	0.01167	1.78	0.01147	0.00	0.01147	0.00	0.01147	0.00	0.01147	0.00	0.01147	0.00	0.01147	0.00
8	0.01892	0.01944	2.76	0.01892	0.00	0.01892	0.00	0.01892	0.00	0.01892	0.00	0.01892	0.00	0.01892	0.00
9	0.02952	0.03068	3.92	0.02952	0.00	0.02952	0.00	0.02952	0.00	0.02952	0.00	0.02952	0.00	0.02952	0.00
10	0.04406	0.04622	4.89	0.04406	0.00	0.04406	0.00	0.04406	0.00	0.04406	0.00	0.04406	0.00	0.04406	0.00
11	0.06340	0.06554	3.37	0.06340	0.00	0.06340	0.00	0.06340	0.00	0.06340	0.00	0.06340	0.00	0.06340	0.00

TABLE 5.5. Results for the Test Problem 3 for the case with 22 primary d.o.f. (continued)

Eigenvalue Number <i>k</i>	Eigenvalues obtained by														
	Solution of the full system <i>N</i> = 142	Static condensation to 22 primary d.o.f.		12x10			6x20			4x30			2x60		
		λ_k	ϵ (%)	λ_k	ϵ (%)	λ_k	ϵ (%)	λ_k	ϵ (%)	λ_k	ϵ (%)	λ_k	ϵ (%)		
12	0.08850	0.1075	21,48	0.08851	0.01	0.08850	0.00	0.08850	0.00	0.08850	0.00	0.08850	0.00	0.08850	0.00
13	0.1204	0.1455	20,82	0.1204311	0.01	0.1204	0.00	0.1204	0.00	0.1204	0.00	0.1204	0.00	0.1204	0.00
14	0.1603	0.1991	24,21	0.1603187	0.03	0.1603	0.00	0.1603	0.00	0.1603	0.00	0.1603	0.00	0.1603	0.00
15	0.2093	0.2707	29,33	0.2094241	0.07	0.2093	0.01	0.2093	0.01	0.2093	0.01	0.2093	0.01	0.2093	0.01
16	0.2688	0.3660	36,20	0.2691	0.14	0.2688	0.03	0.2688	0.03	0.2688	0.03	0.2688	0.03	0.2688	0.03
17	0.3401	0.4934	45,07	0.3409	0.24	0.3403	0.05	0.3403	0.05	0.3403	0.05	0.3403	0.05	0.3403	0.05
18	0.4248	0.6628	56,02	0.4265	0.40	0.4267	0.44	0.4267	0.44	0.4251	0.06	0.4251	0.06	0.4250	0.05
19	0.5245	0.8839	68,54	0.5280	0.61	0.5289	0.84	0.5289	0.84	0.5277	0.61	0.5277	0.61	0.5264	0.36
20	0.6407	1.1592	80,92	0.6477	1.08	0.6503	1.48	0.6503	1.48	0.6478	1.10	0.6478	1.10	0.6635	3.44
21	0.7753	1.4684	89,39	0.7932	2.25	0.8479	8.56	0.8479	8.56	1.0489	26.09	1.0489	26.09	0.9926	21.89
22	0.9301	1.7519	88,35	1.0493	11.36	1.0836	14.16	1.0836	14.16	1.1530	19.33	1.1530	19.33	1.0552	11.85

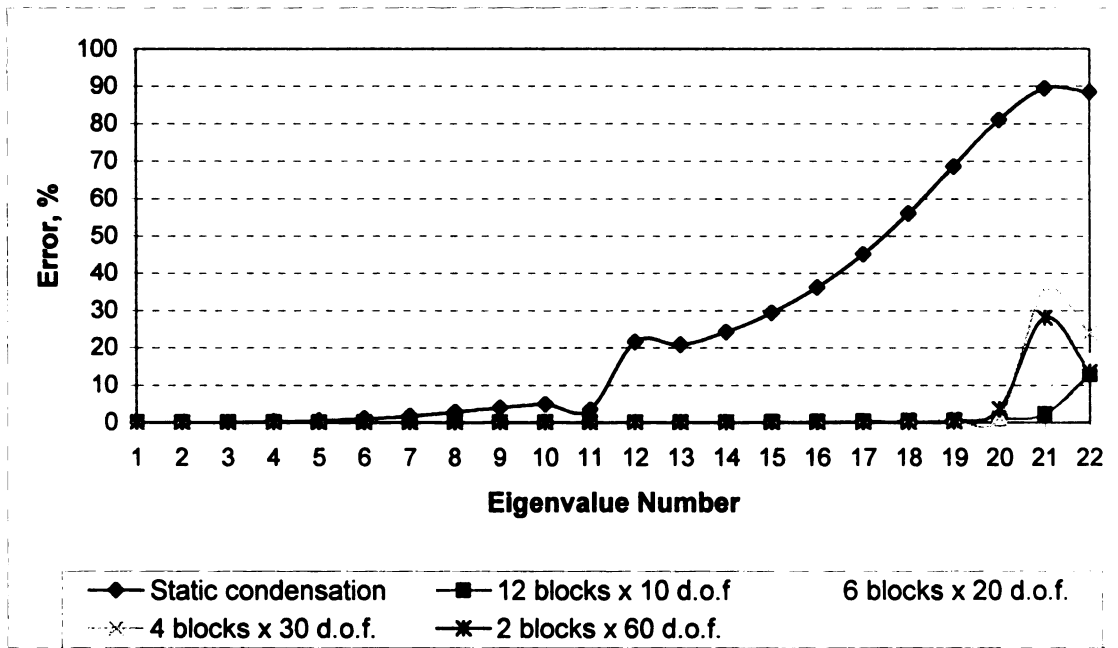


Figure 5.3. Graphs of errors for Test Problem 3 for the case with 22 primary d.o.f.

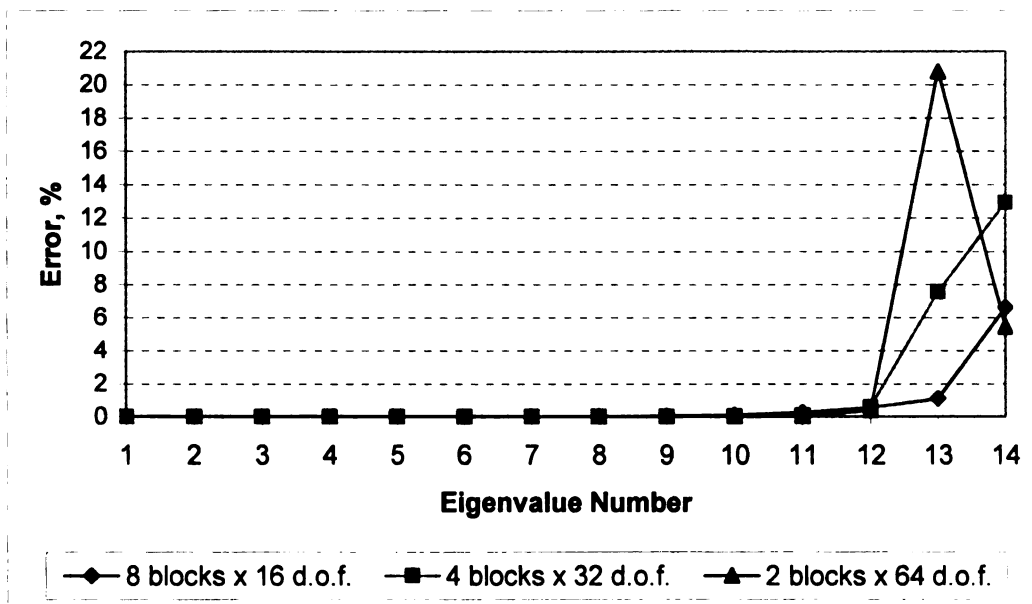


Figure 5.4. Graphs of errors for the Test Problem 3 for the case with 14 primary d.o.f.

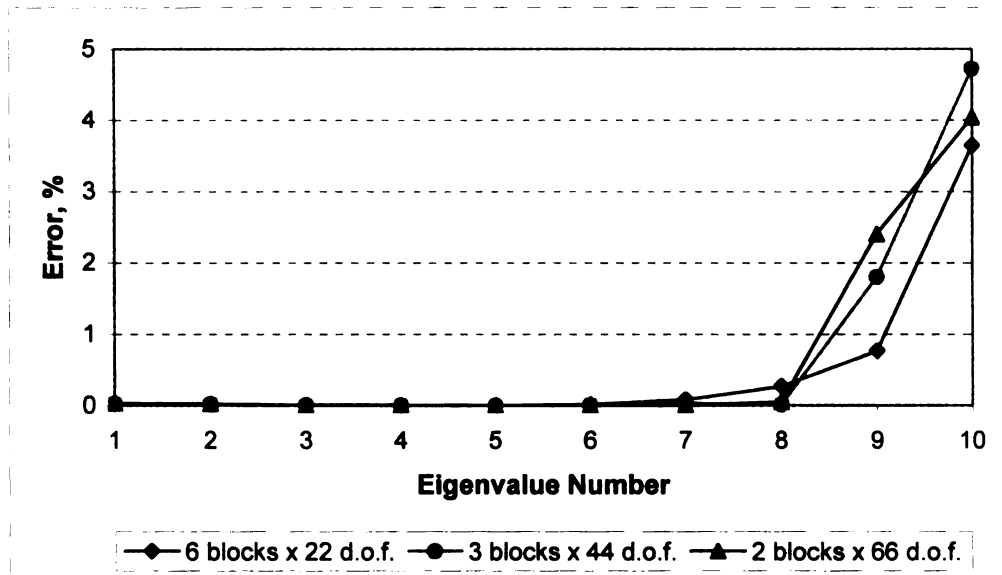


Figure 5.5. Graphs of errors for Test Problem 3 for the case with 10 primary d.o.f.

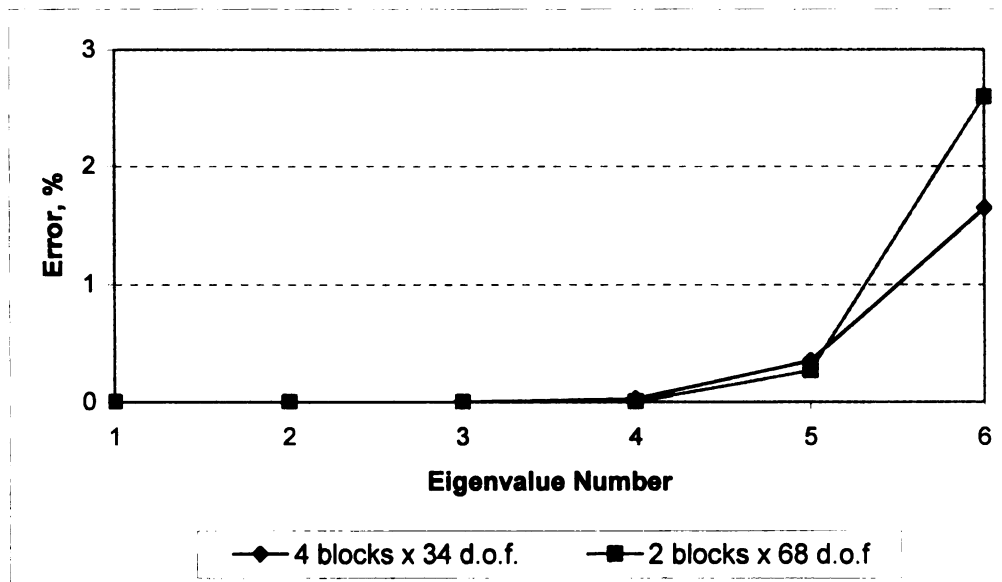


Figure 5.6. Graphs of errors for Test Problem 3 for the case with 6 primary d.o.f.

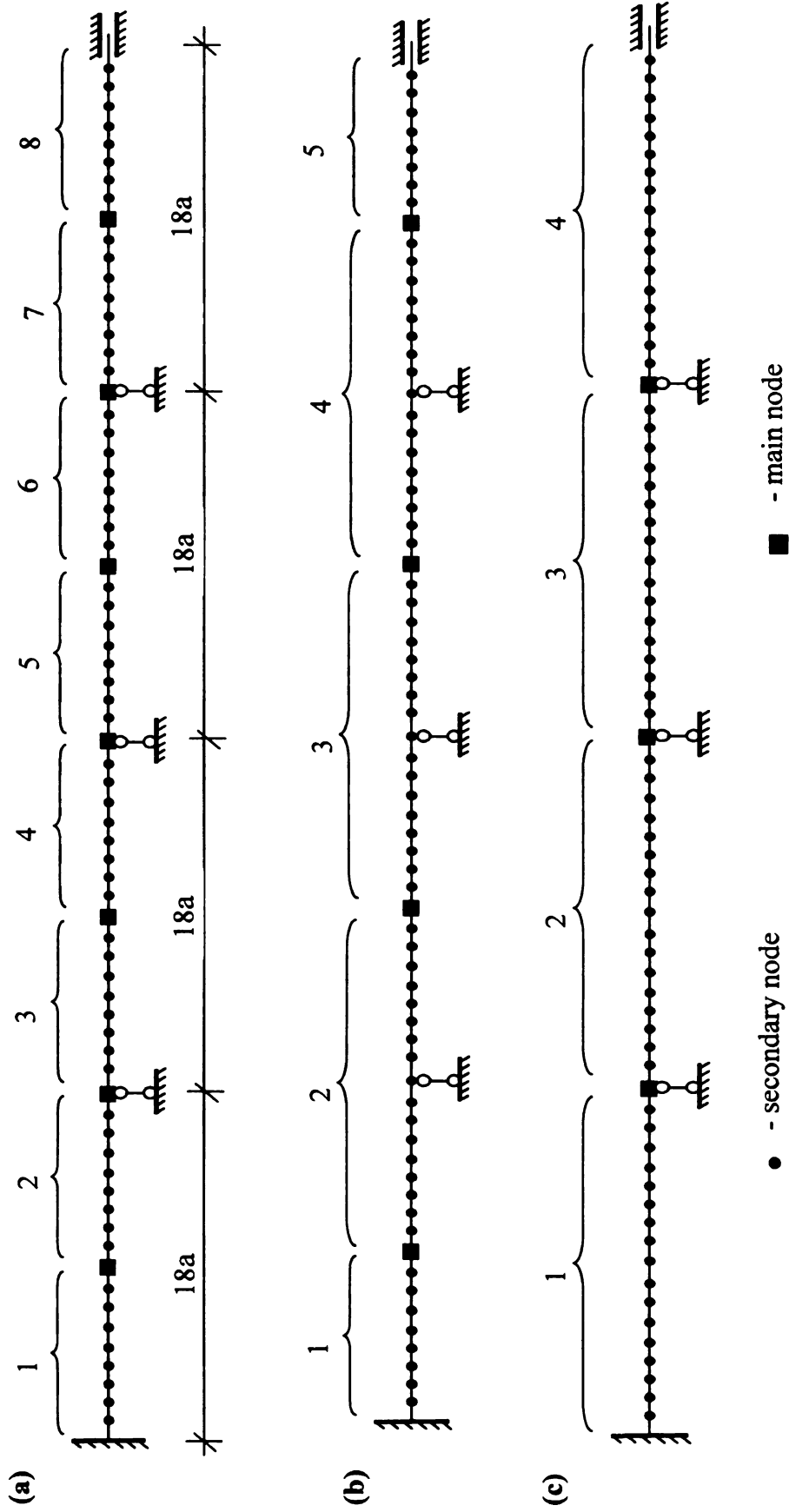


Figure 5.7. Location of the primary d.o.f. and secondary d.o.f. blocks for Test Problem

TABLE 5.6. Results for Test Problem 4 (condensation to 11 primary d.o.f.)

Eigenvalue Number k	Eigenvalues obtained by					
	Solution of the full system $N = 142$	Static condensation to 11 primary d.o.f.		Consecutive dynamic condensation to 11 primary d.o.f.		
		$\lambda_k \times 10^3$	$\lambda_k \times 10^3$	ϵ (%)	$\lambda_k \times 10^3$	ϵ (%)
	λ_k					$ \phi_i $
1	1.2628	1.2763	1,07	1.26287	0.01	0.12
2	2.2645	2.3066	1,86	2.26451	0.00	0.02
3	3.7804	3.8886	2,86	3.78043	0.00	0.2
4	4.7683	4.9242	3,27	4.76842	0.00	0.06
5	17.4851	22.1025	26,41	17.48739	0.01	0.17
6	23.7822	32.4956	36,64	23.78883	0.03	0.27
7	31.6421	49.2494	55,65	31.66137	0.06	0.78
8	36.2342	64.0146	76,67	36.26416	0.08	1.65
9	83.8759	151.1493	80,21	84.6864	0.97	11.02
10	103.539	230.7529	122,87	105.76222	2.15	25.6
11	126.4732	330.8788	161,62	137.7662	8.93	102

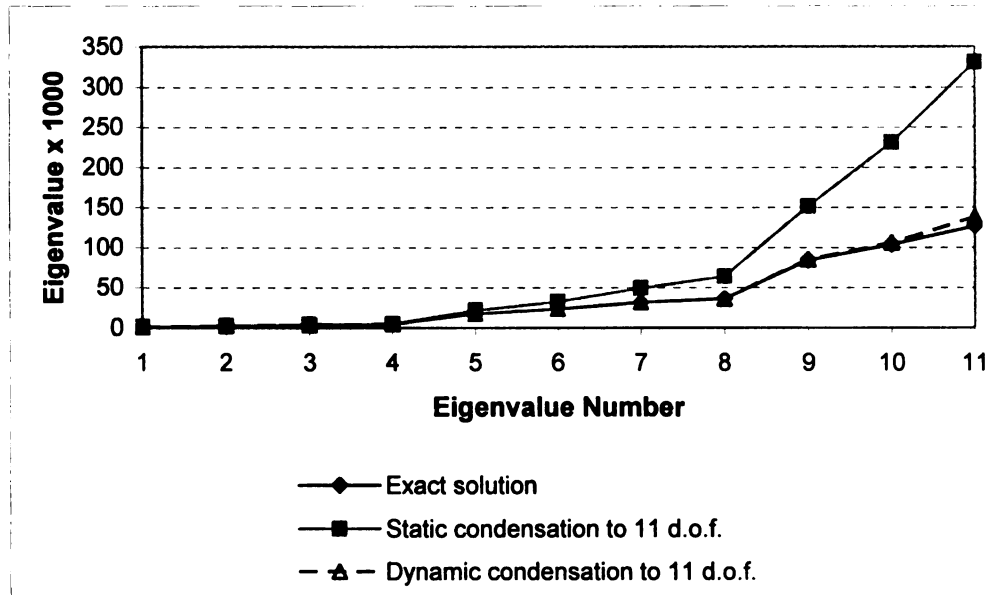


Figure 5.8. Results for Test Problem 4 (condensation to 11 primary d.o.f.)

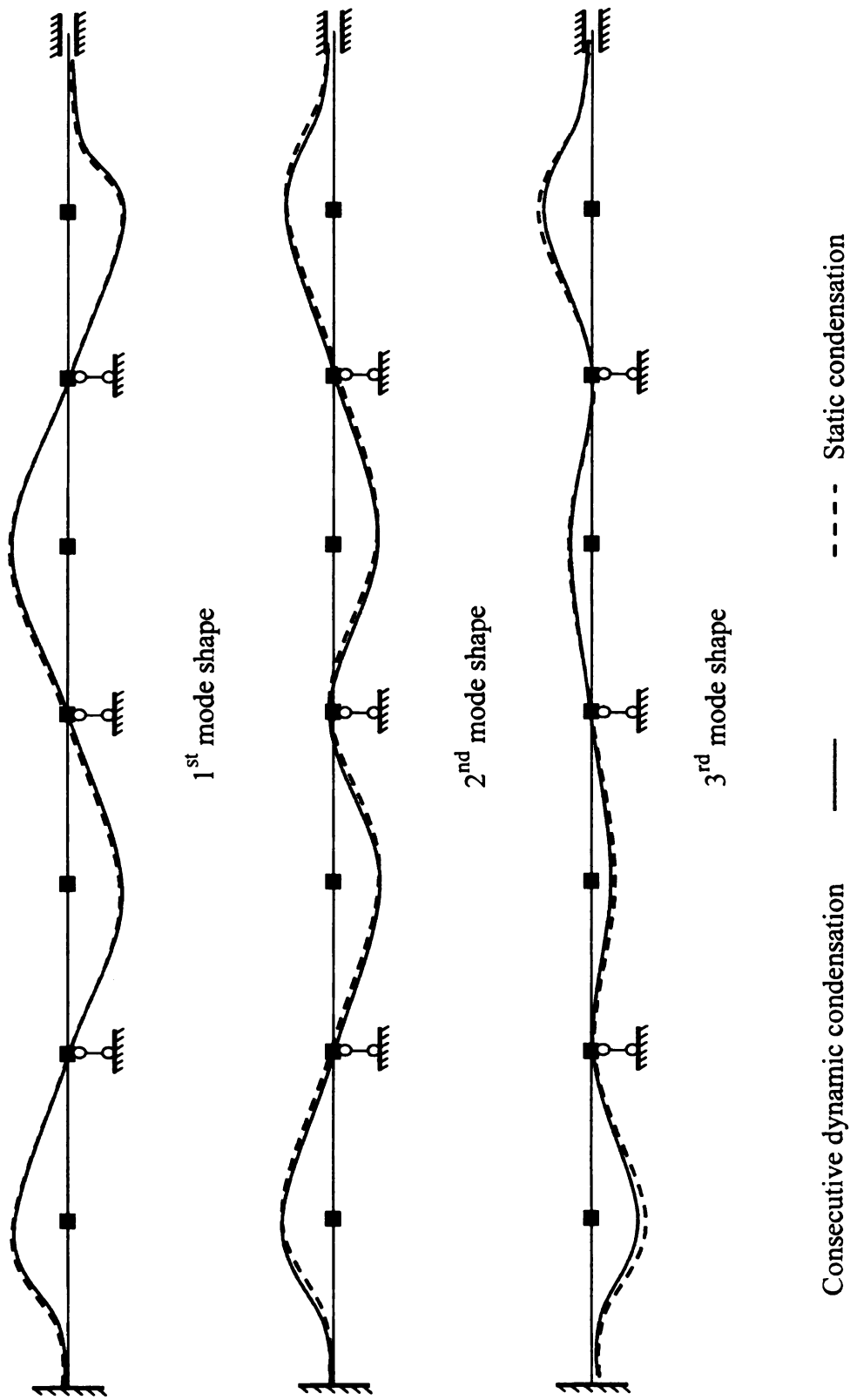


Figure 5.9. Mode shapes for Test Problem 4 (condensation to 11 primary d.o.f.)

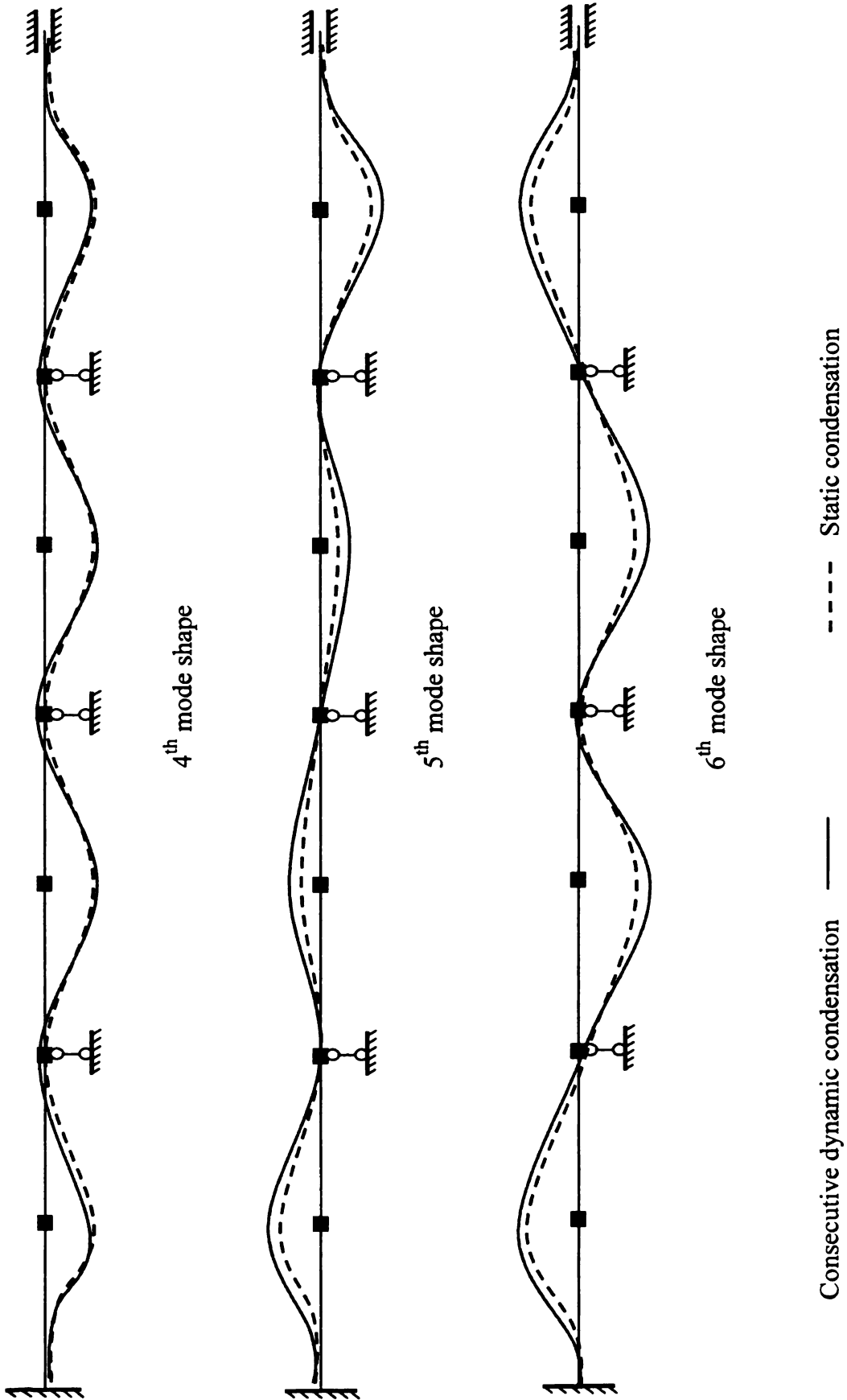


Figure 5.9. Mode shapes for Test Problem 4 (condensation to 11 primary d.o.f.) (Continued)

TABLE 5.7. Results for Test Problem 4 (condensation to 8 primary d.o.f.)

Eigenvalue Number k	Eigenvalues obtained by				
	Solution of the full system $N = 142$	Static condensation to 11 primary d.o.f.		Consecutive dynamic condensation to 11 primary d.o.f.	
		$\lambda_k \times 10^3$	$\lambda_k \times 10^3$	ϵ (%)	$\lambda_k \times 10^3$
1	1.2628	1.28703	1.92	1.26288	0.01
2	2.2645	2.33339	3.04	2.26453	0.00
3	3.7804	3.92298	3.77	3.78049	0.00
4	4.7683	4.92419	3.27	4.76843	0.00
5	17.4851	28.65426	63.88	17.5231	0.22
6	23.7822	40.88108	71.90	23.87258	0.38
7	31.6421	56.21311	77.65	31.83166	0.60
8	36.2342	64.01454	76.67	36.4974	0.73

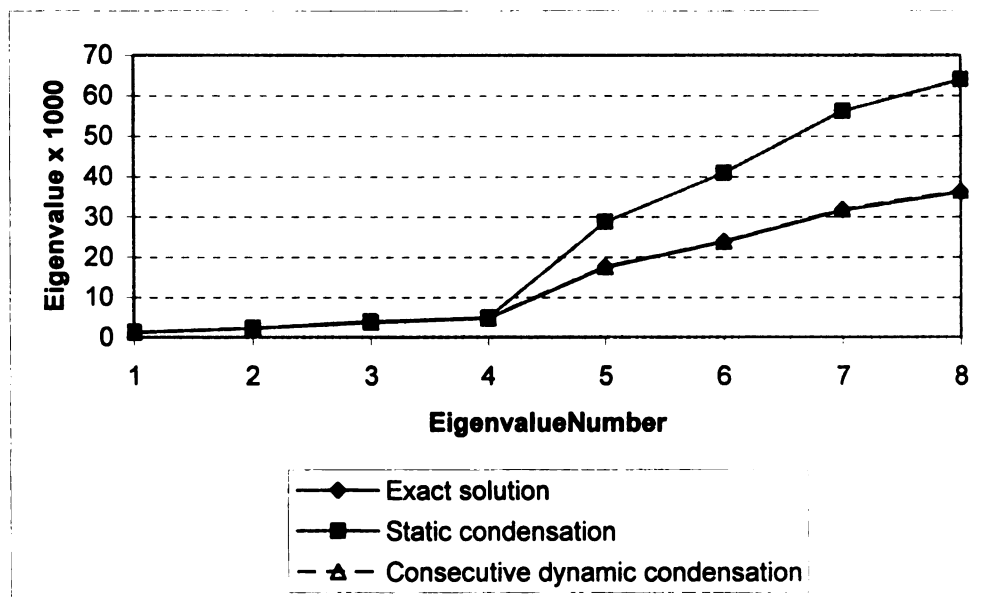


Figure 5.10. Results for Test Problem 4 (condensation to 8 primary d.o.f.)

TABLE 5.8. Results for Test Problem 4 (condensation to 3 primary d.o.f.)

Eigenvalue Number k	Eigenvalues obtained by				
	Solution of the full system $N = 142$	Static condensation to 3 primary d.o.f.		Consecutive dynamic condensation to 3 primary d.o.f.	
		$\lambda_k \times 10^3$	$\lambda_k \times 10^3$	ε (%)	$\lambda_k \times 10^3$
1	1.2628	1,153033	-8,69	1,263967	0,09
2	2.2645	1,690078	-25,37	2,275782	0,50
3	3.7804	4,000915	5,83	3,861551	2,15

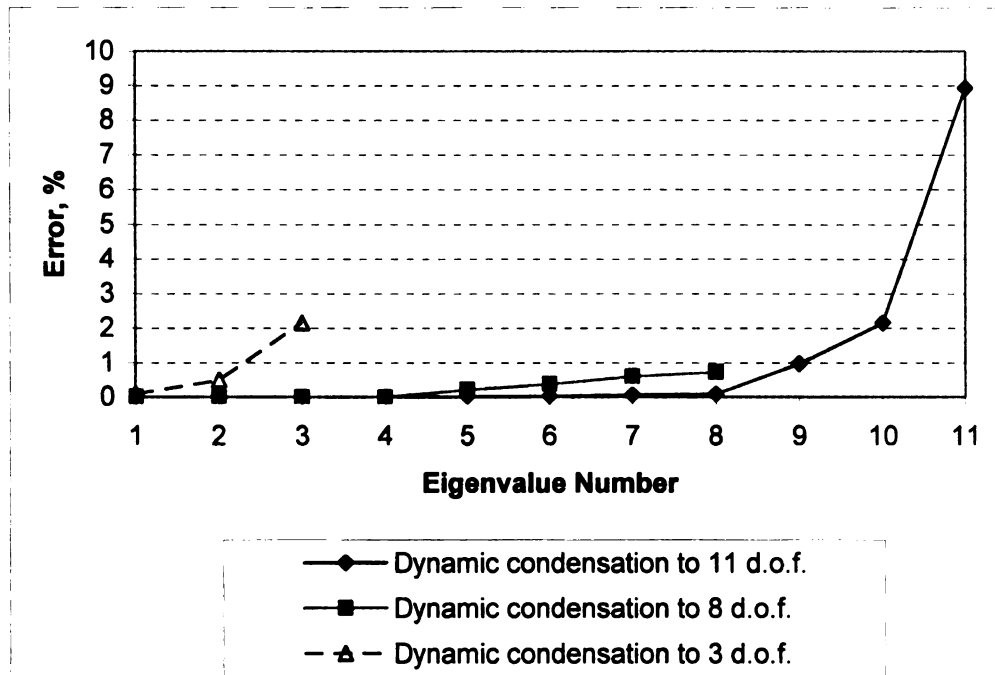


Figure 5.11. Graphs of errors for Test Problem 4

Test Problem 5

Consider a free vibration problem of a rectangular lattice plate with a 16x16 orthogonal grid shown in Figure 5.12. Concentrated masses are applied at the nodes. The problem was solved in the non-dimensional form using the following assumptions: $l_1 = l_2 = l$, $EI_1 = EI_2 = EI$, and $m_{ij} = m$. The transformation to the dimensional form can be done using the expression $\omega = \tilde{\omega} \sqrt{EI/ml^3}$ where $\tilde{\omega}$ is dimensionless frequency.

The problem was solved by the combined static and consecutive dynamic condensation method using three condensation schemes shown in Figure 5.13. The dimensionless values of natural frequencies are presented in Table 5.6. The results obtained by the proposed method are compared with the exact solutions obtained by Ignatiev (1979).

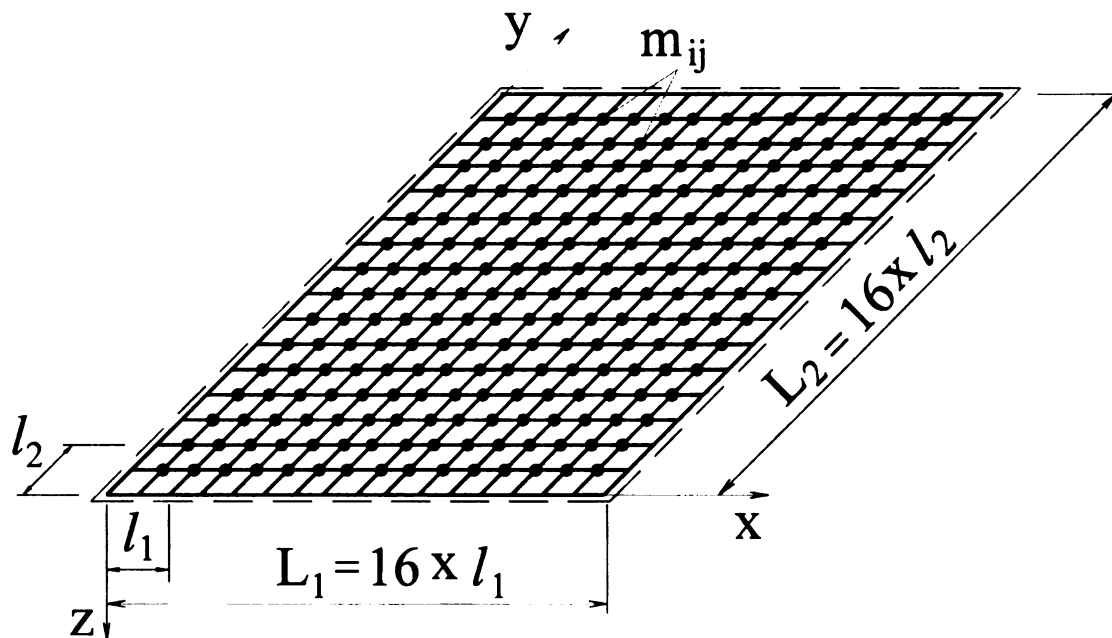


Figure 5.12. Rectangular lattice plate with a 16x16 orthogonal grid

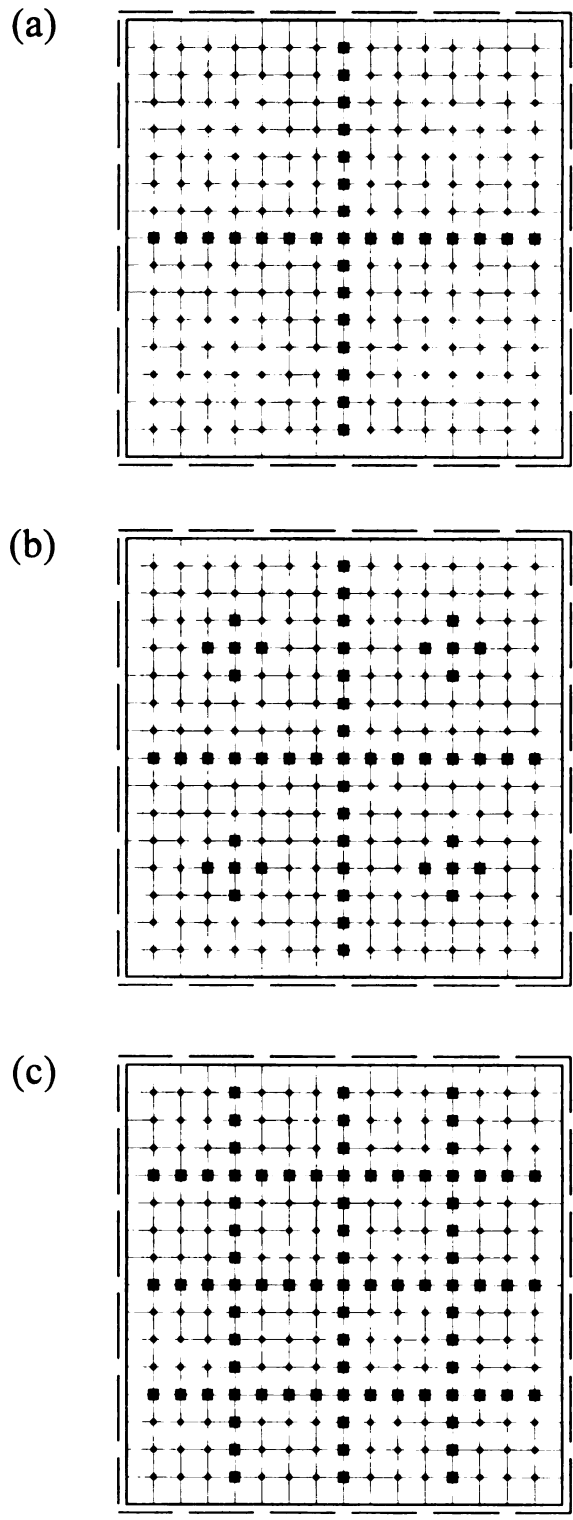


Figure 5.13. Condensation schemes for Test Problem 5: (a) to 29 primary nodes; (b) to 49 primary nodes; and (c) to 81 primary nodes

TABLE 5.6. Results for Test Problem 5

Eigenvalue Number k	Dimensionless frequency values obtained by						
	Exact solution	Combined static and consecutive dynamic condensation method with condensation to					
		29 nodes		49 nodes		81 nodes	
		$\tilde{\omega}_1 \times 10^2$	ε (%)	$\tilde{\omega}_1 \times 10^2$	ε (%)	$\tilde{\omega}_1 \times 10^2$	ε (%)
1	5.452232	5.465317	0.24	5.456594	0.08	5.450051	-0.04
2	21.80858	21.83475	0.12	21.79985	-0.04	21.9089	0.46
3	49.06569	48.96265	-0.21	49.0755	0.02	49.18345	0.24
4	87.20919	87.40977	0.23	87.23535	0.03	87.64523	0.5
5	136.1962	136.4958	0.22	136.1825	-0.01	137.6398	1.06
6	195.9207	191.9827	-2.01	196.0383	0.06	196.7044	0.4
7	266.1501	269.1309	1.12	266.2299	0.03	266.6824	0.2
8	346.4102	359.2966	3.72	346.3755	-0.01	346.7912	0.11
9	435.7914	462.7233	6.18	436.0528	0.06	439.2777	0.8
10	532.6364	554.581	4.12	533.0093	0.07	526.0317	-1.24
11	634.0843	654.1214	3.16	633.8307	-0.04	640.1716	0.96
12	735.5039	774.0443	5.24	733.8858	-0.22	744.6241	1.24
13	830.0138	897.577	8.14	831.1759	0.14	835.4089	0.65
14	908.5588	1001.959	10.28	908.2863	-0.03	910.1034	0.17
15	961.1921	1006.656	4.73	963.4989	0.24	974.9371	1.43
16	979.7959	992.2393	1.27	980.9717	0.12	985.2828	0.56

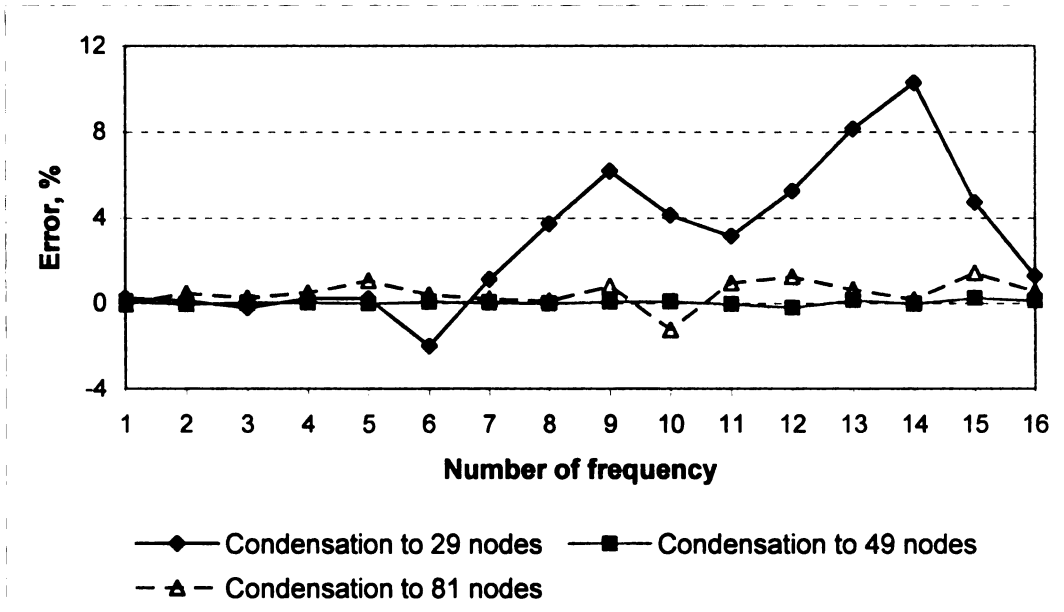


Figure 5.14. Graphs of errors for Test Problem 5

Examples of dynamic analysis of a frame and an isotropic plate using the proposed method are given in Appendix E. Based on the obtained results the following conclusions can be made:

- The proposed technique allows for solution of a broad range of problems
- A preliminary static condensation used in combination with the energy form of the consecutive dynamic condensation method provides better results than both methods used alone
- The proposed technique allows to determine approximately 70% of the reduced spectrum of eigenvalues with sufficient accuracy for different types of problems
- Block form of condensation provides a reduction of computation effort and improves the efficiency of proposed technique

- The number of blocks does not significantly affect the accuracy; therefore it is possible to use lesser number of blocks with larger number of secondary d.o.f. when appropriate
- The number of main d.o.f. and their location play the main role in accuracy of results

CHAPTER 6

CONCLUSIONS AND RECOMMENDATIONS

Two classes of new and effective approximate methods for static and dynamic analysis of large lattice structures using decomposition and consecutive dynamic condensation techniques are developed in this work. The main results of the work are discussed below.

A decomposition method proposed by Pshenichnov is developed for solving bending and free vibration problems of thin isotropic plates with elastic supports. Simple and accurate approximate analytical formulas for the displacements, force responses, and eigenvalues of these boundary value problems are obtained. A comparison of results with well-known solutions for rigid and hinged supports, demonstrates the high accuracy of this method. The merit of this method is the flexibility in the decomposition of the original problem, which provides wide latitude for choosing the auxiliary problems that facilitate the construction of the desired solution.

An effective technique for solving bending and free vibration problems of lattice plates with different combinations of supports is developed based on continuum modeling of lattice plates. The continuum model developed by Pshenichnov is used in this work. It is demonstrated that the continuum model together with the decomposition method yields an accuracy of within 2% for displacements and bending moments, which is adequate for preliminary design and optimization purposes.

It is demonstrated that the developed analytical dependencies can be used to obtain optimal lattice geometries for a class of plate problems. The proposed technique was implemented into the PLAST computer program for analyzing rectangular lattice plates with different types of lattices and different values of support rigidities. PLAST is written in the C programming language and can be used on personal computers.

Analytical formulas for calculating the fundamental frequency are obtained for lattice plates with different combinations of support rigidities. The results obtained for the test problems demonstrate that the decomposition method yields sufficient accuracy for the fundamental frequency. The analytical dependencies obtained can be used for optimization purposes. However, the method is intractable for estimating higher frequencies and mode shapes.

The decomposition method is generalized to include bending and free vibration equations derived from finite difference formulations. This approach allows the original discrete models of lattice plates to be used. Simple approximate analytical solutions are obtained for bending and free vibration problems of lattice plates in the form of systems of orthogonal beams with different types of supports. The results demonstrate that the decomposition method stated in finite difference form for bending problems of lattice plates with different types of grids and support rigidities is sufficiently accurate. The finite difference formulation of the method provides better results than the differential formulation for sparse grids. However, for dense grids both formulations yield similar accuracy.

An energy form of the consecutive dynamic condensation method proposed by Ignatiev is developed. It is demonstrated that preliminary static condensation used in

combination with the energy form of the consecutive dynamic condensation method provides better results than both methods used alone. The proposed technique is capable of determining approximately 70% of the reduced spectrum of eigenvalues with sufficient accuracy for different types of problems. The block form of condensation yields a reduction of computational effort and improves the efficiency of the proposed technique. The number of blocks does not significantly affect the accuracy; therefore it is possible to use fewer blocks with a large number of secondary d.o.f. when appropriate. The proposed technique is computationally efficient due to the resulting block diagonal equations and is suitable for implementation on parallel computers.

Based on the results, the following directions for future research are recommended:

- Inclusion of shear deformation and joint flexibility in the continuum and finite difference formulation of the decomposition method
- Application of the decomposition method to nonlinear static and dynamic problems
- Development of a continuous model for composite laminated plates that will make it possible to use the decomposition method for static and dynamic analysis of laminated structural elements
- Application of the decomposition method to stability problems

- Extension of the proposed technique to broader class of lattice structures including static, dynamic and stability problems of multi-layer lattice plates and large lattice shells
- Use of the finite difference formulation of the method to account for more complicated types of grids, for example grids with openings, grids with double regularity, etc.
- Development of computer programs for static and dynamic analysis of lattice plates and shells
- Application of the energy form of consecutive dynamic condensation method to the analysis of complex structural systems such as lattice shells, thin-walled cellular structures, complex frames, etc.
- Development of computer programs based on the consecutive dynamic condensation method for the analysis of complex structural systems

APPENDICES

APPENDIX A

ARBITRARY FUNCTIONS FOR THE PROBLEM PRESENTED IN SECTION 2.4.2

$$C_0 = 0.$$

$$\begin{aligned} C_1 = & 0.03333333333 (0.3808425 10^7 \lambda^2 k_1^4 + 0.1105425 10^7 \lambda^4 k_1^4 + 0.2652250 10^7 k_1^4 \\ & + 416160. \lambda^4 k_1^3 + 0.1030000 10^7 k_1^3 + 0.1456380 10^7 \lambda^2 k_1^3 + 65178. \lambda^4 k_1^2 \\ & + 151500. k_1^2 + 220980. \lambda^2 k_1^2 + 10000. k_1 + 15660. \lambda^2 k_1 + 4896. \lambda^4 k_1 + 250. \\ & + 153. \lambda^4 + 435. \lambda^2) k_1 / (79866. \lambda^4 k_1^2 + 0.1838550 10^7 \lambda^2 k_1^5 \\ & + 0.2353905 10^7 \lambda^4 k_1^4 + 25. + 809760. \lambda^2 k_1^3 + 0.2541630 10^7 \lambda^2 k_1^4 + 5355. \lambda^4 k_1 \\ & + 611694. \lambda^4 k_1^3 + 87850. k_1^3 + 0.3316275 10^7 \lambda^4 k_1^5 + 14150. k_1^2 + 975. k_1 \\ & + 210. \lambda^2 + 114240. \lambda^2 k_1^2 + 7770. \lambda^2 k_1 + 162225. k_1^4 - 265225. k_1^5 + 153. \lambda^4) \end{aligned}$$

$$\begin{aligned} C_2 = & -0.03333333333 (-1. + k_1) (0.3808425 10^7 \lambda^2 k_1^4 + 0.1105425 10^7 \lambda^4 k_1^4 \\ & + 0.2652250 10^7 k_1^4 + 416160. \lambda^4 k_1^3 + 0.1030000 10^7 k_1^3 + 0.1456380 10^7 \lambda^2 k_1^3 \\ & + 65178. \lambda^4 k_1^2 + 151500. k_1^2 + 220980. \lambda^2 k_1^2 + 10000. k_1 + 15660. \lambda^2 k_1 \\ & + 4896. \lambda^4 k_1 + 250. + 153. \lambda^4 + 435. \lambda^2) / (79866. \lambda^4 k_1^2 + 0.1838550 10^7 \lambda^2 k_1^5 \\ & + 0.2353905 10^7 \lambda^4 k_1^4 + 25. + 809760. \lambda^2 k_1^3 + 0.2541630 10^7 \lambda^2 k_1^4 + 5355. \lambda^4 k_1 \\ & + 611694. \lambda^4 k_1^3 + 87850. k_1^3 + 0.3316275 10^7 \lambda^4 k_1^5 + 14150. k_1^2 + 975. k_1 \\ & + 210. \lambda^2 + 114240. \lambda^2 k_1^2 + 7770. \lambda^2 k_1 + 162225. k_1^4 - 265225. k_1^5 + 153. \lambda^4) \end{aligned}$$

$$\begin{aligned}
C_3 = & -0.050000000000 (250. + 418200. \lambda^2 k_1^2 + 29675. \lambda^2 k_1 + 878500. k_1^3 \\
& + 141500. k_1^2 + 0.2749400 \cdot 10^7 \lambda^2 k_1^3 + 0.1622250 \cdot 10^7 k_1^4 + 0.1574370 \cdot 10^7 \lambda^4 k_1^3 \\
& + 220014. \lambda^4 k_1^2 + 825. \lambda^2 + 9750. k_1 + 0.5527125 \cdot 10^7 \lambda^4 k_1^5 - 0.2652250 \cdot 10^7 k_1^5 \\
& + 15453. \lambda^4 k_1 - 218875. \lambda^2 k_1^5 + 0.5397075 \cdot 10^7 \lambda^4 k_1^4 + 459. \lambda^4 \\
& + 0.7139175 \cdot 10^7 \lambda^2 k_1^4) / (79866. \lambda^4 k_1^2 + 0.1838550 \cdot 10^7 \lambda^2 k_1^5 \\
& + 0.2353905 \cdot 10^7 \lambda^4 k_1^4 + 25. + 809760. \lambda^2 k_1^3 + 0.2541630 \cdot 10^7 \lambda^2 k_1^4 + 5355. \lambda^4 k_1 \\
& + 611694. \lambda^4 k_1^3 + 87850. k_1^3 + 0.3316275 \cdot 10^7 \lambda^4 k_1^5 + 14150. k_1^2 + 975. k_1 \\
& + 210. \lambda^2 + 114240. \lambda^2 k_1^2 + 7770. \lambda^2 k_1 + 162225. k_1^4 - 265225. k_1^5 + 153. \lambda^4)
\end{aligned}$$

$$C_4 = 0.$$

$$\begin{aligned}
C_5 = & 0.050000000000 (0.1400800 \cdot 10^7 \lambda^2 k_1^4 + 368475. \lambda^4 k_1^4 + 0.1326125 \cdot 10^7 k_1^4 \\
& + 138720. \lambda^4 k_1^3 + 515000. k_1^3 + 535680. \lambda^2 k_1^3 + 21726. \lambda^4 k_1^2 + 75750. k_1^2 \\
& + 81280. \lambda^2 k_1^2 + 5000. k_1 + 5760. \lambda^2 k_1 + 1632. \lambda^4 k_1 + 125. + 51. \lambda^4 + 160. \lambda^2) k_1 \\
& / (79866. \lambda^4 k_1^2 + 0.1838550 \cdot 10^7 \lambda^2 k_1^5 + 0.2353905 \cdot 10^7 \lambda^4 k_1^4 + 25. \\
& + 809760. \lambda^2 k_1^3 + 0.2541630 \cdot 10^7 \lambda^2 k_1^4 + 5355. \lambda^4 k_1 + 611694. \lambda^4 k_1^3 + 87850. k_1^3 \\
& + 0.3316275 \cdot 10^7 \lambda^4 k_1^5 + 14150. k_1^2 + 975. k_1 + 210. \lambda^2 + 114240. \lambda^2 k_1^2 \\
& + 7770. \lambda^2 k_1 + 162225. k_1^4 - 265225. k_1^5 + 153. \lambda^4)
\end{aligned}$$

$$\begin{aligned}
C_6 = & -0.05000000000 (-1. + k_1) (0.1400800 10^7 \lambda^2 k_1^4 + 368475. \lambda^4 k_1^4 \\
& + 0.1326125 10^7 k_1^4 + 138720. \lambda^4 k_1^3 + 515000. k_1^3 + 535680. \lambda^2 k_1^3 \\
& + 21726. \lambda^4 k_1^2 + 75750. k_1^2 + 81280. \lambda^2 k_1^2 + 5000. k_1 + 5760. \lambda^2 k_1 + 1632. \lambda^4 k_1 \\
& + 125. + 51. \lambda^4 + 160. \lambda^2) / (79866. \lambda^4 k_1^2 + 0.1838550 10^7 \lambda^2 k_1^5 \\
& + 0.2353905 10^7 \lambda^4 k_1^4 + 25. + 809760. \lambda^2 k_1^3 + 0.2541630 10^7 \lambda^2 k_1^4 + 5355. \lambda^4 k_1 \\
& + 611694. \lambda^4 k_1^3 + 87850. k_1^3 + 0.3316275 10^7 \lambda^4 k_1^5 + 14150. k_1^2 + 975. k_1 \\
& + 210. \lambda^2 + 114240. \lambda^2 k_1^2 + 7770. \lambda^2 k_1 + 162225. k_1^4 - 265225. k_1^5 + 153. \lambda^4)
\end{aligned}$$

$$\begin{aligned}
C_7 = & -0.03333333333 (250. + 10251. \lambda^4 k_1 - 0.1707225 10^7 \lambda^2 k_1^5 \\
& + 0.3316275 10^7 \lambda^4 k_1^5 + 0.1809300 10^7 \lambda^2 k_1^3 + 141500. k_1^2 + 570. \lambda^2 + 9750. k_1 \\
& + 282540. \lambda^2 k_1^2 + 20325. \lambda^2 k_1 + 0.4337490 10^7 \lambda^2 k_1^4 + 0.3459330 10^7 \lambda^4 k_1^4 \\
& + 0.1027854 10^7 \lambda^4 k_1^3 + 145044. \lambda^4 k_1^2 + 878500. k_1^3 + 306. \lambda^4 \\
& + 0.1622250 10^7 k_1^4 - 0.2652250 10^7 k_1^5) / (79866. \lambda^4 k_1^2 \\
& + 0.1838550 10^7 \lambda^2 k_1^5 + 0.2353905 10^7 \lambda^4 k_1^4 + 25. + 809760. \lambda^2 k_1^3 \\
& + 0.2541630 10^7 \lambda^2 k_1^4 + 5355. \lambda^4 k_1 + 611694. \lambda^4 k_1^3 + 87850. k_1^3 \\
& + 0.3316275 10^7 \lambda^4 k_1^5 + 14150. k_1^2 + 975. k_1 + 210. \lambda^2 + 114240. \lambda^2 k_1^2 \\
& + 7770. \lambda^2 k_1 + 162225. k_1^4 - 265225. k_1^5 + 153. \lambda^4)
\end{aligned}$$

$$C_8 = 0.$$

$$\begin{aligned}
C_9 = & 0.02857142857 (0.1488350 10^7 \lambda^2 k_1^4 + 368475. \lambda^4 k_1^4 + 0.1856575 10^7 k_1^4 \\
& + 138720. \lambda^4 k_1^3 + 721000. k_1^3 + 569160. \lambda^2 k_1^3 + 21726. \lambda^4 k_1^2 + 106050. k_1^2 \\
& + 86360. \lambda^2 k_1^2 + 7000. k_1 + 6120. \lambda^2 k_1 + 1632. \lambda^4 k_1 + 175. + 51. \lambda^4 + 170. \lambda^2) k_1 \\
& / (79866. \lambda^4 k_1^2 + 0.1838550 10^7 \lambda^2 k_1^5 + 0.2353905 10^7 \lambda^4 k_1^4 + 25. \\
& + 809760. \lambda^2 k_1^3 + 0.2541630 10^7 \lambda^2 k_1^4 + 5355. \lambda^4 k_1 + 611694. \lambda^4 k_1^3 + 87850. k_1^3 \\
& + 0.3316275 10^7 \lambda^4 k_1^5 + 14150. k_1^2 + 975. k_1 + 210. \lambda^2 + 114240. \lambda^2 k_1^2 \\
& + 7770. \lambda^2 k_1 + 162225. k_1^4 - 265225. k_1^5 + 153. \lambda^4)
\end{aligned}$$

$$\begin{aligned}
C_{10} = & -0.02857142857 (-1. + k_1) (0.1488350 10^7 \lambda^2 k_1^4 + 368475. \lambda^4 k_1^4 \\
& + 0.1856575 10^7 k_1^4 + 138720. \lambda^4 k_1^3 + 721000. k_1^3 + 569160. \lambda^2 k_1^3 \\
& + 21726. \lambda^4 k_1^2 + 106050. k_1^2 + 86360. \lambda^2 k_1^2 + 7000. k_1 + 6120. \lambda^2 k_1 + 1632. \lambda^4 k_1 \\
& + 175. + 51. \lambda^4 + 170. \lambda^2) / (79866. \lambda^4 k_1^2 + 0.1838550 10^7 \lambda^2 k_1^5 \\
& + 0.2353905 10^7 \lambda^4 k_1^4 + 25. + 809760. \lambda^2 k_1^3 + 0.2541630 10^7 \lambda^2 k_1^4 + 5355. \lambda^4 k_1 \\
& + 611694. \lambda^4 k_1^3 + 87850. k_1^3 + 0.3316275 10^7 \lambda^4 k_1^5 + 14150. k_1^2 + 975. k_1 \\
& + 210. \lambda^2 + 114240. \lambda^2 k_1^2 + 7770. \lambda^2 k_1 + 162225. k_1^4 - 265225. k_1^5 + 153. \lambda^4)
\end{aligned}$$

$$\begin{aligned}
C_{11} = & -0.007142857143 (875. + 49420. \lambda^2 k_1 - 0.8579900 10^7 \lambda^2 k_1^5 \\
& + 0.7737975 10^7 \lambda^4 k_1^5 + 0.5677875 10^7 k_1^4 - 0.9282875 10^7 k_1^5 + 495250. k_1^2 \\
& + 1400. \lambda^2 + 0.3074750 10^7 k_1^3 + 675920. \lambda^2 k_1^2 + 0.8975960 10^7 \lambda^2 k_1^4 \\
& + 0.8440245 10^7 \lambda^4 k_1^4 + 34125. k_1 + 0.2537046 10^7 \lambda^4 k_1^3 + 25551. \lambda^4 k_1 + 765. \lambda^4 \\
& + 0.4189360 10^7 \lambda^2 k_1^3 + 360162. \lambda^4 k_1^2) / (79866. \lambda^4 k_1^2 + 0.1838550 10^7 \lambda^2 k_1^5 \\
& + 0.2353905 10^7 \lambda^4 k_1^4 + 25. + 809760. \lambda^2 k_1^3 + 0.2541630 10^7 \lambda^2 k_1^4 + 5355. \lambda^4 k_1 \\
& + 611694. \lambda^4 k_1^3 + 87850. k_1^3 + 0.3316275 10^7 \lambda^4 k_1^5 + 14150. k_1^2 + 975. k_1 \\
& + 210. \lambda^2 + 114240. \lambda^2 k_1^2 + 7770. \lambda^2 k_1 + 162225. k_1^4 - 265225. k_1^5 + 153. \lambda^4)
\end{aligned}$$

APPENDIX B

PROGRAM "PLAS" FOR ANALYSIS OF LATTICE PLATES

```
/******
```

```
PLAS
```

```
Analysis of lattice plates with elastic support
```

```
#include <graphics.h>
#include <stdlib.h>
#include <math.h>
#include <stdio.h>
#include <bios.h>
#include <conio.h>
#include <io.h>
```

```
int errorcode, graphdriver, graphmode;
```

```
char work, str[6][30];
```

```
union inkey char ch[2]; int ii; jj, dd;
```

```
int i, ij, j, ji, k, ki, l, li, m, mi, n, ni, e[5][5];
```

```
double
```

```
    dl, ee, f1, f2, f3, f4, ga, k1, k2, k3, k4, l2, l4, lm, lm1, lm
    2, nu, pi, t1, t2, z1, z2, z3, z4;
```

```
int d1, d2, d3, d4, e0;
```

```
double
```

```
lmm[21], a[5][5], x[9], y[9], v[9][9], w[9][9], f[2][7];
```

```
double
```

```
aa, a0, a1, a2, a3, a4, a5, bb, b0, b1, b2, b3, b4, b5, cc, c0, c1, c2
```

```
,
```

```
    c3, c4, e1, e2, rr, s1, s2, s3, s4, x1, x2, x3, x4, x5, x6, y1,
    y2, y3,
```

```
    y4, y5, y6, u1, u2, u3, u4, v1, v2, v3, v4;
```

```
double o[5][5], g[5], qq, q0, p[5][5], b[2][5], c[4][4];
```

```
void opred(), tire(), ramka(), risl();
```

```

/* переменные графики */

int
i1,i2,i3,i4,i5,i6,j1,j2,j3,j4,j5,j6,i0y,j0x,lx,ly,
lx1,ly1,xx[2][9],yy[2][9],zz[9][2];

FILE *fd; FILE *fp;

main()
{
    clrscr(); /* очистка экрана */

    if ( access("plas.dn",0)==-1 )
printf( "\n Нет файла исходных данных - plas.dn\n" );
    exit(1);
        fd=fopen("plas.dn","r");
        fp=fopen("plas.pr","w");

printf("\n Расчет пластинки на упругом основании\n");

printf("\n Ввод исходных данных\n");
fscanf(fd,"%lf%lf%lf%d",&lm1,&lm2,&dl,&ij);
fscanf(fd,"%lf%lf%lf",&t1,&t2,&ga);
fscanf(fd,"%d%d%d%d",&d1,&d2,&d3,&d4);
fscanf(fd,"%lf%lf%lf%lf",&f1,&f2,&f3,&f4);
fscanf(fd,"%lf%lf%lf%lf",&k1,&k2,&k3,&k4);

    tire();
fprintf(fp,"Расчет пластинки на упругом основании ");
    tire();
fprintf(fp,"\n И с х о д н ы е   д а н н ы е");
    tire();
fprintf(fp,"\n
        lm1          lm2          dl
        ij");
fprintf(fp,"\n%18.2f%15.2f%15.2f%12d\n",lm1,lm2,dl,ij);
fprintf(fp,"\n
        t1          t2          ga");
fprintf(fp,"\n%18.2f%15.2f%15.2f\n",t1,t2,ga);
fprintf(fp,"\n
        dl          d2          d3
        d4");
fprintf(fp,"\n%15d%15d%15d%15d\n",d1,d2,d3,d4);
fprintf(fp,"\n
        f1          f2          f3
        f4");
fprintf(fp,"\n%18.2f%15.2f%15.2f%15.2f\n",f1,f2,f3,f4);
fprintf(fp,"\n
        k1          k2          k3
        k4");
fprintf(fp,"\n%18.2f%15.2f%15.2f%15.2f\n",k1,k2,k3,k4);
    tire();
    n=0;

```

```

        if (lm1<1 || lm1>100) n=1;
        if (lm2<1 || lm2>100) n=1;
        if (d1<0.1 || d1>10) n=1;
        if (t1<0 || t1>5) n=1;
        if (t2<0 || t2>5) n=1;
        if (d1<0 || d1>1) n=1;
        if (d2<0 || d2>1) n=1;
        if (d3<0 || d3>1) n=1;
        if (d4<0 || d4>1) n=1;
        if (f1<-90 || f1>90) n=1;
        if (f2<-90 || f2>90) n=1;
        if (f3<-90 || f3>90) n=1;
        if (f4<-90 || f4>90) n=1;
        if (k1<0 || k1>1) n=1;
        if (k2<0 || k2>1) n=1;
        if (k3<0 || k3>1) n=1;
        if (k4<0 || k4>1) n=1;

        m=(lm2-lm1)/d1+1; /* счетчик цикла по lm */
        if (m>20)
printf("\n Число шагов по /лямбда/ превышает 20 - N =
%d\n",m);
        exit(1);
        if (n==1)
printf("\n Один из исходных параметров имеет недопустимое
значение !\n");
        exit(1);
        pi=3.14159265359; ee=2.71828183; nu=0.3;

        f1=f1*pi/180; f2=f2*pi/180;
        f3=f3*pi/180; f4=f4*pi/180;

printf("\n Начало работы программы\n");

        s1=sin(f1); c1=cos(f1);
        a0=d1+s1*d3+c1*d4;
        rr=d1*(c1*c1*c1*c1)+d4*c1+d1*ga*(s1*s1)*(c1*c1);

/* коэффициенты при неизвестных системы уравнений */
        lm=lm1; l2=lm*lm; l4=lm*lm*lm*lm;
        u1=1+2*k1; u2=1+4*k1; u3=1+6*k1;
        v1=1+2*k2; v2=1+4*k2; v3=1+6*k2;
        a[1][1]=1+4*k2+2*u1*u1*t1/(3*l2)+u2*t2/l4;
        a[1][2]=u2*v1*t1/(15*l2)+2*u3*t2/(15*l4);
        a[1][3]=2*v3+u1*v2*t1/l2;
        a[1][4]=u2*v2*t1/(10*l2);
        a[1][0]=1;
        a[2][1]=(-4)*(v1*t1/l2+u1*t2/l4);

```

```

    a[2][2]=2*(1+4*k2-u2*t2/(5*14));
    a[2][3]=(-6)*(v2*t1/12);
    a[2][4]=4*v3;
    a[2][0]=0;
a[3][1]=(-4)*(1+2*k2+u1*t1/12);
a[3][2]=(-2)*u2*t1/(5*12);
a[3][3]=(-6)*(1+4*k2-5*u2*t2/14);
a[3][4]=4*u3*t2/14;
a[3][0]=0;
    a[4][1]=6*t2/12;
    a[4][2]=(-2)*v1*t1;
    a[4][3]=0;
    a[4][4]=(-3)*v2*t1;
    a[4][0]=0;

        /* единичные коэффициенты при минорах */
for (l=1; l<=4; l++)
    for (m=1; m<=4; m++)
        k=l+m;          e0=-1;
        for (n=1; n<=k-1; n++)          e0=e0*(-1);
    e[l][m]=e0;
        /* вычисление главного определителя */
for (m=1; m<=4; m++)
    for (n=0; n<=4; n++)
        p[m][n]=a[m][n];
    o[m][n]=a[m][n];
opred();          g[0]=qq;

/* вычисление второстепенных определителей */
for (i=1; i<=4; i++)
    for (m=1; m<=4; m++)
        for (n=1; n<=4; n++)
            p[m][n]=o[m][n];
    for (m=1; m<=4; m++)
        p[m][i]=a[m][0];
opred();          g[i]=qq;
        /* значения неизвестных */
    if (g[0]<0.0001)
printf("\n Главный определитель равен нулю !\n");
    exit(1);

    z1=g[1]/g[0];    z2=g[2]/g[0];
    z3=g[3]/g[0];    z4=g[4]/g[0];

/*****
        /* вычисление прогибов и моментов */
    x[0]=0;          y[0]=0;
for (k=1; k<=8; k++)
    x[k]=x[k-1]+0.125;    y[k]=y[k-1]+0.125;

```

```

for (j=0; j<=8; j++)
  for (i=0; i<=8; i++)
    /* координаты */
    x1=x[i];      y1=y[j];
    x2=x1*x[i];   y2=y1*y[j];
    x3=x2*x[i];   y3=y2*y[j];
    x4=x3*x[i];   y4=y3*y[j];
    x5=x4*x[i];   y5=y4*y[j];
    x6=x5*x[i];   y6=y5*y[j];
    /* функции "фи" */
    u1=1+2*k1;    u2=1+4*k1;    u3=1+6*k1;
    v1=1+2*k2;    v2=1+4*k2;    v3=1+6*k2;
    f[1][1]=y4-2*u1*y2+u2;
    f[0][1]=x4-2*v1*x2+v2;
    f[1][2]=y6-3*u2*y2+2*u3;
    f[0][2]=x6-3*v2*x2+2*v3;
    f[1][3]=4*y3-4*u1*y1;
    f[0][3]=4*x3-4*v1*x1;
    f[1][4]=6*y5-6*u2*y1;
    f[0][4]=6*x5-6*v2*x1;
    f[1][5]=12*y2-4*u1;
    f[0][5]=12*x2-4*v1;
    f[1][6]=30*y4-6*u2;
    f[0][6]=30*x4-6*v2;
    e1=1;        e2=1;
    e1=e1/24;    e2=e2/360;
    b1=e1*f[1][1]*(z1*f[0][1]+z3*f[0][2]);
    b2=e2*f[1][2]*(z2*f[0][1]+z4*f[0][2]);
    v[j][i]=b1+b2;
    a1=e1*f[1][5]*(z1*f[0][1]+z3*f[0][2]);
    a2=e2*f[1][6]*(z2*f[0][1]+z4*f[0][2]);
    a3=e1*f[1][1]*(z1*f[0][5]+z3*f[0][6]);
    a4=e2*f[1][2]*(z2*f[0][5]+z4*f[0][6]);
    w[j][i]=a1+a2+nu*(a3+a4);

    /*****/

if (ij==0)

printf("\n\n Вывод результатов на печать\n");

    f1=f1*180/pi;    f2=f2*180/pi;
    f3=f3*180/pi;    f4=f4*180/pi;
    tire();
fprintf(fp, "\n          z1          z2          z3
                z4");
fprintf(fp, "\n%18.4f%15.4f%15.4f%15.4f\n", z1, z2, z3, z4);

```

```

        tire();
        tire();
    fprintf(fp, "\nКоординаты точек пластинки по X и по Y");
        tire();
    fprintf(fp, "    0      1      2      3      4");
    fprintf(fp, "    5      6      7      8");
        tire();
    fprintf(fp, "\n  %8.3f", x[0]);
        for (k=1; k<=8; k++)          fprintf(fp, "%8.3f", x[k]);
    fprintf(fp, "\n  %8.3f", y[0]);
        for (k=1; k<=8; k++)          fprintf(fp, "%8.3f", y[k]);
        tire();
    fprintf(fp, "\nПрогибы пластинки по точкам");
        tire();
    fprintf(fp, "    0      1      2      3      4");
    fprintf(fp, "    5      6      7      8");
        tire();
        for (i=0; i<=8; i++)
    fprintf(fp, "\n  %8.3f", v[i][0]);
        for (k=1; k<=8; k++)          fprintf(fp, "%8.3f", v[i][k]);

        tire();
    fprintf(fp, "\nИзгибающие моменты пластинки по точкам");
        tire();
    fprintf(fp, "    0      1      2      3      4");
    fprintf(fp, "    5      6      7      8");
        tire();
        for (i=0; i<=8; i++)
    fprintf(fp, "\n  %8.3f", w[i][0]);
        for (k=1; k<=8; k++)          fprintf(fp, "%8.3f", w[i][k]);

        tire();

    fprintf(fp, "\n  Конеч результатов \n");

    else
    printf("\n\n Графический вывод \n");

```

```

/*****/

    /* Подготовка графического поля*/

/* координаты графического поля монитора */
/* i1=0; j1=0; i2=639; j2=349; */
i1=0; j1=0; i2=639; j2=479;

    /* координаты поля изображения */
i3=i1+20; j3=j1+25; i4=i2-20; j4=j2-55;
    /* размеры поля кривой */
lx=i4-i3; ly=j4-j3;
    /* координаты координатных осей */
i0y=lx/2+i3; j0x=ly/2+j3;
    /* масштабирование изображения */
a1=lx; b1=ly; e1=a1/b1;
if (lm>e1)
    lx=(lx/16)*16; ly=lx/lm; ly=(ly/16)*16;
    lx1=lx/16; ly1=ly/16;

else
    ly=(ly/16)*16; lx=ly*lm; lx=(lx/16)*16;
    lx1=lx/16; ly1=ly/16;

a1=fabs(w[0][0]); b1=fabs(v[0][0]);
for (i=1; i<=8; i++)
a2=fabs(w[0][i]); a3=fabs(w[i][0]);
b2=fabs(v[0][i]); b3=fabs(v[i][0]);
if (a1<a2) a1=a2;
if (a1<a3) a1=a3;
if (b1<b2) b1=b2;
if (b1<b3) b1=b3;

if (lx1>ly1) e1=lx1; else e1=ly1;
if (a1>b1) e0=3*e1/a1;
else e0=3*e1/b1;
for (i=0; i<=8; i++)
yy[0][i]=w[0][i]*e0;
yy[1][i]=w[i][0]*e0;
xx[0][i]=v[0][i]*e0;
xx[1][i]=v[i][0]*e0;

clrscr(); /* очистка экрана */
/* открытие графического режима */
errorcode = registerbgidriver(EGAVGA_driver);
if (errorcode < 0)
printf("Graphics error: %s\n", grapherrormsg(errorcode));
exit(1);

```

```

detectgraph( &graphdriver, &graphmode);
initgraph( &graphdriver, &graphmode, "");

    setfillstyle(SOLID_FILL, EGA_CYAN);
bar(i1,j1,i2,j2);
    setfillstyle(SOLID_FILL, EGA_WHITE);
    bar(i1+8,j1+8,i2-8,j2-38);
    setfillstyle(SOLID_FILL, EGA_WHITE);
bar(i1+90,j2-30,i2-90,j2-8);
    setcolor(EGA_BLACK);
i5=i1+10;    j5=j2-8; i6=i1+50;    j6=j2-30;
ramka();
outtextxy(i2-60, j2-23, "PLAST");
outtextxy(i1+20, j2-23, "Esc");
i5=i0y-lx/2;    j5=j0x-ly/2; i6=i0y+lx/2;
j6=j0x+ly/2;
ramka();
line(i5,j0x,i6,j0x);    line(i0y,j5,i0y,j6);

    /* пояснения к графикам */
sprintf(str[1],"B/A=%4.2f",lm);
outtextxy(i1+460, j2-23, str[1]);

    setcolor(EGA_RED); line(i1+120,j2-
20,i1+150,j2-20);
sprintf(str[3],"Mmax=%5.3f",a1);
outtextxy(i1+160, j2-23, str[3]);
    i5=i0y;    i6=i0y;
for (i=0; i<=8; i++)
    j5=j0x;    j6=j0x-yy[0][i];
    line(i5,j5,i6,j6);
    zz[i][0]=i6;    zz[i][1]=j6;
i5=i5+lx1;    i6=i6+lx1;
risl();
    j5=j0x;    j6=j0x;
for (i=0; i<=8; i++)
    i5=i0y;    i6=i0y+yy[1][i];
    line(i5,j5,i6,j6);
    zz[i][0]=i6;    zz[i][1]=j6;
j5=j5+ly1;    j6=j6+ly1;
risl();

    setcolor(EGA_BLUE); line(i1+270,j2-
20,i1+300,j2-20);
sprintf(str[2],"Wmax=%5.3f",b1);
outtextxy(i1+310, j2-23, str[2]);
    i5=i0y;    i6=i0y;
for (i=0; i<=8; i++)

```



```

        j5=j0x;          j6=j0x-xx[0][i];
        line(i5,j5,i6,j6);
        zz[i][0]=i6;    zz[i][1]=j6;
i5=i5-lx1;    i6=i6-lx1;
risl();
        j5=j0x;          j6=j0x;
for (i=0; i<=8; i++)
        i5=i0y;          i6=i0y+xx[1][i];
        line(i5,j5,i6,j6);
        zz[i][0]=i6;    zz[i][1]=j6;
j5=j5-ly1;    j6=j6-ly1;
risl();

work=1;
while (work==1)          /* пока не нажата Esc */
        jj.ii=bioskey(0);
        switch (jj.ch[0])
        case 0x1B:      /* Клавиша Esc - выход */
                work=0;
                break;
        default:
                break;

        closegraph();    /* закрытие графического режима */
        clrscr();        /* очистка экрана */

printf("\n  Работа программы закончена\n");
}          /* конец - main() */

/*****

void opred()
        qq=0;
        for (l=0; l<=1; l++)
                for (m=1; m<=4; m++)          b[l][m]=0;
        for (k=1; k<=4; k++)
                b[0][k]=p[1][k];
                switch(k)
                case 1:  li=2;  mi=3;  ni=4; break;
                case 2:  li=1;  mi=3;  ni=4; break;
                case 3:  li=1;  mi=2;  ni=4; break;
                case 4:  li=1;  mi=2;  ni=3; break;
                default: exit(1);

        for (n=1; n<=3; n++)
                c[n][1]=p[n+1][li];
                c[n][2]=p[n+1][mi];
                c[n][3]=p[n+1][ni];
                a2=c[1][1]*c[2][2]*c[3][3]-c[1][1]*c[2][3]*c[3][2];

```

```

        a3=c[1][2]*c[2][3]*c[3][1];
        a1=a2+a3;
        b2=c[1][2]*c[2][1]*c[3][3]-c[1][3]*c[2][1]*c[3][2];
        b3=c[1][3]*c[2][2]*c[3][1];
        b1=b2+b3;
        b[1][k]=(a1-b1)*b[0][k];

    for (k=1; k<=4; k++)
        qq=qq+b[1][k]*e[1][k];
return;
void risl()
    for (i=1; i<=8; i++)
        i5=zz[i-1][0];        j5=zz[i-1][1];
        i6=zz[i][0];          j6=zz[i][1];
        line(i5,j5,i6,j6);
return;
void tire()                    int iv;
    fprintf(fp,"\n ");
    for (iv=1; iv<=74; iv++) fprintf(fp,"-");
    fprintf(fp,"\n");
return;
void ramka()
    rectangle(i5,j5,i6,j6);
return;
/*****
        /*  К о н е ц  п р о г р а м м ы  */

```

APPENDIX C

FORMULAE FOR THE MAIN DIFFERENCES AND SUMS

Differences of the second order	Differences of the 4 th order
$\Delta^2 i^{(2)} = 2$	$\Delta^4 i^{(4)} = 24$
$\Delta^2 i^{(3)} = 6(i-1)^{(1)}$	$\Delta^4 i^{(5)} = 120(i-2)^{(1)}$
$\Delta^2 i^{(4)} = 12(i-1)^{(2)}$	$\Delta^4 i^{(5)} = 360(i-2)^{(2)}$
$\Delta^2 i^{(5)} = 20(i-1)^{(3)}$	
$\Delta^2 i^{(6)} = 30(i-1)^{(4)}$	
Sums	
$S_i = i + C$	$S_i^{(3)} = \frac{(i+1)^{(4)}}{4} + C$
$S_i = \frac{(i+1)^{(2)}}{2} + C$	$S_i^{(4)} = \frac{(i+1)^{(5)}}{5} + C$
$S_i^{(2)} = \frac{(i+1)^{(3)}}{3} + C$	$S_i^{(5)} = \frac{(i+1)^{(6)}}{6} + C$

APPENDIX D

ELEMENTS OF MATRICES OF COEFFICIENTS FOR THE PROBLEM PRESENTED IN SECTION 4.5

Elements of matrix C_i :

$$\begin{aligned}
 c_{11} &= 1 & c_{12} &= -0.5\tilde{k}_1 - 1 & c_{13} &= 3\tilde{k}_1 \\
 c_{21} &= \frac{n^{(3)}}{6} & c_{22} &= \frac{n^{(2)}}{2} & c_{23} &= n \\
 c_{31} &= \frac{(n-1)^{(3)}}{6} (5 + 4\tilde{k}_1) - (4 + 0.5\tilde{k}_1) \frac{(n-2)^{(3)}}{6} + \frac{(n-3)^{(3)}}{6} \\
 c_{32} &= \frac{(n-1)^{(2)}}{2} (5 + 4\tilde{k}_1) - (4 + 0.5\tilde{k}_1) \frac{(n-2)^{(2)}}{2} + \frac{(n-3)^{(3)}}{2} \\
 c_{33} &= (n-1)(5 + 4\tilde{k}_1) - (4 + 0.5\tilde{k}_1)(n-2) + (n-3)
 \end{aligned}$$

Elements of matrix D_i :

$$\begin{aligned}
 d_{11} &= 5 - 0.5\tilde{k}_1 & d_{12} &= 6 - \tilde{k}_1 & d_{13} &= \frac{1}{3} + \frac{1}{6}\tilde{k}_1 \\
 d_{21} &= \frac{n^{(4)}}{4} & d_{22} &= \frac{n^{(5)}}{20} & d_{23} &= \frac{n^{(6)}}{60} \\
 d_{31} &= 5 - 0.5\tilde{k}_1 - (5 + 4\tilde{k}_1) \frac{(n-1)^{(4)}}{4} + (4 + 0.5\tilde{k}_1) \frac{(n-2)^{(4)}}{4} - \frac{(n-3)^{(4)}}{4} \\
 d_{32} &= (4 - 0.5\tilde{k}_1)(n-1) + (n+2) - (5 + 4\tilde{k}_1) \frac{(n-1)^{(5)}}{20} + (4 + 0.5\tilde{k}_1) \frac{(n-2)^{(5)}}{20} - \frac{(n-3)^{(5)}}{20} \\
 d_{33} &= (4 - 0.5\tilde{k}_1) \left((n-1)^{(2)} - \frac{1}{3} \right) + (n+2)^{(2)} - \frac{1}{3} - (5 + 4\tilde{k}_1) \frac{(n-1)^{(6)}}{60} + \\
 &\quad + (4 + 0.5\tilde{k}_1) \frac{(n-2)^{(6)}}{60} - \frac{(n-3)^{(6)}}{60}
 \end{aligned}$$

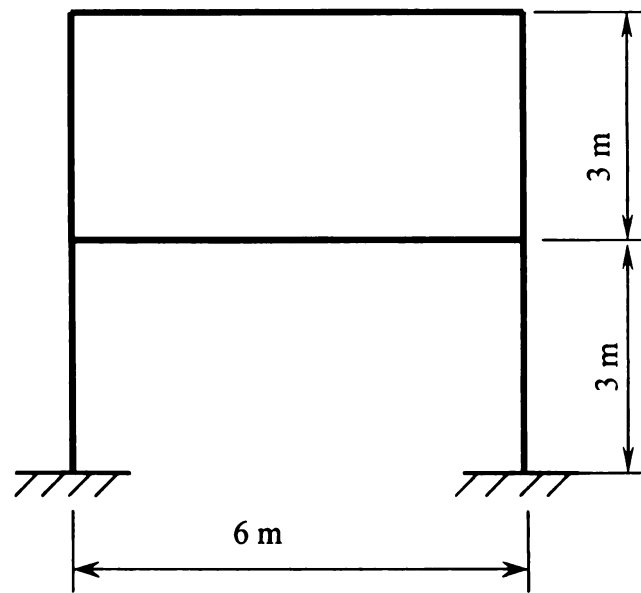
APPENDIX E

EXAMPLES OF DYNAMIC ANALYSIS USING THE COMBINED STATIC AND CONSECUTIVE DYNAMIC CONDENSATION METHOD

Problem 1. Dynamic Analysis of a Two-Story One-Bay Frame with Fixed Supports and Rigid Joints.

Consider the concrete frame shown in Figure E.1 (a). The beams have the following characteristics: dimensions of the cross-section 0.3x0.6 m, the area of the cross-section $A = 0.18 \text{ m}^2$, modulus of elasticity $E = 210 \text{ GPa}$, moment of inertia $I = 0.0054 \text{ m}^4$, mass per unit length $m = 0.45 \text{ (kN}\cdot\text{sec}^2)/\text{m}$. The columns have the following characteristics: dimensions of the cross-section 0.3x0.3 m, the area of the cross-section $A = 0.09 \text{ m}^2$, modulus of elasticity $E = 210 \text{ GPa}$, moment of inertia $I = 0.000675 \text{ m}^4$, mass per unit length $m = 0.225 \text{ (kN}\cdot\text{sec}^2)/\text{m}$. The frame is divided into 24 linear finite elements with equal lengths of beam and column elements: $a = b = 1 \text{ m}$. The condensation was performed using ten main d.o.f. concentrated in the four main joints of the frame (Figure E.1 b). The secondary nodes were structurally subdivided into six groups. Two types of blocks of the secondary unknowns were used. The number of unknowns in the first and the fourth blocks corresponding to the beam groups of nodes was ten, and the number of unknowns in the second, third, fifth, and sixth blocks corresponding to the column groups was four. The problem was solved by the combined static and consecutive dynamic condensation method. Results presented in Table E.1 are compared to the results obtained by solving the original problem with the full set of d.o.f. Results are illustrated in Figures E.2 and E.3.

(a)



(b)

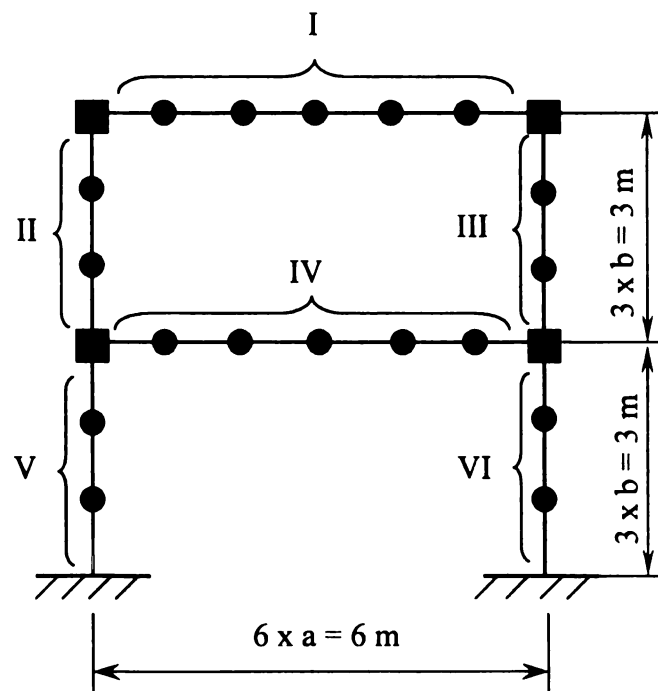


Figure E.1. (a) The frame for Problem 1; (b) Arrangement of the primary d.o.f. and secondary d.o.f. blocks for Problem 1

TABLE E.1. Results for Problem 1

Eigenvalue Number k	Eigenvalues obtained by				
	Solution of the full system $N = 46$	Static condensation to 10 primary d.o.f.		Consecutive dynamic condensation to 10 primary d.o.f.	
		$\lambda_k \times 10^5$	$\lambda_k \times 10^5$	ε (%)	$\lambda_k \times 10^5$
1	0.94334	0,95083	0.79	0.94334	0.00
2	4.15938	5,32689	28.07	4.15985	0.01
3	5.39297	7,71121	42.99	5.39397	0.02
4	8.19999	8.40841	2.54	8.20214	0.03
5	37.927	54.71233	44.26	38.3216	1.04
6	39.5599	66.532	68.18	40.3216	1.93
7	46.4969	80.965	74.13	56.0487	20.54
8	51.9747	128.802	147.82	96.7262	86.10
9	69.0507	219.7353	218.22	135.651	96.45
10	98.5372	356.826	262.12	161.634	64.03

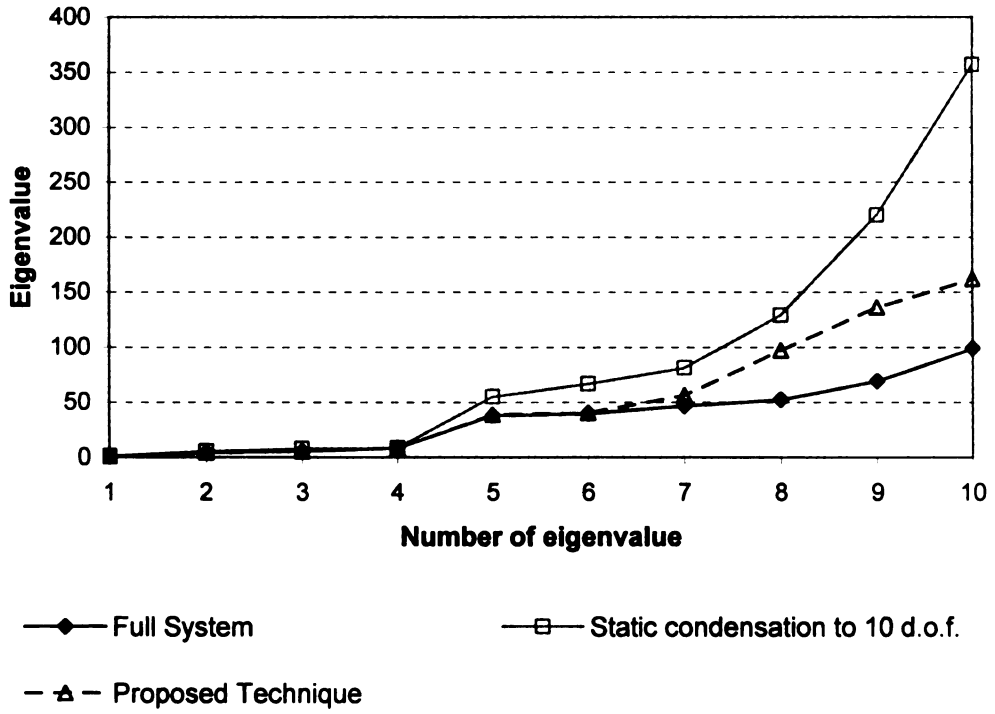


Figure E.2. Results for Problem 1

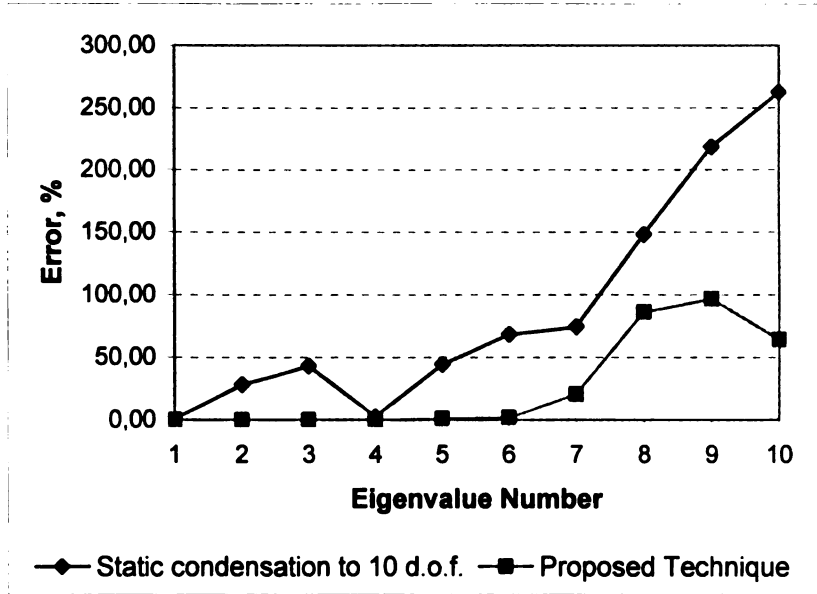


Figure E.3. Graphs of errors for Problem 1

Problem 2. Dynamic Analysis of an Isotropic Plate with Fixed Supports.

Consider a thin rectangular isotropic plate with fixed supports. The plate has the following parameters: length $A = 3$ m, width $B = 2.8$ m, thickness $t = 0.1$ m, Poisson's ratio $\nu = 0.3$, Young's modulus $E = 210$ GPa. The plate is loaded by the uniformly distributed mass of intensity $m = 10$ (kN*s²)/m. The plate is divided into a mesh of rectangular finite elements with dimensions $a = 0.3$ m, $b = 0.2$ m (Figure ED.4 a).

The plate was divided into four substructures by assigning the main nodes along the centerlines of the plate. Additional main nodes were assigned concentrated in the middle of each block. The condensation was carried out using 63, 75, and 99 primary d.o.f. Three variants of the arrangement of condensation nodes are shown in Figure E.4 (a), (b), and (c).

Dynamic analysis of the plate was performed by the combined static and consecutive dynamic condensation method. Results are presented in Table E.2 and illustrated in Figures E.5 and E.6. The eigenvalues obtained by proposed technique are compared with those obtained solving the full system of equations. Alternative calculations were made using the static condensation to 99 primary d.o.f.

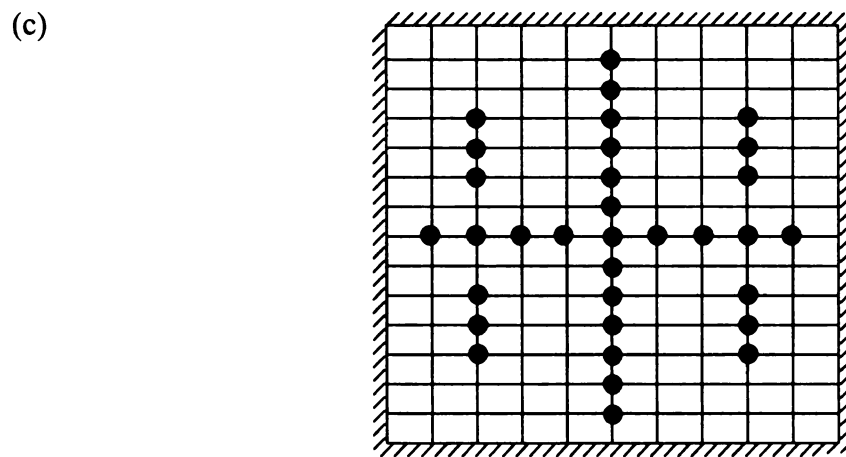
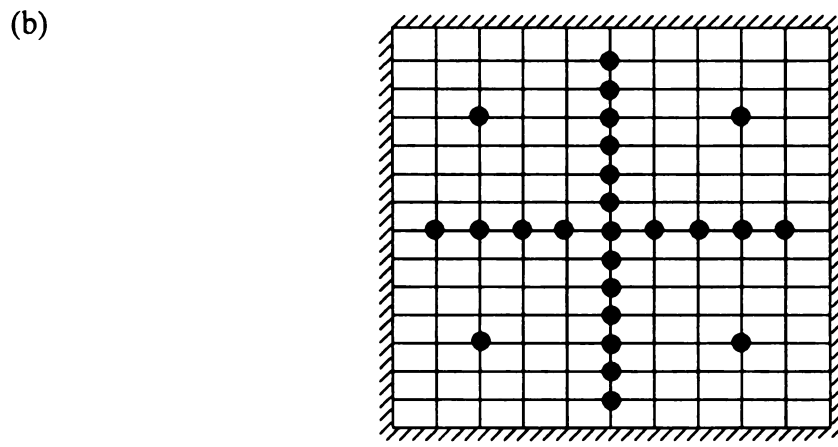
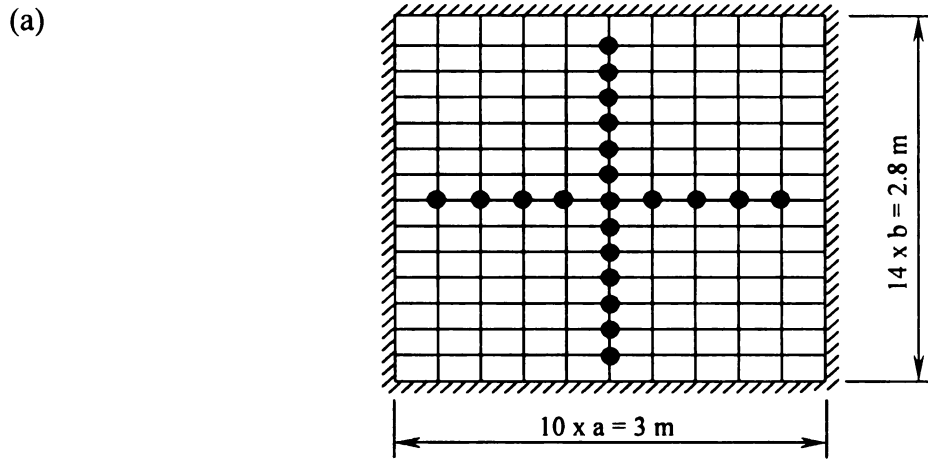


Figure E.4. Location of condensation nodes for Problem 2: (a) condensation to 63 d.o.f.; (b) condensation to 75 d.o.f.; (c) condensation to 99 d.o.f.

TABLE E.2. Results for Problem 2

Eigenvalue Number k	Eigenvalues obtained by											
	Solution of the full system $N = 351$	Static condensation to 99 primary d.o.f.			63 primary d.o.f.			75 primary d.o.f.			99 primary d.o.f.	
		$\lambda_k \times 10^4$	$\lambda_k \times 10^4$	ϵ (%)	$\lambda_k \times 10^4$	ϵ (%)	$\lambda_k \times 10^4$	ϵ (%)	$\lambda_k \times 10^4$	ϵ (%)	$\lambda_k \times 10^4$	ϵ (%)
1	1.6672	1.6815	0.86	1.6700	0.17	1.6658	-0.08	1.6680	0.05	1.6680	0.05	
2	6.3285	6.5680	3.78	6.3300	0.02	6.3284	0.00	6.3280	-0.01	6.3280	-0.01	
3	7.4815	7.9230	5.90	7.4500	-0.42	7.4842	0.04	7.4819	0.01	7.4819	0.01	
4	14.6042	16.3568	12.00	14.6500	0.31	14.6109	0.05	14.6097	0.04	14.6097	0.04	
5	19.8975	20.6490	3.78	19.9400	0.21	19.8990	0.01	19.8968	0.00	19.8968	0.00	
6	24.7990	27.6130	11.35	24.3500	-1.81	24.8140	0.06	24.8089	0.04	24.8089	0.04	
7	31.8452	33.5326	5.30	32.0800	0.74	31.8510	0.02	31.8452	0.00	31.8452	0.00	
8	35.3521	40.1532	13.58	36.9100	4.41	35.3573	0.01	35.3480	-0.01	35.3480	-0.01	
9	50.3620	60.9011	20.93	53.0300	5.30	50.4199	0.11	50.3974	0.07	50.3974	0.07	
10	57.9623	61.6663	6.39	59.5300	2.70	58.0265	0.11	58.0009	0.07	58.0009	0.07	
11	63.9259	81.0490	26.79	65.6800	2.74	64.1208	0.30	63.8880	-0.06	63.8880	-0.06	

TABLE E.2. Results for problem 2 (continued)

Eigenvalues obtained by		Combined static and consecutive dynamic condensation method with condensation to							
		Static condensation to 99 primary d.o.f.			99 main d.o.f.				
		63 main d.o.f.		75 main d.o.f.		99 main d.o.f.			
		$\lambda_k \times 10^4$	ε (%)	$\lambda_k \times 10^4$	ε (%)	$\lambda_k \times 10^4$	ε (%)		
12	66.9040	115.1500	46.89	84.9800	8.40	78.9032	0.65	78.4960	0.13
13	78.3916	129.1660	29.16	111.0900	11.09	100.1792	0.17	99.8750	-0.13
14	100.0042	145.4286	35.61	111.6600	4.12	107.4540	0.20	107.4414	0.19
15	107.2396	151.2050	39.06	119.4400	9.85	109.3400	0.56	109.3400	0.56
16	108.7304	192.0059	46.96	142.8900	9.37	132.3110	1.27	129.4150	-0.95
17	130.6500	216.0000	55.64	143.4800	3.39	140.5680	1.29	139.5647	0.57
18	138.7800	223.7900	42.55	163.4300	4.10	159.2500	1.44	158.9410	1.24
19	156.9886	276.3390	75.18	184.4200	16.91	163.6300	3.73	160.9142	2.01
20	157.7430	297.3950	72.91	191.1300	11.13	173.4220	0.83	172.4805	0.28
21	171.9940	365.2570	90.06	199.5700	3.85	192.7000	0.27	193.8790	0.89
22	192.1749	115.1500	46.89	84.9800	8.40	78.9032	0.65	78.4960	0.13

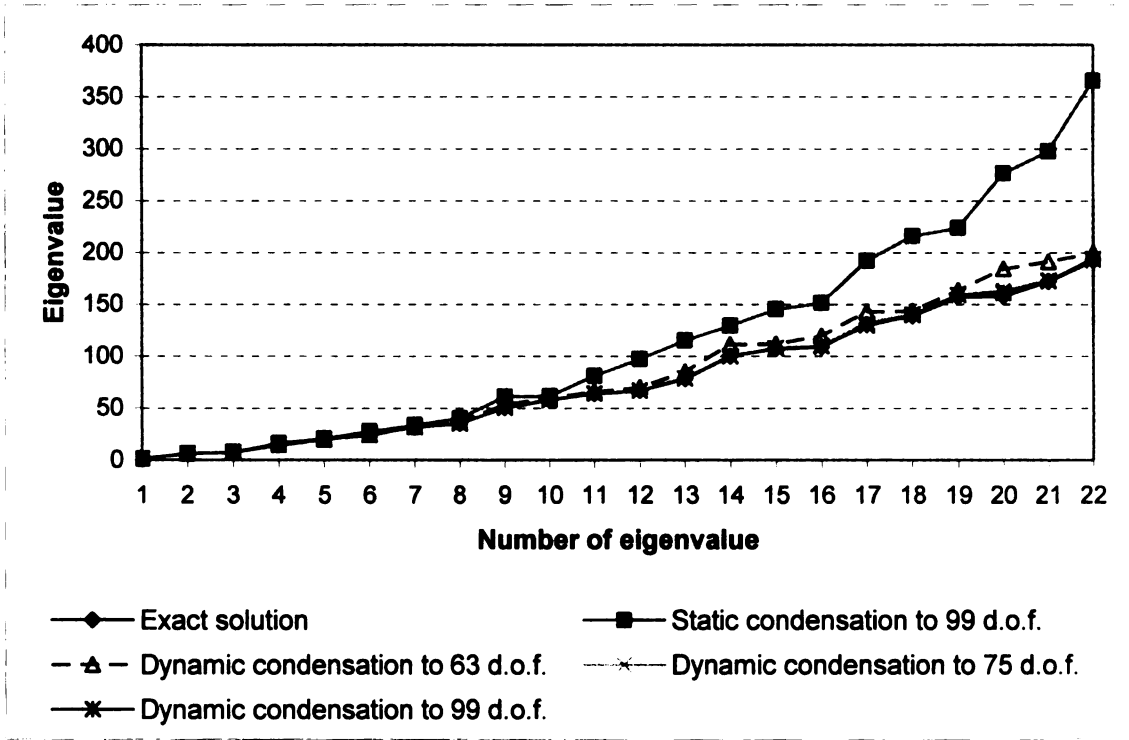


Figure E.5. Results for Problem 2

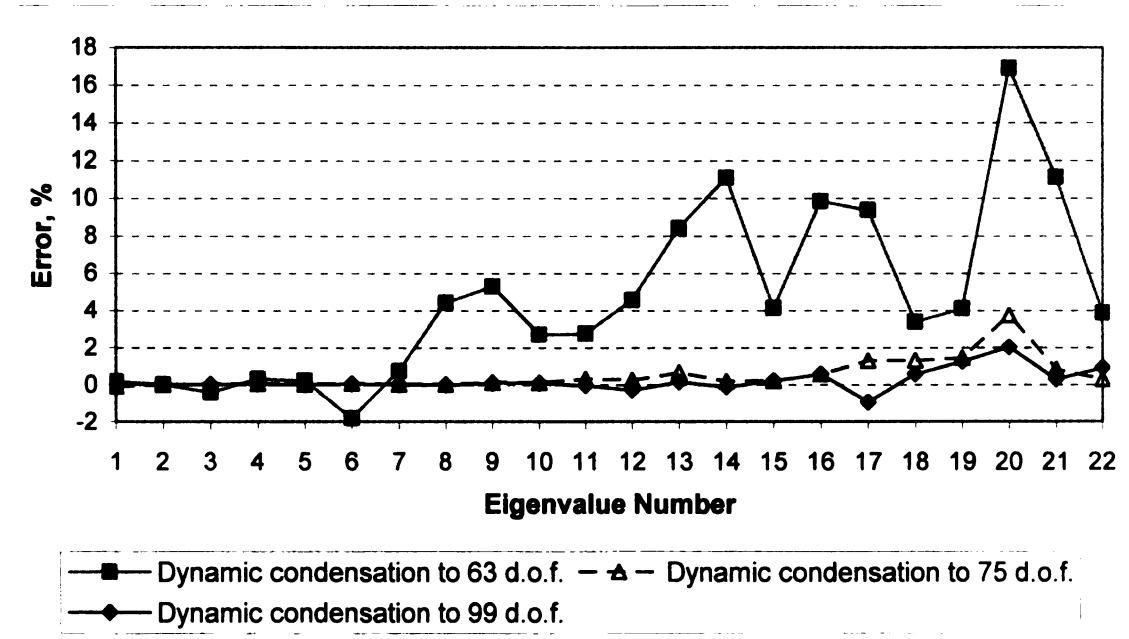


Figure E.6. Graphs of errors for Problem 2

REFERENCES

REFERENCES

- Abrate, S. (1985). "Continuum modeling of latticed structures," *Shock and Vibration Digest*, 17 (1), 15-21.
- Abrate, S. (1988). "Continuum modeling of latticed structures for dynamic analyses," *Shock and Vibration Digest*, 20 (10), 3-8.
- Abrate, S. (1991). "Continuum modeling of latticed structures – Part III," *Shock and Vibration Digest*, 23, 15-20.
- Abrate, S. (1991). "Simple models for periodic lattice," In *Modal analysis, modeling, diagnostics and control-analytical and experimental*, DE,38, Huang, T.C. et al. (eds.), ASME, New York, 725-731
- Bajan, R.L. et al. (1969) "Vibration analysis of complex structural systems by mode substitution," *Shock Vib. Bull.*, 39(3), 99-105.
- Bathe, K-J and Wilson, E.L. (1972) "Large eigenvalue problems in dynamic analysis," ASCE: *J. Eng. Mech. Div.*, 98, 1471-1485.
- Bleich, F. and Melan, E. (1936). *Finite Difference Equations of Statics*. Kharkov, Ukraine, pp. 378 (in Russian).
- Bouhaddi, N. and Fillod, R. (1996¹). "Model reduction by a simplified variant of dynamic condensation," *Journal of Sound and Vibration*, 191(2), 233-250.
- Bouhaddi, N. and Fillod, R. (1996²). "Substructuring by two-level dynamic condensation method," *Computers and Structures*, 60(3), 403-409.
- Bulgakov, V.E., Belyi, M.V., and Mathisen, K.M. (1997). "Multilevel aggregation method for solving large-scale generalized eigenvalue problems in structural dynamics," *Int. Journal for Numerical Methods in Engineering*, 40, 453-471.
- Bykoderov, M.V. and Galishnikova, V.V. (2003). "Application of the collocation form of the decomposition method for a bending problem of a plate with elastic support," *Technical Science, Bulletin of the VolgGASA*, 2-3(8), 3-11 (in Russian).
- Bykoderov, M.V. and Galishnikova, V.V. (2003). "Solution of a bending problem of a plate with elastic support using the collocation method," In: *Reliability and Durability of Construction Materials and Structures Proceedings of 3rd International Conference*, Volgograd, Russia, 2, 144-151 (in Russian).
- Craig, R.R. and Bampton, M.C.C. (1968) "Coupling of substructures for dynamic analysis," *AIAA Journal*, 6(7), 1313-1321.

- Dow, J.O. and Huyer, S.A. (1989) "Continuum models of space station structures," *J. Aerospace Engrg.*, 2(4), 220-238.
- Dow, J.O. and Huyer, S.A.(1987) "An equivalent continuum analysis procedure for space station lattice structures," *Proceeding of the 28th AIAA/ASME/ASCE/ASH/ASC Structures, Struct. Dynam. Matls. Conf.*, Monterey, CA,110-122.
- Galishnikova, V. V. (1991). "Solution of the bending problems of rectangular latticed plates by decomposition method," Thesis presented to Moscow University of Civil Engineering, in partial fulfillment of the requirements for the degree of Candidate of Science (in Russian).
- Galishnikova, V. V., and Harichandran, R. S. (2003). "Application of a decomposition method for analyzing lattice plates with elastic supports." *Proceedings of the 16th Engineering Mechanics Conference (CD-ROM)*, ASCE, Paper 13, Seattle, WA.
- Galishnikova, V., and Harichandran, R. S. (2003). "Analytical solution of boundary value problems in mechanics using a decomposition method." *Proceedings of the 16th Engineering Mechanics Conference*, ASCE, Paper 12, Seattle, WA.
- Guyan, R.J. (1965) "Reduction of stiffness and mass matrices," *AIAA Journal*, 3(2), 380.
- Hurty, W.C. (1960) "Vibration of structural systems by component mode synthesis," *ASCE J. Engr. Mech. Div.*, 51-69.
- Ignatiev, V.A. (1992). *Reduction methods of analysis in statics and dynamics of plate systems*. Saratov State University, Saratov, Russia, 142 pp.
- Ignatiev, V.A. (1979). *Analysis of Periodic Statically Indeterminate Rod Systems*. Saratov State University, Saratov, Russia, 295 pp.
- Ignatiev, V.A. and Sokolov, O.L. (1999). *Thin-Walled Cellular Structures (Methods for their Analysis)*, Oxford & IBH Publishing, New Delhi, 210 pp.
- Kollar, L., and Hegedus, I. (1985). *Analysis and Design of Space Frames by the Continuum Method*. Developments in Civil Engineering, 10, Elsevier.
- Lee, U. (1990). "Dynamic continuum modeling of beamlike space structure, using finite-element matrices," *AIAA Journal*, 18 (4), 725-731.
- Lee, U. (1991). "Dynamic continuum modeling of large platelike space structures," *Machinery Dynamics and Element Vibration*, DE, 36, ASME, 217-222.
- Lee, U. (1993). "Dynamic continuum plate representations of large thin lattice structures," *AIAA Journal*, 31(9), 1734-1736.

- Lee, U. (1994) "Equivalent continuum models of large plate-like lattice structures," *Int. J. Solid Structures*, 31(4), 457-467.
- Lee, U. (1998) "Equivalent continuum representation of lattice beams: spectral element approach," *Engineering Structures*, 20 (7), 587-592.
- Nayfeh, A.M. and Hefzy, M.S. (1978). "Continuum modeling of three-dimensional truss-like space structures," *AIAA Journal*, 16 (8), 779-787.
- Nayfeh, A.M. and Hefzy, M.S. (1981). "Continuum modeling of the mechanical and thermal behavior of discrete large structures," *AIAA Journal*, 19 (6), 766-773.
- Nelson, F.C. (1979) "Review of substructure analysis of vibrating systems," *Shock Vib. Dig.*, 11(11), 3-9.
- Necib, B. and Sun, C.T. (1980). "Analysis of truss beams using a high order Timoshenko beam finite element," *J. Sound Vib.*, 130 (1), 149-159.
- Noor, A.K., Greene, W.H., and Anderson, M.S. (1977). "Continuum models for static and dynamic analysis of repetitive lattices," *Proceedings of the AIAA/ASME/SAE 18th Structures, Structural Dynamics and Material Conference*, San Diego, Calif., 299-310.
- Noor, A.K. (1988). "Continuum modeling for repetitive lattice structures," *Appl. Mech. Rev.*, 41(7), 285-296.
- Przemieniecki, E.S. (1963) "Matrix method of studying structures by substructure analysis," *Raketnaya Technika i Komonavtika*, 1, 88-95.
- Pshenichnov, G.I. (1982). *The thin elastic reticulated shell and plate theory*. Moscow, Nauka, (in Russian).
- Pshenichnov, G.I. (1993). *A theory of latticed plates and shells*. Series on Advances in Mathematics for Applied Sciences, 5, World Scientific.
- Pshenichnov, G.I. (1985). "A decomposition method of solving equations and boundary value problems," *Soviet Math. Reports*, Academy of Sciences USSR, 3 (31), 513-515 (in Russian).
- Renton, J.D. (1970). "General properties of space grids," *International Journal of Mechanical Sciences*, 12, 801-810.
- Sherman, D.R. et al.(1972). "Bibliography on latticed structures," by the Subcommittee on Latticed Structures of the Task Committee on Special Structures of the Committee on Metals of the structural Division, *Journal of the Structural Division*, ASCE, 98 (ST7), 1545-1566.

- Sherman, D.R. et al.(1976). *Lattice structure: State-of-the art report,*” by the Subcommittee on Latticed Structures of the Task Committee on Special Structures of the Committee on Metals of the structural Division, *Journal of the Structural Division*, ASCE, 102 (ST11), 2197-2230.
- Shurygin, S.V. and Galishnikova, V.V. (2000). "Application of the decomposition method for solving a system of linear equations with mixed variables for a regular system of crossing beams," *In: Reliability and Durability of Construction Materials and Structures/ Proceedings of 2nd International Conference*, Volgograd, Russia, p.1, 143-146 (in Russian).
- Suarez, L.E. and Singh, (1992). "Dynamic condensation method for structural eigenvalue analysis," *AIAA Journal*, 30, 1045-1054.
- Sun, C.T. and Yang, T.Y. (1973). "A Continuum approach toward dynamics of gridworks," *Journal of Applied Mechanics*, ASME, 40, 186-192.
- Sun, C.T., and Kim, B.J. (1985). "Continuum modeling of periodic truss structures," *Engrg Mechanics Division of the ASCE in Conjunction with ASCE Convention*, Detroit, MI, 57-71.
- Sun, C.T., Kim, B.J. and Bogdanoff, T.L. (1988). "On the derivation of equivalent simple modals beam-like and plate-like structures in dynamic analysis," *AIAA Paper 81-0624*, 523-532.
- Timoshenko, S. P., and Woinowsky-Krieger, S. (1959). *Theory of Plates and Shells*. New York, London, McGraw-Hill, pp. 580.
- Umansky A. A. (ed.) (1973). *Designer's Handbook. Theoretical & Analytical*, Moscow, Stroyizdat, Vol. 2 (in Russian).

MICHIGAN STATE UNIVERSITY LIBRARIES



3 1293 02736 3039